Ultrasonically assisted emulsion polymerisation

Snell, David John

Award date:
2002

Awarding institution:
University of Bath

Ultrasonically Assisted Emulsion Polymerisation

submitted by **David John Snell**

for the degree of **PhD**

of the **University of Bath**

2002

COPYRIGHT

ProQuest LLC
789 East Eisenhower Parkway
P.O. Box 1346
Ann Arbor, MI 48106-1346

Acknowledgements

There are many people I would like to thank, in no particular order:

I would like to thank Gareth Price for giving me the opportunity to study in his laboratory at the University of Bath. His supervision and guidance were always appreciated, although to some, the humour and satirical comments were not always welcome, they provided a great distraction from the everyday problems. Many thanks also go to my industrial supervisor Peter West who provided a great deal of support and ideas during my thesis and who, via the 'Black Bull', made my time at York very enjoyable.

My time spent at the University of Bath was made all the better through the great company I had there, especially David B, Philip D, Simon C, Roger J and Nia W, Kerry G, Kam Y.

Thanks and appreciation must also go to my parents John and Christine, who have always given their full support and encouragement.

Finally I would like to thank the EPSRC and Smith and Nephew for much needed financial support.

Abstract

This thesis documents the research conducted towards a PhD at the University of Bath, supported by Smith and Nephew through an EPSRC 'CASE' award. The overall aim of the research is the synthesis of emulsion polymers and copolymers though the use of ultrasound.

The research can be conveniently divided into three distinct areas. The initial phase of the research concentrated upon monitoring the rate of radical production in a monomer substitute, and in an emulsion system. This was done with and without an initiator for both systems. The activation energy calculated for these reactions can be compared with the reference and literature values. The work covered in this thesis describes how the activation energy can be changed by the experimental conditions.

The second phase outlines the effect of ultrasound in the preparation of polymers using the emulsion polymerisation technique. The molecular weight, monomer conversion and the particle size are all compared for an ultrasonic reaction and a conventional reaction.

The third phase of the thesis describes the effect ultrasound upon emulsion copolymerisation reactions. Initially the copolymerisation of styrene with acrylates was investigated, then the application of ultrasound to an industrially prepared pressure sensitive adhesive. The reactivity ratios for the styrene/acrylate systems were calculated using ^{1}H NMR, these then could be compared against literature values, reasons for the differences between the reactivity ratios are made.

Contents

1.0 Introduction

1.1 Aims and Objectives

The fundamental aim of this project was to apply ultrasound to emulsion polymerisations in order that the consequences of the cavitational collapse could be utilised. This could be further broken down by;

i) Through the application of ultrasound to an emulsion polymerisation, the effect upon monomer conversions and polymer properties was studied.

ii) In the case of copolymerisations the effect ultrasound had upon the reactivity ratios was determined.

iii) The change in absorbance of a radical trap was followed for a single-phase reaction and the activation energy calculated. This was then carried on to determine the activation energy for a two-phase system.

Therefore this thesis will be described as follows;

Chapter two will present the experimental techniques used and a brief overview of the experiments undertaken during the course of this work.

The use of a radical trap will be described in chapter three. The application to a solution of *o*-xylene containing the radical trap with and without an added initiator will be shown. To further complement this section the activation energy will be determined for a two-phase system.

Through the application of ultrasound to a model system, styrene, the effect upon the monomer conversion, molecular weight and particle size will be described in chapter four.

The determination of the reactivity ratios for a styrene-acrylate copolymerisation will be shown in chapter five. Intensity effects will also be presented for a styrene-butyl acrylate copolymerisation.

Chapter six will explore the practical application of ultrasound to an industrially important emulsion reaction. A patented pressure sensitive adhesive system as used by Smith and Nephew will be utilised for this study.

Final conclusions are drawn in chapter seven and directions for future research are suggested.

1.2 An explanation of ultrasound

Ultrasound can be defined as sound waves having frequencies higher than the limit of human hearing, which is taken as 16 kHz [1]. There is no distinct upper limit but is usually taken to be 500 MHz for liquids and solids and 5 MHz for gases [1]. Ultrasound within this frequency range has two distinct uses; these can be split in terms of their frequency ranges and their uses.

Diagnostic ultrasound; this area of ultrasound is of low power and high frequency. Typically frequencies used are between 1 and 10 MHz with power outputs in the milliwatt range. It is used in non-invasive applications such as medical scanning, chemical analysis and non-destructive testing, all of which utilise the echo-pulse principle. Here a pulse of sound energy is sent through a medium and the detection of the echo as it returns after reflection from the surface of a solid object or phase boundary. Diagnostic ultrasound has found an interesting use in the field of monitoring the reaction medium in flow systems [2]. Here, an emitter is placed upon one side of a tube and a receiver is placed upon the other side, with the frequency being fixed by the diameter of the tube. The velocity of the sound is dependent upon the medium through which it passes, thus any changes in the medium, i.e. the formation of a reaction product [3], will result in a change of sound velocity. This provides continuous monitoring of the reaction medium [4]. Other uses include diagnostics and imaging where the application of the shorter wavelengths result in higher resolution.

Power ultrasound; this range of ultrasound has frequencies that span 20 to 100 kHz [1], with power outputs that can range up to hundreds of watts. Power ultrasound can be used for cleaning, plastic welding and has used throughout this investigation.

1.3 Physical principles of ultrasonic waves

Ultrasound, as with any sound wave, propagates by causing the particles of the medium through which they are moving to vibrate. Thus they are transmitted through any materials that possess elastic properties. They can move as both a longitudinal wave, where the particles of the medium vibrate in the same direction as the wave is travelling, or as transverse waves, where the particles vibrate perpendicular to the direction the wave is travelling. This is shown in figure 1.1

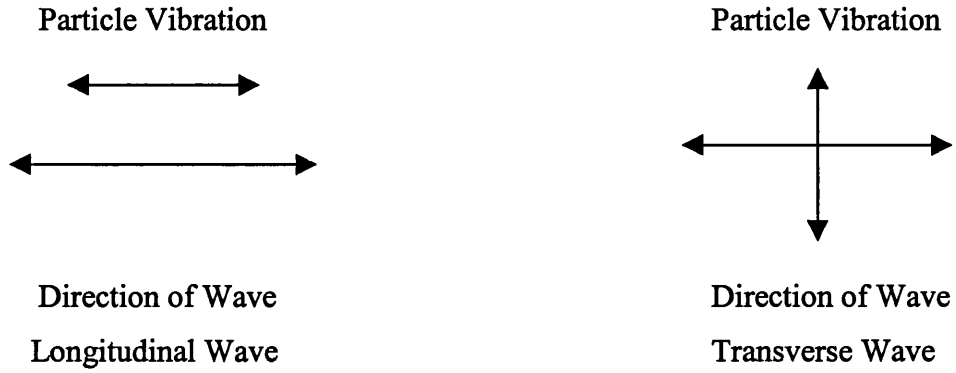

Figure 1.1 Wave and particle movement for longitudinal and transverse waves.

Ultrasound propagates through a solid as both a longitudinal and a transverse wave. However, the attenuation of transverse waves in liquids and gases is so high as to be ignored [5]. Therefore, when an ultrasonic wave passes through a liquid it will be a longitudinal wave. This will consist of an alternating cycle of compressions (where the liquid molecules are 'pushed' together) and rarefactions, (where the liquid molecules are 'pulled' apart). The compression cycle will exert a positive pressure in the liquid (relative to the press in the absence of the acoustic field), while the rarefaction cycle will exert a negative pressure. The cycles of compression and rarefaction can be shown as an acoustic pressure P_A that varies with the time t. This is summarised in figure 1.2 [6].

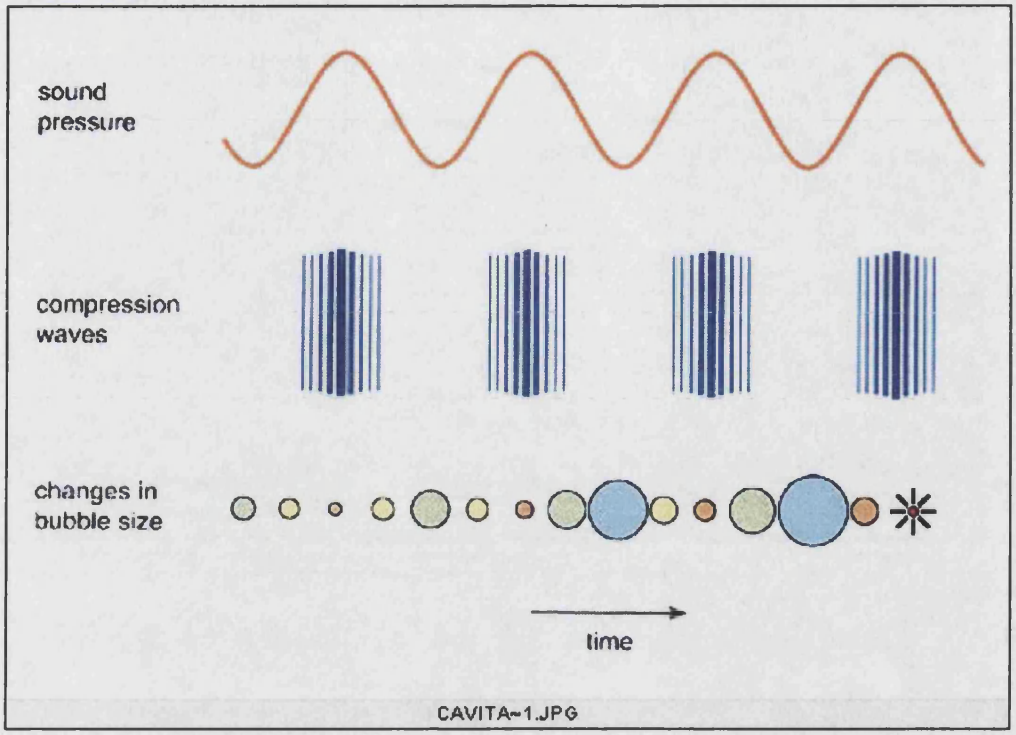

Figure 1.2 The variation of bubble size with the change in pressure [6].

It can be seen from this that the variation of acoustic pressure is sinusoidal. The acoustic pressure at a time t, is related to the frequency of ultrasound f, by.

$$P_A = P_{max} \sin(2\pi ft) \qquad (1.1)$$

Where P_{max} is the maximum acoustic pressure generated. The intensity of the wave can be described as

$$I = \frac{P_{max}^2}{2\rho c} \qquad (1.2)$$

Where ρ is the density of the medium and c is the velocity of the sound in that medium.

During propagation of the sound wave through the liquid the intensity of the wave decreases as the distance from the source increases. This attenuation arises as a result of energy being transferred to the liquid. As the molecules of the

liquid vibrate, due to action of the sound wave, they experience viscous interactions, which lowers the intensity. The energy is transferred to the liquid in the form of heat, which manifests itself as a small rise in the bulk temperature of the liquid during sonication. The attenuation is given by.

$$I_d = I_o \exp(-2\alpha d) \qquad (1.3)$$

Where I_d is the intensity of the source at distance d from the source radiation with an intensity I_o, α the absorption, or attenuation coefficient. The absorption coefficient depends on several factors such as the nature of the medium, temperature and the frequency of the wave. The frequency dependence arises due to the fact that the total energy of the medium is not solely due to the translational energy. It is due to the sum of many components including rotational, vibrational, molecular conformational and structural forms. The sound wave couples with these other energy forms, resulting in an increased frequency and leads to the relationship described in equation 1.3.

As described in figure 1.2, there is a large negative pressure developed during the rarefaction cycle of the sound wave when it is applied to a liquid. When this pressure is sufficient, the distance between molecules exceeds the critical distance necessary to hold the liquid intact, the liquid will form voids. It is these voids, or 'cavitation bubbles' which are the locus of sonochemical activity.

2.0 Cavitation

'Cavitation' is a term given to the formation and the dynamic life of bubbles in liquids. These bubbles, which can be gas or vapour filled, can be formed in a wide variety of liquids and under a wide range of conditions.

During the mid 1800's shipbuilders were developing high powered steam turbines, which could move a propeller through the water fast enough that the propeller lost contact with the water. A wrongly set propeller produces a massive reduction in pressure on the trailing faces of the blades sufficient that the liquid is torn apart. The situation came to a head in 1894 [7] when Sir John Thornycroft

and Sidney Barnaby observed that the destroyer HMS Daring suffered severe vibration and excessive damage to the propellers. Their suggestion that these effects were due to bubble formation, or cavities, being formed by the propellers was the first report of the phenomenon known as cavitation [7]. A second and much greater concern was propeller erosion. This problem was so bad that in 1915 the Admiralty convened a special subcommittee to investigate this problem. With the involvement of Lord Raleigh [8] in 1917, vapour cavity dynamics took a great leap forward with the derivation of a number of equations relating pressure and temperature, which are still useful today.

Acoustic cavitation [9] is thought to involve at least three discrete stages: nucleation, bubble growth, and under proper conditions implosive collapse. It is the principal effect of power ultrasound on liquids.

Formation of cavities in liquids is a nucleated process. The theoretical tensile strength of a pure liquid is so great (1500atm) as to preclude cavity formation [9] simply from the negative pressure of an acoustic wave. In practice cavitation occurs at considerably lower values (< 20atm). Nucleation of bubbles occurs at weak points in the liquid, such as gas filled crevices in suspended particulate matter which lower the liquids tensile strength. Evidence for this comes from the observation that the cavitation threshold (the applied observation intensity needed before cavitation will occur) is raised in rigorously degassed solutions [10,11], or in liquids where suspended particles have been removed by ultra-filtration [12].

As can be seen from figure 1.2, during the rarefaction cycle a bubble may expand. During this expansion cycle liquid vapour may diffuse into the cavity. Thus there can be a number of cavitation bubbles. These are;

1 Empty cavity

2 Vapour filled cavity

3 Gas filled cavity, caused normally by bubbling gas through the liquid.

4 Combination of vapour and gas filled cavities.

They can all be classified into two main classes, stable or resonant and transient cavitation.

1.4.1 Stable or resonant cavitation

If the intensity of the ultrasound is low (between 1 and 3 Wcm^{-2}) oscillations of the bubble around its equilibrium radius occur in the acoustic field. This type of cavitation is known as stable cavitation, because the bubble will oscillate in phase with the compression and rarefaction cycles, continually absorbing energy.

During rarefaction, gas will diffuse into the bubble, while during the compression cycle, it will diffuse out. The amount of gas that diffuses in and out depends on the surface area of the bubble and since this is slightly greater during the rarefaction phase, more gas will diffuse into the bubble than will diffuse out. Thus, over many acoustic cycles a gradual expansion of the bubble will occur. The growing bubble will eventually reach a critical size where it will most efficiently absorb energy from the acoustic field. At this point, the bubble will grow rapidly during a single expansion cycle. This size is determined by the frequency and at 20 kHz the critical size is ~150μm. At this point the bubble will grow rapidly in the course of a single expansion cycle. However, once it has experienced this very rapid growth, it can no longer absorb energy as efficiently from the acoustic field and will no longer be able to sustain itself. The compression forces acting upon the bubble will dominate and the bubble will implode. The process by which the bubble expanded and collapse is termed rectified diffusion. The oscillations of the bubble can cause disruption and movement of adjacent liquid molecules, which can set up shear forces and these can be responsible for some of the mechanical effects associated with cavitation [13].

1.4.2 Transient Cavitation

Transient cavitation bubbles are voids, or vapour filled bubbles believed to be produced using sound intensities in excess of 10 Wcm^{-2} [1] The bubbles formed exist for one, or at most a few acoustic cycles. Such rapid growth leaves little time to allow gas to diffuse into the bubble hence these are either voids or vapour filled cavities [13]. During the rarefaction cycles of the sound wave the bubble grows, such that there is an exponential increase in the radius of the bubble to twice or three times its original size (up to 200 μm) [13] before it collapses

violently. When the bubble collapses, it often disintegrates into smaller bubbles. These smaller bubbles may act as nuclei for further bubbles, or if they are of sufficiently small radius they are absorbed into the bulk of solution.

1.4.3 Bubble Collapse

The collapse or implosion of a cavitation bubble generates extreme conditions, with the collapse of a transient bubble being more violent than that of a stable bubble. This is due to the stable bubble having some gas diffused into it, where as a transient bubble may only contain some vapour. The gas will 'cushion' the collapse of a stable bubble; hence it is not as violent.

As early as 1917, when Lord Raleigh [8] attempted to describe a collapsing bubble mathematically, high pressures and temperatures were predicted upon its collapse. Using his models he predicted local pressures and temperatures of 10300 atm. and 10000K respectively during their collapse. These figures have been somewhat refined since then and with the aid of improved spectral resolution, temperatures up to 5100K $\pm$ 300K [14] have been experimentally recorded. Evidence for this comes from the discovery that sonication of solutions of metal carbonyls, $Fe(CO)_5$, $Cr(CO)_6$, and $Mo(CO)_6$, produced multi-bubble sonoluminescence spectra from the excited states of iron, chromium and molybdenum [15] respectively. Comparison of the spectra with those produced by flame ionisation have resulted in the temperatures of 5100K $\pm$ 300K.

Equations (1.4) and (1.5) were derived by Noltingk and Neppiras [16,17] and later by Flynn [18]. These equations assume adiabatic collapse occurs, i.e. there is no energy exchanged between the bubble and bulk liquid during the collapse. They showed that the maximum temperature (T_{max}) and pressure (P_{max}) generated within the bubble at the moment of total collapse as being;

$$P_{\max} = P\left\{\frac{P_m(\gamma-1)}{P}\right\}^{\gamma/\gamma-1} \qquad (1.4)$$

$$T_{max} = T_0 \left\{ \frac{P_m(\gamma - 1)}{P} \right\} \qquad (1.5)$$

where T_0 is the ambient temperature, P_m is the pressure in the liquid at the moment of transient collapse (equal to the acoustic pressure plus the ambient hydrostatic pressure of the liquid), P is the pressure in the bubble at its maximum size (usually assumed to be equal to the vapour pressure of the liquid) and γ is the ratio of the specific heats of the dissolved gases, or vapour. Using these equations it is calculated that a bubble containing nitrogen gas ($\gamma = 1.33$) in water at 293K and ambient pressure the values for T_{max} and P_{max} are 4200K and 975 bar, respectively. It is the result of these temperature and pressure extremes, within the collapsing transient bubble, that have provided the explanation of much of the increased chemical activity and radical production. This theory of cavitation is often called the 'hot spot' theory. Suslick and co-workers [19,20], have showed that sonoluminescence, the production of light when a liquid cavitates, induced in alkane solvents, is the same as that arising from their combustion at several thousand Kelvin. They have also shown that chemical reactions such as the decomposition of metal carbonyls occurred under cavitation in the same manner as thermal processes at high temperatures.

Although it must be noted that this 'hot spot' theory [21] explains the majority of sonochemical phenomena it does not fully explain all aspects. Margulis [22] has shown that some sonochemical phenomena are not entirely explained by the 'hot spot' theory and put forward his own 'electrical theory' [23]. In this he states that the hot spot theory cannot explain many experimental dependencies of rates of sonochemical reactions and sonoluminescence flux in terms of the temperature of a liquid near the boiling point, the hydrostatic pressure, the amplitude of sound or the viscosity of liquid especially high viscosity. The electrical theory attempts to explain this.

This theory concerns the dipole distribution in a solvent around a cavitation bubble. It has been theoretically shown [24] that during sonication large electrical fields of 10-11 Vm^{-1} are generated which are large enough to cause

chemical bonds to break and therefore cause chemical activity. The major difference being that for the hot spot theory the initial major thermal effects in the collapsing cavitation bubble are the molecule-molecule shocks. For the electrical theory there are electron-molecule shocks. This in principle is the most important difference and leads to explanations to the areas which the hot spot theory fails to cover. However, although this theory accounts for some of the experimental observations, the thermal 'hot spot' theory has gained more acceptance [15].

There may be two conflicting theories to explain certain effects of cavitation and ultrasound, but what is in agreement is that highly reactive species, such as free radicals are formed [13]. For a sonochemist it is convenient to think of three regions around a cavitation bubble [13] figure 1.3.

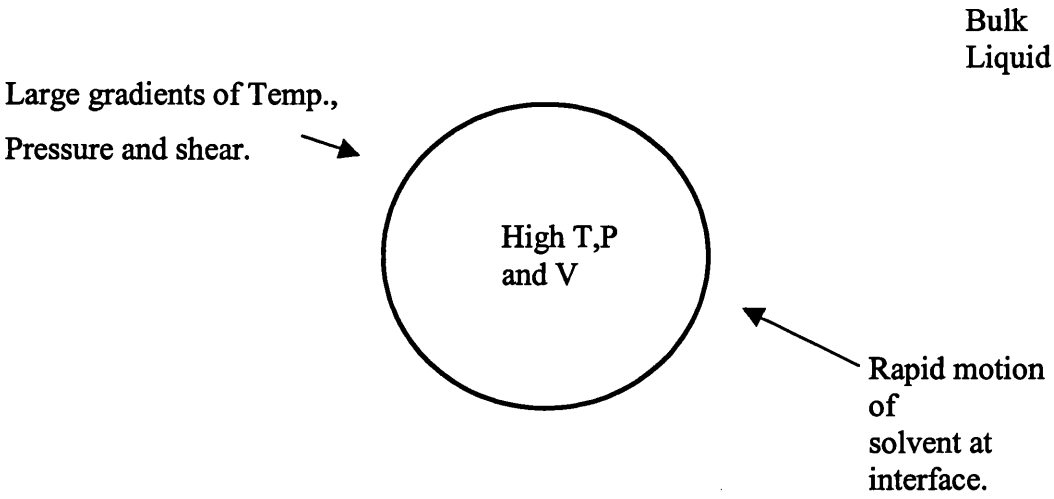

Figure 1.3 The effects of the collapse of a cavitation bubble.

In the bulk liquid there is little effect due to the bubble, except a small heating effect (caused by the attenuation of the ultrasound) and reaction of the intermediates produced. The liquid shell immediately surrounding the imploding cavity is subjected to very large temperature, pressure and electrical field gradients. Rapid movements of the solvent molecules cause very large shear gradients to be set up, causing mixing and stirring of the solution, a process known as acoustic streaming. The primary locus of sonochemical activity, radical

production, occurs within the bubble where the extremes of temperature and pressures are generated.

1.5 Parameters affecting cavitation

The nature of ultrasound reactions depends on several factors two of which, degassing and ultra-filtration have already been mentioned. Removing both the dissolved gases and particulate matter removes the weak spots in the liquid, hence an increase in the cavitational threshold. The presence of particulate matter and the way in which nucleation occurs at these sites, especially the presence of trapped gas in the crevices and recesses of these particles is shown in figure 1.4.

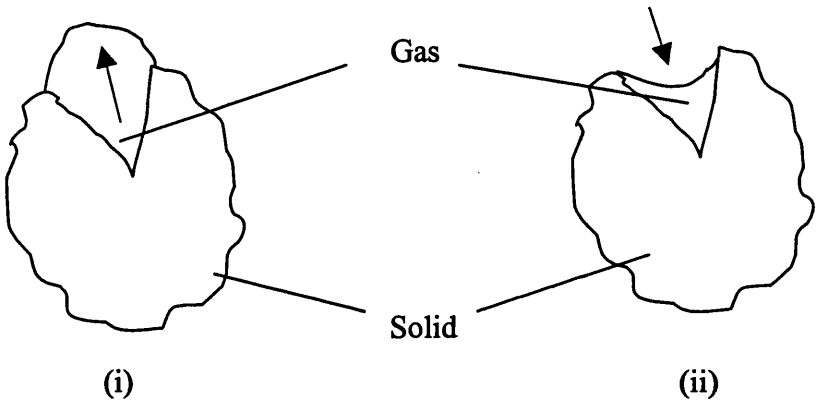

Figure 1.4 Crevice model for the nucleation process for cavitation nuclei.i) For external negative pressure, ii) for external positive pressure.

However, these are not the only parameters to effect cavitation. There are several other factors which should be taken into account.

1.5.1 Effect of temperature

In contrast to most chemical reactions lowering the temperature of the system increases the rate of reaction for selected sonochemical reactions [1]. This is due to a lowering of solvent vapour pressure, which follows the lowering of the solvent bulk temperature. At elevated temperatures, close to the solvent boiling point, the rarefaction cycle will cause the solvent to boil, due to the reduced pressure. Any cavitation bubbles formed will fill with solvent vapour and hence these bubbles will be cushioned during collapse decreasing the extremes of

pressure and temperatures in the bubble. At lower vapour pressures, less vapour has an opportunity to diffuse into the bubble and thus cushion the implosion. Price et al. [25], has demonstrated this effect upon the degradation of polystyrene in toluene. The degradation occurring at a faster rate at –10°C than at +61°C, this causes problems in the treatment of the rate constants by the usual Arrhenius model. A linear relationship was obtained, albeit with a negative apparent activation energy of $-17.3 kJmol^{-1}$. This does not relate to the bond breakage process, the activation energy for which in a thermal degradation experiment is $+164 kJmol^{-1}$.

1.5.2 Effect of solvent

In order to form bubbles, the negative pressure during the rarefaction cycle must overcome the cohesive forces within the liquid. Hence the cavitation threshold is increased in more viscous liquids. Likewise solvents with a lower surface tensions lead to a reduction in the cavitation threshold. However, the vapour pressure of the solvent is the overriding factor. If the volatility of the solvent is high, the amount of vapour entering the bubble will also be high. Thus, the vapour will cushion the collapse of the bubble, reducing the maximum temperatures and pressures. Therefore in solvents with lower vapour pressures the bubble collapse is more violent [13].

1.5.3 Effect of dissolved gases

Gases with a high solubility in the solvent will reduce the cavitation threshold, but also the intensity of bubble collapse. The threshold is lowered as a consequence of the increased number of gas nuclei present in the liquid, whilst the cavitational collapse intensity is decreased as a result of the 'cushioning' effect of the bubble. Although this effect has been demonstrated to occur [25] it is difficult to establish a straightforward relationship due to chemical effects of the gas rather than its physical properties. Oxygen and to a lesser extent carbon monoxide are reactive towards radicals and so will give an increased rate of reaction.

1.5.4 Effect of applied or hydrostatic pressure

Increasing the hydrostatic pressure increases the cavitation threshold and the intensity of bubble collapse. However, by increasing the hydrostatic pressure the inward pressure exerted on the nucleating bubble to the system must also be increased in order to produce bubble growth during rarefaction [9,13]. Raso et al. [26] have shown this effect by studying the effect of applied pressure upon the temperature rise of water for a given power output. They found that an increase in the ultrasonic power could be achieved through increasing the applied pressure up to 600 kPa. after which the ultrasonic intensity fell, due to the ultrasonic field being incapable of overcoming the combined forces of the over pressure and the cohesive forces of the liquid.

1.5.5 Effect of ultrasound intensity

There is generally a minimum intensity below which nucleation of a bubble and thus cavitation does not occur; the cavitation threshold. At very high intensities the chemical effects associated with cavitation may be reduced due to overproduction of bubbles. These bubbles shroud the source of the ultrasound and disperse the acoustic wave. In addition, it is possible that the bubble will grow too large for it to have sufficient time to collapse during the positive pressure phase. Chou and Stoffer [27] found that increasing the intensity from 6.8 to 13 Wcm^{-2}, measured calorimetrically, resulted in an increase in the rate of polymerisation for the emulsion polymerisation of styrene. However, a further increase to 14.4 Wcm^{-2} gave a reduction in the rate of polymerisation. This phenomenon was attributed to the cavitation bubbles being unable to collapse fully within the compression cycle of the applied ultrasonic field. The system then produces fewer, larger and more stable cavitation bubbles resulting in a reduction in the number of potential cavitation nuclei.

1.5.6 Effect of ultrasound frequency

Most experiments conducted in the field of sonochemistry are between 20 and 50 kHz. There are two reasons for this, first is that most equipment operates within this region and secondly it is more difficult to achieve cavitation at higher frequencies. In qualitative terms, at very high frequencies, where rarefaction, (and compression) cycles are very short the time required for the rarefaction

cycle is too small to permit a bubble to grow. Even if a bubble was to be produced, the time required to collapse may be longer than is available in the compression half cycle. The resultant cavitational effect, will therefore be less at higher frequencies.

1.6 Ultrasonic Apparatus

'Transducer'; device for changing variations of quantity e.g. electricity, to those of another e.g. sound. Oxford English dictionary.

Ultrasonic transducers are designed to convert mechanical or electrical energy into high frequency sound waves. Transducers can be split into three main types, gas driven, liquid driven and electromechanical. The most common method used to generate ultrasound is through the use of the piezoelectric properties of certain crystals. For this reason it is the method which will be explained here.

The brothers, Pierre and Jacques Curie, had been investigating the relationship between pyroelectricty and crystal symmetry [28]. Their work had predicted the occurrence of electrical polarisation due to the application of mechanical stress. This led to a theory concerning the effect that could also be used to predict the direction of the applied pressure and to which crystal classes the material exhibiting the effect would belong. In later work they supported these predictions with experimental data showing the piezoelectric effect in several crystals; zinc blende, sodium chlorate, boracite, tourmaline, quartz, calamine, topaz, tartaric acid, cane sugar and Rochelle salt.

By varying the size, type and cut of the piezoelectric material used, ultrasonic generators of different powers and frequencies can be built, although most commercially available equipment operates at 20 or 35 kHz. Crystals such as quartz were initially used to generate ultrasound but more recently various electrically polarised ceramic substances have been used such as barium titanate and lead zirconate. When a rapidly reversing charge is applied to a piezoelectric crystal, the dimensions of the crystal will change. This effect can be utilised to transmit ultrasonic vibrations from the crystal through to the desired medium.

However, optimal performance of the crystal will only be achieved at a natural, or resonance frequency of the particular sample, and this is dependent upon the dimensions of the crystal.

The ultrasound generated can be introduced into a reaction vessel using one of two main techniques:

1.6.1 The ultrasonic bath

This is the least expensive piece of ultrasonic apparatus available and hence the most commonly used type. The construction of the bath is very simple, with a number of transducers clamped to the base, or in some cases the side of the bath, see figure 1.5. The low intensity of the bath combined with the physical size means that for a small bath, a single transducer may be sufficient. The normal method of subjecting a reaction to ultrasound using a bath is to simply dip the reaction vessel into the sonicated reaction medium. The major drawback with this approach is that although there is cavitation in the water outside the flask, due to the attenuation of the ultrasound at the glass/water interface there is a reduction in the intensity of the ultrasound within the flask.

For reactions involving an ultrasonic bath, the vessel should be a flat-bottomed flask, e.g. a conical flask. This is because to the sound waves are radiating vertically from the base of the bath and this energy has to pass through the glass walls, into the reaction itself. This transfer of energy is much more effective when the sound wave impinges onto the flat base of a conical flask rather than hitting the underside of a spherical container at an angle, as more energy will be reflected away.

Despite the ease of use there a number of considerations when using this apparatus

i) Inconsistency in results occur due to the heating of the equipment during operation.

ii) The amount of power dissipated into the reaction from the bath is difficult to quantify, as it will depend upon several factors, such as the size of the bath, the type of reaction vessel and the position of the vessel in the bath.

iii) Although the majority of baths operate at 20 kHz, or 35 kHz, their operating power will vary according to manufacturer. Results that cannot be compared with those from the same equipment cannot therefore, be compared with published data.

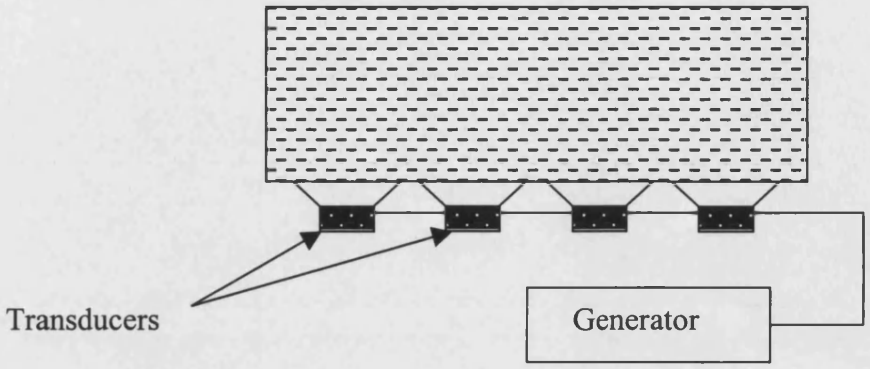

Figure 1.5 A schematic of an ultrasonic bath.

1.6.2 Direct immersion sonic horn

In order to overcome problems associated with the ultrasonic bath the use of the sonic horn is the next logical step for a researcher in the field of sonochemistry. The efficiency of this probe is far higher than that of the ultrasonic cleaning bath as the ultrasonic energy is transmitted directly into the reaction vessel, via a metal probe, see figure 1.6. The main advantages of the sonic horn are that it can be tuned to give optimum cavitation in the reaction and higher powers can be used since energy losses incurred through the cleaning bath are eliminated. However, during prolonged use, erosion of the tip is believed to cause contamination of the reaction mixture with metallic particles. Due to the probe tip being relatively small in size, the zone of high intensity ultrasound is also reduced, thus for a probe 5mm in diameter, the zone is about 7 mm wide and 100 mm long. High intensities are available, although adequate cooling may be necessary, usually through using a jacketed vessel, as large temperature rises can occur. However, unlike the bath, the intensity can be controlled, while the use of a jacketed vessel allows easier control over the temperature.

These drawbacks were considered to be minimal for the purposes of this study as it was this type of apparatus that was used for the present study.

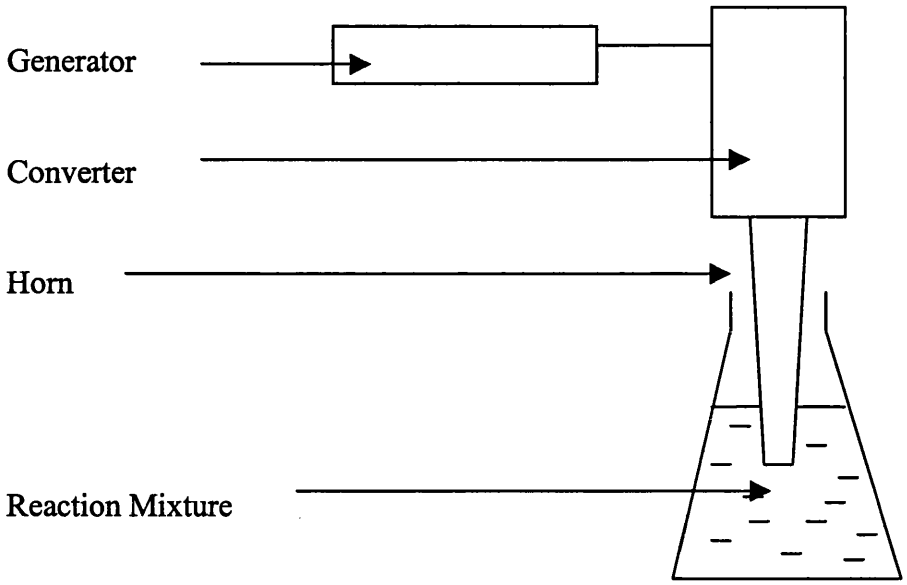

Figure 1.6 A schematic of an ultrasonic horn.

1.7 Previous work in Sonochemistry

Loomis and Wood in 1927 [29], made the first reports of the chemical effects of ultrasound when they published a paper entitled 'The physical and biological effects of high frequency sound waves of great intensity'. They described some effects such as the heating of liquids, the formation of emulsions and the destruction of red blood cells. In a further study by Loomis and Richards [30], they described the degassing effect of ultrasound along with the acceleration of two reactions, the hydrolysis of dimethyl sulphate and the 'clock' reaction, the reaction of potassium iodate with sulphuric acid. In a follow up study by Flosdorf and Chambers [31] reported that egg albumin was instantly coagulated and the hydrolysis of sucrose to glucose was accelerated, although they used audible sound and not ultrasound.

Since the effects of ultrasound where first noted, there has been a diverse range of published work detailing the positive effects of ultrasound on many different chemical reactions [1,9,13]. Luche has attempted to rationalise this huge range of reactions and has proposed a system where sonochemical reactions can be classified into three types [32,33].

Luche type 1.

These are homogeneous reactions in solution in which a single electron transfer occurs in a rate-determining step, i.e. the mechanism involves radical intermediates. Homogenous processes that have a purely ionic mechanism will be insensitive to sonication.

An example of this class of reaction is the Kornblum-Russell reaction [34,35], figure 1.7. The reaction was expected to display sonochemical switching, the reaction of 4-nitrobenzyl bromide can follow either a polar two electron pathway leading to the O-alkylation product, or a single electron transfer, responsible for the formation of the C-alkylated dinitro compound [36].

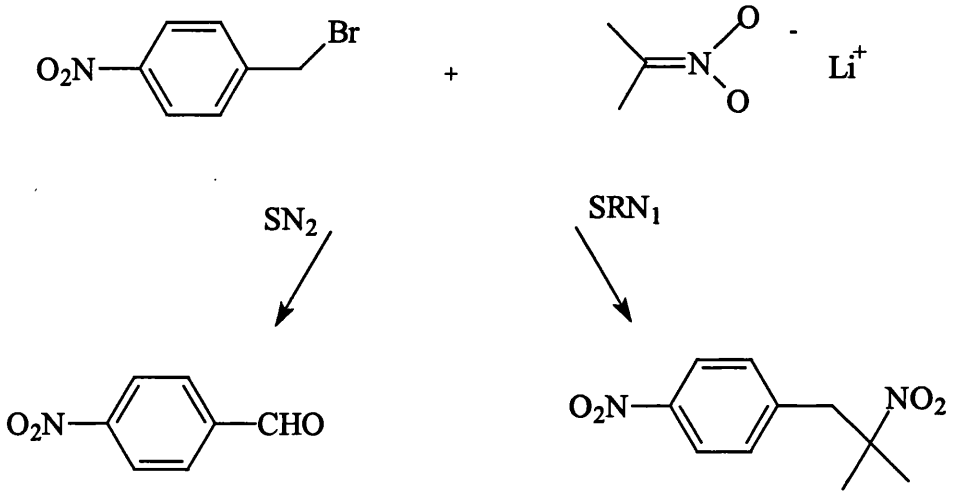

Figure 1.7 The Kornblum-Russell reaction.

Luche type 2.

These are heterogeneous reactions, which follow an ionic mechanism. The ionic mechanisms are not affected by sonication and so any effects seen will be due to the mechanical effects of ultrasound. This second class was christened 'false sonochemistry' since the role of ultrasound is essentially similar to that of a highly efficient agitation system rather than involving a specific generation of reactive chemical species.

An example of this class of reaction is in the generation of cyclic ketene acetals from cyclic β–bromo acetals and potassium hydroxide [37]. Diaz-Barra et.al. found that the best results were obtained by using a combination of ultrasound and solvent free phase transfer catalyst. A number of reactions were carried out and the results summarised below in figure 1.8.

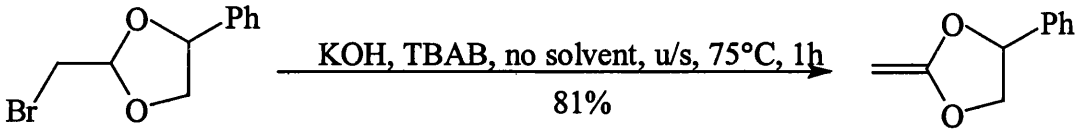

Other conditions; stir, no PTC, 1.5h, 90°C, 37%

Stir, PTC, 1.5h, 90°C, 68%

U/S, no PTC, 1h, 75°C, 65%

Figure 1.8 A summary of the published results of Diaz-Barra [37].

An advantage of this method is that the products can be directly isolated from the reaction mixture by distillation at a reduced pressure.

Luche type 3.

These are heterogeneous reactions, which involve radical intermediates in the mechanism. These will be subject to both the mechanical and chemical effects of ultrasound. This class includes most of the reactions where a metal reacts with an organic or inorganic substrate via an initial electron transfer. An example of this class of reaction is the Barbier reaction [38] as shown in figure 1.9. Here once there is physical contact between the reaction partners the metallic surface can react. Using ultrasound both increases the mass transport of the system and cleans the surface of the metal. Plus the initial electron transfer is accelerated by sonication, which then has a true chemical role.

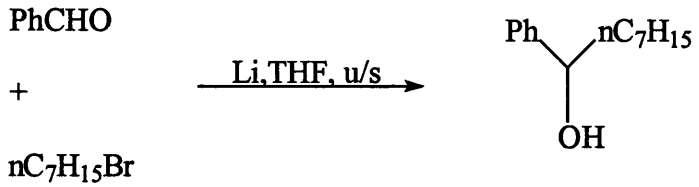

Figure 1.9 The Barbier reaction.

1.7.1 Previous work in polymer sonochemistry.

The most basic effect of applying sound waves to polymer chemistry was first reported in the 1930's [39]. Szalay used ultrasound to degrade the natural polymers gelatin, starch and gum arabic [39], the degradation being followed by the change in viscosity. The cleavage of polymer chains when irradiated in solution is known as 'sonochemical degradation'. The effect arises when polymer chains are caught in the rapid solvent flows around collapsing cavitation bubbles resulting in the stretching out and eventual breakage of the chains. The process flows has many parallels with other 'extensional flow' degradations.

During the late 1930's, Schmid and Rommel [40,41] published their results on the irradiation of polystyrene and poly(acrylates) with ultrasound. They found that there was a permanent reduction in viscosity, which was initially quite fast, but after a period of time it reached a limiting value. This suggested that the polymer chains were being broken, resulting in a lowering of the molecular weight until a limiting molecular weight is reached. This initial rapid degradation and the existence of a limiting molecular weight, where no further degradation occurs, has been observed by several other workers. Indeed, this limiting molecular weight is regarded as a characteristic of ultrasonic degradation [13,42,43,44]. Evidence for this effect comes from the observation that at low ultrasonic intensity, when no cavitation is produced, no degradation occurs, while at higher intensities, degradation does occur [45].

The cleavage of a polymer chain as a result of cavitation gives rise to active sites at chain ends. The nature of the chain ends was a matter of some debate for a

number of years with the possibility of homolytic cleavage, producing radicals at the chain ends, or heterolytic cleavage producing ions at the chain ends.

$P_{n+m} \longrightarrow P_n^{\bullet} + P_m^{\bullet}$ homolytic cleavage

$P_{n+m} \longrightarrow P_n^{+} + P_m^{-}$ heterolytic cleavage

The majority of common polymers have a carbon backbone and these are homolytically cleaved. The first evidence for this came from Henglein [46] who used the stable free radical 2,2-diphenyl-1-picrylhydrazyl (DPPH) to trap the macromolecular radicals produced during the degradation of poly(methyl methacrylate). Further evidence came from the work of Melville and Murray [47] who further demonstrated the existence of radicals by sonicating polymers in the presence of vinyl monomers. The macromolecular radicals formed initiated the polymerisation of the monomers present, to form copolymers.

As mentioned above the possibility of using ultrasound as a method for making block copolymers, by sonicating polymer in the presence of a monomer, was first reported by Melville and Murray [47]. The macromolecular radicals acting as initiators for the polymerisation of the monomer. This method has been used to produce a number of copolymers, such as poly(styrene) and poly(methyl methacrylate) [13], as well as water soluble copolymers, such as poly(acrylonitrile) and poly(ethylene oxide) [48]. A related approach is to replace the monomer with a species that is also susceptible to radical attack in order to produce end capped or telechelic materials [44].

An alternative method of producing block copolymers is to sonicate a solution containing two homopolymers. The macromolecular radicals produced can recombine to produce a block copolymer. This was reported at the same time, although independently, by Melville [49] and Henglein [50], both of whom sonicated poly(styrene) and poly(methyl methacrylate) to produce the block copolymer. This method is problematic however, as the amount of copolymer produced is small and recovery is difficult. An interesting development to this method is that the block copolymers formed can act as 'in-situ' generated

compatabilisers. Here they act as a detergent to otherwise immiscible polymer mixtures [51].

Although the degradation of polymer chains was observed very early in the historical development of sonochemistry, it was not until 1950 that the first observation of ultrasound initiating polymerisation was reported. Lindstrom and Lamm [52] investigated the polymerisation of acrylonitrile in dilute aqueous solution at several different frequencies and intensities. HO• radicals produced from the decomposition of the water were said to have initiated the polymerisation. The early view was that an initiating species was necessary for polymerisation to occur under ultrasound, i.e. application of ultrasound to pure, dried monomers would not lead to polymerisation [13]. Several workers have since investigated the effect of ultrasound upon a variety of monomers [1], although Kruus and co-workers [53,54] first demonstrated that monomers such as styrene and methyl methacrylate could be polymerised simply by sonication. Cavitation in the monomer gave rise to free radicals that initiated the polymerisation of the monomer. Using ultrasound in this way, there is no need for an added initiator. Using this approach, several monomers have been polymerised, including vinyl acetate and vinyl carbazole [44].

Price et al. [55, 56] have studied the ultrasonic polymerisation of methyl methacrylate and found that radical production under ultrasound at room temperature is comparable to that for an added initiator azo-bis(isobutyronitrile) (AIBN) at 70-80°C. As a consequence of the more violent cavitational collapse at lower temperatures, radical production was faster at lower temperatures. However, the conversions were rather low at approximately 25%. This is due to the increased viscosity as the polymerisation progressed suppressing cavitation and so preventing further formation of radicals. Performing the polymerisations in solution gave a higher conversion as the viscosity was lower.

Ultrasound has been found to affect other types of polymerisations. Emulsion polymerisations will be discussed later. Reactions employing organometallic reagents have also been enhanced using ultrasound. The most industrially

important of these is the Ziegler-Natta polymerisation of poly(ethylene) and poly(propylene), which uses a mixed metal catalyst such as alkyl aluminium with titanium tetrachloride. The major advantage of this reaction is that the polymers produced have a stereospecific structure, however, molecular weight control is difficult due to the complexity of the reacting system. By performing the reaction under ultrasound it has been found to speed up the reaction and the polymers produced had a narrow, well defined molecular weight distribution. This was achieved without loss of stereospecificity [13].

1.7.2 Previous work in emulsion sonochemistry.

In the majority of cases ultrasound has been used purely as a dispersant to prepare a homogeneous emulsion, the reaction being initiated by an added chemical initiator, such as potassium persulphate. In these cases the initiator is activated to produce free radicals either by heating or by U.V. irradiation. Ultrasonic waves have been found to increase the rates of emulsion [57,58] and suspension [59] polymerisations. The acceleration is thought to be due to two properties of ultrasound. The first is the degassing effect of ultrasound [1], which causes the efficient depletion of oxygen from the reaction medium and thus causes a lowering of the threshold or induction period experienced before polymerisation begins and a higher overall particle number and therefore polymerisation rate. The second effect is due to the localised heating of the reaction medium caused by the cavitation process. It is possible therefore that any polymerisation reaction occurring in the vicinity of a collapsing cavity will be accelerated and contribute to the overall rate increase observed.

The first report of ultrasound increasing the conversion for an emulsion was in 1950 [57]. Using laboratory made equipment operating at a frequency of 500kHz Ostroski and Stambaugh sonicated solutions of water, styrene, surfactant and potassium persulphate at 50°C and 40°C. They found that at 50°C the main effect of using ultrasound was reducing the induction period, with only a slight increase in the actual rate of reaction as given by the slope of the conversion/time graphs. At 40°C, the effect of the irradiation was much more pronounced. In order to establish that the increase in yield was from the ultrasound an aluminium rod was

inserted into the reaction, in place of the transducer, and a current passed through the rod. The runs, which were carried out using this heated rod, showed that the rod temperature did have some effect, but not enough to explain the rapid reaction when ultrasonic agitation was applied.

Although this initial work showed that ultrasound could have beneficial effects to an emulsion polymerisation, no follow up work was carried out until 1989. Lorimer et al. demonstrating the rate of polymer production is enhanced under ultrasound [60]. Again, no follow up work was carried out until Biggs and Grieser [61], irradiated a solution of water, styrene and various concentrations of surfactant. They found a dramatic increase in the rate of polymerisation when the concentration of surfactant is above the critical micelle concentration, indeed it is possible to polymerise styrene without surfactant and added chemical initiator.

Novel work reported by Liu, Chou and Stoffer [62] involving the identification of radical species within an ultrasonic irradiated emulsion. Here methyl methacrylate was the monomer and sodium dodecyl sulphate (SDS) was the emulsifier. It was found that a high yield of poly(methyl methacrylate) (PMMA, M_W=2,000,000) was obtained even without a conventional free radical initiator. They proposed that the surfactant, SDS, is dissociated into free radicals according to equation 1.6.

$$C_{12}H_{25}OSO_3Na \longrightarrow C_{12}H_{25}\bullet + \bullet OSO_3Na \qquad (1.6)$$

The emulsion systems were prepared by first adding SDS to bromoform and water, then subjecting it to ultrasonic irradiation. The emulsions irradiated by ultrasound were directly injected in a gas chromatograph interfaced with a mass spectrometer (GC-MS). From the resulting spectrum it was possible to identify the peak corresponding to 1-bromododecane, resulting from the reaction of $C_{12}H_{25}\bullet$ and bromoform. Using this method they showed that the radical concentration increased with, increasing surfactant concentration, acoustic intensity (between 6.8 Wcm^{-2} and 13.0 Wcm^{-2}) and the argon flow rate.

There have recently been a number of reports [58,63,64] concerning the ultrasonic polymerisation of styrene and methyl methacrylate. These however, do not expand upon the work already in the literature.

1.8 Historical development of emulsion polymerisation

The method of polymerising one or more monomers in an emulsion can be traced back as far as 1927. Industrial laboratories in Germany, America, and Russia were developing a process to produce synthetic latexes, similar to natural rubber. Patents describing processes in which monomer emulsions could be stabilised by soap or synthetic detergents and thermally polymerised were filed by the Goodyear Tire and Rubber Co. of Akron [65] and the I.G. Farbenindustrie Ludwigshafen laboratories [66] in 1927. Several excellent reviews of this early work in the development of emulsion and suspension polymerisation have been published [67,68,69,70]. Later [71] cold rubber produced at low temperatures using a redox initiating system was found to have superior properties and a wide variety of initiating systems were then employed, comprising a peroxide or hydroperoxide and a reducing agent. Eventually it became standard practice to polymerise at 5°C, using diisopropylbenzene activated by ferrous ions complexed with ethylene diamine tetracetate. Industrial development was supported by an extensive programme of research in academic and industrial laboratories and has been reviewed by Bovey [72].

1.9 Basic ingredients

An emulsion polymerisation is a free radical chain polymerisation, where the monomer or monomers are polymerised in the presence of an aqueous solution of a surfactant to form a product, called a latex. A typical laboratory recipe for an emulsion polymerisation, besides monomer and water, includes surfactants, initiators, chain transfer agents, and a buffer. Water is the major ingredient in both a suspension and an emulsion polymerisation. It acts as the inert continuous phase helping to maintain a low viscosity and providing good heat transfer. It does however, isolate the polymerisation loci. This is called compartmentalisation and it gives emulsion polymerisation a particular

advantage over other free radical polymerisations, in terms of rates of polymerisation and molar masses. The water also acts as the medium of transfer of monomer from droplets to particles and as will be seen later it acts as the locus of initiator decomposition and oligomer formation.

1.9.1 Initiators

The majority of initiators used in emulsion polymerisations are water-soluble. A commonly used laboratory and industrial initiator is the inorganic salt of persulphuric acid, such as potassium persulphate, which dissociates into two sulphate radical anions. Persulphate produces free radicals as a result of bond scission [73], according to equation 1.7 and equation 1.8.

$$K_2S_2O_8 \longrightarrow 2K^+ + S_2O_8^{2-} \qquad (1.7)$$

$$S_2O_8^{2-} \longrightarrow 2SO_4^{\bullet-} \qquad (1.8)$$

At high temperatures (50°C or higher) persulphate is employed as the sole initiator as the activation energy for the reaction shown is quite high. Strong evidence [73] suggests water reacts with the persulphate radical to form HSO_4^-. As shown in equation 1.9;

$$SO_4^{\bullet-} + H_2O \longrightarrow OH^{\bullet} + HSO_4^- \qquad (1.9)$$

Since HSO_4^- alters pH which can drastically reduce initiator efficiency [73] a buffer should be used with the initiator, in this case sodium hydrogen phosphate. Indeed it has been shown [73,74] that below a pH of 3 persulphate decomposes by a different mechanism and does not produce free radicals, as in equation 1.10.

$$H_2S_2O_8^- + H_2O \longrightarrow H_2SO_5 + 2HSO_4^- \qquad (1.10)$$

Redox initiators, typically a mixture of an oxidising agent and a reducing agent whose reaction generates radicals are useful for reactions at lower temperatures, less than 50°C as in equation 1.11 and 1.12.

$$S_2O_8^{2-} + Cu^{+} \longrightarrow SO_4^{\bullet -} + SO_4^{2-} + Cu^{2+} \quad (1.11)$$

$$H_2O_2 + Fe^{2+} \longrightarrow OH^{\bullet} + OH^{-} + Fe^{3+} \quad (1.12)$$

It is common to perform industrial emulsion polymerisations at low temperatures, through use of a redox initiator. In the case of synthetic rubbers this reduces the amount of branching of the chains, which then also reduces the time taken to incorporate carbon black into the rubber.

Finally it is possible to employ an organic phase initiator such as azoisobutyronitrile (AIBN) in an emulsion polymerisation, although the mode of initiation of such a species is frequently different in an emulsion polymerisation from that in bulk and solution polymerisation. Oil soluble initiators, such as azo compounds, can be employed under unique circumstances in the preparation of large particle size (up to 2.5μm) mono-disperse latexes, [75,76] they can be used in order to control particle morphology and grafting reactions within the particles. They can also be employed to reduce the residual monomer at the end of the polymerisation.

1.9.2 Surfactants.

The surfactant, sometimes referred to as an emulsifier or soap, is a molecule with both a hydrophilic (water loving) and hydrophobic (water hating) segments. They have a dual role to play in an emulsion polymerisation. They provide sites for particle nucleation, as well as imparting colloidal stability to the latex particles, which are the loci of polymerisation. The most common type of surfactant used in an emulsion polymerisation is an anionic surfactant i.e. the hydrophilic part is an anion, such as sodium dodecyl sulphate and the Aerosol series; these are sodium dialkyl sulphosuccinates. Polymerisations in which they are employed produce relatively monodisperse particle size distributions, hence, the Aerosol series are favoured industrially. Other conventional surfactants are also used such as cationic surfactants i.e. the hydrophilic part is a cation, for making charged latex particles in the paper and asphalt industries, and non-ionic

surfactants for controlling latex particle morphology and for enhancing the colloidal stability against mechanical shear, freezing and added electrolytes. Reactive surfactants, which are surface active molecules with an active vinyl group, are used in order to bind the surfactant chemically to the surface of the particles. This gives the added advantage of reduced desorption during film formation and reduced water sensitivity of the latex films.

1.9.3 Other ingredients.

Buffers are a usual additive to the system and are added for several reasons. Their main role is to control the pH of the reaction, which prevents hydrolysis of the surfactant and maintains the efficiency of the initiator. The use of a buffer can also induce particle size monodispersity. However, since electrolytes may also have the detrimental effect of promoting particle coagulation care needs to be exercised when using them.

It is often common to add a chain transfer agent. Emulsion polymerisations often result in a very high molecular weight polymer. Therefore to control the molecular weight, chain transfer agents, usually mercaptans, are introduced. The mercaptan is introduced into the vessel together with the monomer. This is in order that the consumption of the mercaptan is kept in balance with the monomer consumption.

1.10 Particle Formation Mechanism

An emulsion polymerisation is a form of a free radical addition polymerisation i.e. there is an initiation, propagation and termination stage. However, the heterogeneous nature of the polymerisation adds some complications, due to the partitioning of the reagents between the various phases; these being the micellar phase, the aqueous phase, the monomer droplet phase and the particle phase. This leads to the possibility that the initiation stages take place in all the phases, then shifts to the aqueous phase and the particle phase in the latter stages, after the monomer droplets have disappeared.

There have been three major mechanisms proposed for particle nucleation in emulsion polymerisation, these are described below.

The particle formation mechanism starts with the simplest case, absence, or an amount below the critical micelle concentration (CMC), of the surfactant. In this mechanism the governing particle formation is homogeneous nucleation [77,78,79,80,81,82]. An empirical approach to this model is given below;

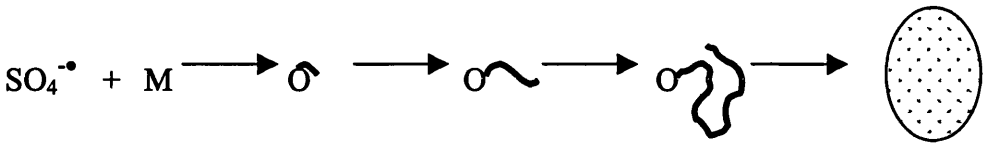

propagation 'precipitation' particle

Here, aqueous phase radicals propagate, by adding monomer units, so that they form water-soluble oligomers. Oligomeric free radicals in the aqueous phase propagate until they attain a sufficiently high degree of polymerisation, j_{crit} (j_{crit} ~5 for styrene [83]) to precipitate. These 'primary particles' then have to adsorb surfactant molecules in order to bring about their stabilisation and adsorb monomer allowing further propagation and growth. The primary particles can persist or coagulate with themselves or with growing stable radicals. From this mechanism the profile of particle size (and number) development during the course of the polymerisation and the final particle size (and number) are determined by the concentration of surfactant and how effective it is in stabilising the primary and growing particles. This model was first quantified by Fitch and co-workers and has become known as the 'HUFT' (Hansen-Ugelsted-Fitch-Tsai) theory [80]. The model requires some adjustment in order to take into account the advances since the original theory. The main one being that entry only occurs after an initiator radical has attained the critical degree of polymerisation z, where $z<j_{crit}$.

If particle formation occurs at concentrations of surfactant above the CMC, then micellar formation can be considered. This basic approach summarised below is based upon the pioneering work of Harkins [84,85] and of Smith and Ewart [86,87] which assumes that particle nucleation occurs entirely through the entry of free radicals into micelles, 'micellar entry' [88,89,90,91].

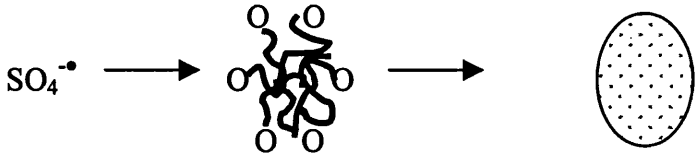

micelle particle

Here, initiator radicals from the aqueous phase enter the monomer swollen surfactant micelles and initiate the polymerisation to form monomer swollen polymer particles. These can then grow via propagation reactions. The capture efficiency is very low with every one out of 100-1000 micelles capturing a radical and becoming a polymer particle. Micelles that have not been entered by a radical give up their surfactant and any monomer molecules to the growing particles. The disappearance of the micelles signifies the end of the particle nucleation, after which the number of particles generated remains constant. The monomer droplets now serve as reservoirs, feeding monomer to the growing particles by diffusion through the aqueous phase, until they disappear at about 30-40% conversion.

If the monomer droplets are of sufficiently small in size, <0.2μm, the radicals generated in the aqueous phase enter monomer emulsion droplets as single radicals and propagate to form particles. Colloidal stability is imparted from the adsorption of surfactant molecules on the surfaces of the monomer droplets and growing polymer particles. This mechanism is thought to be predominant in micro [92,93] and mini [94,95,96] emulsion polymerisations, where the small size droplets can compete effectively for radicals. However, both systems require the use of a 'cosurfactant', which is used in addition to the main surfactant. In microemulsion polymerisations the cosurfactant is usually a low molar mass alcohol such as pentanol or hexanol, whereas in miniemulsions the cosurfactant is usually hexadecanol or cetyl alcohol, both of which have a low molar mass and low water solubility.

Although in principle all three particle formation mechanisms may be operating simultaneously, in a conventional emulsion polymerisation, their relative contributions can vary considerably. It is thought that one mechanism will

dominate depending upon, the surfactant concentration, the monomer solubility in water and the size of the monomer droplets.

The mode of particle nucleation is a source of controversy and has existed since the development of the Smith-Ewart theory. Roe [97] was the first to question the role of micellar nucleation when he derived equations identical to those from the Smith-Ewart theory without invoking micellar entry. In a recent review paper Hansen [98] re-examined the role of surfactant micelles in particle nucleation and attempted to answer the question as to what degree these micelles are the main locus of nucleation at high surfactant concentrations. Casey [99] studied the role of the aqueous phase events and concluded that nucleation below the CMC and for surfactant free systems, homogeneous-coagulative nucleation is the dominant mechanism. While above the CMC particles are formed by both micellar and homogeneous nucleation mechanisms.
Figure 1.10 shows the main components and phases in an emulsion polymerisation system.

Monomer (i) will usually exist in droplets; (ii) some monomer (depending on water solubility) will be dissolved in the continuous phase; (iii) some monomer will be within micelles.

Emulsifier (i) will be partly dissolved in the continuous phase; (ii) if the concentration is above the CMC, the excess will form micelles; (iii) some emulsifier will be adsorbed on, or even within monomer droplets.

Initiator (i) will be mostly dissolved in the continuous phase as water-soluble initiators.

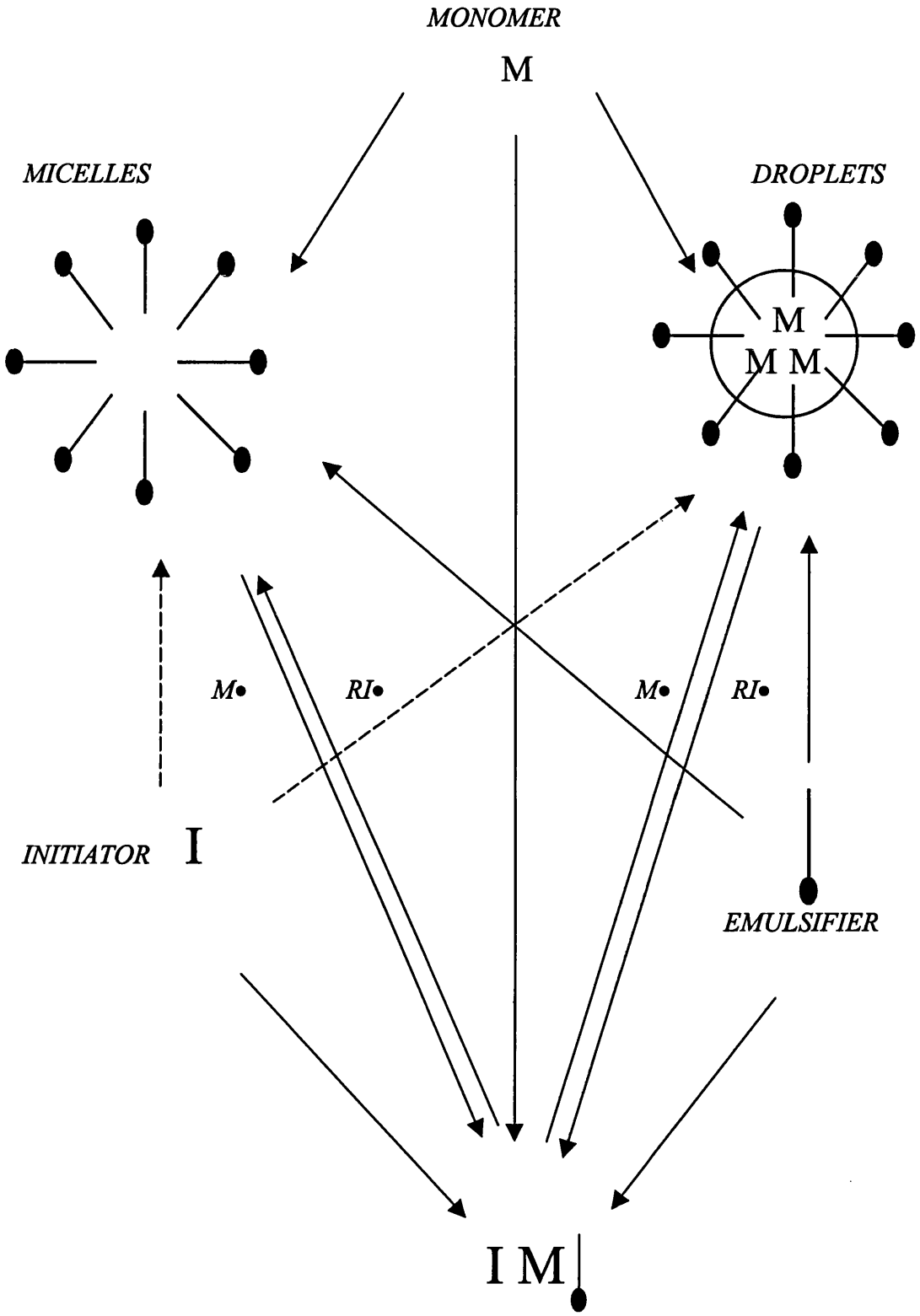

Figure 1.10 Schematic of the components and phases usually present in an emulsion polymerisation system. The arrows indicate the possible distribution of components among phases.

1.11 Polymerisation kinetics

Due to the nature of an emulsion polymerisation, with the polymerisation taking place in isolated loci, the kinetics are different from those of other radical addition polymerisations taking place in bulk, solution or suspensions. General free radical kinetics dictates that to increase the rate of polymerisation a possibility is to increase the initiator concentration, or the temperature. This however, reduces the molar mass of the resulting polymer. Emulsion polymerisations are not only quicker, but also yield a polymer with a higher molar mass than would be obtained in a bulk polymerisation. This is illustrated by comparing the following general expressions for the instantaneous rate of polymerisation, R_p, and the number average degree of polymerisation, X_n, for an emulsion versus bulk, solution or suspension polymerisations. For an emulsion polymerisation these can be expressed as;

$$R_p = k_p[M]nN / N_A \qquad (1.13)$$

$$X_n = k_p[M]nN / R_I \qquad (1.14)$$

Where k_p is the rate coefficient for propagation, [M] the monomer concentration in the particles, n the average number of radicals per particle, N the number of latex particles per unit volume, R_I the rate of radical generation or radical absorption and N_A the Avogadro constant.

For bulk free radical polymerisations:

$$R_P = k_P[M](R_I / 2k_t)^{1/2} \qquad (1.15)$$

$$X_n = k_P[M](2 / R_I k_t)^{1/2} \qquad (1.16)$$

Where, k_t is the rate coefficient for termination. Equations 1.13 and 1.14 demonstrate that the polymerisation rate and the molar mass can be simultaneously increased in an emulsion polymerisation by increasing the number of polymer particles, N, at a constant initiation rate. The polymerisation

rate may also be increased by increasing the rate of initiation, in bulk however, this leads to a reduction in the molar mass as shown by equation (1.16).

1.12 Copolymerisation reactivity ratios

Copolymerisations are processes which lead to the formation of polymers containing two or more discrete types of monomer units. It is important to note that the copolymer is not a mixture of two homopolymers, but contains units of both monomers incorporated into each copolymer molecule. The sequence of monomer units in a copolymer can vary, and the variation in structure can manifest itself dramatically in the physical properties of the final copolymer. The reaction scheme can be represented as;

Random copolymers have a random arrangement of monomer units in the chain.

$$M_A + M_B \longrightarrow M_AM_BM_BM_AM_BM_BM_BM_BM_AM_A \quad (1.17)$$

Alternating copolymers as their name suggests, have an alternating sequence of monomer units.

$$M_A + M_B \longrightarrow M_AM_BM_AM_BM_AM_BM_AM_BM_AM_B \quad (1.18)$$

Block copolymers consist of a block of one type of monomer unit connected a block of the other.

$$M_A + M_B \longrightarrow M_AM_AM_AM_AM_BM_BM_BM_B \text{ -diblock} \quad (1.19)$$

$$M_A + M_B \longrightarrow M_AM_AM_AM_BM_BM_BM_AM_AM_A \text{ –triblock} \quad (1.20)$$

Graft copolymers consist of a main homopolymer chain with branches of another type of homopolymer.

$$M_A + M_B \longrightarrow \begin{array}{c} M_AM_AM_AM_AM_AM_AM_AM_A \\ \quad\quad | \quad\quad\quad\quad | \\ \quad M_B \quad\quad\quad M_B \\ \quad\quad | \quad\quad\quad\quad | \\ \quad M_B \quad\quad\quad M_B \end{array} \quad (1.21)$$

It was observed many years ago [100] that the relative rates of homopolymerisation bore little relation to their copolymerisation rates. Some

monomers are more reactive than predicted by their rates of homopolymerisation, whilst others are less reactive. A number of monomers such as stilbene, maleic anhydride and fumaric esters undergo copolymerisation, although they have little tendency to undergo homopolymerisation. Thus from a knowledge of the homopolymerisation rates the copolymerisation rates cannot be determined. The number of parameters required to describe a given copolymerisation accurately is potentially very large. Studies on radical copolymerisation and related model systems have demonstrated that many factors influence the rate and course of polymerisation. These include;

i) The structure of the propagating species and the likelihood of significant remote unit effects.

ii) The possibility of complex formation between monomers, between monomer and solvent, etc.

iii) The kinetics and thermodynamics of copolymerisation and the possibility that depropagation is competitive with propagation.

iv) The nature of the medium and the manner in which it changes during the course of the copolymerisation.

Copolymerisation models can take several routes, terminal, penultimate, bootstrap, complex dissociation and complex participation [101]. These models should not be considered as alternative descriptions. They are approximations made through necessity to reduce complexity and should be considered a subset of some overall scheme for copolymerisation. If such a theory is possible, it would have to take into account all of the factors mentioned above. The models used are chosen as the simplest possible model capable of explaining the experimental data. As such for the purposes of this study the terminal model is the only one considered here. The terminal model was used by Maxwell et al [102] to study the compositional data of Fukuda etal [103], who also used the terminal model and came to the conclusion that there is no penultimate effect in the styrene / methyl methacrylate copolymerisation. Arehart and Matyjaszewski [104] have demonstrated the validity of the terminal model for the copolymerisation of styrene and butyl acrylate.

1.13 The terminal model

Consider the case for the copolymerisation of two monomers M_A and M_B. This leads to two types of propagating species, one with M_A* and the other with M_B*, where the dot represents a radical species. If it assumed that the reactivity of the propagating species is dependent upon the monomer unit at the end of the chain four propagating reactions are then possible.

$$M_A^* + M_A \longrightarrow M_A^* \quad (k_{AA}) \qquad (1.18)$$

$$M_A^* + M_B \longrightarrow M_B^* \quad (k_{AB}) \qquad (1.19)$$

$$M_B^* + M_A \longrightarrow M_A^* \quad (k_{BA}) \qquad (1.20)$$

$$M_B^* + M_B \longrightarrow M_B^* \quad (k_{BB}) \qquad (1.21)$$

Where k_{AA} is the rate constant for a propagating chain ending in M_A adding to monomer M_A, k_{AB} that for a propagating chain ending in M_A adding to monomer M_B etc. It is assumed that the chains are long and therefore the influence of the initiation and termination steps on the rate of monomer consumption can be neglected. Monomer M_A is consumed by reactions 1.18 and 1.20, while monomer M_B is consumed by reactions 1.19 and 1.21. The rates of disappearance of the two monomers, which are synonymous with their rates of entry into the copolymer, are given by equations 1.22 and 1.23;

$$-\frac{d[M_A]}{dt} = k_{AA}[M_A^*][M_A] + k_{BA}[M_B^*][M_A] \qquad (1.22)$$

$$-\frac{d[M_B]}{dt} = k_{AB}[M_A^*][M_B] + k_{BB}[M_B^*][M_B] \qquad (1.23)$$

Dividing the two equations yields the ratio of the rates at which the two monomers enter the copolymer

$$\frac{d[M_A]}{d[M_B]} = \frac{k_{AA}[M_A^*][M_A] + k_{BA}[M_B^*][M_A]}{k_{AB}[M_A^*][M_B] + k_{BB}[M_B^*][M_B]}$$

(1.24)

In order to remove the concentration of M_A^* and M_B^* a steady state concentration is assumed for each of the reactive species M_A^* and M_B^*. For the concentrations M_A^* and M_B^* to remain constant their rates of reaction must be equal i.e. reactions 1.19 and 1.20 are equal.

$$K_{BA}[M_B^*][M_A] = k_{AB}[M_A^*][M_B] \qquad (1.25)$$

This allows elimination of the radical concentrations from the above equation and the Mayo-Lewis equation can now be derived:

$$\frac{d[M_A]}{d[M_B]} = \frac{[M_A](r_A[M_A] + [M_B])}{[M_B](M_A] + r_B[M_B])}$$

(1.26)

Where r_A and r_B are the reactivity ratios

$$r_A = \frac{k_{AA}}{k_{AB}} \qquad r_B = \frac{k_{BB}}{k_{BA}}$$

(1.27)

Each reactivity ratio as defined above is the ratio of the rate constant for a reactive propagating species adding to its own type of monomer to the rate constant for its addition of the other monomer. The tendency of two monomers to copolymerise is noted by r values between zero and unity. An r_A value greater than unity means that M_A^* preferentially adds M_A instead of M_B, while an r_A value less than unity means that M_A^* preferentially adds M_B.

The terminal model has proven very successful in correlating a large number of copolymerisation data. Greenley [105] has provided the most recent tabulation of reactivity ratios, where some 900 ratios were recalculated using the equations of

Kelen and Tudos [106,107], from the original experimental data. All reactivity patterns can be distinguished from one another on the basis of r_A and r_B. This can be summarised as follows;

(i) $r_A \sim r_B \sim 1 (k_{AA} = k_{AB}\ ;\ k_{BA} = k_{BB})$. Neither radical shows substantial preference for either M_A or M_B, so that the relative rates of monomer consumption are determined only by the relative monomer concentrations in the feed mixture.

Equation 1.26 thus becomes

$$\frac{d[M_A]}{d[M_B]} = \frac{[M_A]}{[M_B]} \qquad (1.28)$$

in this instance the copolymer and monomer feed compositions are identical. Systems which approximate to this are styrene-butadiene (r_A = 1.35-1.83; r_B = 0.37-0.84) and vinyl acetate-vinyl chloride (r_A = 0.24-0.98; r_B = 1.03-2.30). Each shows small but significant deviations, however, so that compositional drift with conversion becomes an important experimental concern. The phenomenon composition drift is a feature of most copolymerisations and is due to the greater reactivity of one of the monomers in the reaction. Hence, in a copolymerisation it is necessary to distinguish between the composition of a copolymer being formed at any one given time in the reaction and the overall composition of the polymer at a given degree of conversion.

This situation arises when the growing polymer shows little or no preference for either monomer radical and the copolymerisation is then random. When $r_A = r_B = 1$ the two monomers show equal reactivities toward both propagating species. Therefore, the copolymer composition is the same as the comonomer feed with a random placement of the two monomers along the copolymer chain. Under these conditions any copolymer where $r_A = r_B = 1$ are called ideal copolymers.

(ii) $r_a \sim r_b \sim 0$. Here, the radical centre shows a preference for cross propagation. In the extreme case, the copolymer is perfectly alternating and of 1 : 1 composition, regardless of the monomer feed mixture. Each of the two types of

propagating species preferentially adds the other monomer, i.e. M_A* adds only M_B and M_B* adds only M_A. Equation 1.26 thus becomes

$$\frac{d[M_A]}{d[M_B]} = \frac{[M_A][M_B]}{[M_B][M_A]} = 1 \tag{1.29}$$

The copolymerisation of maleic anhydride(r_A = 0.00 – 0.02) with styrene (r_B = 0.00 – 0.0097) behaves in this manner.

(iii) r_A>1; r_B<1. Each of these radical centres prefers to add M_A, so that the copolymer is always enriched in M_A relative to the feed. This situation arises frequently in radical copolymerisation. A special case is that in which $r_A r_B$ = 1 ($k_{AA}/k_{AB} = k_{BA}/k_{BB}$); where both centres show the same preference for addition of one of the monomers. Equation 1.26 now becomes

$$\frac{d[M_A]}{d[M_B]} = r_A \frac{[M_A]}{[M_B]} \tag{1.30}$$

(iv) r_A<1; r_B<1. The radical centres now prefer cross propagation but the preference is not absolute. This results in a tendency toward alternation, which increases as r_A and r_B approach zero. The copolymerisation of acrylonitrile (r_A = 0.00 – 0.17) with styrene(r_B = 0.29 – 0.55) provides a good example. A characteristic of such polymerisations is the existence of the so-called azeotropic composition, at which the copolymer and feed compositions are equal. This situation arises when

$$\frac{d[M_A]}{d[M_B]} = \frac{[M_A]}{[M_B]}$$

which requires that

$$\frac{r_A[M_A]+[M_B]}{[M_A]+r_B[M_B]} = 1 \tag{1.31}$$

so that

$$\frac{[M_A]}{[M_B]} = \frac{1-r_B}{1-r_A} \tag{1.32}$$

at the azeotropic point. The azeotropic composition is of some practical significance in that at this point compositional drift with conversion may be neglected. This allows batch copolymerisations to be run to high conversions without the introduction of substantial compositional heterogeneity into the product.

These patterns of copolymerisation behaviour can be summarised in the form of composition curves in which the copolymer composition is plotted as a function of the monomer feed composition. Composition curves for each of the four classes of copolymerisations discussed above are shown in figure 1.11.

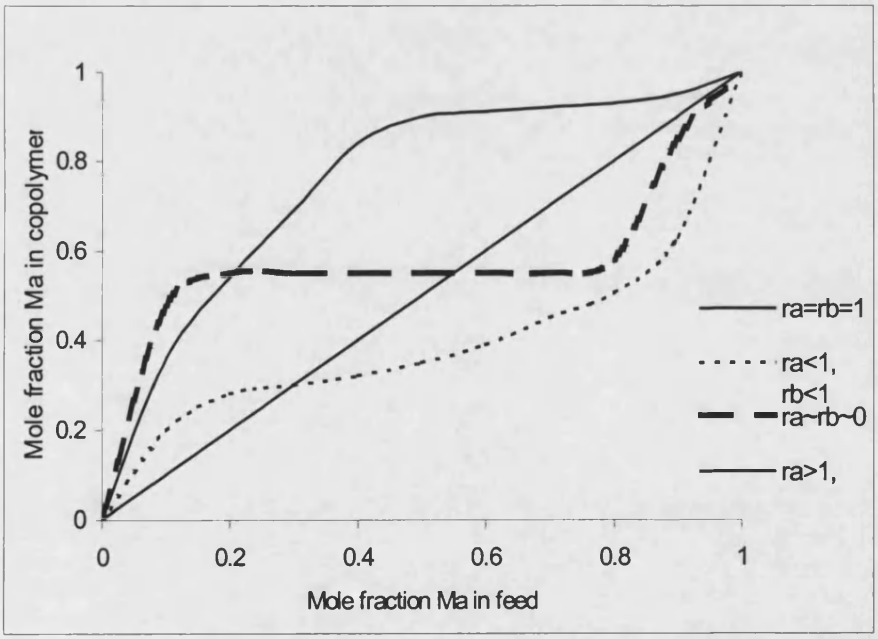

Figure 1.11 Variation of mole fraction M_A for copolymerisations.

1.14 Determination of reactivity ratios

There are two basic types of information that can be analysed to give the reactivity ratios. These are the copolymer composition/conversion data and the monomer sequence distribution.

1.14.1 Monomer composition

The more established method for determining reactivity ratios involves determinations of the overall copolymer composition for a range of monomer feeds at 'zero conversion' [108,109,110]. Copolymerisations are carried out to low conversions in order to minimise errors in the use of the copolymerisation equation. The experimental methods that have been employed for copolymer analysis include elemental analysis, radioisotopic tagging and spectroscopy (IR, UV, ^{1}H NMR).

A number of methods can be found in the polymer literature which illustrate how to calculate reactivity ratios from polymer composition and initial monomer concentrations. Early methods [111,112] do not give equal weighting to the experimental points and do not allow for a non linear dependence of the error on the composition. Thus, although the linear forms of the copolymer equation shown by Fineman and Ross [109] or by Mayo and co-workers [111,113] are algebraically correct, they are not in a useful form for estimation purposes. A good estimation procedure should include;

i) The method should give unbiased estimates of the parameters.

ii) The method should utilise all, or nearly all of the information resident in the data with regard to the parameters to be estimated so providing precise estimates.

iii) The parameter values calculated by the method should not depend upon arbitrary factors, such as which monomer is subscripted A and the starting point of the calculation.

iv) The method should supply a valid measure of the errors of the resulting estimates.

v) The method should be reasonably straightforward to use.

The method of least squares, as described [114] in the literature is a method which meets the first four of the above criteria. The procedure for estimation of reactivity ratios was addressed by Tidwell and Mortimer [110,114]. They advocated numerical analysis by non-linear least squares and later by Kelen and Tudos [106,107] who proposed an improved graphical method for data analysis, equation 1.35, that is derived from the Fineman Ross [109] equation. Fineman Ross related the molar ratio of monomer *A* to monomer *B* in the co-monomer feed (*h*) to that in the copolymer (*H*), as shown in equation 1.33;

$$G = r_1 F - r_2 \tag{1.33}$$

Where

$$G = \frac{h(H-1)}{H} \qquad F = \frac{h^2}{H} \tag{1.34}$$

Kelen and Tudos modified the above linear method to give equal weighting to all data points. They expressed the copolymerisation equation in terms of an arbitrary positive constant α.

$$\eta = \left(r_A + \frac{r_B}{\alpha}\right)\xi - \frac{r_B}{\alpha} \tag{1.35}$$

Where $\alpha = (F_m F_M)^{1/2}$ a constant and, F_m and F_M are the minimum and maximum F values.

$$\xi = \frac{F}{\alpha + F} \qquad \eta = \frac{G}{\alpha + F} \tag{1.36}$$

A plot of η against ξ will yield a straight line with intercepts of $-r_B/\alpha$ and r_A at $\xi=0$ and $\xi=1$ respectively.

Various other methods of analysing feed and copolymer composition data to determine r_A and r_B have been described [115,116]. The different methods of

data analysis are all attempts to minimise the inherent error involved in using the differential form of the copolymerisation equation. The relative merits of the different methods of data analysis have been reviewed as have the use of computational methods for minimising error [117].

1.14.2 Monomer sequence length determination

The use of NMR spectroscopy has made possible the characterisation of copolymers in terms of their monomer sequence distribution. Information on monomer sequence distribution is much more powerful than simple composition data with respect to model discrimination [118,119,120]. The use of triad fractions, analysing the tacticity of three repeat units, has been mainly used to confirm the adequacy or otherwise of various models. A number of researchers have gone one stage further and used triad fractions to calculate reactivity ratios directly [118,121,122], however, it is common for papers to be published purporting to correct the interpretation of the ^{1}H NMR [128]. For this reason the use of triad sequences was not used in this study. The area has been reviewed by Randall [123], Bovey [124], Tonelli [125] and others.

Using ^{1}H NMR spectroscopy the reactivity ratios can be determined from the sequence distributions by using equations 1.36 and 1.37.

$$\frac{N_{11}+\frac{N_{12}}{2}}{\frac{N_{12}}{2}}=\frac{N_{212}+N_{211}+N_{111}}{N_{212}+\frac{N_{112}}{2}}=r_A\frac{[M_A]}{[M_B]}+1 \qquad (1.36)$$

Likewise for r_B

$$\frac{N_{22}+\frac{N_{12}}{2}}{\frac{N_{12}}{2}}=\frac{N_{121}+N_{221}+N_{222}}{N_{212}+\frac{N_{112}}{2}}=\frac{\frac{[M_A]}{[M_B]}+r_B}{\frac{[M_A]}{[M_B]}} \qquad (1.37)$$

Where N_{ij} is the fraction of all diads which are of the type M_iM_j. The triad symbols follow by analogy. Thus N_{212} is the number of $M_2M_1M_2$ triads

normalised with respect to the total number of 1-centred and 2-centred triads. It must be noted that utilising this method to determine the reactivity ratios is not foolproof and papers on peak reassignment are quite common [126]. Indeed, in a recent paper by Maxwell, Aerdts and German [126] they stated all previous attempts to fit triad sequence distributions of styrene/methyl methacrylate using the terminal model are invalid since they utilise ^{1}H NMR spectra, which has been shown to be due to pentad sequences [127]. Further, in an accompanying paper [128] they proposed that all previous triad sequence assignments of ^{13}C NMR spectra are invalid and put forward new assignments.

A drawback with sequence distributions is that they are subject to more experimental noise than compositional data. However, this must be balanced against greater information content. Reactivity ratios can, in principle, be calculated from a single triad concentration and feed composition. A more serious problem is that unambiguous assignments of NMR signals to monomer sequences are only available for a few systems. Assignments are complicated by the fact that the sensitivity of chemical shifts to tacticity may be equal or greater than their sensitivity to monomer sequence [129].

As is usual, a series of copolymers each containing a different ratio of the monomers is prepared. A correlation of expected and measured peak intensities may then enable peak assignment [118,119]. The analysis of complex systems has been greatly facilitated by the use of, 2D NMR methods [129], decoupling experiments [127], special pulse sequences [118], and analyses of isotopically labelled systems [130,131]. In principle these methods allow a 'mechanism free' assignment.

1.15 Radical scavengers

Emulsion polymerisation is a free radical polymerisation, where the kinetics are severely affected by the presence of small amounts of inhibitors and retarders. These substances are polymerisation suppressors with different degrees of effectiveness [132]. Inhibitors completely stop the polymerisation, whereas retarders are less efficient and cause only a reduction of the polymerisation rate. Inhibition and retardation are often the cause of run to run irreproducibility. Retardation of the rate of reaction between radicals is, in some cases so effective as to produce complete inhibition of polymerisation.

Many compounds retard or inhibit polymerisation via radical addition reactions to produce a radical, which again is unreactive towards the monomer. Quinones are probably the most important class of inhibitors of this type; for example the inhibitor found in commercial methyl methacrylate is hydroquinone monomethylether.

Molecular oxygen is also an effective inhibitor for radical polymerisations, it is often considered to be an ideal inhibitor, i.e. it has to disappear completely from the reaction mixture to start the polymerisation [133,134]. It reacts with chain radicals to form the relatively unreactive peroxy radical. In some cases, notably those of styrene and methyl methacrylate, reaction proceeds further by addition to the monomer to produce an alternating copolymer [135]. Stable free radicals are also inhibitors for polymerisation. While they are too stable to initiate polymerisation they are active enough to react with free radicals. 2,2-diphenylpicrylhydrazyl (DPPH) is perhaps the best example of this class of inhibitor.

2,2-diphenylpicrylhydrazyl is an extremely efficient inhibitor, being capable of producing induction periods in the vinyl polymerisation of vinyl monomers when present in concentrations as low as 10^{-4}M [54]. This radical scavenger is very useful for quantitative measurements. Hence DPPH was used in this study to monitor the rate of production of radicals produced during the sonication period i.e. of the initiation process.

There are several possible mechanisms, which may be envisaged to account for the consumption of DPPH [136]. For example, solvent molecules may undergo pyrolysis to yield radical entities, which then react with the radical scavenger DPPH (equations 1.38-40). DPPH, being itself a radical entity, may abstract a hydrogen radical from the solvent to yield DPPH-H (equation 1.41). There may be the possibility of both of the above reactions occurring concurrently. Finally, since DPPH is a radical entity, there is the possibility that two DPPH molecules may react together, i.e. bimolecular combination (equation 1.42). However, it must be recognised that sterically it will be extremely difficult for two DPPH molecules to undergo combination termination reaction.

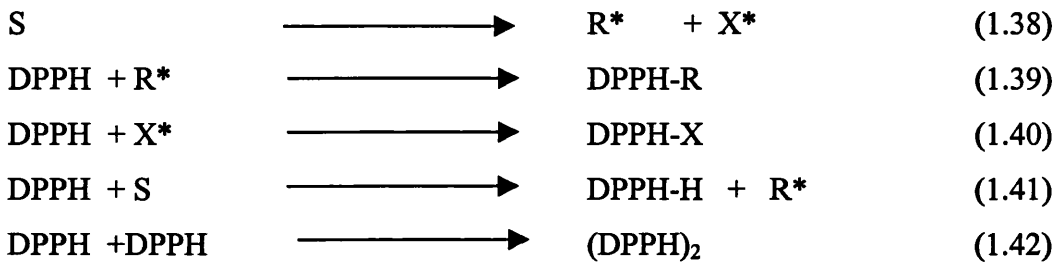

In the study of a reaction proceeding via a radical mechanism, it is vital to accurately know the rate of radical generation in the system. DPPH itself is stable but interacts with reactive radicals to give stable products. It has a strong purple colour, with λ_{max} at 520nm and the rate of fading of this colour has been used for measuring the rate of radical formation [137]. Provided that the DPPH concentration is exceedingly small, the calculated rate of radical production of radicals is independent of the concentration. This result suggests that the scavenger reacts with all of the radicals which are produced. Indeed a number of groups have studied the reaction of DPPH under a great deal of experimental conditions, including sonolysis [138,139].

Although the actual mechanism of the reaction between DPPH and radicals is not certain, the reduction of DPPH to 2,2-diphenylpicrylhydrazine ($DPPH_2$) has been noted to occur in the presence of air, oxygen and argon. It was found that the absolute amount of DPPH converted was greatest with oxygen. This is believed to be due to oxygen combining with the primary free radicals produced in the

cavitation process, giving a greater concentration of stable free radicals which can diffuse out of the bubble to react with DPPH. Segal [139] noted that the reaction of DPPH to $DPPH_2$ decreases with increasing methanol concentration. This is believed to be due to the volatile alcohol inhibiting the cavitation process [139].

1.16 Adhesive preparation

A number of years ago Smith and Nephew decided to replace the use of solvents, which are considered to be environmentally undesirable, in their polymerisation processes and move towards water based systems. One of the reactions which they changed to an emulsion process was the preparation of an adhesive as described by European patent application number 0194881 [140]. Here the copolymerisation of a number of acrylates, butyl, hydroxy-ethyl, 2-ethyl hexyl acrylate and methyl methacrylate together with a polymerisable surfactant, sodium mono-lauryl itaconoxy propane, produces a pressure sensitive adhesive. The basis of the adhesive is acrylic esters that yield polymers of low glass transition temperatures. The use of a polymerisable surfactant avoids the extra process of removing any residual surfactant.

The term 'pressure sensitive adhesive' (PSA) refers to that type of adhesive which, when in a dry state, will adhere to a variety of surfaces merely by application of light hand pressure. Such combinations are inherently soft, permanently tacky materials which exhibit a balance of adhesive and cohesive strength depending upon the visco-elastic nature of the adhesive and the performance requirements of the particular end use. Therefore, from a performance point of view, the properties that are most important to the formation of a satisfactory PSA bond are surface tack, peel adhesion and shear resistance.

1.16.1 Surface tack

Surface tack is the property of a PSA that allows it to adhere to a surface under light pressure and to resist removal almost instantly. Softer polymers generally exhibit a higher degree of tack, but also lower cohesive shear strength than

harder polymers. Tack is also a function of the thickness of the adhesive film with higher film thickness contributing to higher levels of tack.
There are a number of methods to measure the tack the oldest being the rolling ball technique [141,142]. Here, a flat plane is inclined at a certain angle to the horizontal and the adhesive film is placed on this surface, tacky surface uppermost. The ball is allowed to roll down the plane for a predetermined distance before rolling onto the tacky surface where its movement is slowed to a stop. The distance the ball moves on the tacky surface is an inverse measure of the tack of that surface.

1.16.2 Peel adhesion

Peel adhesion is determined by measuring the force required to remove a pressure sensitive material by peeling at a constant rate, either at 90 or 180° to the substrate. The peeling force required for de-bonding is measured under defined geometry, rate of separation and temperature conditions.
The disadvantage of all peel test methods used to assess adhesion is that the measured peel force is dependent on several factors such as modulus and thickness of substrate and adhesive bond. Hence, the peel test for the assessment of tack is mainly used as a quality control tool.

1.16.3 Shear resistance

Shear resistance is the force required to remove a pressure sensitive material from a surface in a direction parallel to the surface to which it is fixed. It is a measure of the cohesive strength of the adhesive. Shear resistance can be enhanced by increasing the molecular weight or the crosslink density of the polymer, however, a decrease in tack and peel adhesion will result.

1.16.4 Influence of polymer structure on performance properties

The characteristics for a PSA, namely the tack, adhesive and cohesive force, can be correlated with three basic properties; molecular weight, glass transition temperature (T_g) and the polarity of the polymer [143].

1.16.4.1Molecular weight

The molecular weight and the molecular weight distribution will influence the viscosity of the resultant PSA, the presence of lower molecular weight species contributes to a lower viscosity. The viscosity at bonding temperatures is a prime factor in how well the adhesive wets upon a substrate and hence forms a bond. When the viscosity is lower the wetting is improved due to the increased mobility of the polymer molecules. However, as the molecular weight is decreased the cohesive strength of the bond is also decreased.

The influence of the molecular weight on the performance of an idealised PSA is shown in figure1.12.

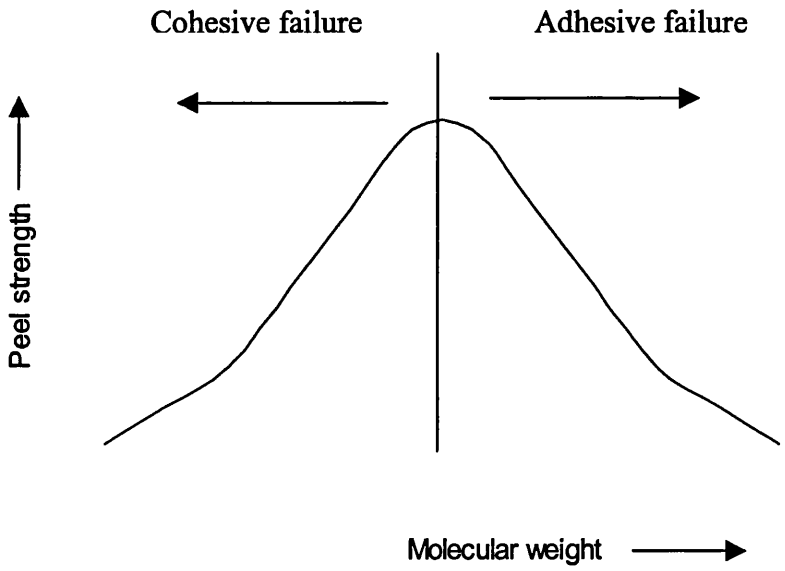

Figure 1.12 An idealised representation of the relationship between the molecular weight and the peel strength of a PSA.

Starting with a low molecular weight polymer, an increase in the molecular weight results in higher peel values due to an increase in cohesive strength, whilst the wetting of the substrate remains excellent within this range. As the molecular weight is further increased a decrease in peel strength is observed and failure on a macroscopic scale takes place at the interface between the adhesive and the substrate.

To improve the cohesive strength and the shear resistance of PSAs, without adversely affecting the peel, crosslinking is often used especially at elevated

temperatures. The improvement of resistance to creep can be quite significant even at low crosslinking densities. Crosslinking decreases the free movement of polymer molecules and a decrease in tack is normally observed. In the polymerisation of acrylates, multifunctional monomers or reactive groups carrying monomers can be introduced into the polymer chain for crosslinking purposes. For example crosslinking of simple acrylate based polymers can be accomplished very easily using free radical reagents; gelation will occur in a few minutes by heating with 2% benzoyl peroxide at 100°C. Alternatively, a short exposure to ultra violet light in the presence of a sensitiser such as benzophenone will often suffice. The beneficial effects of incorporating very low levels of multifunctional monomers into a PSA are shown in figure 1.13. Here, the shear resistance improves markedly, while the peel strength remains unaffected until higher levels of monomer were used.

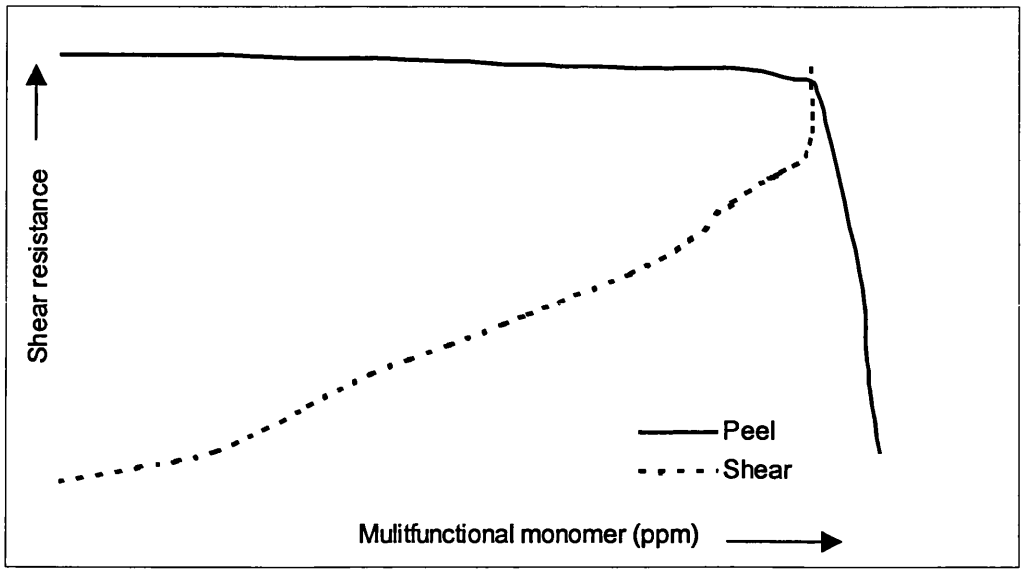

Figure 1.13 Effect of multifunctional monomer on a PSA.

1.16.4.2 Glass transition

The greater the difference between the end use temperature and the T_g for the PSA, then the lower the viscosity and the better the wetting will be. There will be an optimum T_g where a balance between polymer mobility and cohesion properties will exist. When a PSA is synthesised consideration must be given to the T_g, the molecular weight and their interplay with the mobility of the polymer molecules. Glass transition and molecular weight must be considered simultaneously when correlating the adhesive performance of polymers with physiochemical properties.

1.16.4.3 Polar effects

Other bonds besides the covalent bonding also influence the cohesive strength of a polymer. The most common bonds are the ones caused by dispersion forces that act between all atoms and are largely responsible for intermolecular cohesion [144]. Cohesive properties can be affected by the introduction of polar groups that interact forming secondary bonding. Such interactions can be hydrogen bonding, dipole-dipole and dipole induced dipole bonding. While the effect of such bonding is similar to covalent crosslinking, such polymers are soluble and the strength of such bonds decreases rapidly with increasing temperature as the bond strength decreases with increasing distance between atoms. In general, polar adhesives have a tendency to adhere to polar or high

surface energy substrates, by virtue of dipole-dipole interactions. It is for this reason that cyano-acrylate adhesives form some of the strongest adhesive bonds.

1.16.5 The polymerisation of PSA's

Polymerisation of acrylates by either solution or emulsion polymerisation are well known processes, therefore, the techniques are well known in industry. Solution and emulsion polymerisation processes have their own advantages and disadvantages, table 1.1summarises the most important differences between these two processes.

Property	Solution	Emulsion
Molecular weight	Low	High
Branching	High	Low
Residual monomer	High	Low
Impurities	Low	Low
Cost	Higher, due to solvent	Low
Yield per reactor space	Lower	High
Polymerisation rate	Low	High
Ease of tailoring	Poorer	Good
Coating	Directly	Directly, or coagulated and dissolved

Table 1.1 Differences between solution and emulsion polymerisation process and products.

1.16.5.1 Solution polymerisation

Solution polymerisation is a homogeneous free radical polymerisation process, where the monomers are soluble in the solvent and the polymer is also usually soluble in the same solvent. The main advantage of this process is that a pure polymer is obtained in a ready to coat condition. Unfortunately, the solvent can also act as chain transfer agents and cause a decrease in the molecular weight that has a negative effect upon the physical properties of the adhesive. This combined

with increasing environmental pressures to reduce volatile organic emissions means a trend away from solution polymerisation.

1.16.5.2 Emulsion polymerisation

The deposition of PSA films from a water medium has a number of advantages when compared to deposition from solvents. Water is the cheapest carrier obtainable and presents no supply problem It is odourless, non-toxic (an important consideration in medical applications), non-polluting and non-flammable. Due to the insolubility of the polymer in water the viscosities of a latex are not affected by molecular weight and are considerably lower than for a solvent based process. The solids level of the resultant latex can be as high as 70%, much higher than for a solvent process.

2.0 Experimental

The research carried out during this project involved a number of differing areas. These include radical trapping in a one phase and two-phase system, the emulsion polymerisation and copolymerisation of vinyl monomers and the preparation of a pressure sensitive adhesive. The experimental details of the main aspects that are common to these studies are described here. Greater description on the methodology for the individual studies is presented in the chapters that follow.

2.1 Materials

The chemicals used were obtained from - Aldrich, Merck, Fisher and Smith and Nephew.

Potassium persulphate : (Aldrich) 99%

Ammonium persulphate : (Aldrich) 98+% ACS grade

Azo-bisisobutyronitrile : (Aldrich) 99%

Benzoyl peroxide : (Aldrich) 99%

Styrene : (Aldrich), 99% contained the inhibitor 4-tertbutylcatechol (65 ppm), prior to purification.

Methyl methacrylate (Aldrich), 99% containing the inhibitor monomethyl ether hydroquinone (10-100ppm) prior to purification.

Butyl acrylate (Aldrich), 99% containing the inhibitor monomethyl ether hydroquinone (10-100ppm) prior to purification.

2-Hydroxy ethyl methacrylate : (Aldrich) 97% containing the inhibitor monomethyl ether hydroquinone (300ppm) prior to purification.

2-Ethyl hexyl acrylate : (Aldrich) 98% containing the inhibitor monomethyl ether hydroquinone (10ppm) prior to purification

Sodium hydrogen phosphate : (Aldrich) 99%

Sodium tripolyphosphate : (Aldrich) Tech.85%

Sodium dodecylsulphate : (Aldrich) 70%

Sodium mono lauryl itaconoxypropane sulphonate : (Smith and Nephew) 99+%

Methanol : (Aldrich) standard laboratory grade

Tetrahydrofuran : (Aldrich) 99%

Water : Milli-Q_{plus} 185 distilled and de-ionised

DPPH : 2,2-diphenylpicrylhydrazyl, (Aldrich) 98%

o-Xylene : (Merck), general reagent grade 99%

2.2 Experimental Apparatus

2.2.1 Ultrasonic horn

The apparatus used to carry out experiments using the ultrasonic horn is shown in figure 2.1.

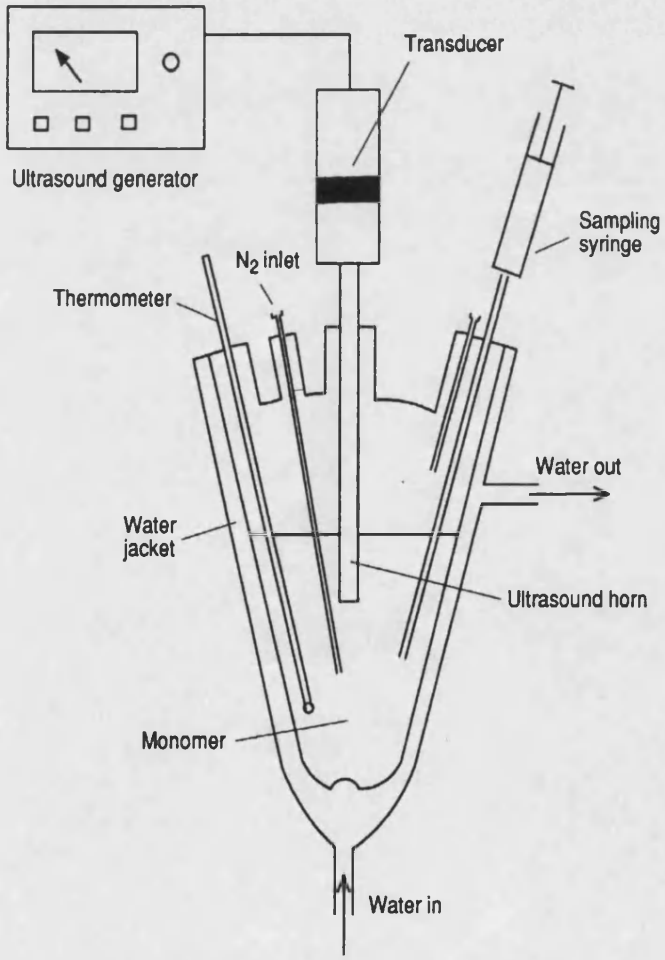

Figure 2.1 Ultrasonic apparatus.

The indentation at the bottom of the glass cell is to assist the mixing caused by acoustic streaming. The outer jacket allowed thermostatted water to be circulated around the reaction mixture, allowing the sonications to be controlled to within ± 1°C. The ultrasound generator was either; 1) Sonic Systems P100 sonicator, 2) Sonic Systems L500 sonicator, both operating at a nominal frequency of 20kHz or, 3) Sonics and Materials VC600 sonicator operating at a nominal frequency of 23kHz.

2.2.2 Conventional reaction

The apparatus used to carry out experiments that were to be heated and stirred, is shown in figure 2.2.

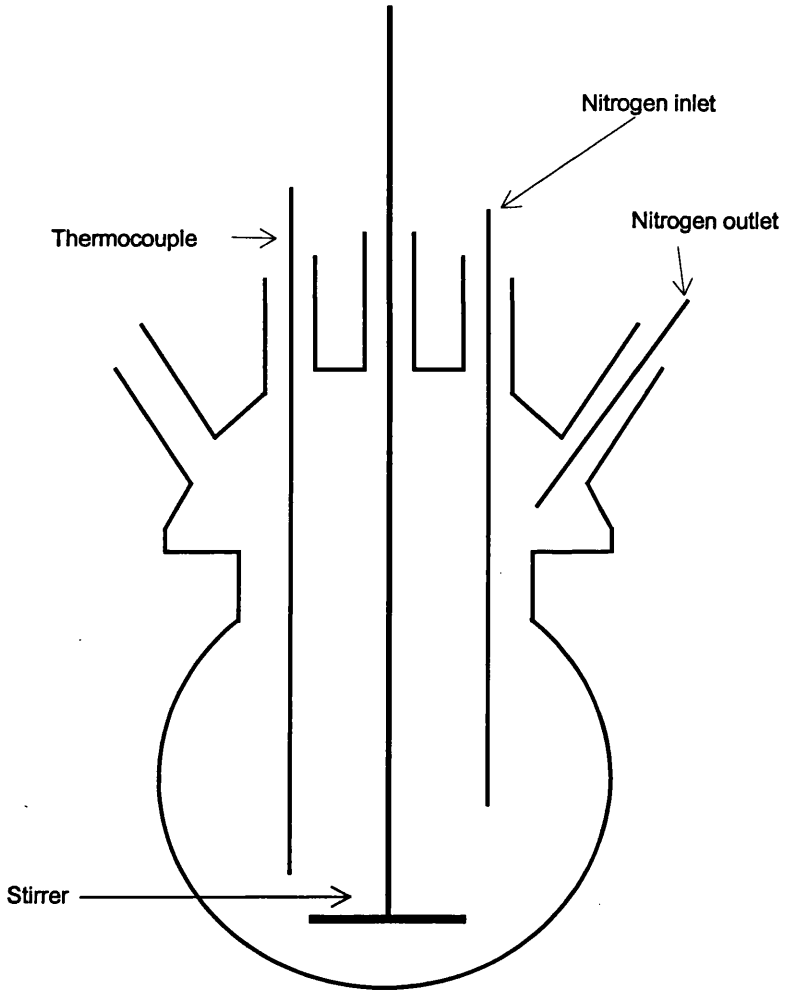

Figure 2.2 Conventional reaction apparatus.

An oil bath surrounded the bottom of the reaction flask that was connected to the thermocouple in the reaction, therefore, ensuring that the correct temperature was maintained. The stirring speed could be controlled via a variable speed motor, although for the purposes of this study it was kept to approximately 600 rpm.

2.3 Calibration of ultrasound intensity

All three ultrasonic generators are capable of delivering a variable amount of power. This is shown as a percentage of the maximum theoretical power output; however this does not give any indication of the power that is being transferred from the transducer to the solution via the horn. Therefore the system was calibrated to determine the ultrasonic intensity, the energy transferred through a unit area in a unit time, at a number of different power settings. Using a calorimetric approach [13] this was achieved using the following method.

The reaction vessel was set up as intended for a polymerisation reaction. To calibrate the P100 horn 200cm^3 of distilled water was added to the reaction vessel; to calibrate the other two horns 100cm^3 of distilled water was added to the reaction vessel. The outer jacket was filled with water, but not circulated, and an electric heater was placed into the solution. The system was allowed to equilibrate at room temperature before the heater was switched on. The heater was then switched on and the voltage and current measured using a Thander TS3021S multimeter and the temperature rise was monitored using a Digitron thermocouple every minute for five minutes. In order to assess the reproducibility, this was repeated three times to determine the average temperature rise.

The energy supplied to the heater can be calculated from equation (2.1)

$$E = VIt \tag{2.1}$$

Where, V is the voltage, I is the current and t is the time in seconds. As the energy supplied is now known, the heat capacity C, of the system can now be calculated from equation (2.2)

$$E = C\Delta T \tag{2.2}$$

The method was then repeated using the ultrasonic horn instead of the heater. The ultrasonic power was calculated using equation (2.3).

$$P = \frac{C\Delta T}{t} \tag{2.3}$$

Where, P is the ultrasonic power supplied at that intensity and T is the temperature rise recorded in time t. The result is then divided by the area of the horn tip to determine the power per unit area, or the ultrasonic intensity.

2.3.2 Calibration of Sonic Systems P100 horn

Electrical heating ; Voltage = 30.7 V, Current = 0.307 A.

Time in seconds	Temperature (°C)	Temperature rise
0	22.3	0
60	23.0	0.7
120	23.6	1.3
180	24.2	1.9
240	24.6	2.3
300	24.9	2.6

Temperature rise over 300 seconds = 2.6 °C.

Energy supplied = VIt = 30.7 *x* 0.307 *x* 300 = 2827.47 J.

Heat capacity, C = E / T = 1087.49 JK^{-1}.

The horn was calibrated for a range of ultrasonic powers, summarised below.

Generator Setting	8	10	16
Temperature rise (°C)	4.86	6.04	9.24
Power (W)	17.63	21.88	33.49
Intensity (Wcm^{-2})	5.61	6.96	10.66

2.3.3 Uncertainties involved with calibrating P100 horn.

The quantifiable errors arise from the stop clock and thermocouple readings.

Each thermocouple reading is subject to ±0.1 °C.

Each stop clock reading is subject to ±1 second.

The uncertainty in the thermocouple is:

$$= [(0.1)^2 + (0.1)^2]^{½} = 0.1°C$$

The uncertainty in the heat capacity is:

$$= 1087.5\ [\ (1/300)^2 + (0.14)^2\ ]^{½} = 59\ JK^{-1}$$

Hence, the heat capacity, $C = 1087.5 \pm 59JK^{-1}$.

For the ultrasonic horn the uncertainty in the heat capacity also needs to be taken into consideration. Therefore, for a power setting of 8 microns the uncertainty is:

$$5.61\ [\ (1/300)^2 + (0.14/4.86)^2 + (59/1087.5)^2\ ]^{½} = 0.35\ JK^{-1}.$$

Thus the final intensities should be quoted as:

Power setting (microns Pk. to Pk.)	Intensity (Wcm^{-2})
8	5.61 ± 0.35
10	6.96 ± 0.41
16	10.66 ± 0.6

2.3.3 Calibration for Sonic Systems L500 horn.

Using the method described above the following intensities were calculated:

Power setting (Microns Pk. to Pk.)	Intensity (Wcm^{-2})
5	10.64 ± 0.63
7	14.53 ± 1.08
10	21.47 ± 1.33

2.3.4 Calibration for Sonic and Materials VC600 horn.

Using the method described above the following intensities were calculated::

Power setting	Intensity (Wcm^{-2})
3	13.6 ± 0.97
4	17.3 ± 1.28
5	23.8 ± 1.72
8	36.5 ± 2.31

2.4 Analytical instrumentation

^1H NMR. NMR spectra were recorded in $CDCl_3$ with TMS as the internal reference, using a JEOL GX 400 FT-NMR spectrometer.

Mass spectroscopy. Mass-spectrometry were conducted on a Micromass VG autospec. EI, FAB+, FAB- and CI, using iso-butane, ionisation were measured.

TEM. TEM images were obtained on a JEOL 2010 200 KeV transmission electron microscope.

GPC. Both Smith and Nephew and RAPRA carried out GPC analysis. Smith and Nephew carried out the GPC analysis using a Phenomenex 10 μm mixed bed column with guard and refractive index detection was used, with THF as the solvent and polystyrene as the standard. RAPRA's analysis was performed using a Polymer Laboratories 10μm gel2 mixed bed column and refractive index detection with THF as the solvent.

DSC Differential Scanning Calorimetry was carried out on a TA instruments 2910 DSC. Aluminium pans and lids were utilised with the reference being an empty pan and lid, both lids were crimped prior to any cooling/heating cycle being carried out.

FTIR All FTIR spectra were carried out using a Perkin Elmer model 330 spectrometer with NaCl plates.

Particle sizer All samples were analysed using a Coulter LS 230 machine equipped with a small volume module and the Coulter LS control program.

2.5 Polymerisation of vinyl monomers

All the monomers except 2-hydroxy ethyl methacrylate were purified according to the following procedure:
i) Washed twice with an equal volume of 10%w/v sodium hydroxide solution.
ii) Washed with equal volumes of distilled water until neutral to universal indicator paper.
2-Hydroxy ethyl methacrylate was dissolved in water and then extracted using n-heptane.

To purify further, the monomers were distilled under vacuum to remove any remaining residuals. The purified monomer was then stored in dark bottles in a refrigerator to minimise thermal and photo-initiated polymerisation. Using this method of purification it has been shown [145] to give monomer purity in excess of 99.5%, by G.L.C analysis.

Every reaction was performed three times to ensure reproducibility.

2.5.2 Ultrasonic polymerisation of styrene.

The ultrasonic polymerisation of styrene has been carried out. The effect of changing the ultrasonic intensity, temperature and the solution concentration have been investigated. Although the exact experimental details will be described with the relevant results a representative procedure is described here.

In a typical polymerisation experiment, the glassware was thoroughly washed using distilled water, then washed using Milli-Q_{plus} 185, distilled and de-ionised water. The flask was then charged with sodium hydrogen phosphate (0.05g), potassium persulphate (0.05g), sodium dodecyl sulphate (1g) and Milli-Q_{plus} 185

water (190cm^3), from a dropping funnel, purified styrene (10cm^3) was added. The system was then flushed with nitrogen for thirty minutes, to remove any traces of oxygen. The addition of the monomer was taken to be time zero. A nitrogen atmosphere was maintained throughout the course of the reaction. Coolant was circulated around the reaction flask, so maintaining the desired temperature. 1 cm^3 samples were extracted at regular intervals and injected into a tenfold excess of methanol to precipitate the polymer. The sample was then dried to a constant weight and the conversion calculated.

After the desired time the ultrasound was switched off and adding a tenfold excess of methanol precipitated the polymer and terminated the polymerisation.

2.5.3 Conventional (or 'silent') polymerisations of styrene.

The polymerisation of styrene was carried out using the apparatus shown in figure 2.2. The effect of changing the temperature and the solution concentration was investigated. The exact experimental details will be described with the relevant results.

A typical emulsion polymerisation was carried out in a 500cm^3 multi-necked glass reaction vessel equipped with an overhead mechanical stirrer (4 bladed stirrer, 5.5cm diameter) and thermocouple. All apparatus was washed thoroughly with distilled water and then with Milli-Q_{plus} 185, distilled and de-ionised water. The flask was charged with sodium hydrogen phosphate (0.05g), potassium persulphate (0.05g), sodium dodecyl sulphate (1g) and Milli-Q_{plus} 185 water (190cm^3), in a dropping funnel styrene (10cm^3) was added. The system was then flushed with nitrogen for thirty minutes to remove any traces of oxygen. The stirrer and hotplate were switched on and the temperature controller was set to the desired temperature. The addition of the monomer was taken to be time zero. A nitrogen atmosphere was maintained throughout the course of the reaction. Samples were extracted at regular intervals and the conversion was calculated as described in section 2.5.2.

2.5.4 Copolymerisation reactions.

The ultrasonic copolymerisation of styrene-methyl methacrylate and styrene-butyl acrylate was conducted, using a Sonic and Materials VC600 horn. For each series of reactions the ultrasonic intensity and temperature were kept constant. In order to obtain a sufficient number of molar feed ratios, nine experiments were carried out at various monomer ratios.

In a typical polymerisation experiment, the glassware was thoroughly washed using distilled water, then washed using Milli-Q_{plus} 185, distilled and de-ionised water. The flask was then charged with sodium hydrogen phosphate (0.05g), potassium persulphate (0.05g), sodium dodecyl sulphate (2.25g), Milli-Q_{plus} 185 water ($75cm^3$) and the two monomers (25g total). The system was then flushed with nitrogen for thirty minutes to remove any traces of oxygen. A nitrogen atmosphere was maintained throughout the course of the reaction. Coolant was circulated around the reaction flask, so maintaining the desired temperature. The total conversion was controlled below 10%, by sonicating the solution for fifteen minutes. After this period of time, the ultrasound was switched off and a tenfold excess of methanol was added to precipitate the polymer and terminate the polymerisation. The surfactant had to be removed from the microgels by a 3-fold reprecipitation. Here, the crude product is redissolved in tetra-hydrofuran and then reprecipitated in methanol. After this procedure, no surfactant can be detected in the solution by chloride, bromide analysis [146].

2.6 Adhesive preparation

2.6.1 Conventional adhesive preparation.

The pressure sensitive adhesive was synthesised according to the method described in European Patent number 0 194 881, a patent awarded to Smith and Nephew in 1986. The synthesis involved a number of steps as follows;
To a open topped beaker Milli-Q_{plus} 185 water (65g), sodium tripolyphosphate (0.02g), sodium mono-lauryl itaconoxy propane sulphonate (0.17g) and hydroxy ethyl acrylate (0.85g) was added under continuous stirring. A second mixture of 2-ethyl hexyl acrylate (42g), n-butyl acrylate (38g) and methyl methacrylate (4.25g) was added over a period of fifteen minutes. When the addition was

complete the mixture was sonicated for a further fifteen minutes, the sonication was then stopped and the mixture added to a dropping funnel.
Milli-Q_{plus} 185 water (60g) was added to the reaction vessel as shown in figure 2.2 and heated to 82°C, upon the addition of ammonium persulphate (0.0442g) the system was deoxygenated by bubbling oxygen through the reactants for thirty minutes prior to the addition of the monomer emulsion
The monomer emulsion was slowly added to the reaction vessel over a period of one and a half hours whilst stirring and maintaining the temperature between 85-90°C.
The reaction was allowed to continue for a further three hours before the resultant polymer emulsion was cooled to 40°C and transferred to a storage jar.

2.6.2 Ultrasonically initiated adhesive polymerisation

All the reagents were added to the reaction vessel as shown in figure 2.1. The reagents were deoxygenated by bubbling nitrogen through the reactants for thirty minutes prior to the addition of the initiator. The addition of the initiator was taken as time zero and the horn switched on.

2.7 Radical trapping experiments

2.7.1 Measurement of extinction coefficients.

The solvent chosen for this study was *o*-xylene because of its similar physical properties and hence, cavitational properties to the monomer styrene. A comparison of their properties is shown in table 2.1. The solvent was chosen to reproduce the behaviour of the respective monomer without polymerising during sonication.

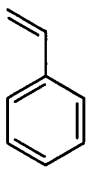

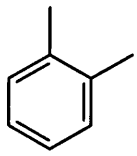

	Styrene	Ortho-Xylene
Molecular Weight	104.2	106.2
Boiling Point (°C)	145.2	144.4
Density (g cm^{-3})	0.9060	0.8802
Saturated vapour pressure (Torr)	7.22	6.48

Table 2.1 A comparison of the physical properties for *o*-xylene and styrene.

A stock solution (1×10^{-3} M) of 2,2-diphenylpicrylhydrazyl (DPPH) dissolved in *o*-xylene was prepared. The stock solution was then accurately diluted so as to prepare a number of solutions with a range of concentrations at which the maximum absorbance at the wavelength λ_{max} 520 nm, was measured. The solutions were between 0.2×10^{-4}, to 2×10^{-4} M and were measured using quartz cells of 1 cm path length and a Perkin-Elmer 330 spectrophotometer.

2.7.2 Sonication of DPPH in *o*-xylene.

DPPH is capable of acting as a radical scavenger in concentrations as low as 10^{-4}M. A solution ($100cm^3$) of approximately this concentration, known to give a maximum absorbance at $\lambda_{max} = 520$ nm, was added to the reaction vessel as shown in figure 2.1. The system was deoxygenated using nitrogen for thirty minutes simulating the conditions for a polymerisation. An initial absorbance reading was then taken by removing a sample prior to sonication and subsequent readings were taken at intervals throughout the sonication. Using the kinetic treatment outlined later, a value for the rate constant was then calculated. A range of temperatures was studied in order to calculate the Arrhenius parameters and hence determine the activation energy for the system.

To further complement the polymerisation studies the sonication of DPPH in *o*-xylene was repeated including 0.1%w/v of the initiators azo-isobutyronitrile,

(AIBN)and benzoyl peroxide (BPO). Again values for the rate constants were calculated and a comparison with the results obtained without inclusion of the initiators could be made.

2.7.3 Two phase radical trapping.

The system was set up as shown in figure 2.1. Milli-Q_{plus} 185 distilled and de-ionised water ($90cm^3$) was then added to the vessel and $10cm^3$ of a $1 \times 10^{-4}M$ DPPH pipetted into the reaction vessel. The system was then deoxygenated using nitrogen for thirty minutes simulating the conditions for a polymerisation. The ultrasound was then applied for the desired length of time. In order to obtain the organic layer containing DPPH from the emulsion, $250cm^3$ of a saturated salt solution (30%w/v NaCl) was added upon completion of the reaction. The organic layer could then be removed for analysis in the manner described in section 2.7.2. A range of temperatures were studied in order to determine the Arrhenius parameters. To further complement the polymerisation studies the sonication of DPPH was repeated including 0.025g of the aqueous initiator, potassium persulphate.

3.0 The Use of radical scavengers

Vinyl polymerisations generally have a radical initiation step. This does however present its own problems as monomers such as styrene can self polymerise during storage. In order to stop this manufacturers add a small amount, typically less than 20ppm, of a quinone to act as a radical scavenger. While these radical scavengers are too thermodynamically and kinetically stable to initiate polymerisation, they are active enough to react with free radicals. The thermodynamic stability of the inhibitor depends upon conjugation, hyperconjugation and hybridisation, these factors all contribute to the stability of the scavenger.

Hydrazyl radicals are also an important class of stable radicals with 2,2-diphenylpicrylhydrazyl (DPPH) being used for many years to obtain a measure of the rate of free radical production in a wide variety of free radical polymerisations [54,137]. Several investigators have used this highly coloured material to measure the rate of free radical production in sonochemical reactions [147,46]. Although the reaction mechanism has not been fully elucidated, what is certain is that the change in intensity of DPPH can be accurately measured against time. DPPH is an extremely efficient scavenger, being capable of producing induction periods in the vinyl polymerisation of vinyl monomers when present in concentrations as low as 10^{-4}moldm^{-3}. Hence DPPH was used in this study to monitor the rate of production of radicals produced during the sonication period i.e. of the initiation process.

This work was therefore directed at trying to identify if DPPH could be used to determine the rate of production of radicals during sonication of a solution of *o*-xylene, with and without an added initiator and in a two-phase system again with and without added initiator. An additional aspect of this section was to attempt to determine the reaction products from the sonication of DPPH. This was to be achieved by analysing the reaction products using a mass spectrometer.

3.1 Measurement of the extinction coefficient for DPPH in *o*-xylene.

To assist in the modelling of the initiation step of styrene a trapping method was chosen. The rates of initiation can be estimated by trapping the radicals formed as a result of cavitation using an excess concentration of DPPH. If styrene is used as the solvent during these reactions then there are obviously other reactions occurring besides just the initiation step. Therefore, the use of a model solvent avoided complications from reactions with styrene and from growing or degrading polymer chains. There will be a degree of radical recombination and other side reactions, but since the radical must escape from the collapsing cavitation bubble and solvent 'primary cage', whether to initiate polymerisation or to be trapped by DPPH it is felt that the rate of trapping will closely mimic the rate of initiation. For the model solvent, a liquid was needed that would behave in an identical manner to styrene when sonicated except that it would not polymerise. As explained in chapter 1 the cavitational behaviour of a solvent is determined mainly by its physical properties and the liquid most closely matching styrene is *o*-xylene. Therefore, the application of ultrasound to these cavitationally similar liquids would be expected to produce similar number of radicals upon sonication. The physical properties of *o*-xylene and styrene are shown in table 3.1.

	Styrene	*o*-Xylene
Molecular Weight	104.2	106.2
Boiling Point (°C)	145.2	144.4
Density (g cm^{-3})	0.9060	0.8802

Table 3.1 Comparison of the physical properties of styrene and *o*-xylene.

However, before a kinetic study could be made, the extinction coefficient for DPPH dissolved in *o*-xylene had to be measured. This was achieved by using the Beer-Lambert law, equation 3.1.

$$A = \varepsilon cl \qquad (3.1)$$

Where A= absorbance, ε = extinction coefficient, c = concentration ($moldm^{-3}$), l= path length (1cm). This is summarised in table 3.2.

Concentration of DPPH $x\ 10^{-4}$M.	Average absorbance
2.01	1.917 ±0.004
1.51	1.459 ±0.030
1.01	0.926 ±0.012
0.80	0.732 ±0.009
0.60	0.535 ±0.010
0.40	0.324 ±0.024
0.20	0.136 ±0.016

Table 3.2 The absorbance values for DPPH in *o*-xylene.

Therefore if the absorbance of a range of solutions of known concentrations are measured, a plot of absorbance versus concentration where the gradient will give the extinction coefficient, shown in graph 3.1.

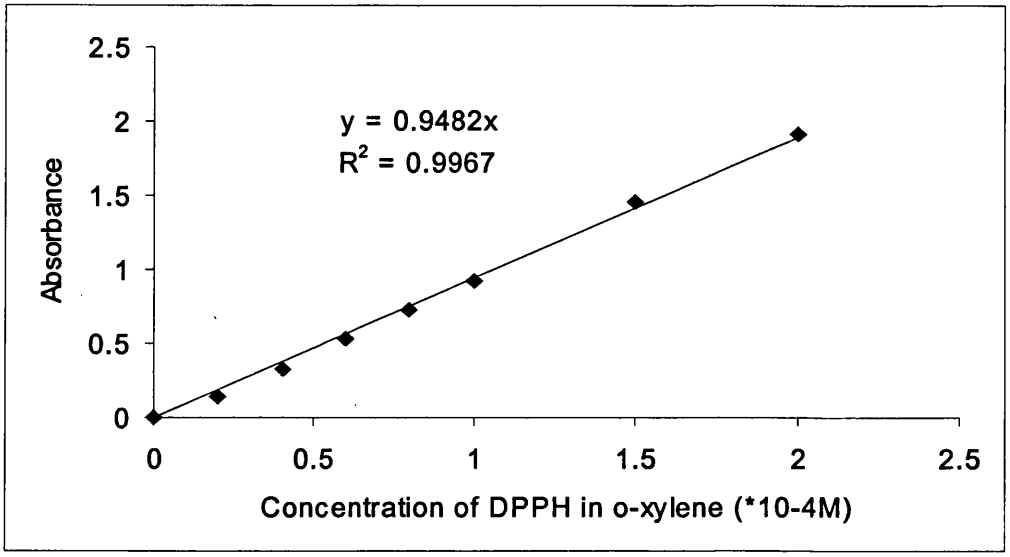

Graph 3.1 Determination of the extinction coefficient for DPPH in o-xylene.

Therefore the extinction coefficient for DPPH dissolved in *o*-xylene is 9482 ±230 $dm^3mol^{-1}cm^{-1}$. This value compares well with published data on the extinction coefficient for DPPH in an organic solvent [148]. Hence, as the absorbance of the solution, the path length and the molar absorption coefficient are known, the concentration can be determined. Plotting concentration against sonication time therefore allows the rate of consumption of DPPH to be determined. As DPPH will react with short lived radicals, its disappearance and therefore the appearance of the radical will be equal to the rate of production of radicals in the solution.

3.2 Sonication of DPPH in *o*-xylene.

The experiments were carried out as outlined in section 2.7, using a Sonic and Materials VC600 horn operating at a fixed frequency of 23kHz and a power output of 23.8 ±1.72 Wcm^{-2}.

As DPPH is a highly coloured solution the change in absorbance can be followed as a function of time. A solution of approximately 1×10^{-4}M was made up and sonicated. Through the application of first order kinetics the rate constant for a known temperature can be found.

$$C_t = C_0 e^{-kt} \quad (3.2)$$

$$\ln C_t = \ln C_0 - kt \quad (3.3)$$

Hence a graph of $-\ln C_t / C_0$ versus time can be plotted, where the gradient is the rate constant k, this is shown in graph 3.2. If zero or second order kinetics are used to calculate the rate of reaction then a straight line is not achieved. This is shown in graphs 3.3 and 3.4 respectively.

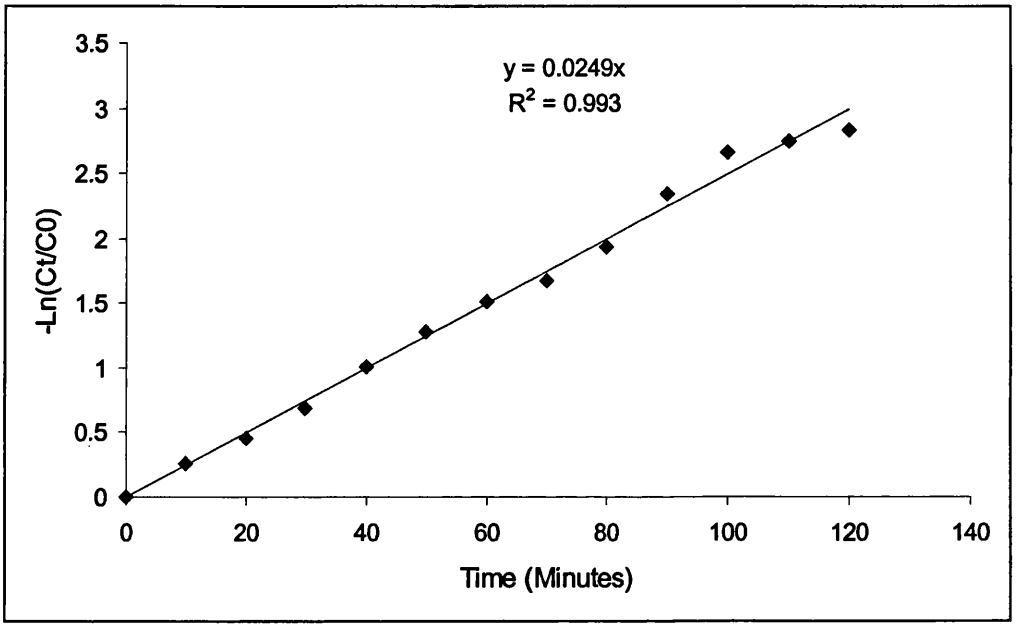

Graph 3.2 A graph demonstrating first order reaction kinetics for the consumption of DPPH in o-xylene sonicated at an intensity of 23.8 ± 1.72 Wcm^{-2} and at a temperature of 55°C.

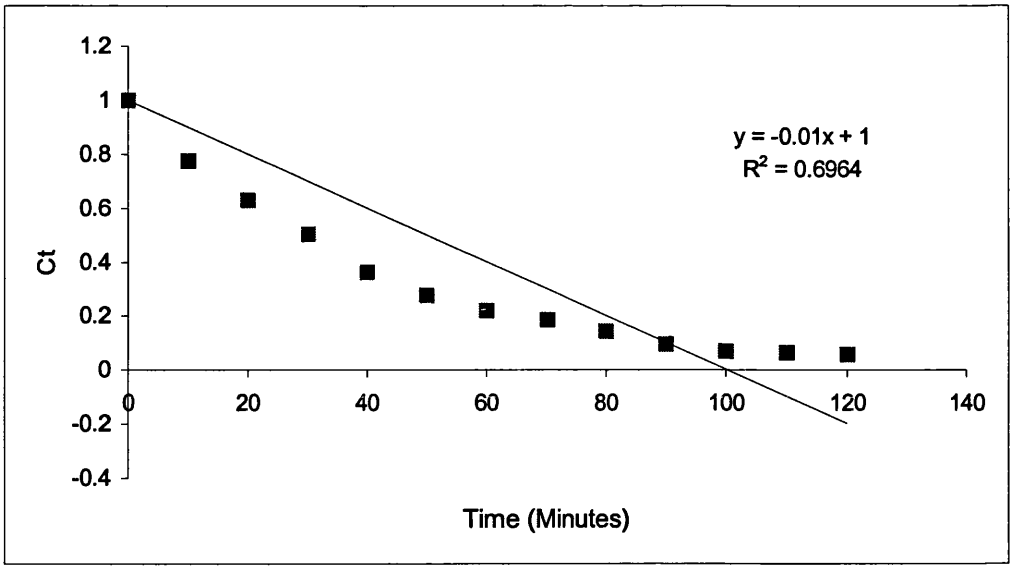

Graph 3.3 A graph demonstrating zero order reaction kinetics for the consumption of DPPH in *o*-xylene sonicated at an intensity of 23.8 ± 1.72 Wcm^{-2} and at a temperature of 55°C.

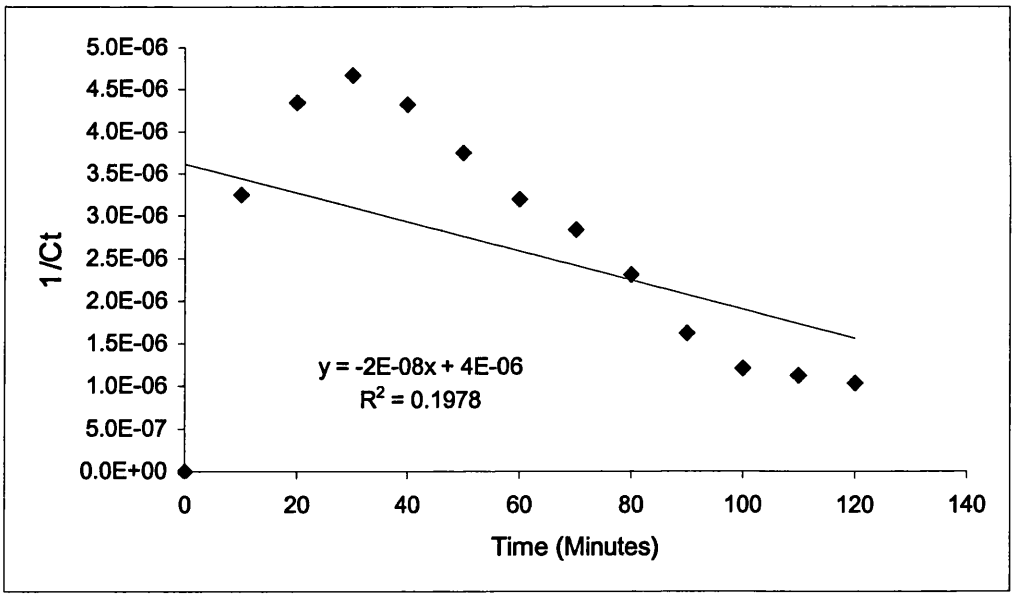

Graph 3.4 A graph demonstrating second order reaction kinetics for the consumption of DPPH in *o*-xylene sonicated at an intensity of 23.8 ± 1.72 Wcm^{-2} and at a temperature of 55°C.

The application of first order kinetics has been utilised by Mason and Lorimer [137] who sonicated solutions of DPPH in toluene, benzene and 1,2,4-

trichlorobenzene at 142°C and 156°C. They proposed that the consumption of DPPH could occur by one of two mechanisms, abstraction alone, or concurrent pyrolysis plus abstraction. If the graph of change of absorbance against DPPH concentration passed through the origin that is indicative of abstraction only, whereas a plot having a positive intercept would be indicative of abstraction plus pyrolysis. At 142°C and 156°C, within experimental error, they found that there was no significant contribution from pyrolysis of the solvent, hence, they proposed that abstraction alone is the mechanism. Other workers have also demonstrated this relationship, including Price [56], Kruus [54], and Suslick [149], who have all sonicated solutions of DPPH in various organic solvents.

Using first order kinetics, the rate constants can be found for a range of temperatures, including the radical initiators azobisisobutyronitrile (AIBN) and benzoyl peroxide (BPO). These reactions are summarised in table 3.3.

Temperature (± 0.5 °C)	DPPH	DPPH + 0.1%w/v AIBN	DPPH + 0.1%w/v BPO
-5	0.0035 ±0.0003	0.0027 ±0.001	0.0076 ±0.0015
20	0.0027 ±0.00028	0.0043 ±0.0004	0.0113 ±0.0029
35	0.0024 ±0.00021	0.0093 ±0.0003	0.0181 ±0.0037
45	0.002 ±0.00025	0.012 ±0.002	0.0187 ±0.0015
55	0.0018 ±0.00027	0.0221 ±0.0018	0.0249 ±0.0014

Table 3.3 Rate constants (min^{-1}) for the sonication of DPPH in *o*-xylene sonicated at an intensity of 23.8 ± 1.72 Wcm^{-2}.

It may be noted that proportionally the error is larger for a decrease in the temperature. This is due to the greater accuracy to control the temperature above ambient temperatures.

3.2.1 Sonication of DPPH in *o*-xylene

Using the values for the sonication of DPPH in solution and by applying the Arrhenius equation, a graph of the Ln rate constant against 1/T can be plotted where the activation energy for the system can be found. This is shown in graph 3.5.

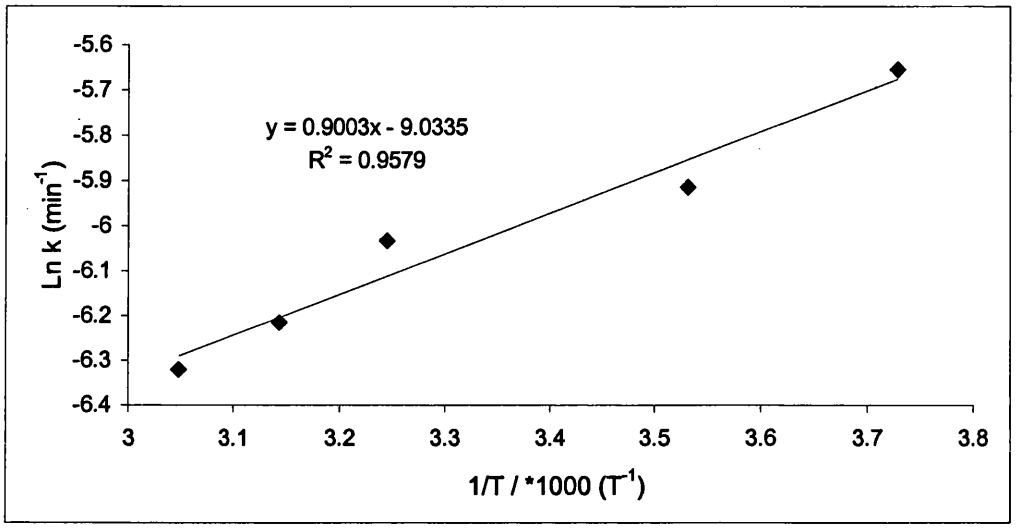

Graph 3.5 Arrhenius Graph for DPPH in o-xylene sonicated at an intensity of 23.8 ± 1.72 Wcm^{-2}.

Therefore the activation energy for the system can be calculated to be –7.49 $kJmol^{-1}$. This is a typical occurrence for a reaction performed using ultrasound, the reaction apparently occurring at a faster rate at a lower temperature, giving a negative activation energy for the system. This feature of sonochemical processes has been reported by a number of workers [54,149,150] and can be explained by the fact that the vapour pressure decreases at lower temperatures therefore cavitational collapse is more violent [1].

Attempts to quantify the rate of radical production (for an ultrasonic reaction) and relate it to the Arrhenius equation have given rise to equation 3.4. This equation was put forward by Kruus et al. [54] who suggested that the maximum temperature reached within the collapsing cavitation bubble should be used in the Arrhenius equation rather than the bulk liquid temperature. If reversible adiabatic

collapse is assumed then reasonable correlation has been achieved for the consumption of DPPH [54].

$$\ln(k) = \ln(A) - \frac{E_a P_v}{RT_0 P_A(\gamma - 1)} \tag{3.4}$$

Where k is the rate constant, A is the Arrhenius factor, E_a is the activation energy, R is the gas constant, T_0 is the reaction temperature, γ is the ratio of the heat capacities within the bubble, P_v and P_A are the vapour pressure of the solvent and the acoustic pressure at the initiation of collapse respectively. Using this equation and setting P_A to 1 atm. a value for the activation energy is calculated to be 25.07 ±2.96 kJmol^{-1}. However, the calculated activation energy is linearly dependent upon the value for the acoustic pressure generated at the point of bubble collapse. It has been suggested that P_A [16] is likely to be an order of magnitude or more, higher. If P_A is set to 10 atm. then the activation energy increases to 250 ±29.6 kJmol^{-1}.

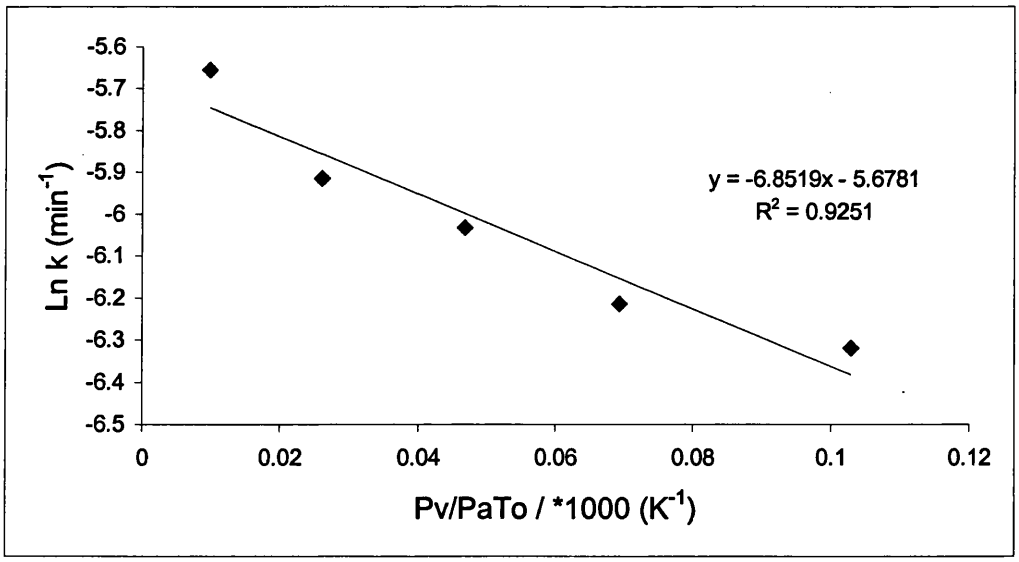

Graph 3.6 A plot of Ln k against $P_v/(P_A T_o)$ for the derived Arrhenius equation 3.4.

The value calculated for the activation energy, using the amended Arrhenius +25.07 ±2.96 kJmol^{-1}, is between the published values by Kruus et al. [54] (8

$kJmol^{-1}$) and Lorimer et al. [148] (76-140 $kJmol^{-1}$). This can be accounted for by the choice of the experimental conditions. Kruus chose to sonicate DPPH in methyl methacrylate between -17°C and +40°C. and to use a value of 1atm for equation 3.4. Whilst Lorimer studied a number of solvents, from 1,2,4-trichlorobenzene to toluene between the range of 125°C and 156°C, but did not report what value for the acoustic pressure was used in their calculations.

The apparent negative activation energy when the Arrhenius equation is used and the difference when the modified Arrhenius equation is used can be attributed to the overall reaction scheme. When the consumption of DPPH occurs in a thermally activated reaction the activation energy observed is equal to the thermal rate constant, equation 3.5.

$$E_{A(observed)} = E_{A(thermal\ reaction)} \quad (3.5)$$

In this case the Arrhenius equation is still valid. However, when the reaction is performed using ultrasound an additional factor comes into equation 3.5. If it is assumed that two concurrent processes take place, the conventional thermal reaction and the ultrasonic process then the observed activation energy will be given by equation 3.6.

$$E_{A(observed)} = E_{A(thermal\ reaction)} + E_{A(ultrasonic\ reaction)} \quad (3.6)$$

It is the addition of this extra factor that causes the breakdown of the Arrhenius equation arising from the unknown temperature i.e. the bulk temperature or the temperature reached upon bubble collapse, and pressures i.e. the magnitude of P_{max} reached at the end of bubble collapse, to be substituted into the Arrhenius equation.

Equation 3.4 also assumes reversible adiabatic bubble collapse, which given that there is no gas flowing through the solvent so that transient cavitation is the major type of cavitation is a valid assumption. However, there is the possibility

that irreversible collapse could occur, i.e. stable or resonant cavitation. Therefore, in such conditions equation 3.7 would be valid.

$$\ln k = \ln(A) - \left(\frac{P_v C_p}{P_{max}}\right)\left(\frac{E_a}{R^2 T_0}\right) \qquad (3.7)$$

Where C_p is the heat capacity of the vapour in the bubble, P_v is the liquid vapour pressure (assumed to be the pressure at the start of the bubble collapse), P_{max} is the pressure at the end of the bubble collapse. A graph of ln *k* against $P_vC_p/P_{max}T_o$ can be plotted using the same values as previously and the heat capacity of the cavity contents (primarily monomer vapour) as 100 $JK^{-1}mol^{-1}$ by analogy to similar compounds [54] and is shown in graph 3.7.

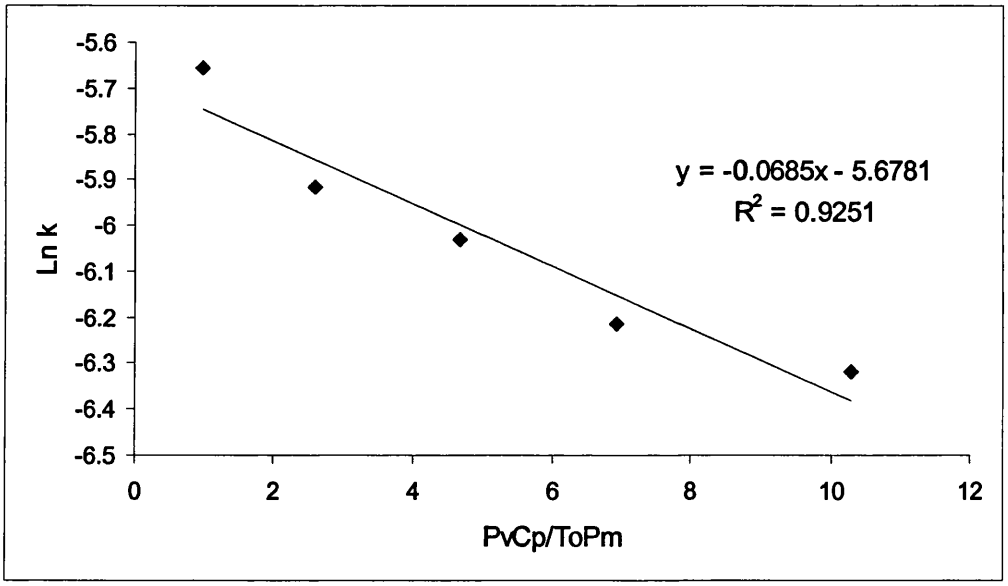

Graph 3.7 A plot of Ln *k* against $P_vC_p/P_{max}T_o$ for the derived Arrhenius equation 3.7.

Using this relationship a value of +4.74 $kJmol^{-1}$ is found for the activation energy. Again, as with equation 3.4 the value for the activation energy is linearly dependent upon the value assumed for P_{max}.

What is apparent from using the Arrhenius equations to describe the sonication of DPPH in a solvent is that a straightforward relationship between the temperature measured and the temperature and subsequently, the pressure values required to substitute into the Arrhenius equations are not obeyed.

3.2.2 Sonication of DPPH in o-xylene with AIBN

Using the conventional Arrhenius equation, the addition of 0.1w/v% AIBN has a remarkable effect upon the Arrhenius graph, shown in graph 3.8.

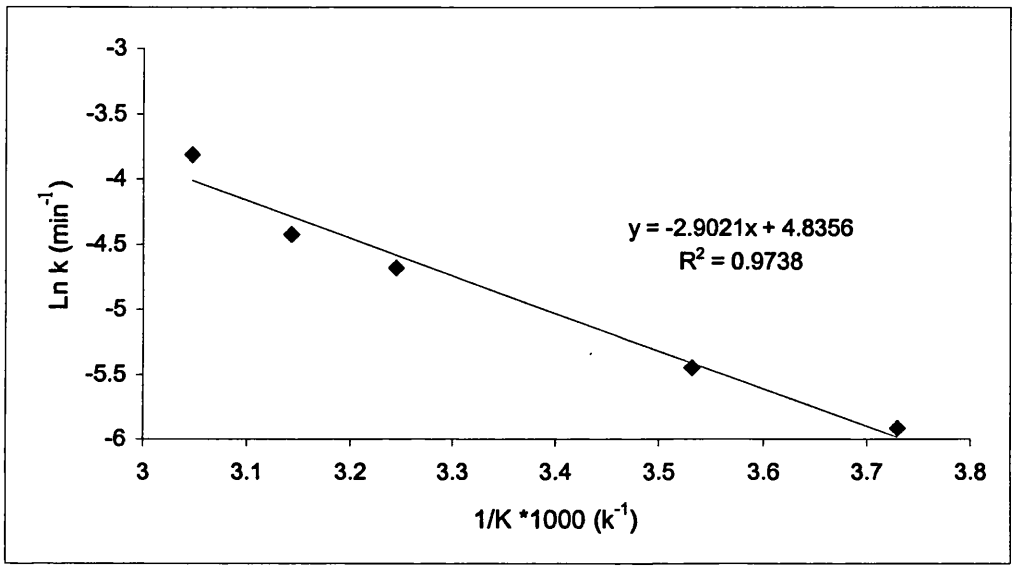

Graph 3.8 Arrhenius graph for DPPH in o-xylene with 0.1w/v% AIBN sonicated at an intensity of 23.8 ± 1.72 Wcm^{-2}.

This is in contrast to the Arrhenius graph found for the sonication of DPPH alone in o-xylene. The activation energy for the system is calculated, using the conventional Arrhenius equation, to be +24.1±3.35 $kJmol^{-1}$. The change of slope can be attributed to the addition of an extra factor to the overall system. As stated in equation 3.6 the reaction performed using ultrasound introduces an additional factor into the Arrhenius equation. The addition of AIBN causes the addition of yet another factor to be considered, the activation energy for the bond breakage of AIBN, giving equation 3.7.

$$E_{A\ observed} = E_{A\ Thermal} + E_{A\ Ultrasound} + E_{A\ AIBN} \quad (3.7)$$

It is the addition of this factor that causes the break down of the Arrhenius equation. Likewise if the modified Arrhenius equation, 3.4, is used to calculate the activation energy then a breakdown in the relationship also occurs for this equation, as shown in graph 3.9.

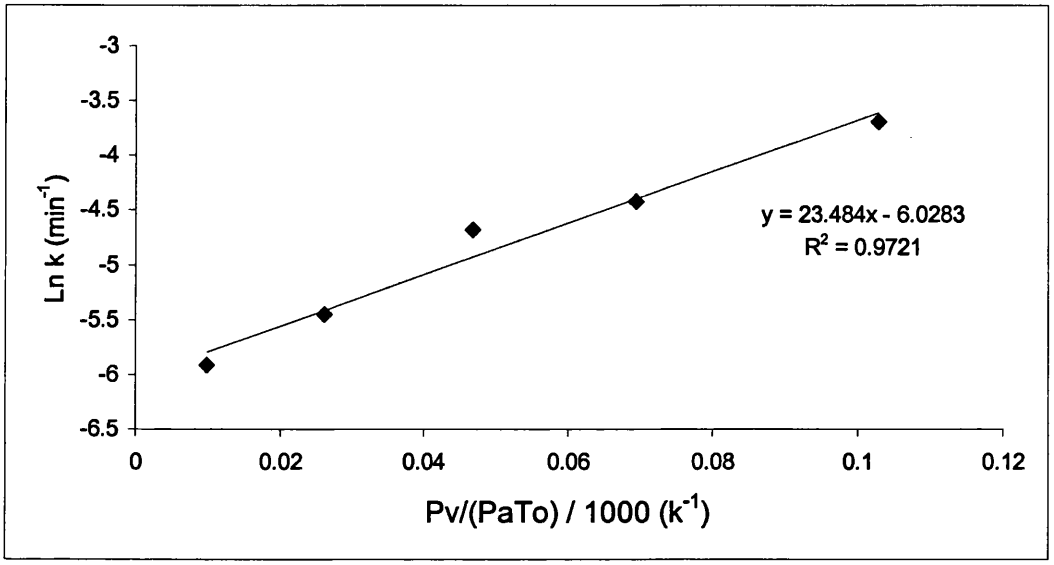

Graph 3.9 Arrhenius graph for DPPH in o-xylene and 0.1%w/v AIBN using equation 3.4.

If equation 3.4 is used to calculate the activation energy then an apparent negative activation energy is found for the reaction –85.91 ±9.79 $kJmol^{-1}$, shown in graph 3.9.

Although the values for the activation energy are not in agreement with published data, see table 3.4, upon closer inspection of the decomposition rates it is found that using ultrasound can accelerate the rate of AIBN decomposition. The sonochemical process at 25°C occurring at the same rate as the purely thermal reaction at 85°C [151, 152], so that the use of AIBN for initiation becomes possible.

Solvent	Temp. range (°C)	E_A (kJmol^{-1})	Reference
Xylene	80	130.96	153
Toluene	50-80	142.26	154
Benzene	49-76	128.45	138
Xylene	56-88	134.31	155
Benzene	60-80	130.96	156
Toluene	50-65	133.89	157
Toluene	70-80	131.38	158
Toluene	90-105	128.03	158
Xylene	90-107	130.12	159

Table 3.4 A sample of the literature values for the thermal decomposition of AIBN.

3.2.3 Sonication of DPPH in o-xylene with BPO

This situation also applies when the addition of 0.1%w/v benzoyl peroxide is included in the system. If the conventional Arrhenius equation is used to calculate the activation energy, a value of +15.36 ±2.17 kJmol^{-1} is calculated, as shown in graph 3.10

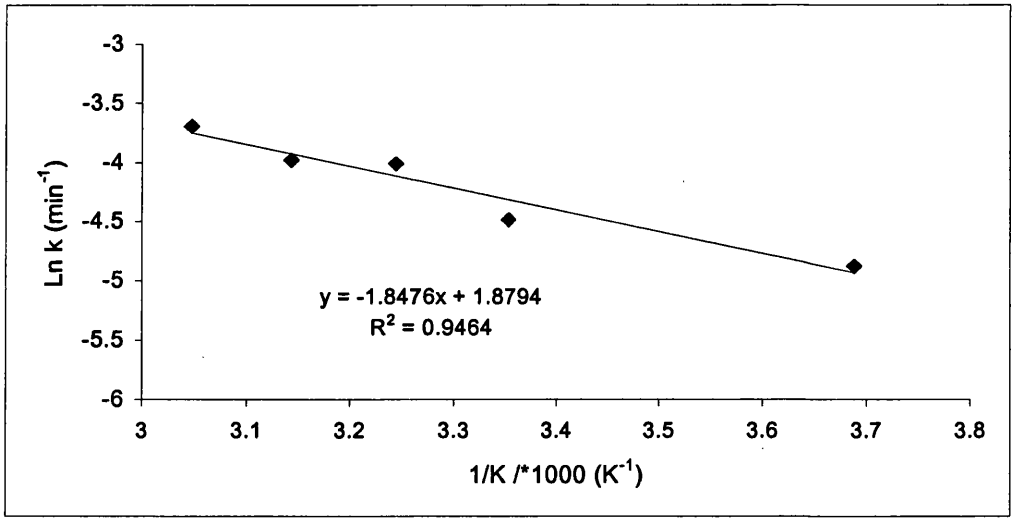

Graph 3.10 Arrhenius graph for DPPH in o-xylene with 0.1w/v% BPO sonicated at an intensity of 23.8 ± 1.72 Wcm^{-2}.

Likewise if equation 3.4 is used to calculate the activation energy then an apparent negative value of -39.75 ±4.67 $kJmol^{-1}$ is found, this is shown in graph 3.11

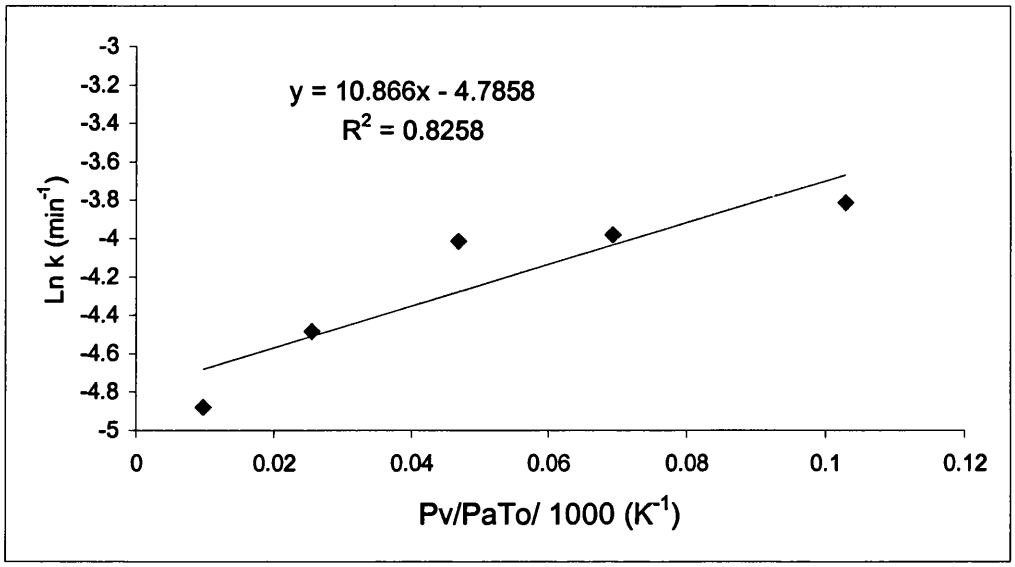

Graph 3.11 Arrhenius graph for DPPH in o-xylene and 0.1%w/v AIBN using equation 3.4

The application of both the conventional Arrhenius equation and the modified Arrhenius equation to the sonication of DPPH with a radical species has shown that a straightforward relationship is not obeyed. This can be accounted for by considering the type of cavitation that occurs within the system, transient and or stable/resonant. Through a combination of both types of cavitation the Arrhenius equations 3.4 and 3.7 used to determine the activation energy, breakdown. Previous published papers have not noted this problem due to the chosen experimental conditions. Kruus [54] choosing to sonicate DPPH in MMA. For that system equation 3.7 is valid, however, upon the addition of an initiator equation 3.7 breaks down. Lorimer [148] chose to sonicate DPPH in a number of solvents again without the addition of an initiator. The measured rate constant is the sum of three rate constants, *k* bond breakage of the solvent, *k* bond breakage of the radical species and *k* bond formation. It is the addition of the *k* bond breakage of the radical species that causes the break down of the Arrhenius equation.

3.3 Radical trapping in a two-phase system.

The experiments were carried out as outlined in section 2.7, using a Sonic and Materials horn operating at a fixed frequency of 23 kHz, with a power output of 23.8 ±1.72Wcm^{-2}. The system was set up using 90cm^{-3} of distilled and de-ionised water, with 10 cm^3 of 1 x 10^{-4}M solution of DPPH added last. The sonic horn was switched on for the desired length of time and the resulting emulsion was cooled in ice and 250cm^{-3} of a saturated sodium chloride solution was added to assist the coagulation and separation of the organic layer. Using this method it was found that the organic layer, containing the DPPH, could be removed and analysed much quicker and more conveniently than centrifugation. The organic layer was then analysed using a Perkin Elmer UV-Visible spectrometer.

A typical graph of the change in absorbance against time is shown in graph 3.12.

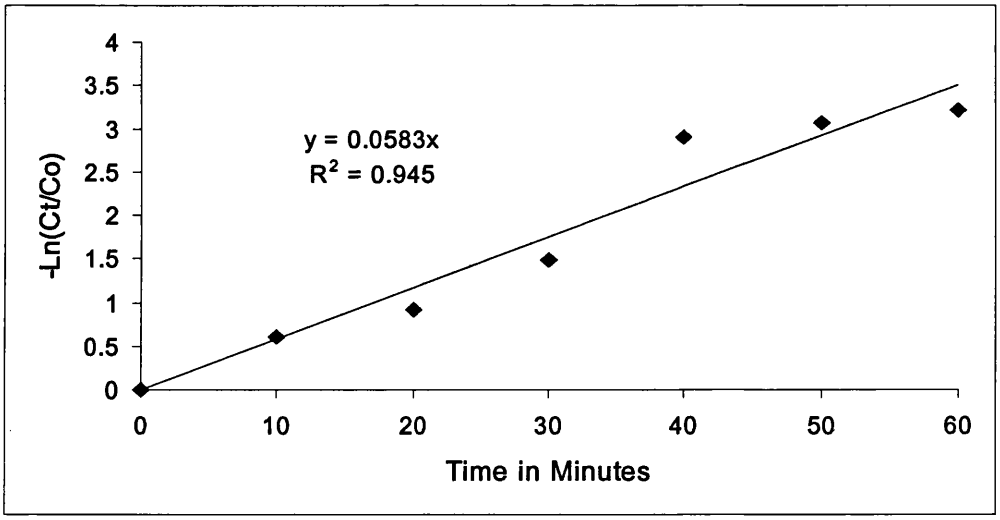

Graph 3.12 Change of absorbance for DPPH in o-xylene and water with time at 35°C sonicated at an intensity of 23.8 ±1.72Wcm^{-2}.

The rate constants for the sonication of DPPH in o-xylene and water are shown in table 3.5.

Temperature (°C ±0.5)	DPPH in o-xylene/water
2	0.0381 ±0.0052
25	0.048 ±0.0037
35	0.0583 ±0.0025
45	0.0661 ±0.0023
55	0.0657 ±0.0025

Table 3.5 Rate constants, min^{-1}, for DPPH in o-xylene and water sonicated at an intensity of 23.8 ±1.72Wcm^{-2}.

Again the same situation applies here as it does to the reactions performed in a bulk solution, the error being less the higher the temperature, due to the difficulty in controlling the reaction temperature below ambient. From these values the Arrhenius graph can now be plotted and the activation energy for the system can be found. This is shown in graph 3.13.

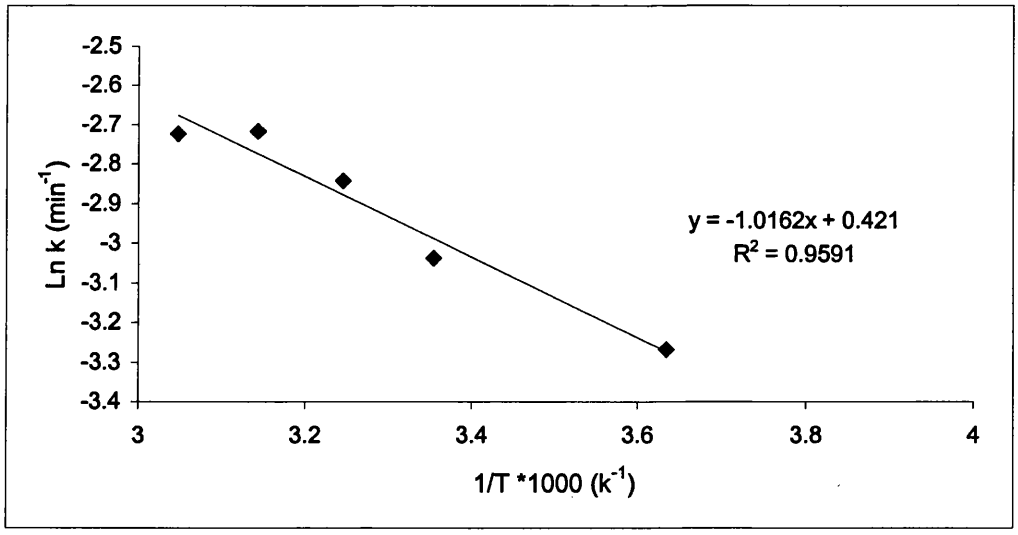

Graph 3.13 Arrhenius graph for DPPH in o-xylene and water sonicated at an intensity of 23.8 ±1.72Wcm^{-2}.

The activation energy is calculated to be +8.45 ±1.59 kJmol^{-1} well below the energy required to break chemical bonds but it is a positive activation energy. This is in contrast to the situation when DPPH is sonicated alone in a bulk reaction, when an apparent negative activation energy is calculated. This can be explained by the simple fact that the reaction is being performed in a two-phase system. With the increase in temperature the surface tension between the two phases decreases, so allowing the DPPH molecules into the aqueous phase. Therefore the reaction with DPPH and hydroxy radicals, produced from the breakdown of water, can occur. The reduction in ultrasonic intensity due to the increase in temperature is offset against the decreased interfacial tension between the two liquids.

If equation 3.4 is used to calculate the activation energy then an apparent negative activation energy of -20.75 ±3.24 kJmol^{-1} is found, this is shown in graph 3.14

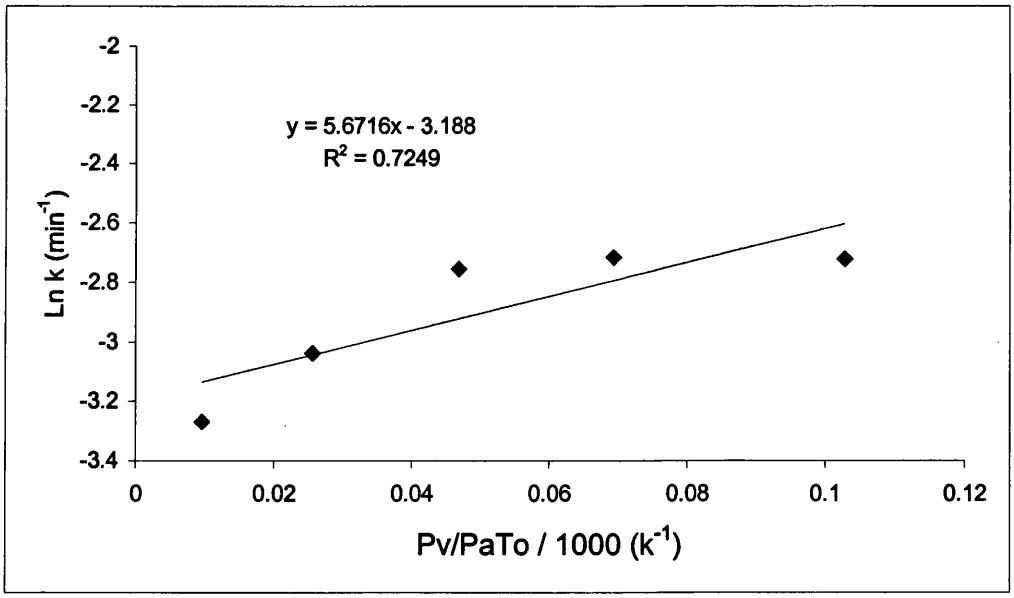

Graph 3.14 Arrhenius graph, using equation 3.3, for the sonication of DPPH in a water/o-xylene system sonicated at an intensity of 23.8 ±1.72Wcm^{-2}.

Once again, it is the addition of an additional factor to equation 3.6, bond breakage of water, that causes the breakdown of the Arrhenius equation and hence a negative activation energy to be calculated.

3.3.1 Radical trapping in a two-phase reaction with potassium persulphate.

As potassium persulphate is an aqueous initiator and is the initiator used in the laboratory preparation of emulsion polymerisations it was chosen to determine the effect it has upon DPPH in solution. Again the system was set up as described in section 2.7, also included was 0.025g of potassium persulphate. The results are shown in table 3.6.

Temperature (°C ±0.5)	DPPH in o-xylene/water + potassium persulphate.
2	0.0398 ±0.0061
25	0.0496 ±0.0034
35	0.0526 ±0.0021
45	0.0541 ±0.0024
55	0.0759 ±0.0028

Table 3.6 Rate constants, min^{-1}, for DPPH in o-xylene and water with 0.025g of potassium persulphate sonicated at an intensity of 23.8 ±1.72Wcm^{-2}.

Using the Arrhenius equation a graph could now be plotted to determine the activation energy for the system. This is shown in graph 3.15.

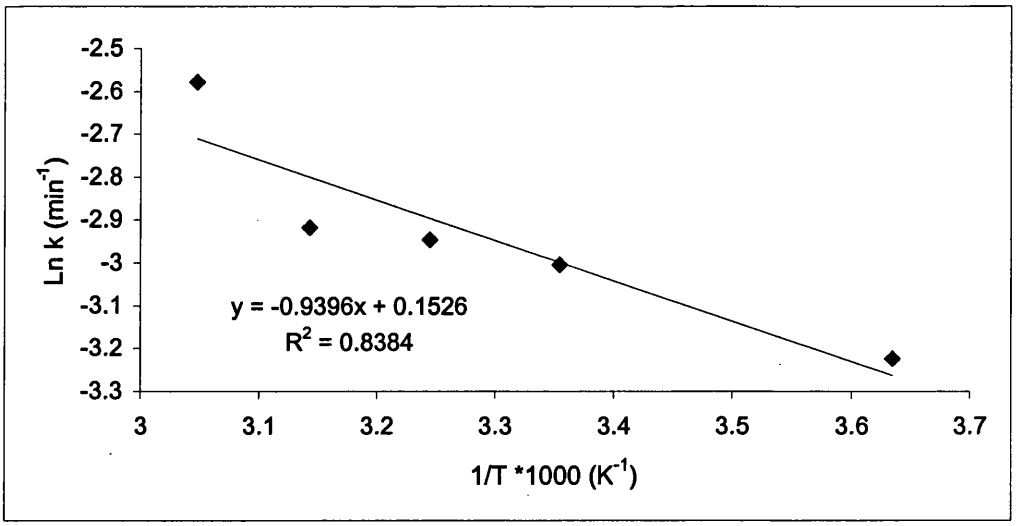

Graph 3.15 Arrhenius graph for DPPH in o-xylene/water with potassium persulphate sonicated at an intensity of 23.8 ±1.72Wcm^{-2}.

This results in an activation energy of +7.8 ±1.82 $kJmol^{-1}$, which is lower than when potassium persulphate is not included into the system. This is surprising given that potassium persulphate is an aqueous phase initiator. In comparison with other trapping reactions [150] the activation energies calculated for this system are very low. Price and Clifton [150] used N-*t*-butyl-α- phenyl nitrone, TBPN, as a radical trap to determine the activation energy of potassium persulphate when in an ultrasonic field. Although they experienced similar problems to this work, the thermal process yielding a value of 121 ±12 $kJmol^{-1}$, whilst the activation energy for the sonochemical process giving an apparent activation energy of –21.1 $kJmol^{-1}$.

However, the activation energies with and without potassium persulphate, within experimental error, can be regarded as the same. This tends to suggest that DPPH either stays in the organic phase and does not cross over into the aqueous phase or if it does go into the aqueous phase then it does not react with the persulphate radical. It is the latter that is the most logical conclusion as the high shear rates that occur upon the collapse of a cavitation bubble will emulsify the solution to an extent where DPPH will be in the aqueous phase.

Again if equation 3.4 is used to determine the activation energy then a value of -22.05 ±4.61$kJmol^{-1}$ is calculated, this is shown in graph 3.16.

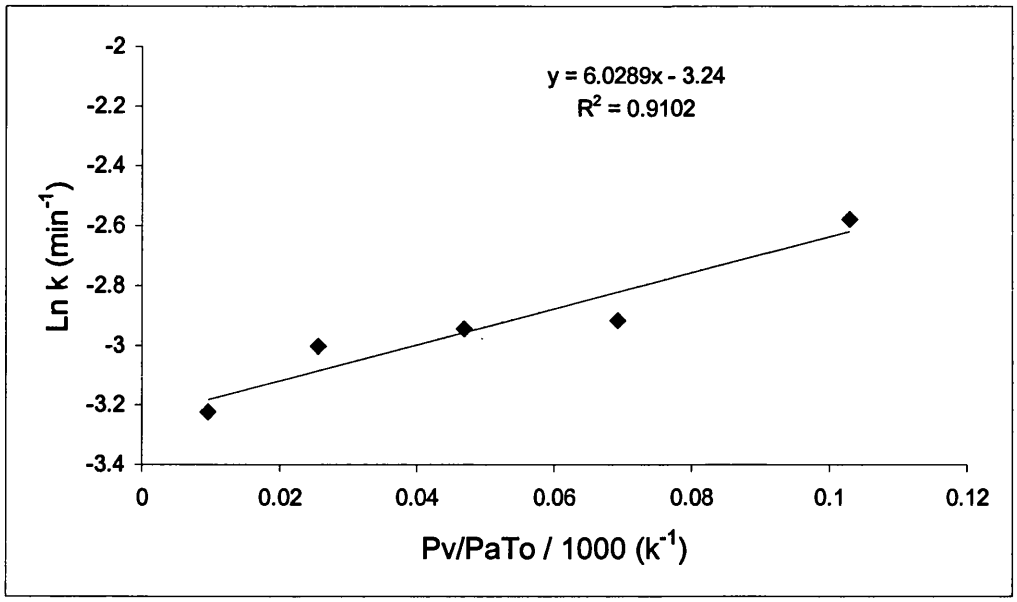

Graph 3.16 Arrhenius graph, using equation 3.3, for the sonication of DPPH in a o-xylene/water/potassium persulphate system at an intensity of 23.8 $\pm 1.72 Wcm^{-2}$.

The radical trapping of DPPH in a two-phase system has agreed with the conclusion from the trapping of DPPH with an organic initiator, that the Arrhenius equation is not obeyed. This is due to the differences in the bulk temperature and the temperatures and pressures found upon bubble collapse. Any attempt to fully describe the activation energy of this system would have to include the collapsing bubble temperature and pressures and the effect of irreversible and reversible bubble collapse.

3.4 Identification of DPPH reaction products via mass spectrometry.

The reactions were carried out as outlined in section 2.6. However, no samples were withdrawn for analysis in the spectrophotometer. This was to ensure that the maximum amount of reaction product would be in the solution, therefore making recovery and subsequent analysis easier. The mass spectra were recorded for a number of different reactions in order to assess the effect the initiator had upon the reaction and to try and elucidate the reaction scheme. Although a number of authors have used DPPH as a way of measuring the rate of reaction there have been no reported attempts at determining the reaction products between DPPH and other radical species.

Mass spectrometry was used to determine the reaction products, as it is the most sensitive and appropriate method for molecular analysis. The method can be broken down into two basic types of ionisation, 'hard' where the ionised molecules have such high internal energy that they fragment before leaving the ion source; the masses of these fragment ions are the basic substructure information used in the interpretation. 'Soft' ionisation minimises such further fragmentation, which is particularly useful, for example, for characterising mixtures. Typical experiments for such methods are electron ionisation for 'hard' ionisation, chemical ionisation and fast atom bombardment for 'soft' ionisation. These and other techniques are summarised in a variety of texts [160, 161].

The first spectrum to be recorded was that of DPPH alone. The chemical ionisation spectra is shown in figure 3.1, with the electron ionisation spectra shown in figure 3.2.

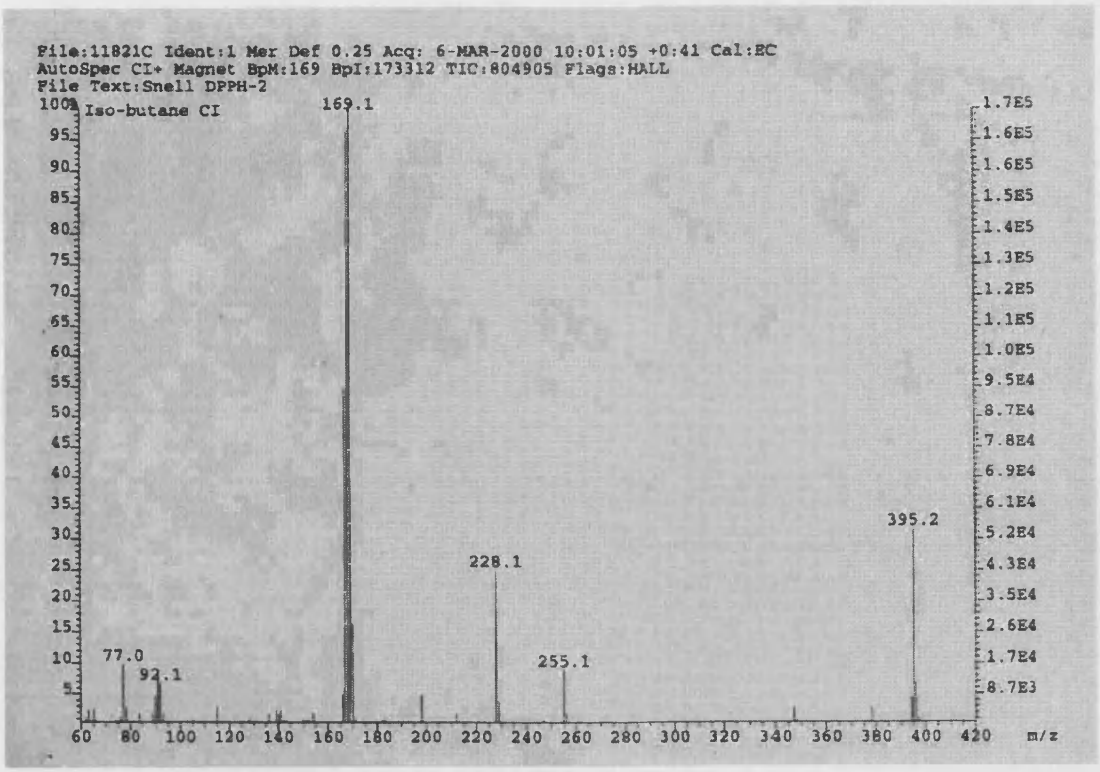

Figure 3.1 The chemical ionisation mass spectrum of DPPH

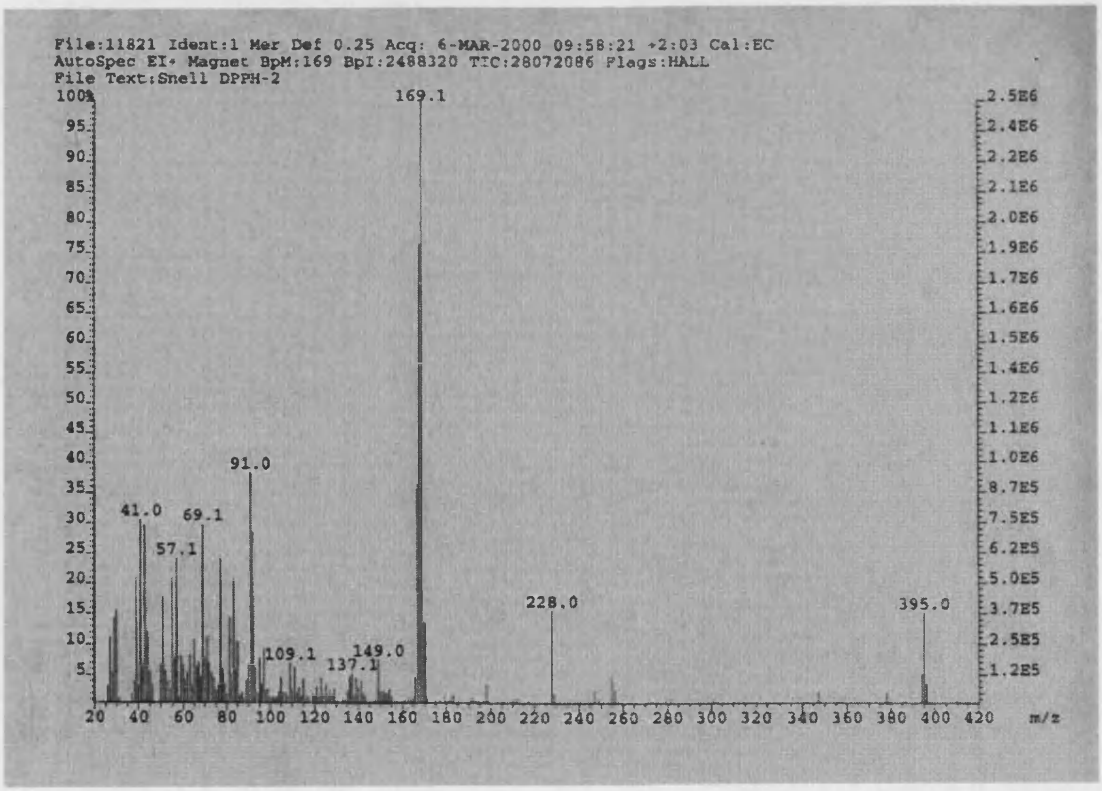

Figure 3.2 The electron ionisation spectra of DPPH.

These spectra are, as expected, straightforward to interpret. The DPPH molecule gives the M+ ion at 395,

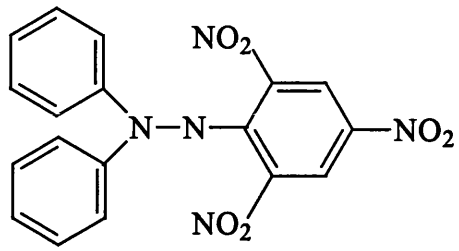

This is the peak at 228

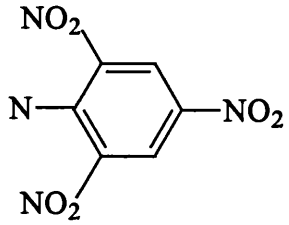

This is the peak at 169.

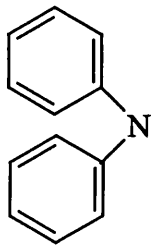

The remainder of the peaks are fragmentations of these ions with the peak at 77 is representative of aromatic rings.

The spectra of DPPH now can act as a reference so that the reactions of DPPH with an initiator can be identified more easily. The sonication of DPPH with 0.1% w/v AIBN in a solution of 1 x 10^{-4} M *o*-xylene was the first reaction to be carried out at an intensity of 23.8 ±1.72Wcm^{-2}. Again the reaction was set up exactly as for the trapping experiments, however, no samples were withdrawn. The mass spectra are shown in figures 3.3 and 3.4 for the chemical ionisation and the electron ionisation respectively.

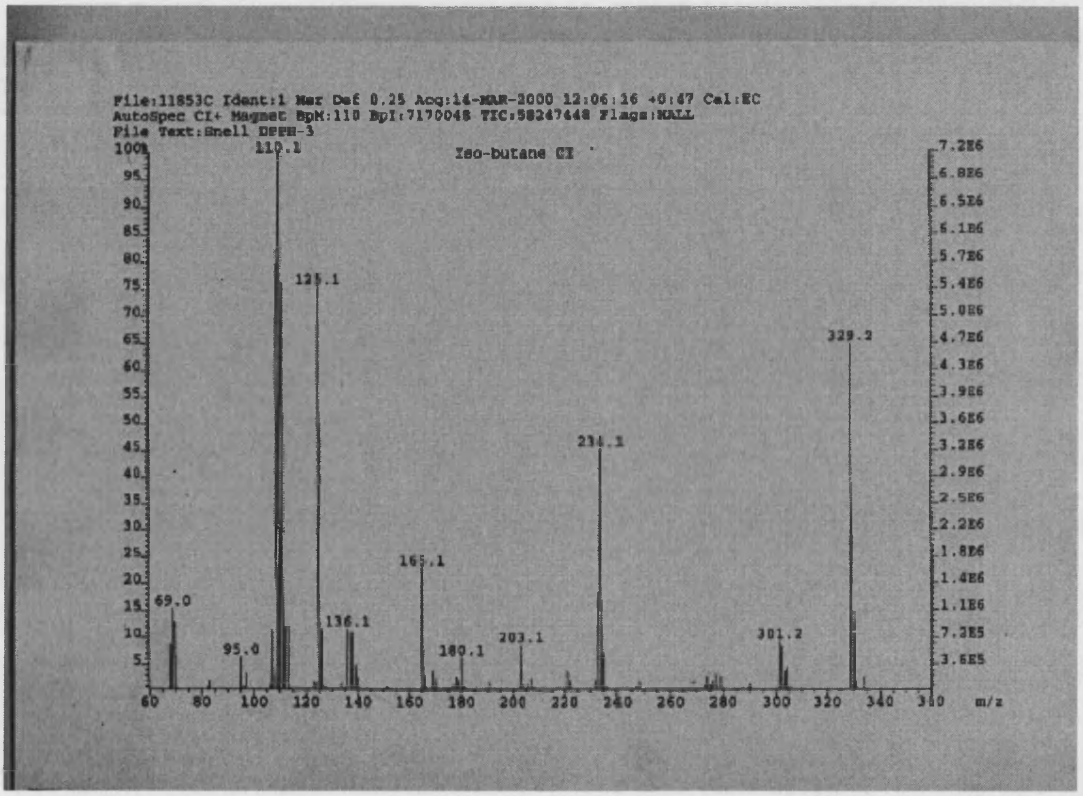

Figure 3.3 The chemical ionisation spectra for DPPH and 0.1%w/v AIBN.

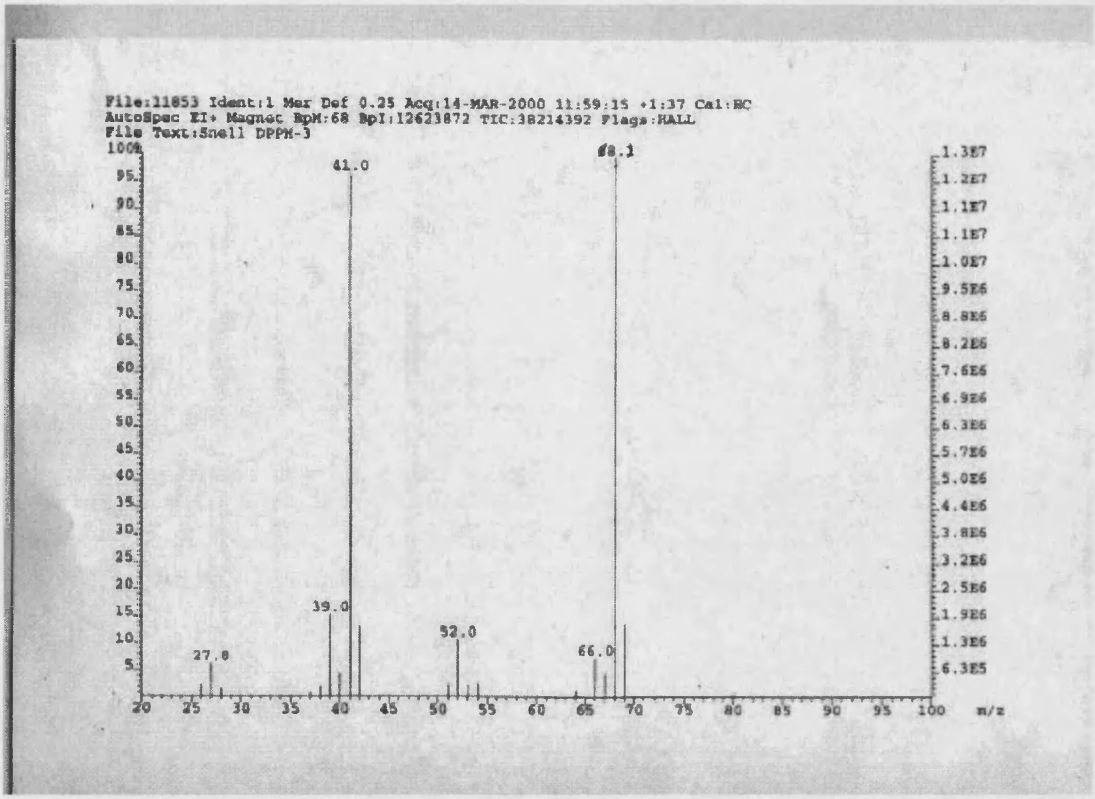

Figure 3.5 Electron ionisation spectra for the sonication of DPPH in *o*-xylene with 0.1%w/v AIBN.

From these two spectra there are only three peaks that are identifiable, these being;

A 'soft' ionisation method was now attempted in order to try and identify a greater number of peaks. Figures 3.6 and 3.7 show the FAB- and FAB+ spectra respectively.

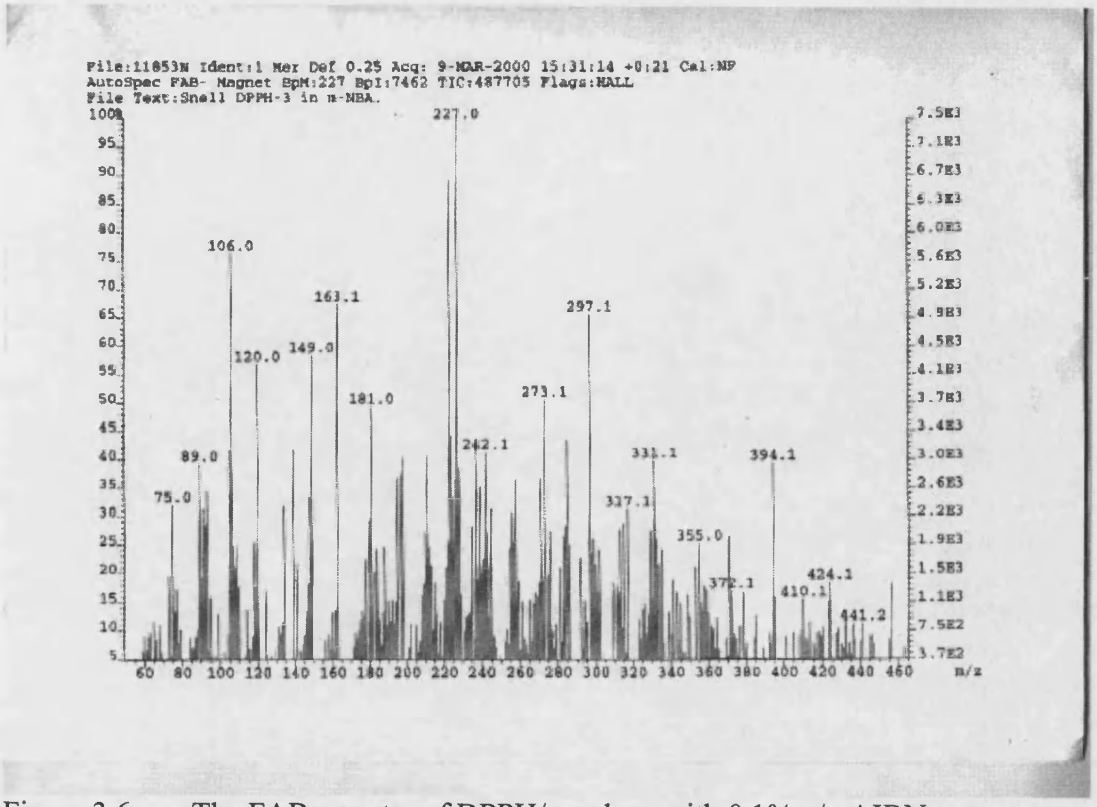

Figure 3.6 The FAB- spectra of DPPH/o-xylene with 0.1%w/v AIBN.

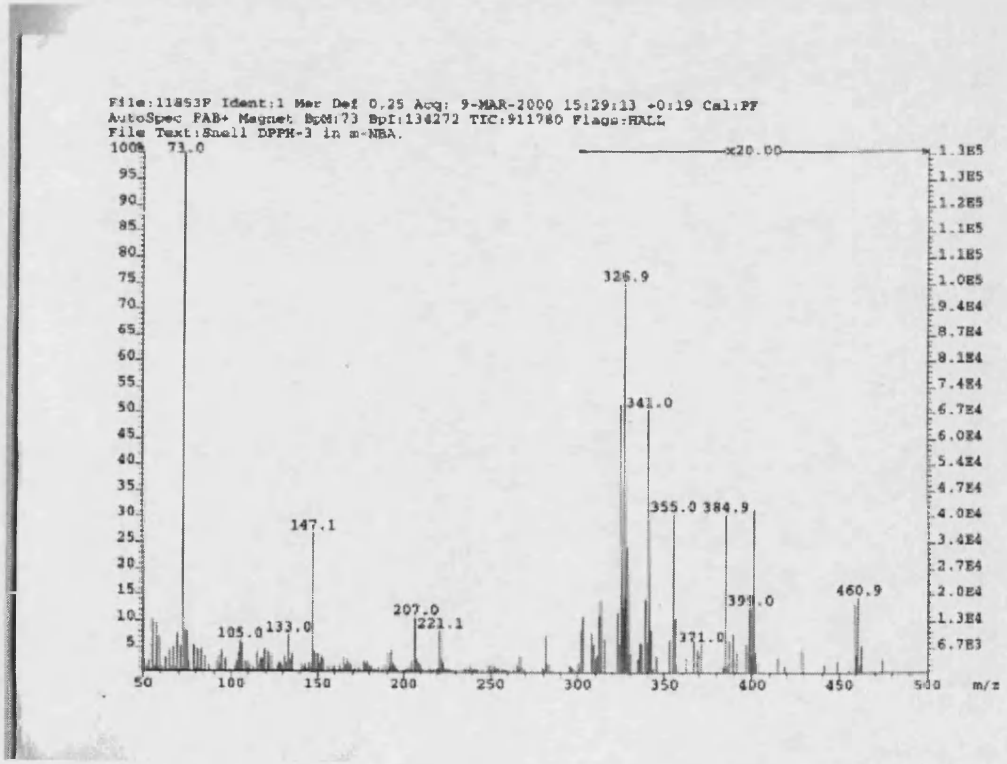

Figure 3.7 The FAB+ spectra of DPPH/o-xylene with 0.1% w/v AIBN.

From the FAB spectra there is further evidence of the reaction of DPPH with AIBN. The following peaks can be assigned as;

spectra is the result of the reaction of DPPH with the AIBN, which is not surprising given the relative concentrations of the two reagents, 1^{-4}M and 6.1^{-4}M, respectively.

The major peaks can be identified as follows;

The second reaction to be carried out was the sonication of DPPH with 0.1 %w/v benzoyl peroxide (BPO). The spectra are shown in figures 3.8, 3.9, 3.10, 3.11 for the chemical, electron, FAB^+, and FAB^- respectively. Fast Atom Bombardment spectra were recorded due to the complexity of the spectra recorded with AIBN and it was hoped that due to the 'soft' ionisation method of FAB then this would yield more information than just CI or EI alone. The spectra are shown below;

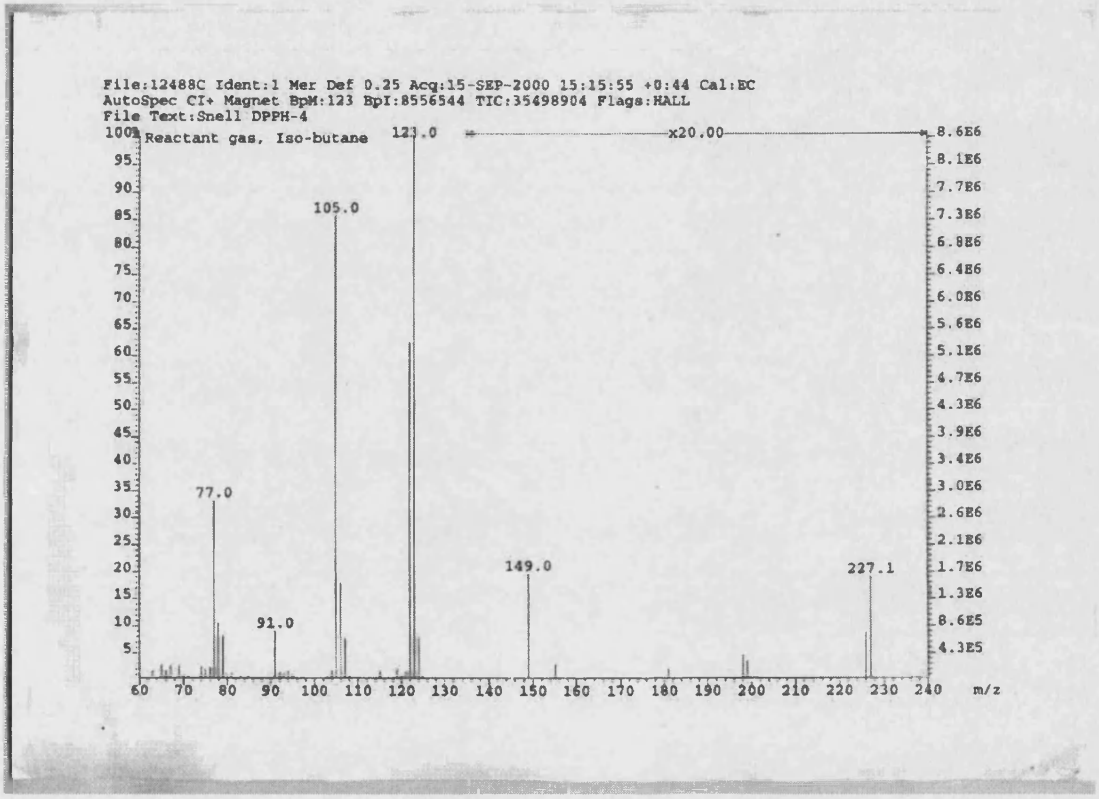

Figure 3.8 The chemical ionisation spectra for the reaction of DPPH/*o*-xylene with 0.1%w/v BPO.

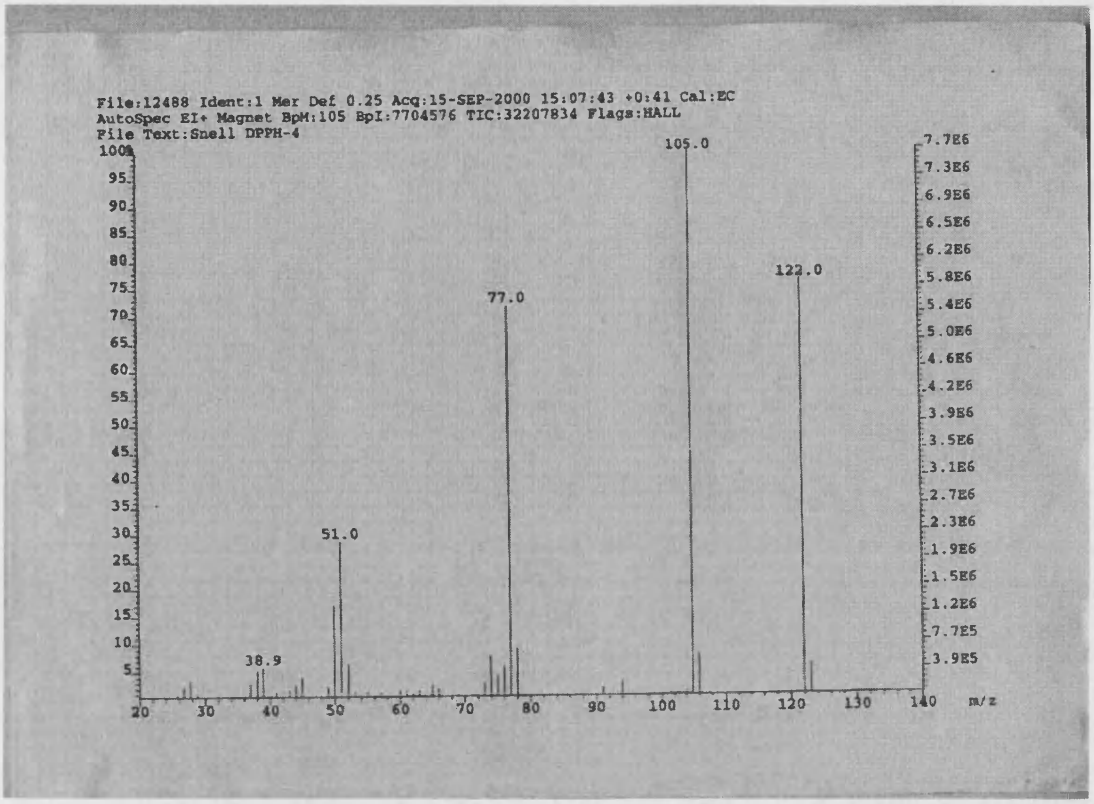

Figure 3.9 The electron ionisation spectra for the reaction of DPPH/*o*-xylene with BPO.

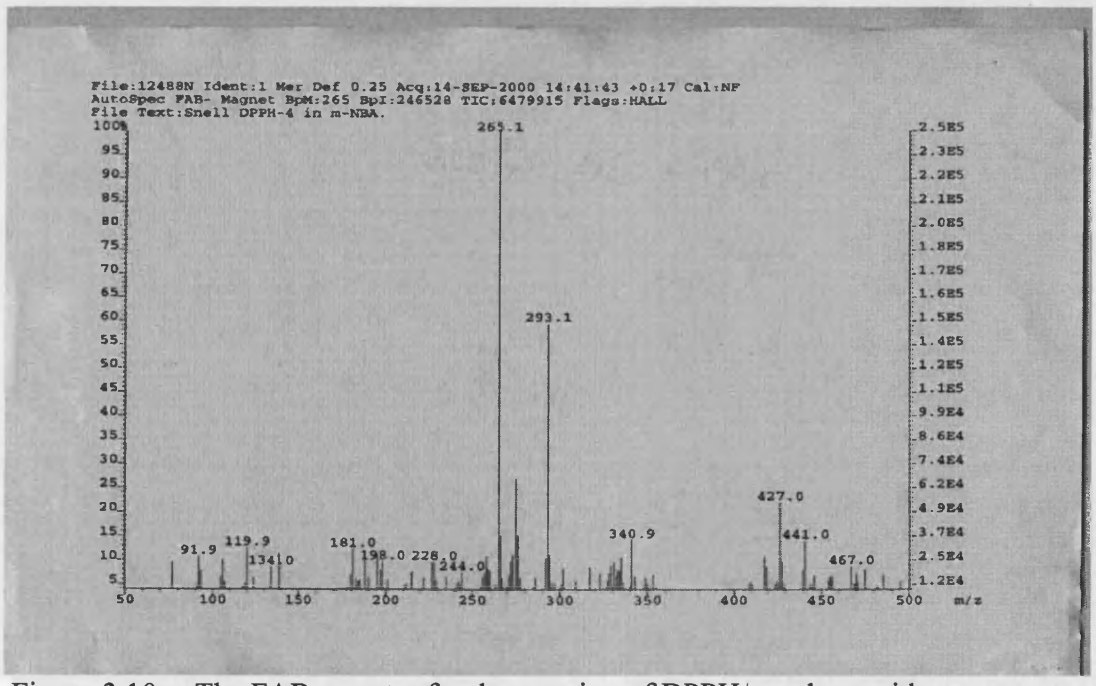

Figure 3.10 The FAB- spectra for the reaction of DPPH/*o*-xylene with 0.1%w/v BPO.

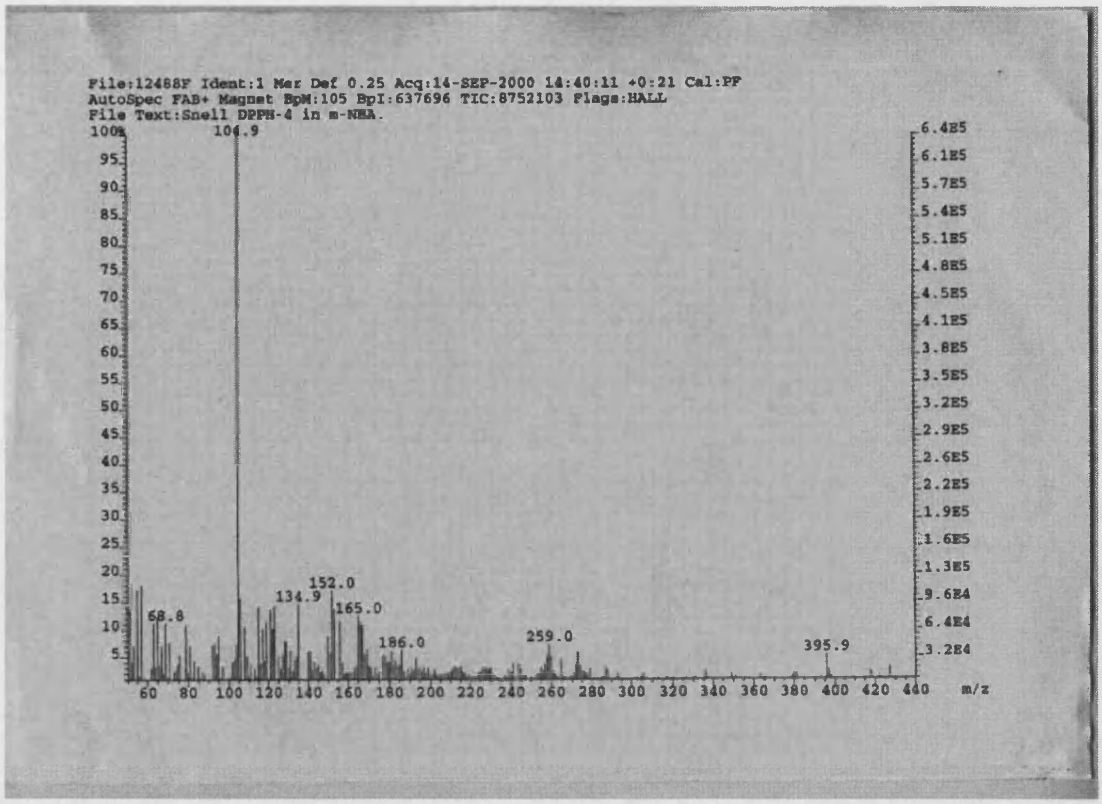

Figure 3.11 The FAB+ spectra from the reaction of DPPH/*o*-xylene with 0.1%w/v BPO.

As in the reaction of DPPH with AIBN the spectra do not many strong peaks that are due to DPPH, demonstrating that the reaction between the two radicals has gone to completion. The major peaks that have been recorded are due to the following ions:

The final reaction to be carried out was the two-phase reaction, water /*o*-xylene and with potassium persulphate could be ascertained. The chemical and electron ionisation spectra are shown in figures 3.12 and 3.13.

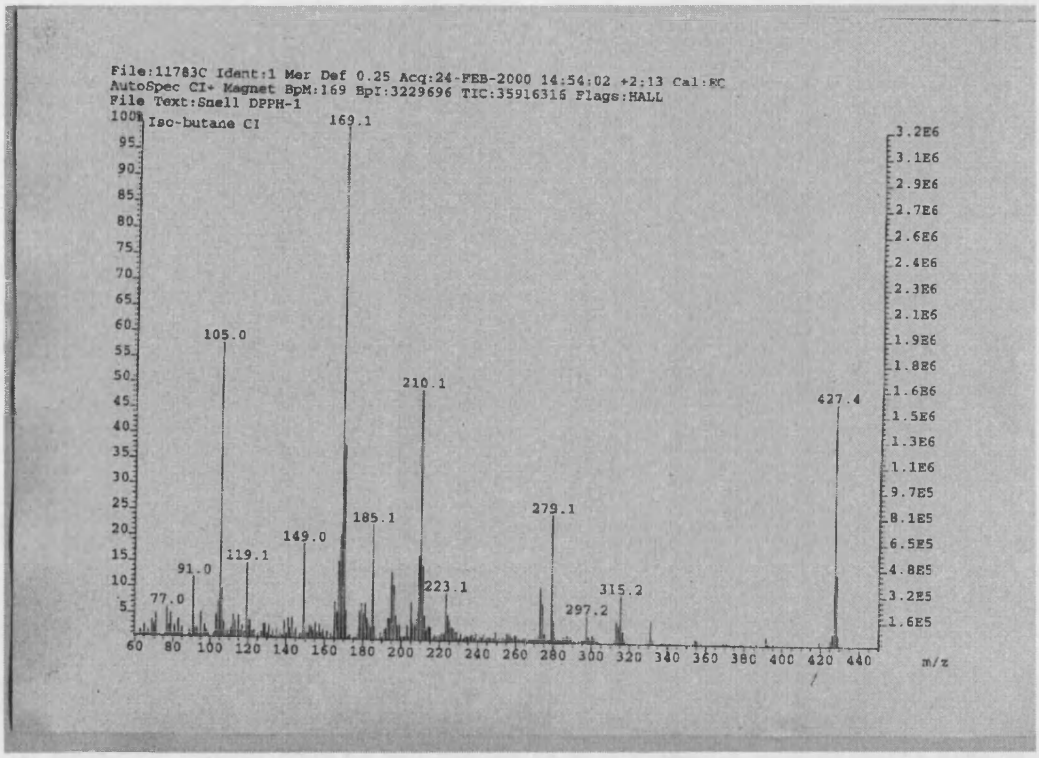

Figure 3.12 The chemical ionisation spectra for DPPH/*o*-xylene/water with 0.025g potassium persulphate.

The

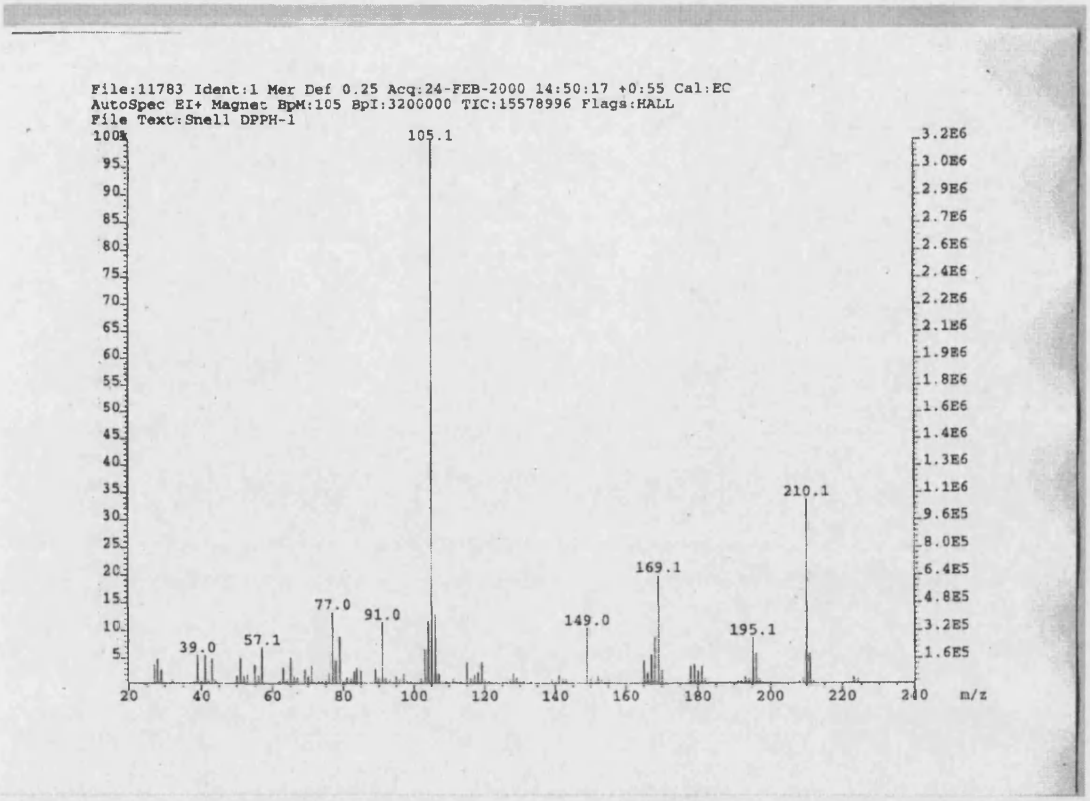

Figure 3.13 The electron ionisation spectra for DPPH/*o*-xylene/water with 0.025g of potassium persulphate.

From these spectra it can be noticed that there is only one easily identifiable peak at 169, in the electron ionisation spectra, from DPPH. The rest of the spectral peaks cannot be identified using this method.

The reactions of DPPH with either AIBN or BPO show that all of the DPPH is consumed in the reaction between the radical trap and the initiator. However, in the reaction containing the aqueous initiator potassium persulphate there are no peaks resulting from the reaction of DPPH with the persulphate radical. This suggests that the use of DPPH as a radical trap for persulphate radicals is not possible.

3.5 Conclusions.

The sonication of a radical scavenger, DPPH, has been carried out at an intensity of 23.8 ±1.72Wcm^{-2} and at a number of temperatures, in order to determine the activation energy. For the sonication of DPPH in *o*-xylene an activation energy of –7.49 ±kJmol^{-1} was calculated using the conventional Arrhenius equation. If a modified Arrhenius equation is used to determine the activation energy then a value of +25.07 ±2.96 kJmol^{-1} is calculated. The sonication of DPPH in a bulk reaction shows a typical behaviour for an ultrasonic reaction, the reaction proceeding faster at a lower temperature. This can be attributed to the decrease in the vapour pressure within the collapsing cavitation bubble.

The organic initiators AIBN and BPO were also reacted with DPPH in *o*-xylene in order to determine the activation energy for each system. Using the conventional Arrhenius equation these were found to be +24.1 ±3.35 kJmol^{-1} and +15.36 ±2.17 kJmol^{-1} respectively. The change in slope for these reactions in comparison with the sonication of DPPH in *o*-xylene can be explained of in terms of the number of factors that go to make up the calculation for the activation energy.

Through the use of the modified Arrhenius equation the activation energy for the sonication of DPPH/*o*-xylene with AIBN and BPO has been calculated as –85.91 kJmol^{-1} and –39.75 kJmol^{-1} respectively. The breakdown of the modified Arrhenius equation is caused by the assumption that only transient cavitation occurs within the reaction. If resonant or stable cavitation occurs then the assumption that the collapsing bubble does some work is not valid and although irreversible collapse can be described the assumption that it is the only type of cavitation is incorrect.

The use of DPPH in a two-phase system has also been attempted. Using both the conventional and the modified Arrhenius equations the activation energy has been calculated. The addition of an aqueous initiator has also been studied. As with the sonication of DPPH in a bulk reaction the Arrhenius equations cannot

describe the reaction and hence cannot be used to calculate the activation energy. This is the first reported attempt to use DPPH as an aqueous phase radical trap.

Therefore further modification to the Arrhenius equation is required before the activation energy can be determined through the use of a radical trap. Modifications would have to include both types of cavitation that can occur within the reaction and include the effect of an additional factor i.e. bond breakage of an initiator.

The reaction product from all of these reactions has been studied using a mass spectrometer. However, due to the limitations upon the type of equipment full separation of the reaction product is not possible. Therefore, it can only be said that the reaction of DPPH with AIBN and BPO goes to completion. Whereas the reaction with potassium persulphate is inconclusive, there appears to be no peaks that indicate the presence of DPPH/persulphate product.

4.0 Emulsion polymerisation of styrene

Emulsion polymerisation offers a number of advantages over a conventional bulk polymerisation. Amongst these it provides a way of exploiting the higher number of radicals generated in an aqueous solution whilst still being able to polymerise water insoluble monomers and from an industrial view point it offers a way of controlling any exotherm that is generated during the polymerisation.

The emulsion polymerisation of styrene is a well-documented system. Indeed styrene was chosen to be an 'ideal' monomer in the study of emulsion kinetics by Smith and Ewart in 1948 [87], through to the most recent advances in the theory of emulsion kinetics by Asua et al in 1996 [162]. This is due to the low solubility of styrene in water (3.6×10^{-3} moldm^{-3} at 50°C [85]) which led to the assumption that styrene is present in the aqueous phase only in micelles or stabilised emulsion droplets. Indeed it was this assumption that led to the Smith and Ewart derived theory, which found favour amongst numerous text until Gardon [89] derived the same theory but by invoking micellar collision rather than diffusion.

As styrene has been studied in an emulsion polymerisation for almost 60 years it was chosen to be the monomer that would be used during this study. In order to assess how effective ultrasound is in creating an emulsion and in monomer conversion, a comparison with a conventional reaction is necessary. Therefore for every ultrasonic reaction a similar conventional reaction will be carried out.

4.1 Polymerisation of styrene

The emulsion polymerisation of styrene was carried out as outlined in section 2.4., using a Sonic Systems P100 horn at an intensity of 10.66 Wcm^{-2}. Although the heating effect of ultrasound is well documented the temperature that was chosen to perform the reactions was 25°C. This represents the balance between the reduction in the vapour pressure entering the collapsing cavitational bubble and the ability to control the reaction temperature.

4.1.1 Comparison of an ultrasonic and conventional reaction – all reagents.

The first reaction to be carried out was described in section 2.5. The resulting monomer conversion against time graph is shown in graph 4.1.

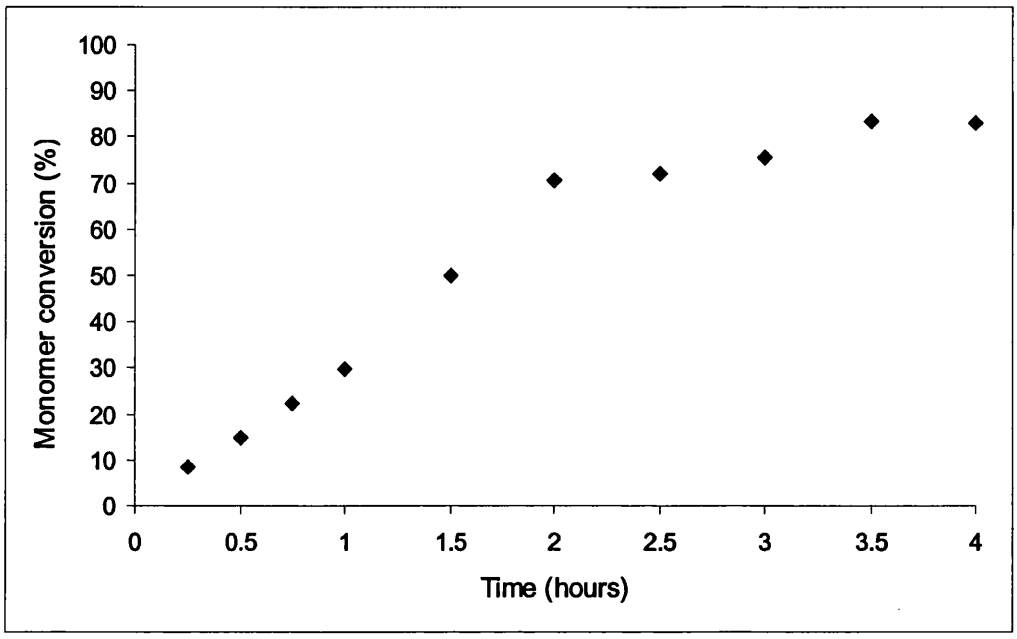

Graph 4.1 Monomer conversion for an ultrasonic reaction at 10.66 ±0.6 Wcm^{-2},25°C.

The total monomer conversion is lower than that first reported by Ostroski and Stambaugh in 1950 [57], 75 % after one hour and much later by Cheung and Gaddam [64], 85 % after two hours, although neither quoted the intensity used during the reaction. Ostroski merely estimated the amount of ultrasonic energy being put into the reaction cell as 100 watts, with an input of 200 watts into the oscillator. This combined with a usable radiating area of $8cm^2$ implies that Ostroski was irradiating the experiments with approximately 12.5 Wcm^{-2}. In both cases elevated temperatures were used 50°C and 40°C for Ostroski, 50°C and 70°C for Cheung , so the monomer conversion could have a significant contribution from the thermal energy as well as the ultrasonic energy.

Due to the compartmentalised nature of an emulsion polymerisation, the initiation step taking place in one phase and the termination step taking place in another the average molecular weight is of great interest. Typically the average molecular weight of a solution polymerisation is about 200kDa, this can increase

five fold for an emulsion polymerisation [163]. The plot of weight average and number average molecular weight is shown in graph 4.2.

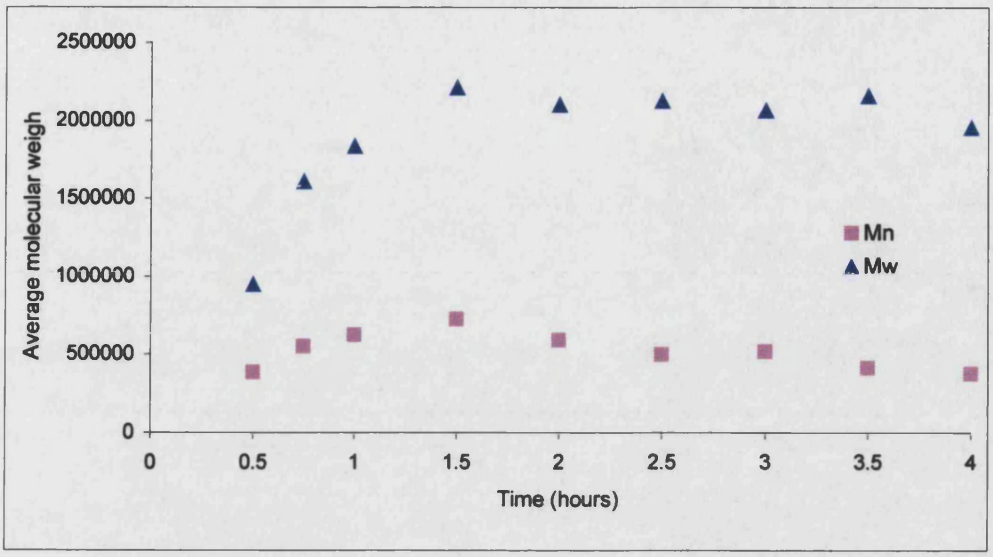

Graph 4.2 Average molecular weight for the ultrasonic polymerisation of styrene at 10.66 ±0.6 Wcm^{-2}.

Given that a typical molecular weight from an emulsion polymerisation is $1x10^6$ the polymer produced here is almost twice that value. This caused significant problems when processing the polymer including filtering the polymer and passing the polymer through a column. Indeed, analysis carried out at Smith and Nephew was curtailed when two columns were blocked whilst analysing samples that had been previously been passed through a 0.2μm filter.

In comparison with a conventional reaction ultrasound can have a twofold effect upon the reaction scheme, i.e. an increase in the radical concentration and an increase in the rate of formation of the emulsion. An increase in the radical concentration will increase the termination rate and hence decrease the chain length. This is not in evidence here. An increase in the rate of formation of the emulsion should lead to a higher monomer conversion for any given time point, again this is not in evidence here. So the process that is occurring here must be related to the application of ultrasound. As stated in chapter 1 the collapse of a cavitation bubble will lead to not only localised high pressures and temperatures being generated but to high shear rates as the surrounding liquid moves to fill the

void. It is this process to cause the polymerisation to proceed via a droplet nucleation pathway rather than micellar nucleation that results in the much higher molecular weight and the reduced monomer conversion in comparison with a conventional reaction at 75°C. In switching to a droplet nucleation pathway the radicals generated in the aqueous phase can enter the monomer droplets as single radicals and propagate to form particles. This mechanism is considered to be predominant in both mini-emulsions and micro-emulsions [163,164]. In comparison with a micro and mini emulsion polymerisation of styrene [165] the monomer conversion and the molecular weight data are very similar for a number of reasons: 1) the molecular weight distribution in a microemulsion is very broad (typically 4-6), 2) due to the high shear rates monomer swollen micelles are available to act as nucleation sites so allowing continuous nucleation to occur.

There are a number of published methods for calculating the rate of polymerisation, from the derivative of the third order polynomials used to fit the conversion time data [58], to using the rate of change of monomer conversion per unit time [166]. It is the latter method that is used to calculate the rate of polymerisation in this study.

If the rate of polymerisation is analysed for an ultrasonic reaction then it can be seen that there is a gradual increase until two hours into the reaction, after which the polymerisation rate decreases. This is shown graphically in graph 4.3.

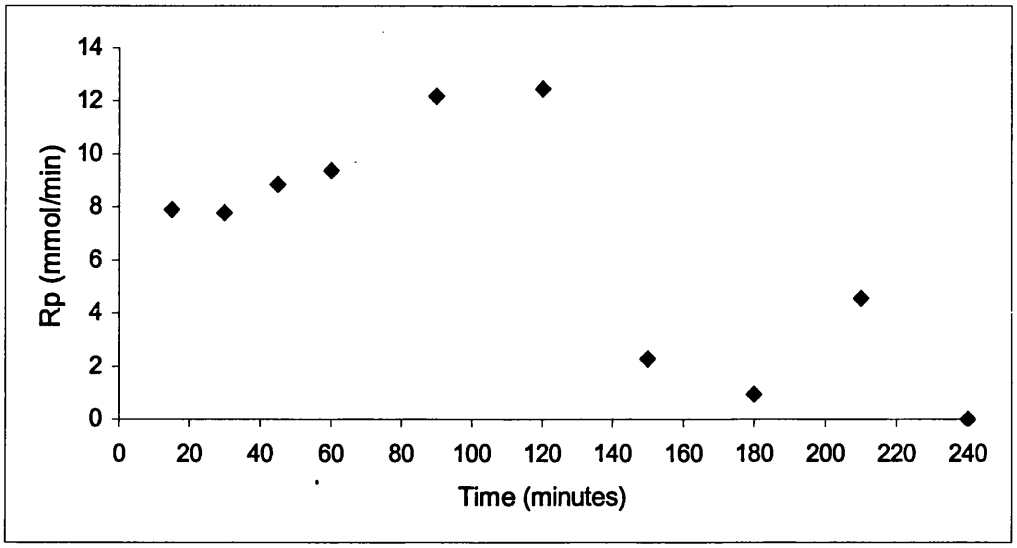

Graph 4.3 The rate of polymerisation in $mmolmin^{-1}$ for an ultrasonic reaction at 10.66 ±0.6 Wcm^{-2}.

Ooi and Biggs [58] calculated the rate of polymerisation by the derivative of the third order polynomial used to fit the conversion time data. Using this method a quadratic equation is obtained which when used to fit the conversion data will give a curve. They concluded that this is indicative of droplet nucleation rather than monomer-swollen nucleation. The rate of polymerisation determined in this study although not giving a curve is typical of a micro emulsion type system i.e. droplet nucleation rather than monomer swollen nucleation [165,167]. The low rate of polymerisation and the minimal change in the rate can be explained by considering the rate of formation of new growing particles and the rate of termination of growing particles. Initially the rate of formation of new growing particles is much higher than the terminating rate of the growing particles. After time the terminating rate will equal the nucleating rate and so the number of growing particles will acquire a balance value. If the polymerisation loci are still saturated with monomer the polymerisation rate will be relatively unaffected. So it will be the number of growing polymer particles being kept constant rather than the total number of polymer particles.

Although the emulsion polymerisation of styrene is a well-researched system in order to compare the effect of ultrasound the same concentrations of reagents were polymerised but using what can be termed 'silent' or 'conventional' conditions. The method is described in section 2.5.3, with the temperature set to 75°C. The graph of monomer conversion against time is shown in graph 4.4.

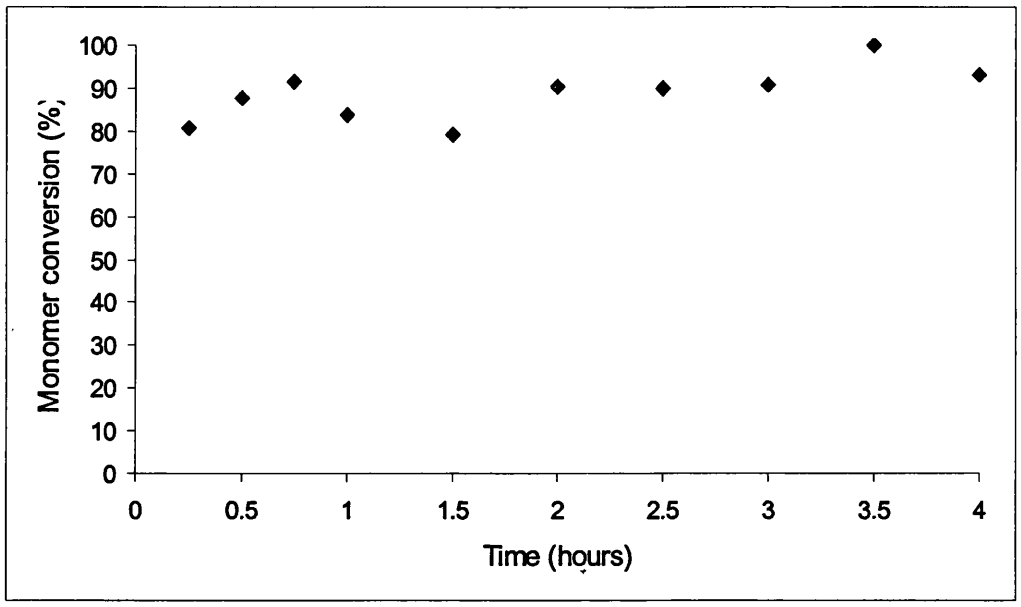

Graph 4.4 Monomer conversion for a conventional reaction at 75°C.

It is immediately apparent that the reaction when performed at 75°C is much faster than that of an ultrasonic reaction at 25°C. This can be attributed to the rise in temperature. Although ultrasound has been calculated to produce extremes of pressure and temperature [13] these extremes are very localised. However, the effect can be seen in a gradual rise in temperature of the system. The increase in temperature effects not only the rate of reaction but it affects the rate of radical formation, the rate of collision between a radical and a micelle and hence the chance of a radical being captured by a micelle.

The increased rate of radical production and capture by the micelles can be seen from the molecular weight data, as shown in graph 4.5

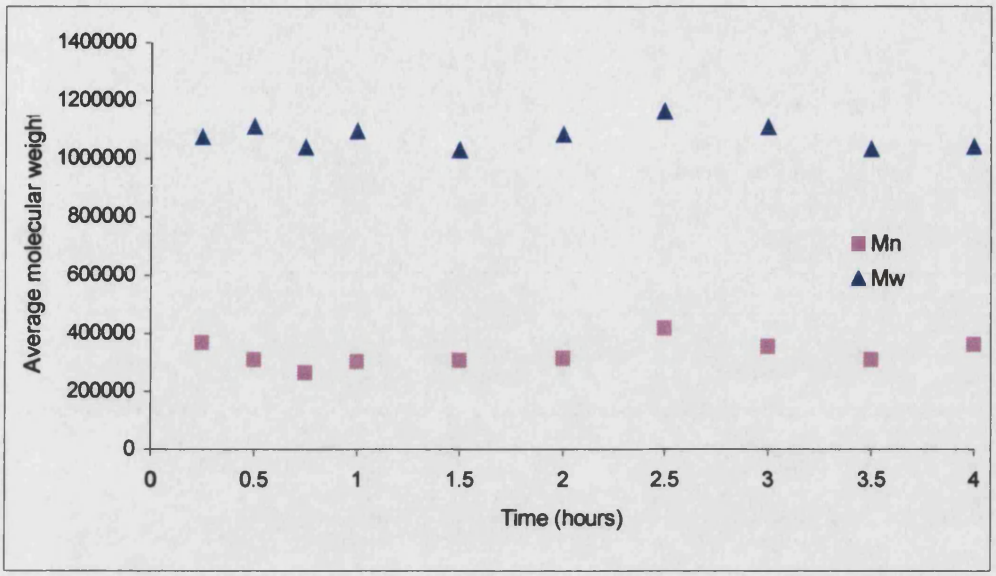

Graph 4.5 Average molecular weight for the emulsion polymerisation of styrene at 75°C.

If the rate of radical production were similar to that in an ultrasonic reaction then the molecular weight would be much higher. This is due to the complex nature of an emulsion polymerisation, a growing polymer chain inside a micelle contains only one radical, if the concentration of radicals is increased then the chance of another radical entering a micelle also increases. The result of two radicals in a micelle is termination of the growing polymer chain, hence the reduction in the molecular weight. The fact that more polymer is produced can be attributed to twice the number of particles being in the system, see section 4.4. Therefore, although the total monomer is the same, there are twice as many particles for the monomer to be absorbed by and thereby not only reducing the chance of a termination reaction occurring but also the molecular weight.

The rate of polymerisation for a conventional reaction at 75°C is not typical of a styrene emulsion polymerisation, i.e. there are no definitive three stages of polymerisation. The graph of the rate of polymerisation against time is shown in graph 4.6.

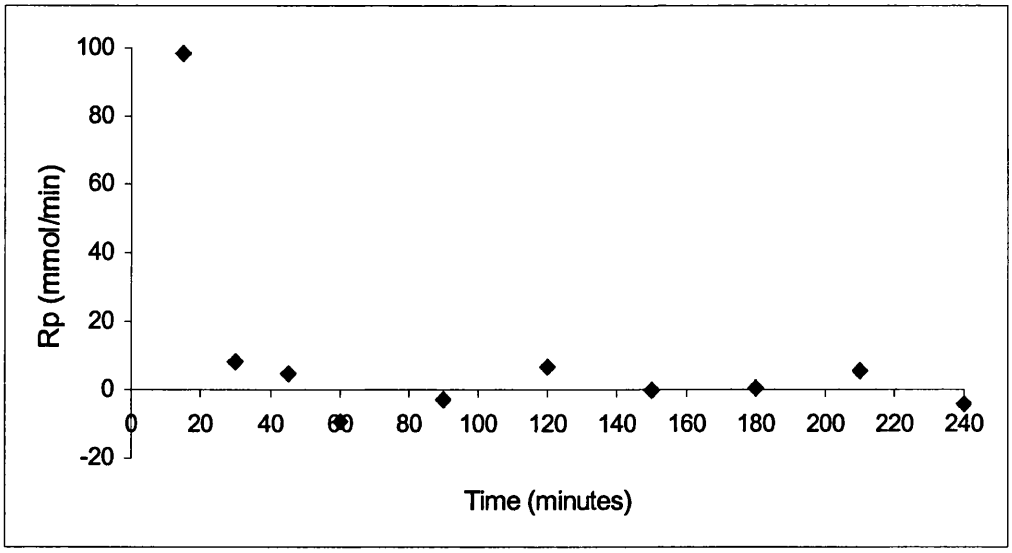

Graph 4.6 The rate of polymerisation in $mmolmin^{-1}$ for the conventional reaction performed at 75°C.

The discrepancy between the rate of polymerisation for this study and that for a classical emulsion polymerisation of styrene [164] can be explained by;

i) Generation of the particle nuclei does not cease beyond the classical Smith-Ewart interval I due to the mixed mode of the particle nucleation, micellar and homogenous nucleation.

ii) The range of constant polymerisation rate region, Smith-Ewart interval II will become narrower increasing the temperature from 50 -75°C [166].

iii) Polymerisation operated at higher temperature (>60°C) does not obey the Smith-Ewart case 2 kinetics (where the average number of free radicals per particle equals 0.5) [166]. In this case, the reaction system can be described by Smith-Ewart case 1 kinetics () <0.5).

Using equation 4.1 and literature values for k_p the propagation rate constant, $[M]_p$, the monomer concentration in the latex particles and the experimentally determined values for the number of latex particles per unit volume in section 4.4, N_p then the average number of radicals per particle can be determined.

$$R_p = k_p [M]_p ()N_p/N_A) \qquad (4.1)$$

Where N_A is Avogadro's number. Using equation 4.1 then the average number of latex particles per unit volume can be determined to be 0.048 for the majority of the polymerisation and only 0.57 for the very high rate of polymerisation at the start of the reaction. The population of inactive particles containing no radicals in the reaction system becomes larger, thereby leading to a reduction in $\rangle$.

Another contributing factor for the low value of $\rangle$, is the increased desorption of radicals out of the latex particles with temperature. The desorption mechanism involves transfer of activity of a macro-radical to monomer, followed by diffusion of the mobile monomeric radical to the particle surface. The relatively water-soluble species may cross the interface into water. The radical exit is complete by diffusion of the monomeric radical to the bulk aqueous phase. The desorbed radical may be reabsorbed into another particle or terminated with an oligomeric radical in the aqueous phase. The small size of the latex particles, see section 4.4, means that there is greater probability for the monomeric radical generated by the chain transfer reaction to diffuse from the particle phase into the aqueous phase.

4.1.2 Comparison of an ultrasonic and conventional reaction – No surfactant.

A number of authors [58,61,62] have reported that through the use of ultrasound an emulsion polymerisation can proceed without any added surfactant. The high shear rates that are created by an ultrasonic field are sufficient to create and sustain an emulsion. It is unclear though if the source of radicals necessary to initiate the polymerisation are from the formation of styrene radicals within a cavitation bubble, or whether it is the primary radicals formed from the cleavage of water i.e. H•, OH•, which act as the initiating species. The presence of dissolved styrene in the aqueous continuous phase implies that that its presence inside any cavity cannot be discounted although its effective concentration will be low, total concentration is 5 %v/v. It therefore seems more probable that it is the radicals generated by the cleavage of water that will contribute primarily to the initiation of the polymerisation.

Therefore in order to assess these reports the apparatus was set up as for an ultrasonic polymerisation. However, the surfactant concentration was changed from 1g to 0.5g and then finally omitted, but keeping all other parameters identical. The graph of monomer conversion is shown in graph 4.7.

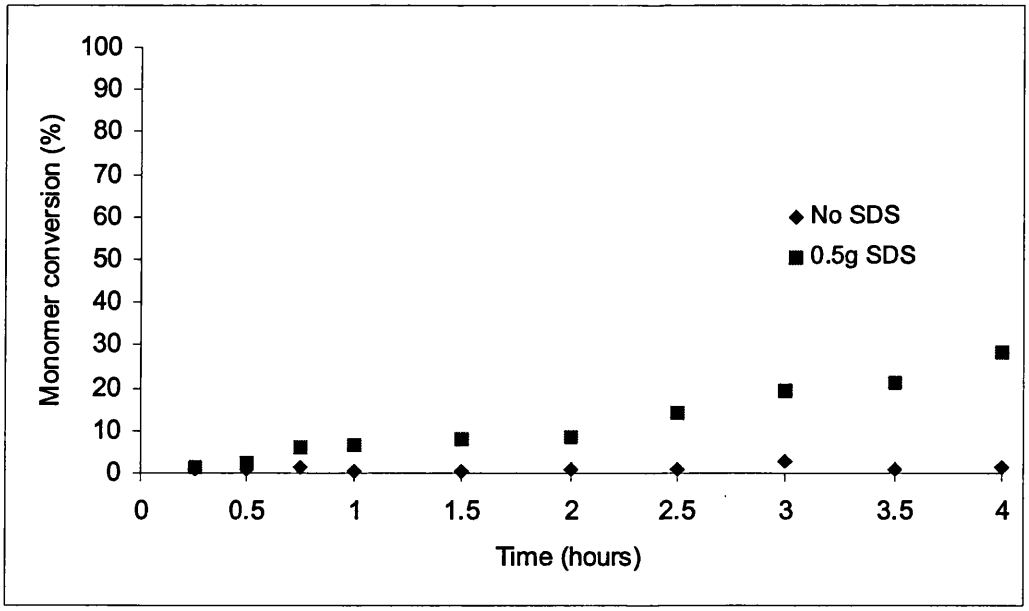

Graph 4.7 Monomer conversion for an ultrasonic reaction at 10.66 ±0.6 Wcm^{-2}, 0.5g and 0g of surfactant.

The low monomer conversion for the reaction with 0.5g of surfactant was rather surprising but reproducible. The conversion is lower than expected only if a droplet nucleation pathway is considered, as this will require the presence of a high concentration of surfactant and even a co-surfactant [164]. If a micellar pathway is considered then with the surfactant concentration above the CMC, 8.1 $x\ 10^{-3}$ mol dm^{-3} [168] and as the main locus of the polymerisation is the monomer-swollen micelles then the monomer conversation should be higher.

The poor monomer conversion, even with the surfactant above the CMC, is more evidence for the polymerisation switching to a droplet nucleation pathway in the presence of an ultrasonic field. The collapsing cavitation bubble is proposed to cause the decomposition of the SDS molecule into free radicals as in equation 4.2 [62].

$$C_{12}H_{25}OSO_3Na \longrightarrow C_{12}H_{25}\bullet + \bullet OSO_3Na \qquad (4.2)$$

However, without the stabilisation of the surfactant or the omission of a co-surfactant the monomer droplets do not have a sufficient half life to capture a radical and provide stability for polymerisation to occur. Therefore, the concentration of 0.5g is too low to provide sufficient stability to the monomer-swollen micelles.

The reaction omitting the surfactant although giving negligible conversion is comparable with the conversion reported by Biggs and Grieser [61]. In their study a power rating of 10-20 Wcm^{-2} was used which is of a similar rating used in this study. Due to the low conversion not enough sample could be collected for GPC analysis. However, the molecular weight data for the reaction with 0.5g of surfactant is shown in graph 4.8.

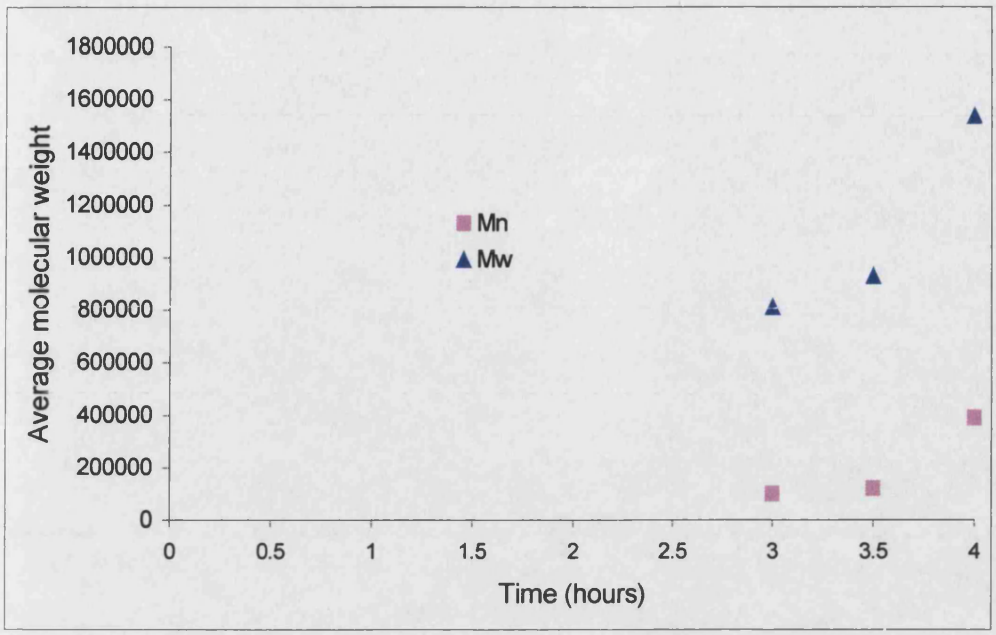

Graph 4.8 Average molecular weight for the emulsion polymerisation of styrene at 10.66 ±0.6 Wcm^{-2}, 0.5g of surfactant.

There are no data points prior to three hours due to the lack of sample. The very high molecular weight of the resultant polymer is approximately three times higher than that obtained by the sonication of styrene in a bulk reaction [13]. Therefore, the monomer is polymerising via a micellar pathway. This may seem a contradiction to the statement above. However, if none of the micelles were providing stability then a bulk reaction would result and the molecular weight would be considerably less. If only a small number of micelles were stabilising the polymerisation then the conversion would be reduced and the molecular weight would also be reduced.

The increase in surfactant concentration will mainly assist in the stabilisation of the monomer droplets, rather than producing a greater number of monomer-swollen micelles. Using ultrasound the larger monomer droplets which are ~0.3-10μm [58,61] in size are constantly being sheared into smaller droplets. This process of increasing the surface area is thermodynamically unstable due to the interfacial tension. Therefore, the small monomer droplets will have a tendency to coagulate unless they can be stabilised. If a sufficient amount of surfactant is present, 1g, then the small monomer droplets can be stabilised so lowering the

interfacial tension. The net result of this will be increased lifetimes for the small droplets and so a greater opportunity to scavenge a radical and form a primary particle. Further evidence for this is discussed in section 4.4 where there is invariance of particle size distribution data for an increase in the surfactant concentration.

Again, the same reaction was carried out for a conventional reaction keeping all other parameters constant. The graph of monomer conversion is shown in graph 4.9.

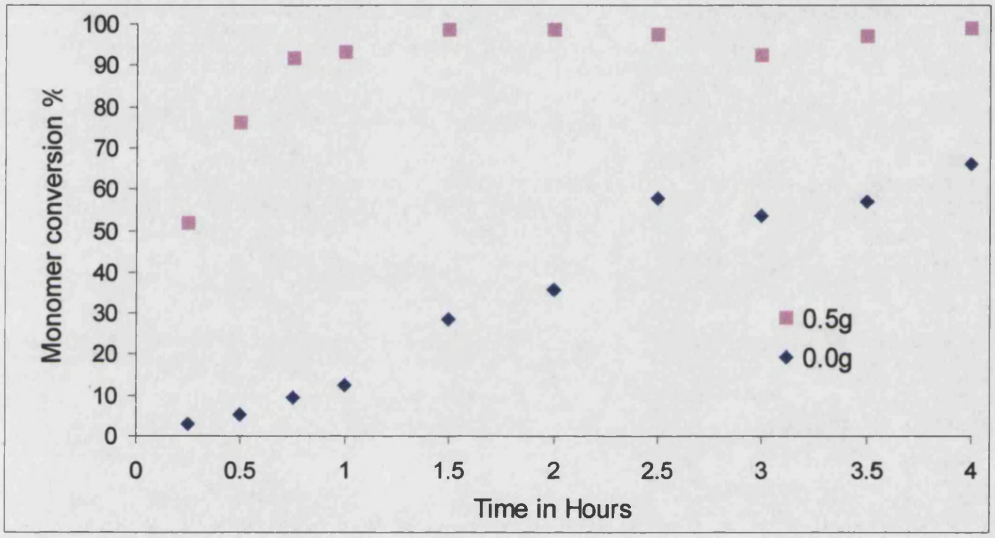

Graph 4.9 Monomer conversion for a conventional reaction at 75°C, with 0.5g and no surfactant.

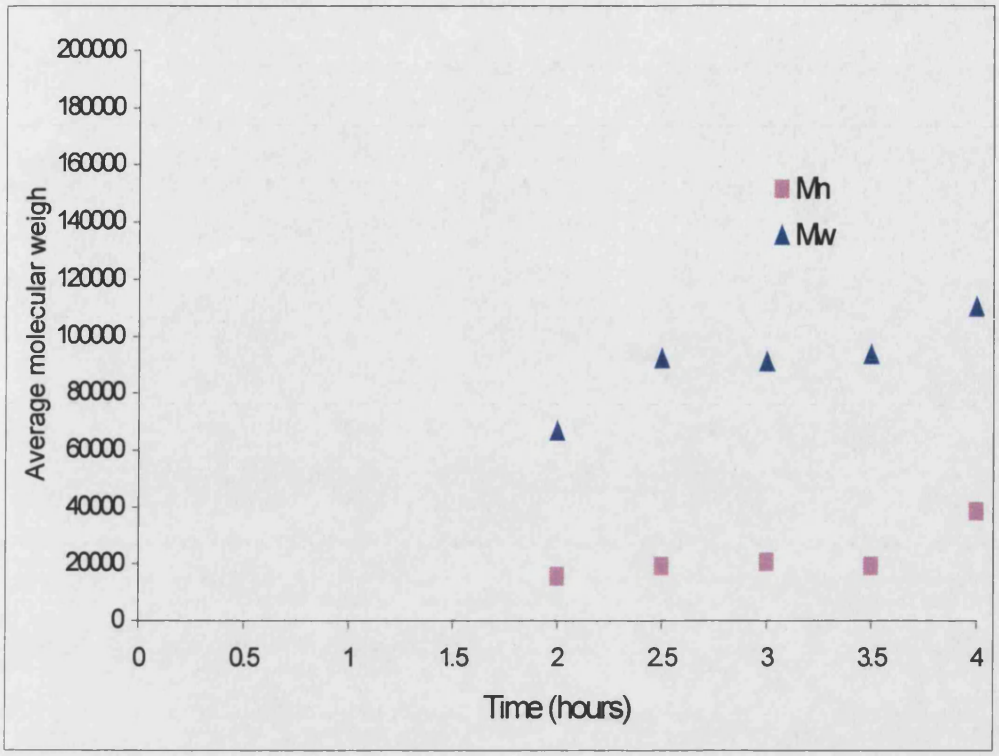

Graph 4.10. Average molecular weight for the emulsion polymerisation of styrene at 75°C, no surfactant.

It is immediately apparent from the graph of monomer conversion against time that with 0.5g of SDS then the reaction gives a monomer conversion similar to that with 1g of surfactant and almost as quick. This shows that for a conventional reaction then the reaction proceeds via a micellar pathway where the CMC of SDS has been reached, 8.1×10^{-3}mol dm^{-3}.

When the surfactant has been omitted from the reaction the conversion still gives ~60% polymer. This is because the polymerisation is proceeding via a bulk polymerisation pathway. In the conventional reaction, at 75°C, the rate of stirring and blade design is insufficient to cause the large monomer droplets to shear into smaller droplets. Therefore, the system can be said to be phase separated with the monomer only polymerising via a bulk polymerisation pathway. Indeed, comparison with a bulk reaction at 75°C the graph of monomer conversion is very similar [13].

4.1.3 Comparison of an ultrasonic and conventional reaction – no initiator.

Leading reports of recent years were by Biggs and Grieser [61], and subsequently by Ooi and Biggs [58] who reported that using ultrasound in a system where there was no added initiator could give a monomer conversion of up to 80% after 3 hours. This work built upon the work of Liu, Chou and Stoffer [62] who demonstrated that the surfactant SDS could dissociate in an ultrasonic field to give free radicals, according to equation 4.3, capable of initiating the emulsion polymerisation of methyl methacrylate.

$$C_{12}H_{25}OSO_3Na \longrightarrow C_{12}H_{25}\bullet + \bullet OSO_3Na \qquad (4.3)$$

The presence of the $C_{12}H_{25}\bullet$ radical was detected by mixing SDS, water and bromoform and irradiating the solution with ultrasound. The generated free radicals then react with $CHBr_3$ to give $C_{12}H_{25}Br$, which could then be detected by GC-MS analysis. Hence, if the chemical initiator potassium persulphate were omitted, the main source of radicals would be from the surfactant SDS. The reaction apparatus was set up as for an ultrasonic reaction, however, no initiator was added. The graph of monomer conversion is shown in graph 4.11.

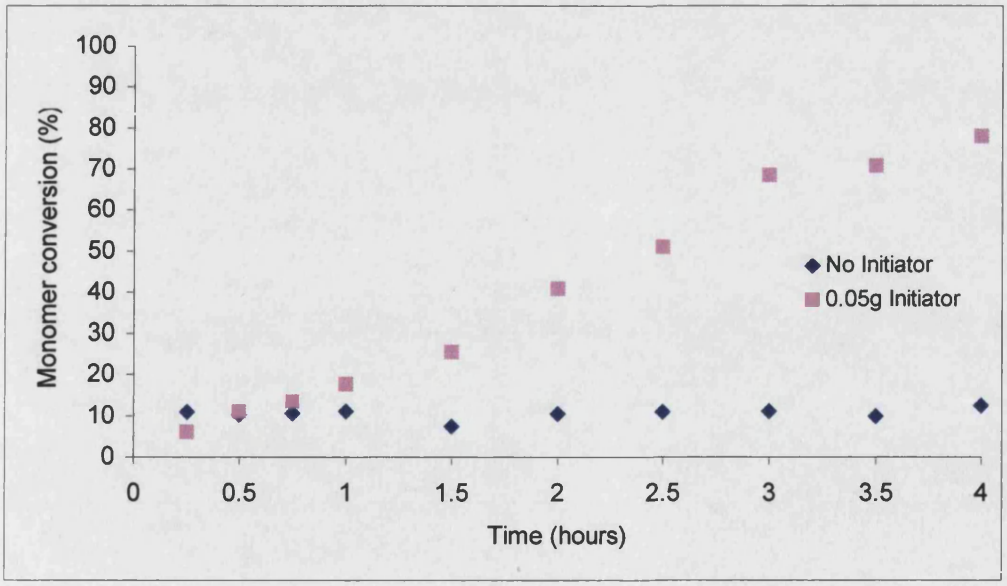

Graph 4.11 Monomer conversion for an ultrasonic reaction at 10.66 $\pm 0.6 Wcm^{-2}$, 0.05g and no initiator.

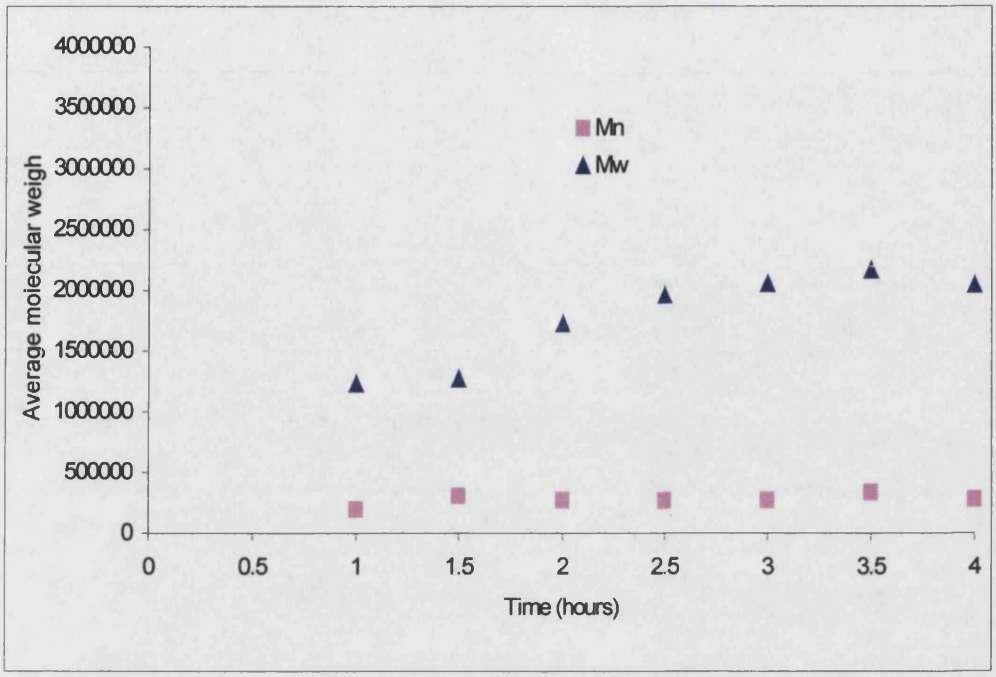

Graph 4.12 Average molecular weight for the ultrasonic polymerisation of styrene at 10.66 ±0.6 Wcm^{-2}, 0.05g initiator.

There are no data points prior to one hour due to the lack of sample. Likewise there are no data points for the reaction with no initiator due to lack of sample. The reaction omitting the initiator gave a poor yield and was repeated twice more to confirm the result. Chou and Stoffer [62] demonstrated the presence of sulphate ion radicals and alkyl radicals at an intensity from 6.8 to 14.4 Wcm^{-2}, so why is the monomer conversion so low?

The answer lies in the type of cavitation produced by the ultrasonic horn, either transient or resonant [1,13] and the experimental design. Transient (or vapour) cavitation, occurs when there is no gas flow through the solution and results from the formation and collapse of a bubble within a few cycles. The audible noise from this type of cavitation is loud and harsh. Due to short lifetime of a bubble the internal pressures and temperatures produced are much higher than resonant cavitation [1], it is this type of cavitation that is utilised in this study. In the study published by Chou and Stoffer [27,169] they tried to utilise resonant cavitation by bubbling argon through the solution and allowing the bubbles to be broken

into micro-bubbles which through the streaming caused by ultrasound distributes these bubbles throughout the solution. The net result is that local temperatures reached when a resonant bubble collapses are lower than those produced for transient cavitation. It is this increased temperature which is the cause of the low monomer conversion. Rather than promoting a polymerisation reaction a pyrolysis type reaction is promoted, where the surfactant is destroyed rather than splitting into radicals.

This is less of a problem when all of the reactants are in the system as the presence of potassium persulphate provides a source of radicals to allow the polymerisation to continue.

Again, the comparable reaction was now carried out for a conventional reaction but omitting the chemical initiator potassium persulphate. The graph of monomer conversion is shown in graph 4.13.

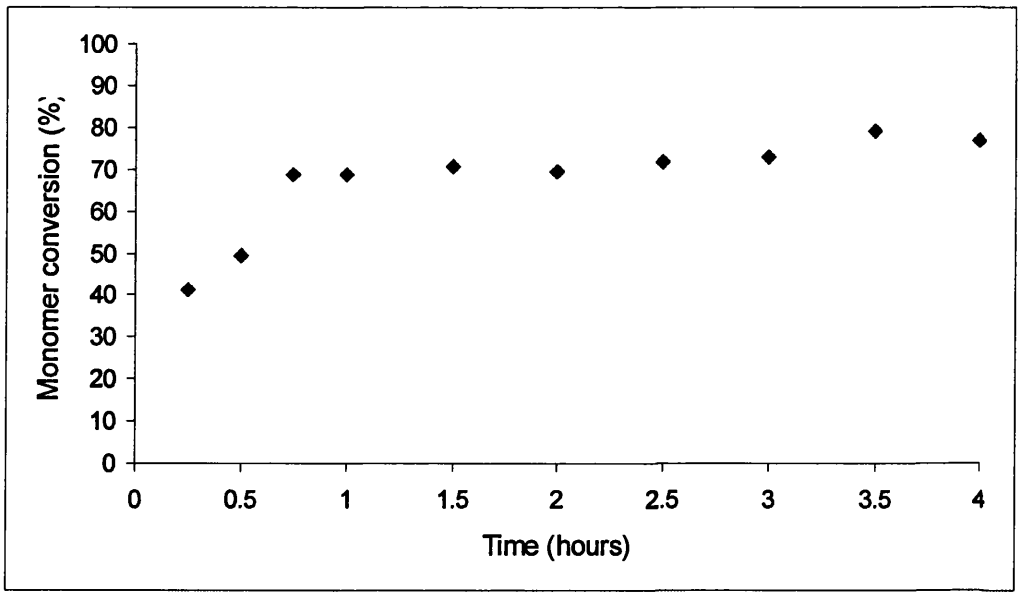

Graph 4.13 Monomer conversion for a conventional reaction at 75°C, no initiator.

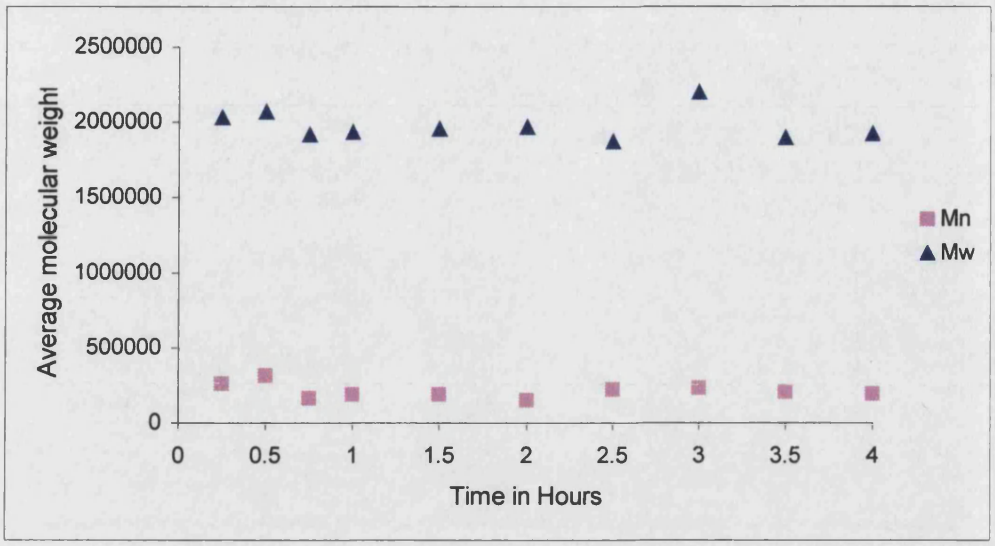

Graph 4.14 Average molecular weight for the emulsion polymerisation of styrene at 75°C, no initiator.

The conventional reaction only has thermal energy to cause initiation, therefore the number of radicals is much smaller and hence there is a smaller proportion of micelles with growing chains inside them leading to an increase in the molecular weight.

4.2 Change of ultrasonic intensity

The acoustic intensity is the main influencing factor upon the number of cavitation bubbles produced, all other things being equal. At a lower acoustic intensity, the rate of formation of small monomer droplets capable of directly scavenging free radicals is predicted to be lower. Also lower radical flux into these monomer droplets will give a decreased nucleation rate. Therefore, as the acoustic intensity decreases the number of cavitation bubbles will also decrease. Thus, the rate of radical production is expected to decrease resulting in lower polymerisation rates and lower conversion for a given time point. Reducing the ultrasonic intensity from 10.66 ±0.6 Wcm^{-2} to 5.61 ±0.35 Wcm^{-2}, but keeping all other factors equal tested this hypothesis.

The experiments were carried out as described in section 2.5. The monomer conversion with all the reagents is shown in graph 4.15.

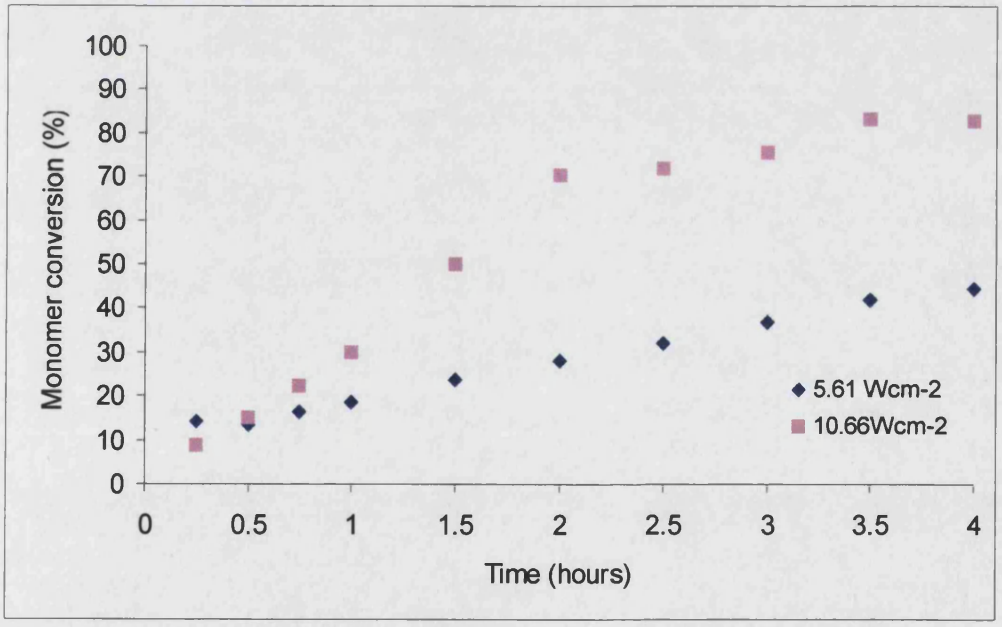

Graph 4.15 Monomer conversion for an ultrasonic reaction at 5.61±0.35 and 10.66 ±0.6 Wcm^{-2}, 25°C.

The monomer conversion, at 5.61 ±0.35 Wcm^{-2}, although much lower than that found for an intensity of 10.66 ±0.6Wcm^{-2} is in line with the conversion that

Chou and Stoffer and Ooi and Biggs reported [27,58]. The reason for this is that under the conditions of constant ultrasonic irradiation there is a continuous production of both high radical numbers and a high concentration of small monomer droplets. The production of large numbers of small monomer droplets is the result of the high shear rates caused by the ultrasound acting upon large monomer droplets. By decreasing the acoustic intensity there will be a smaller number of monomer droplets at any given instant. Consequently, there are lower radical fluxes into these monomer particles as the cavitation process is not as efficient in producing numbers of radicals.

The number of monomer-swollen micelles is predicted to be relatively insensitive to changes in the acoustic intensity and will depend upon the surfactant concentration [58]. Therefore, the ratio of small monomer droplets to monomer swollen micelles is expected to decrease as a function of acoustic intensity for a given surfactant concentration. For an intensity of 5.61 ±0.35 Wcm^{-2} the monomer droplets cannot be sheared into small enough droplets. Since the primary sites for radicals to be captured will be dependent upon relative surface areas and as there will be a higher number of large monomer droplets i.e. a low surface area, will lead to a lower rate of polymerisation, monomer conversion and molecular weight.

The graph of average molecular weight is shown in graph 4.16.

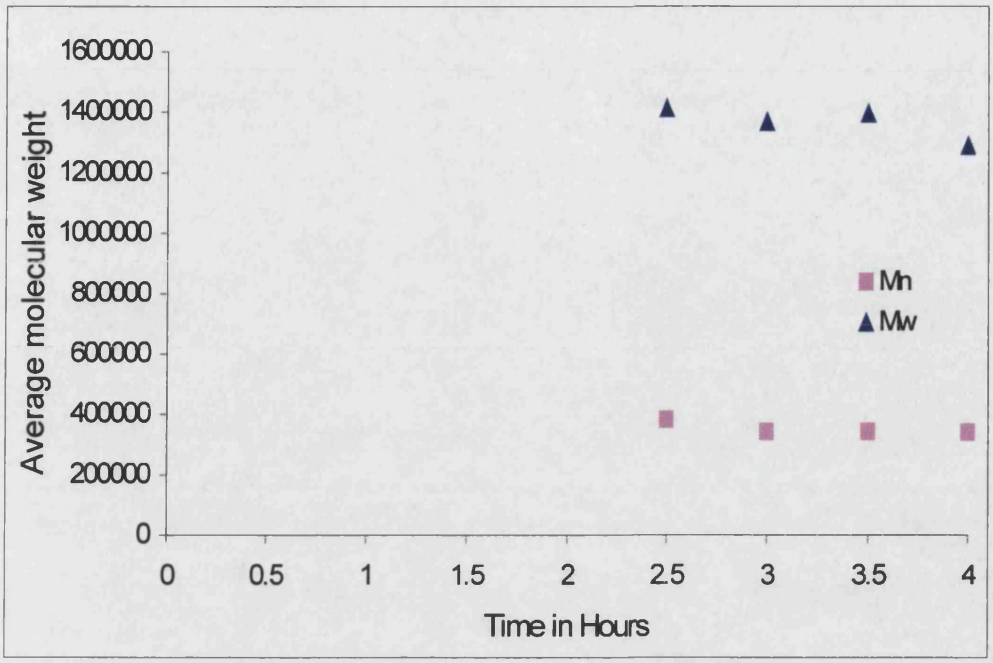

Graph 4.16 Average molecular weight for the ultrasonic polymerisation of styrene at 5.61 ±0.35 Wcm^{-2}.

There are no points prior to 2 ½ hours due to a lack of reaction product. The molecular weight results support the view that at an intensity of 5.61 ±0.35 Wcm^{-2} the monomer droplets are too large a size to be absorbed by micelle, leading to a decrease in the molecular weight.

By using the same method to determine the rate of polymerisation as in section 4.1.1 the rate of polymerisation against time is shown in graph 4.17.

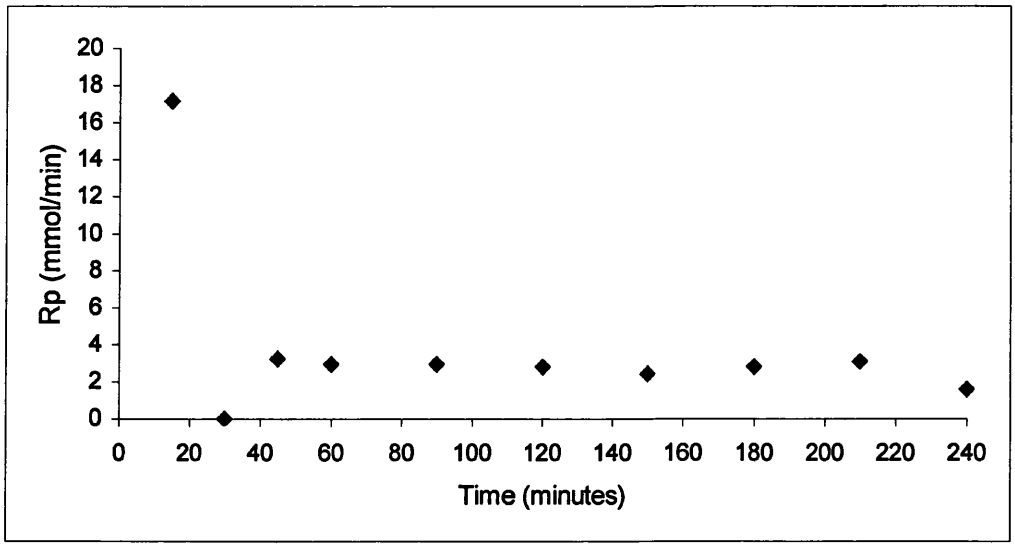

Graph 4.17 The rate of polymerisation in $mmolmin^{-1}$ for an ultrasonic reaction at 5.61 ±0.35 Wcm^{-2}.

Although the initial rate is much higher than for a reaction performed at 10.66 ±0.6 Wcm^{-2} the overall rate is, as the monomer conversion graph suggests, much lower and far more constant. The reason for this plateau can be explained in the same manner as explained in section 4.1.1. The initial rate of generating new particles is much higher than the termination rate. After time the termination rate will equal the nucleating rate, the number of growing polymer particles will acquire a constant value. However, as the polymerisation loci are still saturated with monomer a plateau in the rate of polymerisation will appear. The length of the plateau will depend upon the number of growing particles and the remaining monomer concentration. In a true micro emulsion monomer diffusion is fast enough to maintain thermodynamic equilibrium [170]. Therefore, as the monomer concentration is the same as for the reaction at 10.66 ±0.6 Wcm^{-2}, then the number of growing particles must be less. In order to shorten the plateau for a given intensity an increase in the initiator concentration or a decrease in the monomer concentration is necessary.

As for an intensity of 10.66 ±0.6 Wcm^{-2} the next reagent to be changed was the surfactant concentration. The change in surfactant concentration is shown below in graph 4.18.

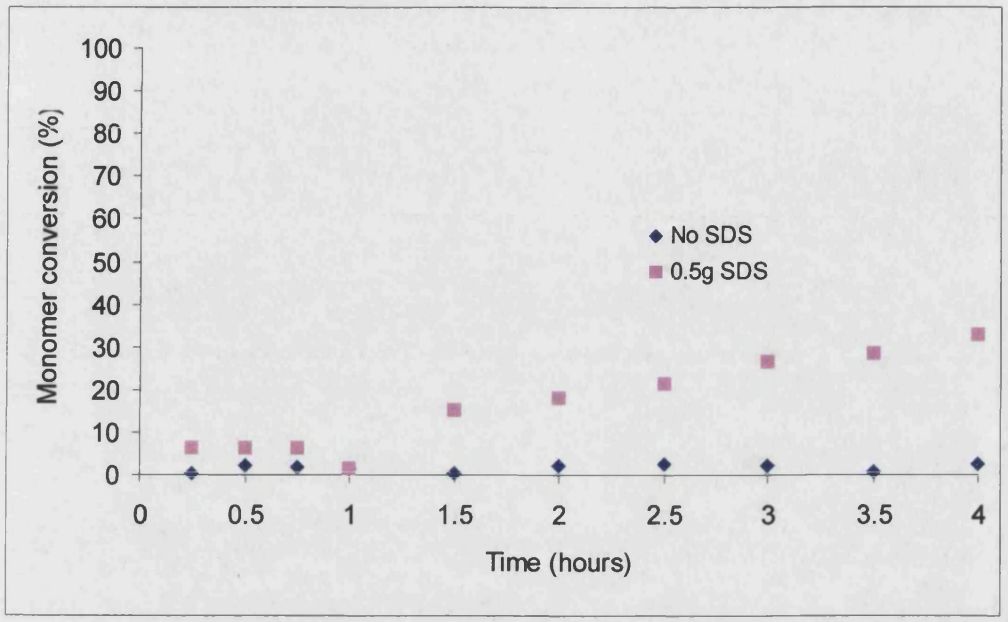

Graph 4.18 Monomer conversion for an ultrasonic reaction at 5.61±0.35 Wcm^{-2}, 0.5g and 0g of surfactant.

As in the reaction with an intensity of 10.66 ±0.6 Wcm^{-2} omitting the surfactant does not produce any polymer. With half the concentration of surfactant the conversion is only 15 % less than that obtained with 1g of surfactant. At a lower acoustic intensity, the time required to produce a similar average number of latex particles increases. This is justified by the lowering of the monomer conversion. The graph showing the molecular weight is below in graph 4.19.

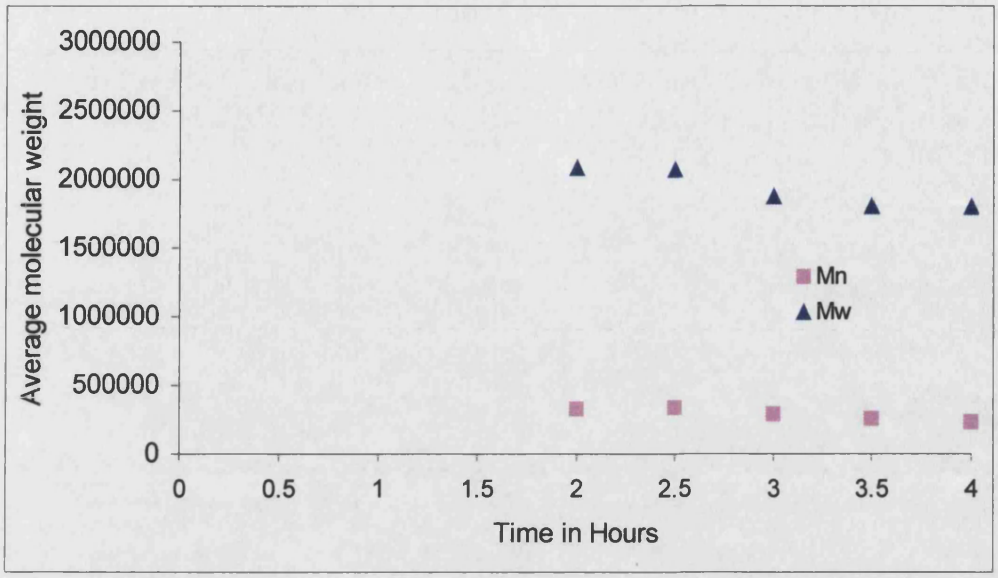

Graph 4.19. Average molecular for the ultrasonic polymerisation of styrene at 5.61 ±0.35 Wcm^{-2}, 0.5 g of surfactant.

There are no data points prior to two hours due to the lack of sample, likewise there are no data points for the reaction with no surfactant due to lack of sample. Initially the high molecular weight was surprising, given that the molecular weight for an intensity of 10.66 ±0.6 Wcm^{-2} is almost half of that recorded here. If however, the intensity of the reaction is considered then the reason for such a high molecular weight can be understood. At the higher intensity the rate of radical production is higher than that at the lower intensity. The reduction in radical concentration means that the likelihood of a termination reaction occurring i.e. two radicals combining in a micelle, is also reduced leading to an increase in the molecular weight.

The next reagent to be omitted was the initiator, the monomer conversion is shown in graph 4.20.

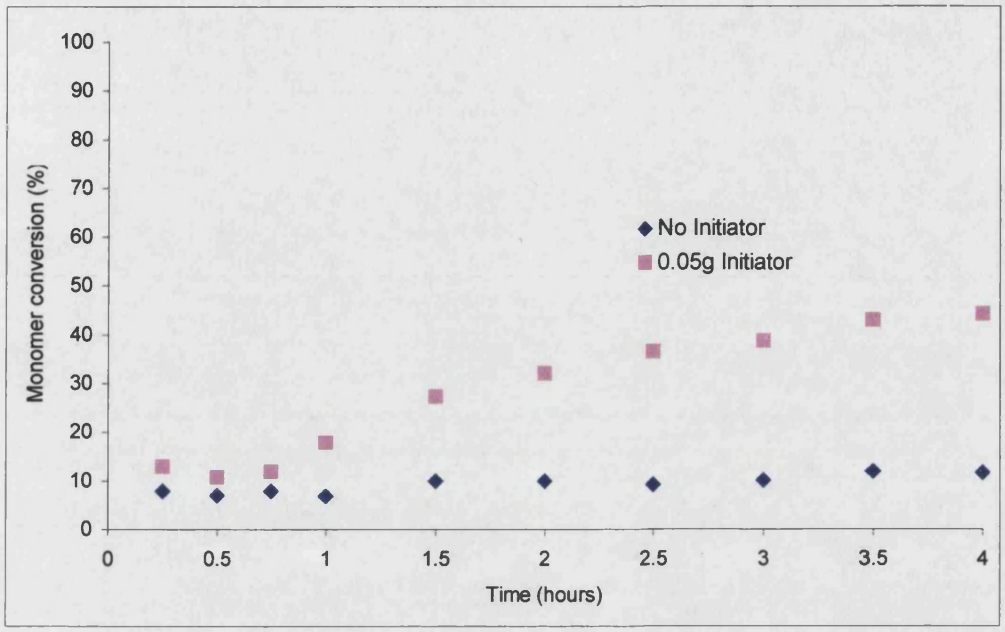

Graph 4.20 Monomer conversion for an ultrasonic reaction at 5.61±0.35 Wcm^{-2}, 0.05g and no initiator.

Omitting the initiator, again, does not produce any significant monomer conversion. As explained in section 4.1, this is due to the type of cavitation that occurs in the reaction, transient rather than resonant cavitation. The higher temperatures being produced during the collapse of a transient bubble causing a pyrolysis type reaction rather than a radical forming reaction.

4.2 Change in the bulk temperature

As shown in chapter three, an increase in the bulk reaction temperature does not always translate into an increase in the rate of an ultrasonic reaction. For this reason the effect of changing the reaction temperature was investigated whilst keeping the reaction reagents constant. The monomer conversion against time graph for the polymerisation of styrene at an intensity of 10.66 ±0.6 Wcm^{-2} is shown in graph 4.21.

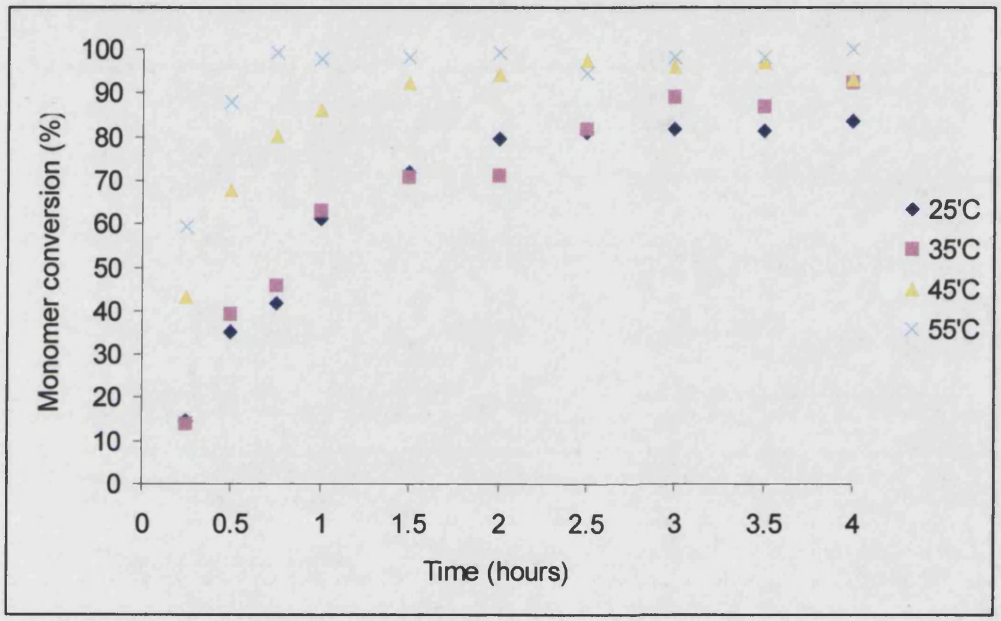

Graph 4.21 Monomer conversion against time for the ultrasonic polymerisation of styrene at 10.66 ±0.6 Wcm^{-2}.

The results from graph 4.21 clearly show that there is a significant rise in the rate of polymerisation and monomer conversion with increasing temperature. This relationship is shown for the majority of chemical reactions. However, the results shown in graph 4.21 are in disagreement with that which is normally predicted of an ultrasonic reaction [13]. The rise in temperature will increase the vapour pressure of the system, which in turn causes more vapour, water or styrene monomer, to diffuse into an expanding cavitation bubble. The expanding bubble will therefore contain more vapour that will in turn cushion its collapse. Hence, a decrease in temperature and pressures will occur in the vicinity of the collapsing

bubble, leading to a decrease in the number of radicals capable of initiating the polymerisation. Hence, it is predicted that for an ultrasonic reaction a decrease in temperature will increase the rate of reaction, From the results shown in graph 4.21 this trend was not in evidence.

For the emulsion polymerisation of styrene the increase in the vapour pressure is insignificant compared with the increased rate of polymerisation due to the effects of enhanced thermal activation. A comparison between the two differing methods of conducting the reaction can be made by comparing graph 4.21 with graph 4.22, monomer conversion against time using the same reagents as for graph 4.21. However, rather than using ultrasound a conventional method was used, stirred and heated.

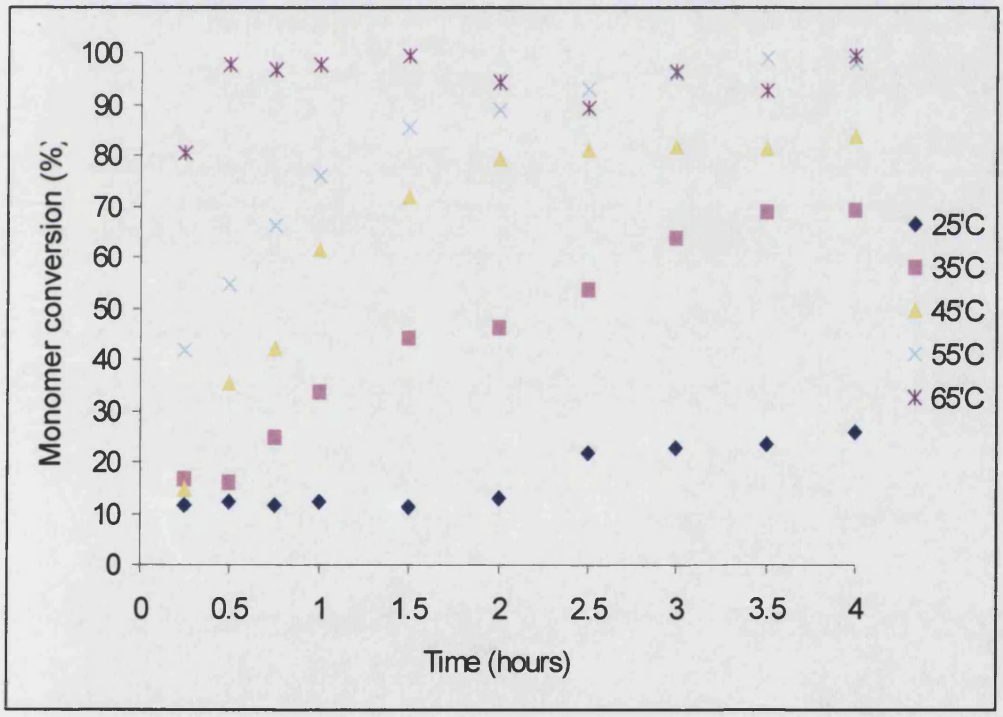

Graph 4.22 Monomer conversion against time for the polymerisation of styrene using an overhead stirrer and a heated oil bath.

Using the graphs of conversion versus time the rates of polymerisation can be determined for a reaction containing exactly the same ingredients but with differing experimental methods. Shown in graph 4.23 are the rates of

polymerisation for an ultrasonic reaction and in graph 4.24 are the rates of polymerisation for a conventional reaction.

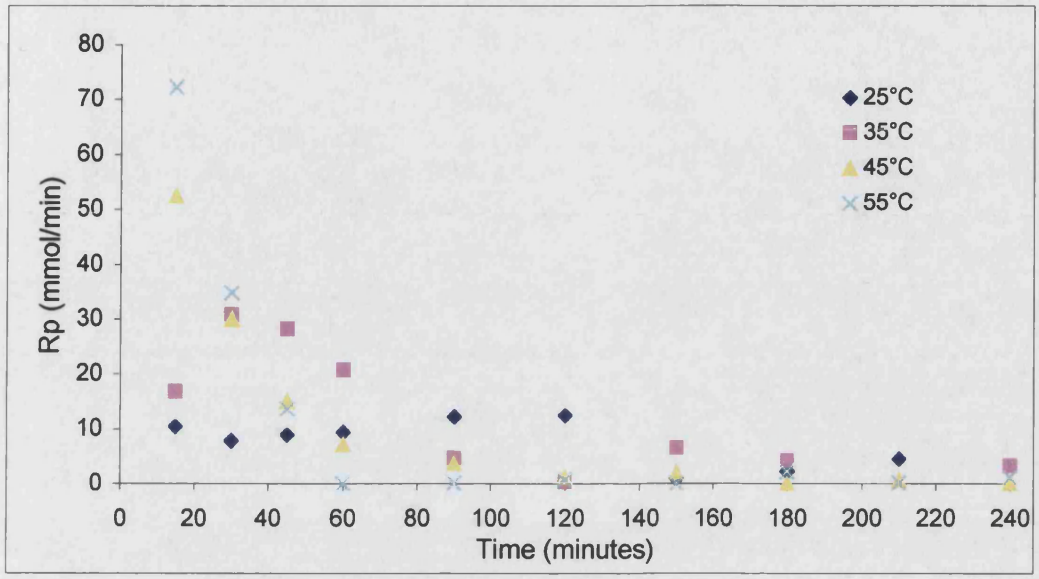

Graph 4.23 The rates of polymerisation for an ultrasonic reaction, with increasing temperature

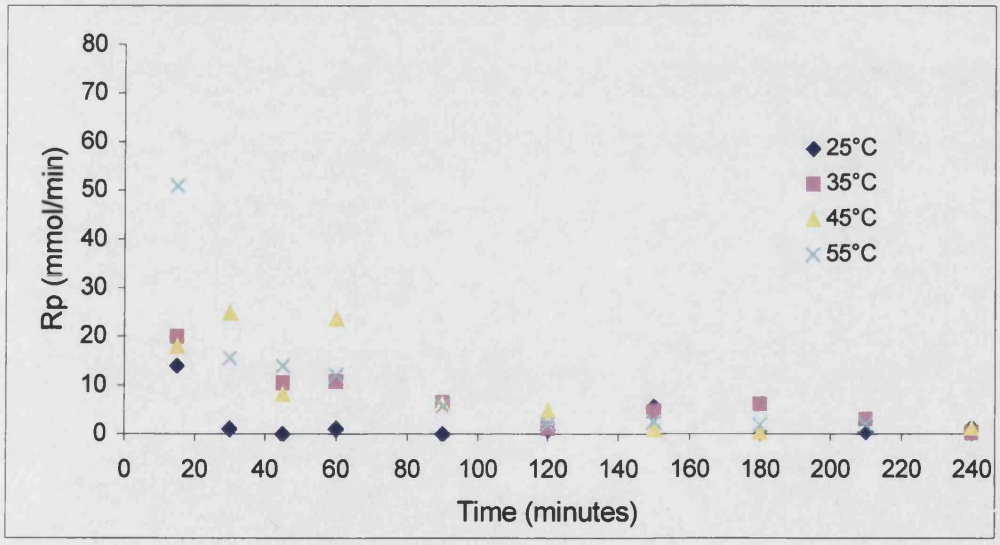

Graph 4.24 The rates of polymerisation for a conventional reaction, with increasing temperature.

Through a comparison of the two graphs then it can be seen that for a comparable bulk temperature the rate of polymerisation is faster for an ultrasonic reaction than for a conventional reaction. This can be seen in graph 4.25 where the rates for an ultrasonic reaction and a conventional reaction at 35°C are compared.

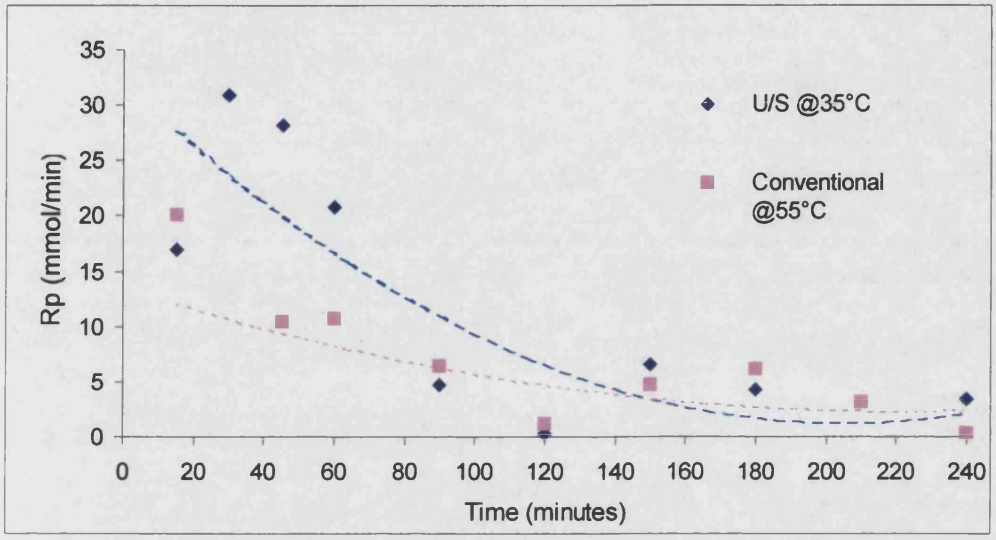

Graph 4.25 A comparison of the rates of polymerisation for an ultrasonic and a conventional reaction at 35°C and 55°C respectively.

The increased rate of polymerisation for a comparable temperature can be explained in terms of the mechanism of the formation of nucleating particles. During the conventional reaction the particle formation mechanism is predominately one of micellar nucleation [84,163]. Usually only one out of every 100-1000 micelles captures a radical and becomes a polymer particle. Unentered micelles give up their surfactant and monomer molecules to the growing particles [163]. During an ultrasonic reaction the predominate mechanism for particle nucleation is via a droplet nucleation mechanism, where radicals generated in the aqueous phase can enter monomer emulsion droplets as single radicals or oligoradicals and propagate to form particles. Thus the probability of radical capture by micelles remains very high throughout and the rate of coagulation is negligible. The net result is that every oligoradical enters an 'unstung' micelle, initiating a new particle. Therefore new particles are nucleated continuously throughout the polymerisation and the particles on average contain only one polymer chain.

4.4 Particle sizing experiments

As stated in section 2.5, all the experiments were carried out using a Coulter LS230 that can measure particles in the range 0.04μm-2000μm. It is dependent upon one type of light scatter, termed diffraction. An inherent problem when measuring particle size is what average to measure namely weight, volume or the number distribution? This is demonstrated in figure 4.1.

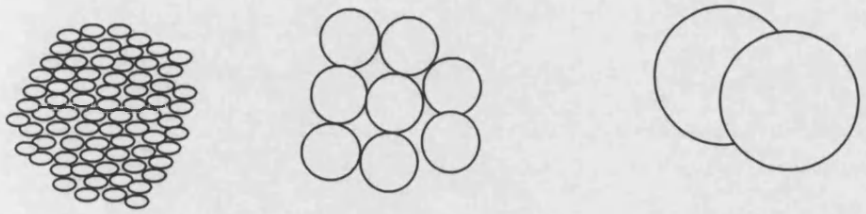

70 Ball bearings 8 Marbles 2 Golf Balls

Figure 4.1 A comparison of a sample distribution.

A wide distribution of particles can have a huge number of tiny particles whose weight may be negligible in comparison to the overall weight of the sample. In figure 4.1, many ball bearings are required to give the same volume as one golf ball. For this reason number distributions show more readily significant changes at the small size end of the distribution while volume or weight distributions are often used to monitor significant changes at the large size end. As the expected particle size for a monomer-swollen micelle in a styrene emulsion is 0.02-0.09μm [163], the number distribution, as shown in equation 4.4, will be displayed and quoted in this study.

$$d_n = \frac{\sum n_i d_i}{\sum n_i} \tag{4.4}$$

Also quoted alongside the number average, is the Sauter diameter. This is shown in equation 4.5 and represents a surface average.

$$d_{32} = \frac{\sum n_i d_i^3}{\sum n_i d_i^2} \tag{4.5}$$

Where n_i is the number of particles of diameter d_i.

The experiments were carried out as outlined in section 2.5, but with varying concentrations of the initiator, potassium persulphate. Both ultrasonic and conventional reactions were performed in order to have a direct comparison between the two reaction systems. Published papers comment upon either the particle size as obtained in an ultrasonic reaction or a conventional reaction. No comparison has been made between two systems that have identical reagents, but different methods of creating the emulsion.

The two most influential factors that control particle size are the surfactant concentration and the initiator concentration, for any given reactants. This can be shown by relating the number of particles per unit volume, N_p to the concentrations of the surfactant and initiator. The derivation is a complex one but the Smith-Ewart approach [86,87], which includes a number of simplifying assumptions and has been expanded upon by a number of authors, gives equation 4.6.

$$N_p = 0.53\left(\frac{\rho_r}{\mu}\right)^{0.4}\left(a_s[S]^{0.6}\right) \qquad (4.6)$$

Where ρ_r is the rate at which effective radicals are generated, μ is the rate at which a polymer swollen particle is growing, a_s is the surface area occupied by one mole of surfactant and S is the surfactant concentration. The total number of particles per unit volume should vary with surfactant concentration to the 0.6 power and with initiator concentration to the 0.4 power. This derivation can be further modified to take into account radicals entering particles in competition with micelles.

The number of particles generated per millilitre of water can be calculated from equation 4.7.

$$Np = \frac{\text{Total mass of monomer}}{4/3\ \pi\ r^3 D_p} \qquad (4.7)$$

where r is the radius of the latex particle and D_p is the polymer density.

Hence, the change in surfactant concentration and the change in initiator concentration has been studied for the emulsion polymerisation of styrene using both a heated and stirred reaction system and an ultrasonic reaction system.

4.4.1 Change in initiator concentration

From the Smith-Ewart derived equation, (4.6) it is predicted that increasing the initiator concentration via ρ_r then the total number of particles N_p will also increase to the 0.4 power, therefore increasing the number of particles per unit volume but also decreasing the particle size.

$$N_p = 0.53\left(\frac{\rho_r}{\mu}\right)^{0.4}\left(a_s[S]^{0.6}\right) \tag{4.6}$$

For an initiator concentration of 4.6×10^{-4}M time points of 1, 10, 20, 40 and 60 minutes were recorded. A comparison with the conventional reaction is shown in the following graphs with the blue line representing the ultrasonic reaction and the red line representing the conventional reaction.

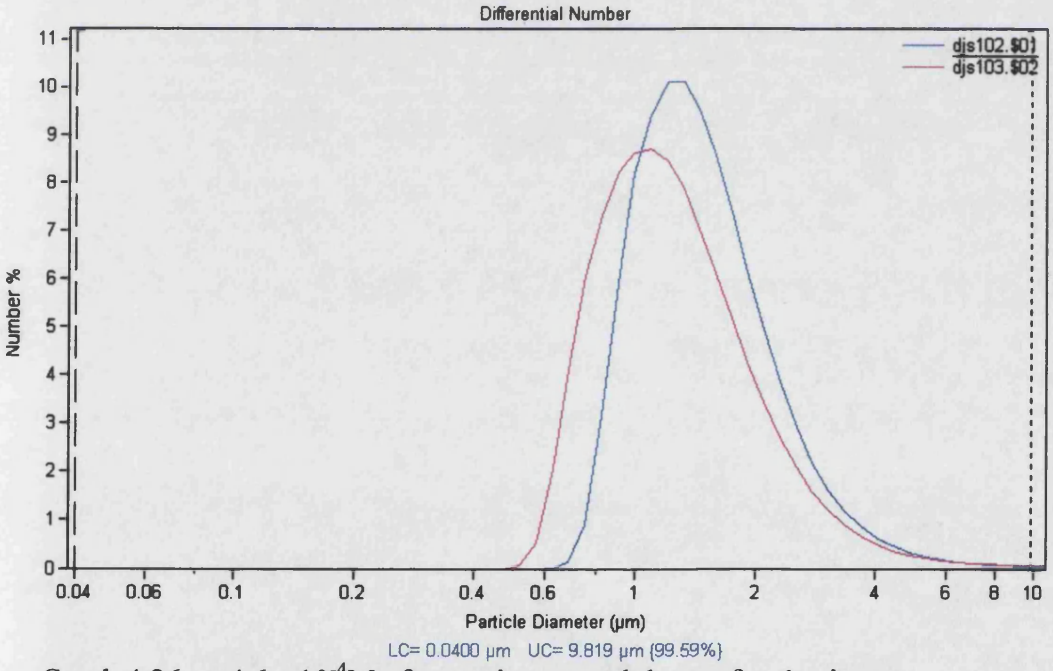

Graph 4.26 4.6×10^{-4}M of potassium persulphate, after 1 minute.

The results are summarised in table 4.1.

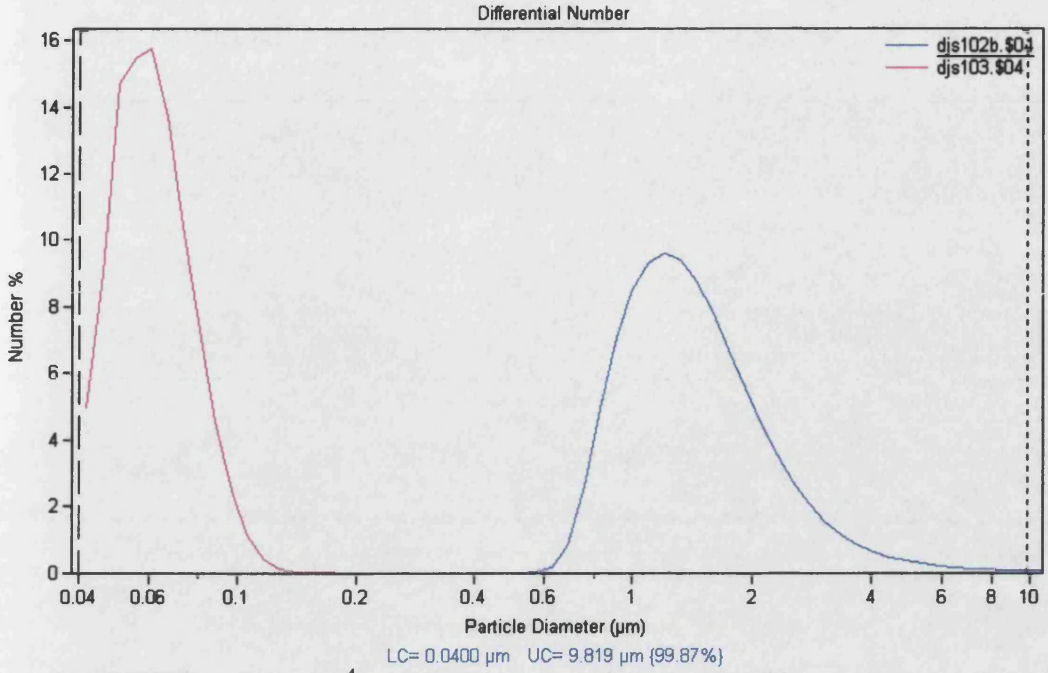

Graph 4.27 4.6×10^{-4}M potassium persulphate, after 10 minutes.

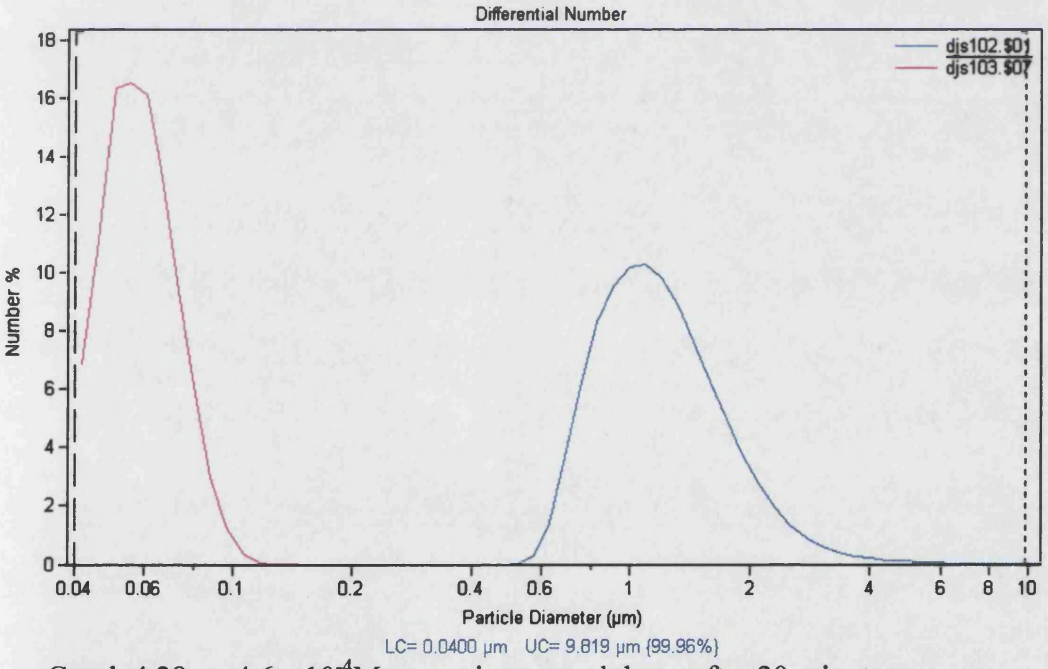

Graph 4.28 4.6×10^{-4}M potassium persulphate, after 20 minutes.

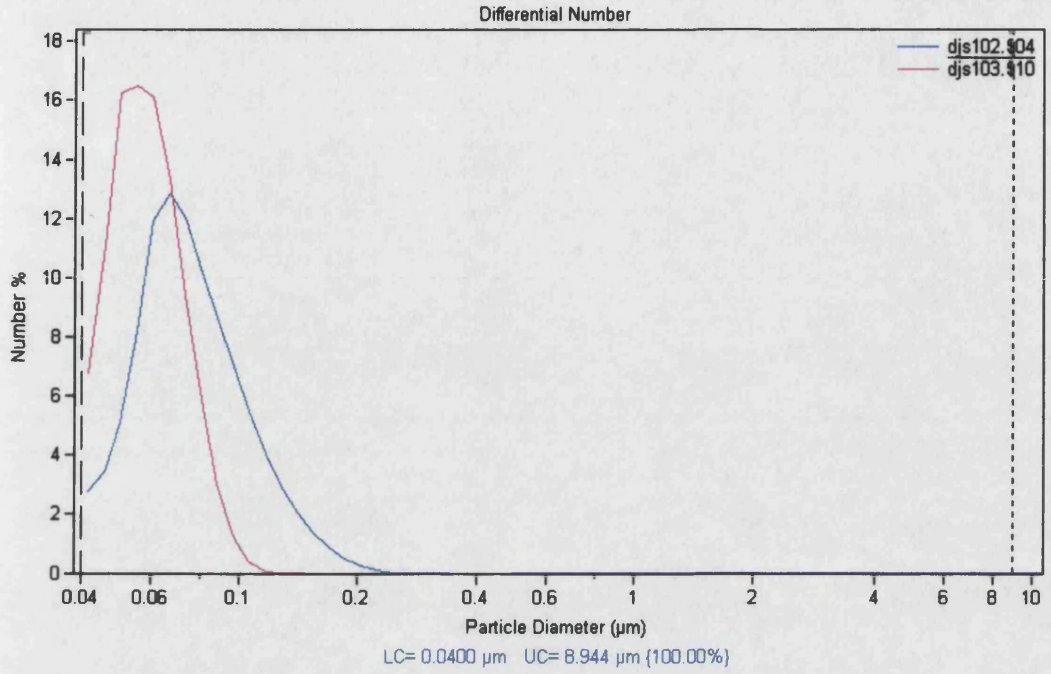

Graph 4.29 4.6×10^{-4}M potassium persulphate, after 40 minutes.

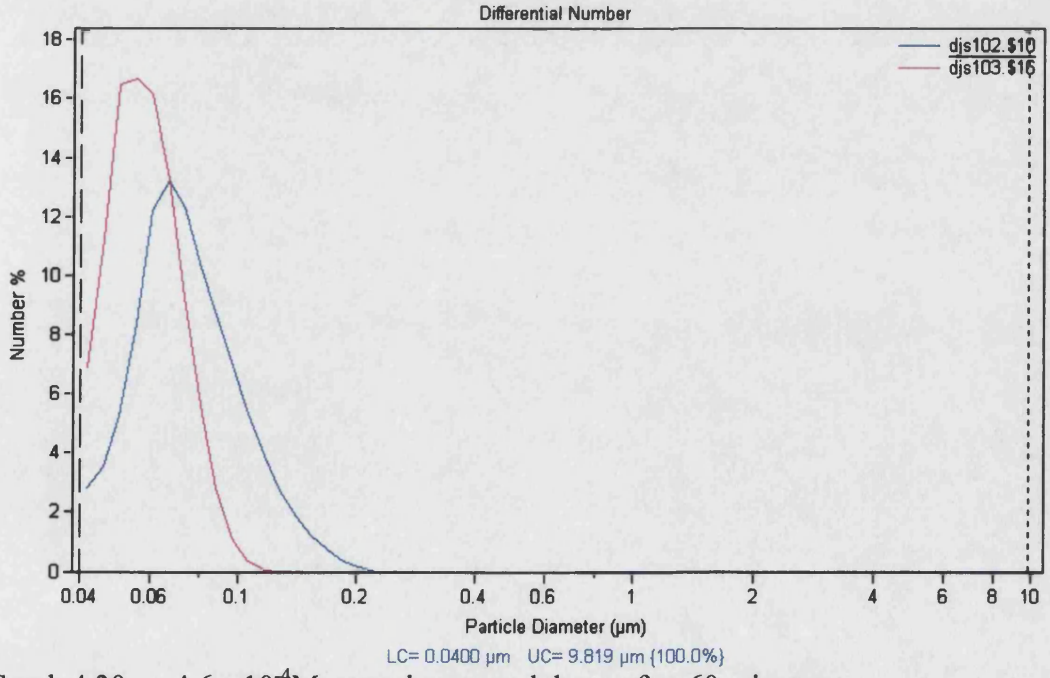

Graph 4.30 4.6×10^{-4}M potassium persulphate, after 60 minutes.

Ultrasonic reaction 10.66 Wcm^{-2}.				Conventional reaction.	
Time (mins)	D_n (μm)	$D_{(3,2)}$ (μm)		D_n (μm)	$D_{(3,2)}$(μm)
1	1.665	2.803		1.761	12.00
10	1.664	3.38		0.0615	0.068
20	1.632	3.28		0.0599	0.0656
40	0.0804	0.515		0.06	0.0656
60	0.0784	0.206		0.0597	0.0652

Table 4.1 Average particle sizes for the reaction containing 4.6×10^{-4}M of potassium persulphate.

At first the results here were rather surprising given the large number of papers detailing how ultrasound gives smaller particles [171]. However, these studies all involved the use of a model system i.e. corn oil or kerosene and not always the same surfactant used here. Indeed it has been demonstrated that small changes in the position of the ultrasonic horn produce large variation in the emulsion properties [172]. What is apparent from the results is that the conventional emulsion polymerisation soon reaches a stable particle size that does not change significantly from ten minutes to the final time point of sixty minutes. If this is compared with the monomer conversion then it can be seen that this corresponds with 100% monomer conversion and an average molecular weight of 1×10^6. In the ultrasonic reaction the particle size has a major change in size between 20 and 40 minutes. This corresponds with the monomer conversion increasing from less than 10% to approximately 20%, and an average molecular weight of $1\text{-}1.5 \times 10^6$. This is suggesting that all of the monomer has been absorbed into monomer-swollen micelles and that the polymerisation reaction is continuing in the micelles.

Further experiments to establish the relationship were carried out by changing the initiator concentration from 4.6×10^{-4}M to 9.3×10^{-4}M and finally to 1.9×10^{-3} M. The results are shown in the following pages.

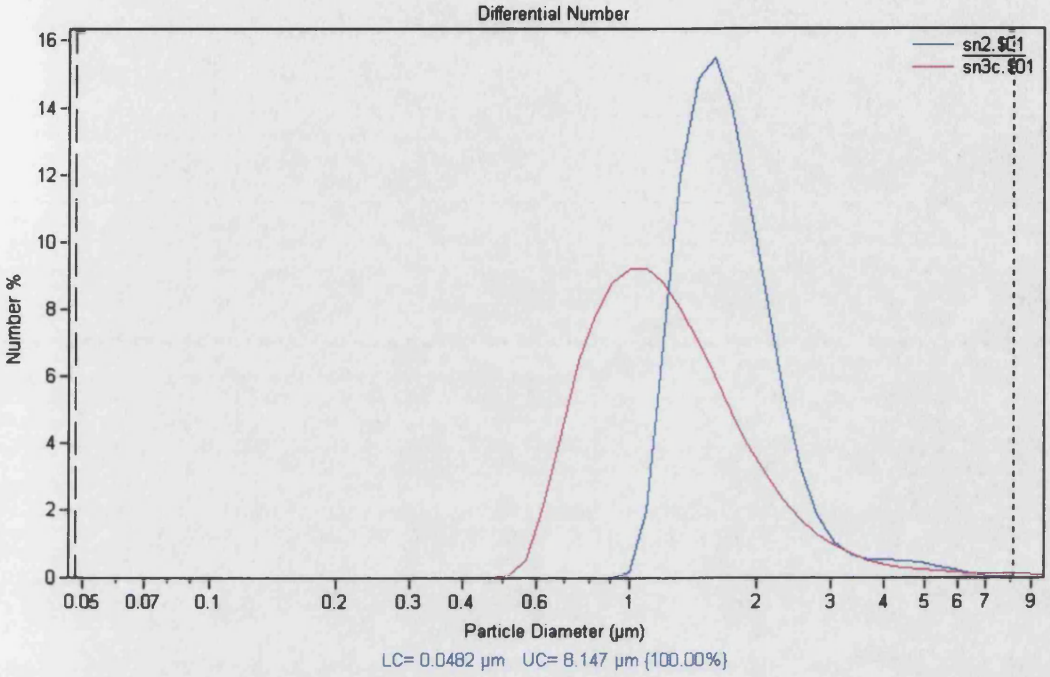

Graph 4.31 9.3×10^{-4}M potassium persulphate after 1 minute.

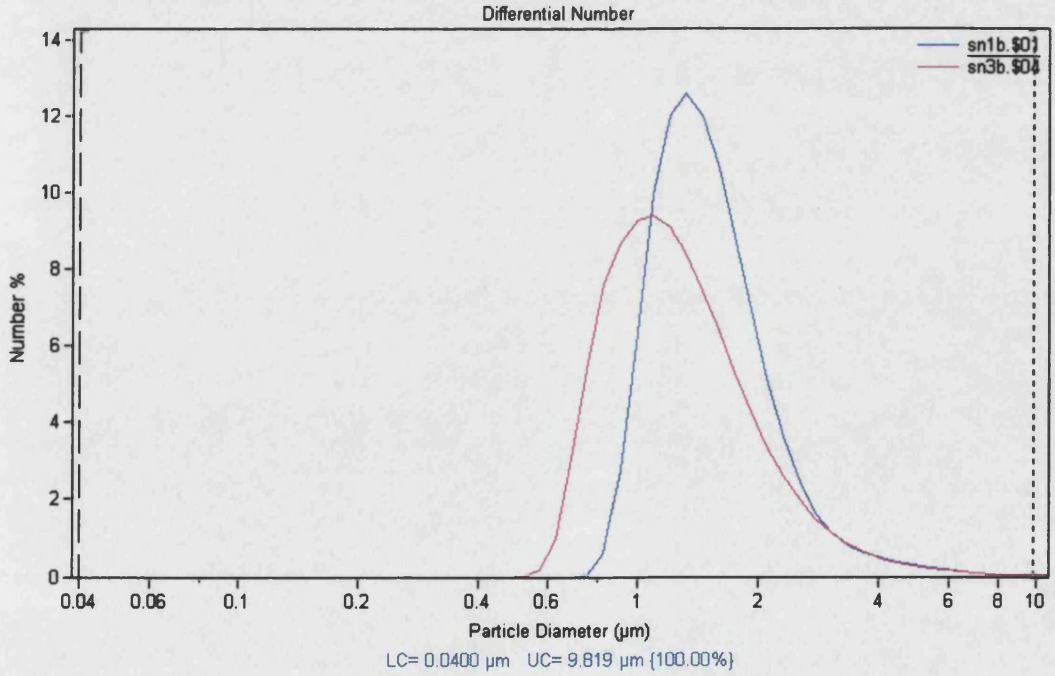

Graph 4.32 9.3×10^{-4}M potassium persulphate, after 10 minutes.

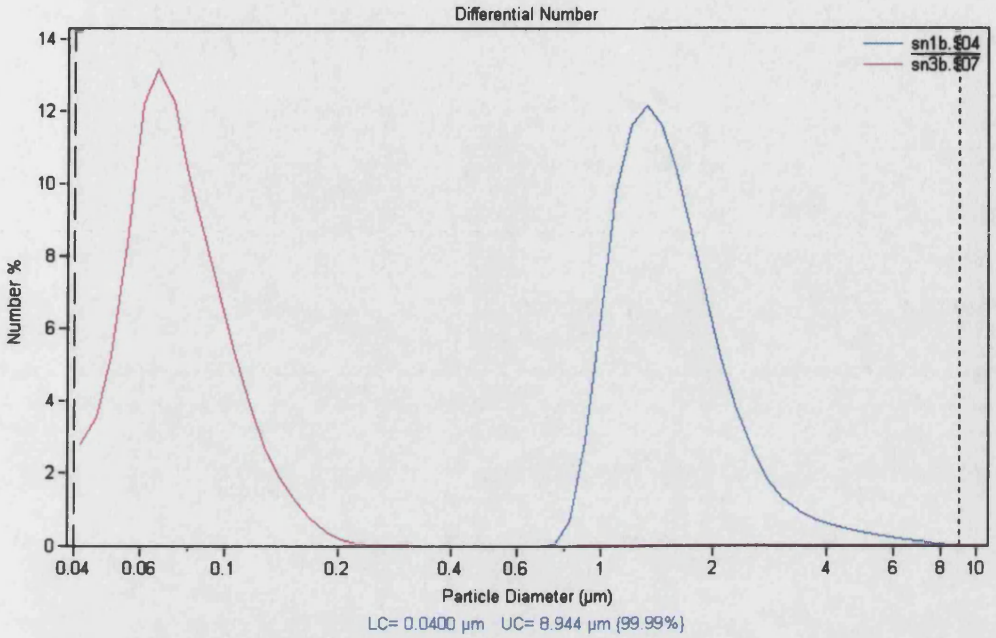

Graph 4.33 9.3 x 10^{-4}M potassium persulphate, after 20 minutes.

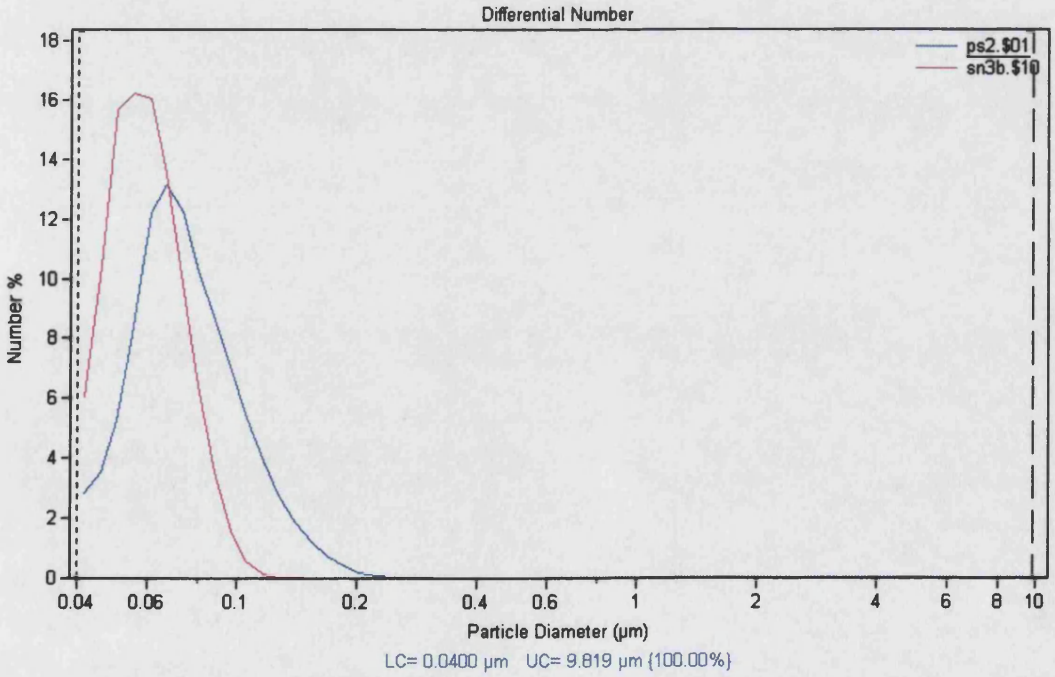

Graph 4.34 9.3 x 10^{-4}M potassium persulphate, after 40 minutes.

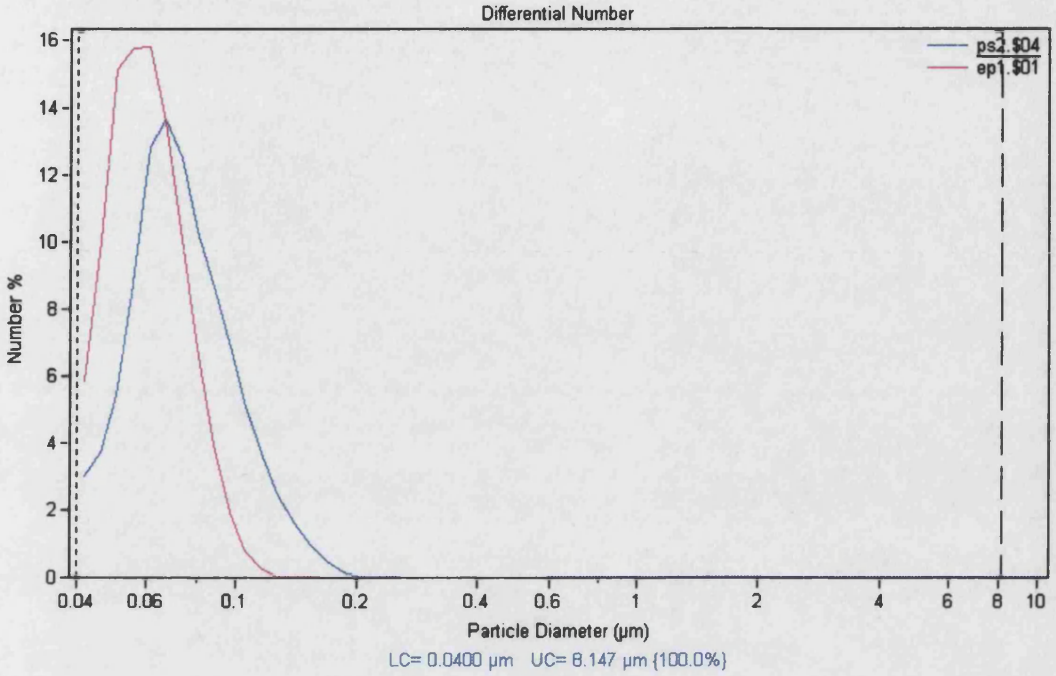

Graph 4.35 9.3×10^{-4}M potassium persulphate, after 60 minutes.

Ultrasonic reaction at 10.66 Wcm^{-2}			Conventional reaction	
Time (mins)	D_n (µm)	$D_{(3,2)}$ (µm)	D_n (µm)	$D_{(3,2)}$(µm)
1	1.832	2.359	1.505	8.543
10	1.665	2.625	1.497	9.735
20	1.679	2.900	0.0784	0.1557
40	0.0684	0.303	0.0608	0.0668
60	0.0784	0.403	0.0615	0.0680

Table 4.2 Average particle sizes for the reaction containing 9.3×10^{-4}M potassium persulphate.

The experiment was then repeated using 1.9×10^{-3} M of initiator.

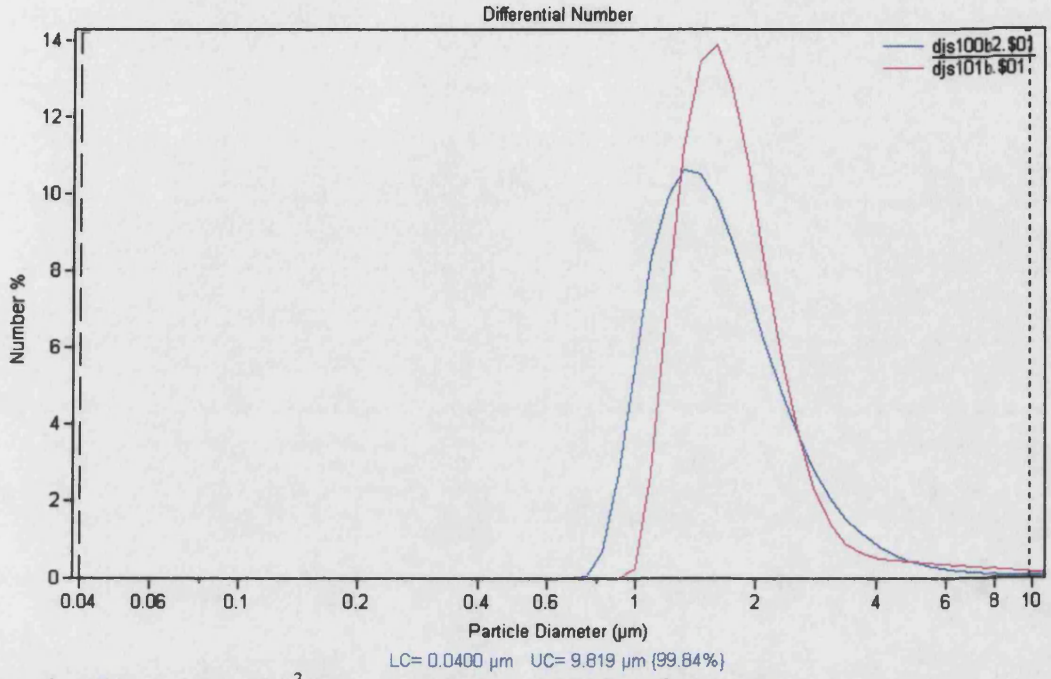

Graph 4.36 1.9×10^{-3} M potassium persulphate, after 1 minute.

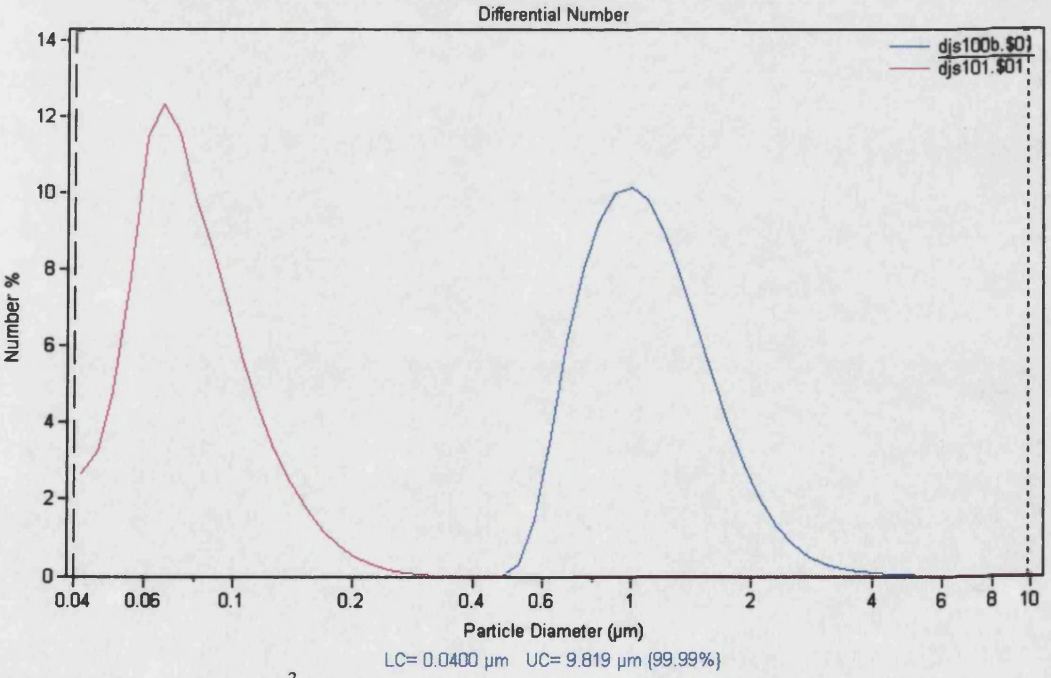

Graph 4.37 1.9×10^{-3} M potassium persulphate, after 10 minutes.

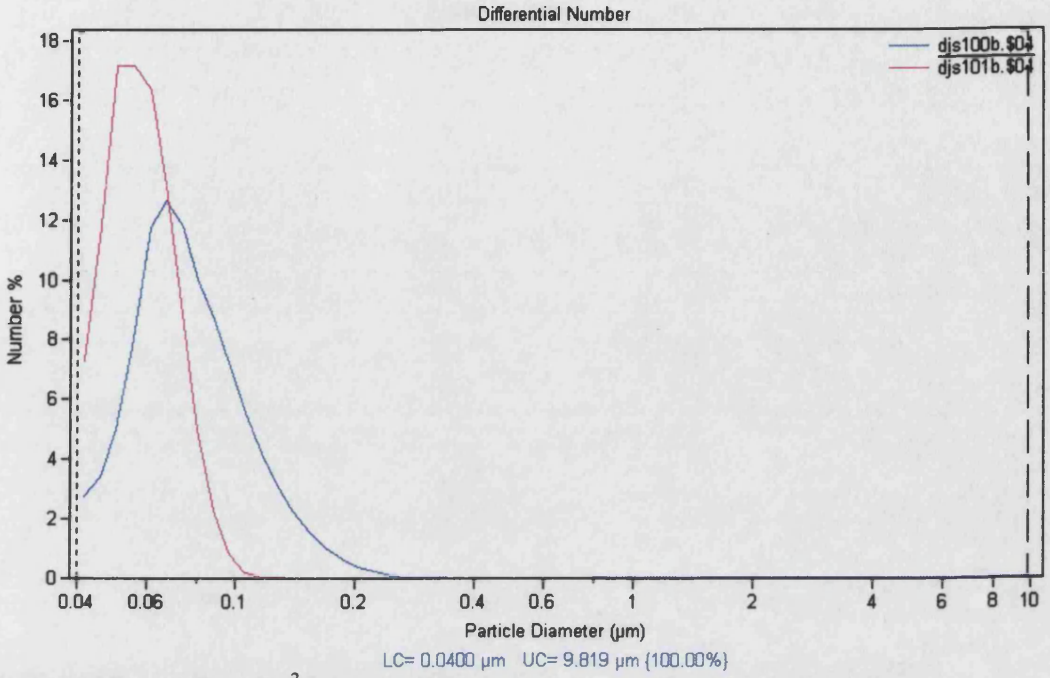

Graph 4.38 1.9×10^{-3} M potassium persulphate, after 20 minutes.

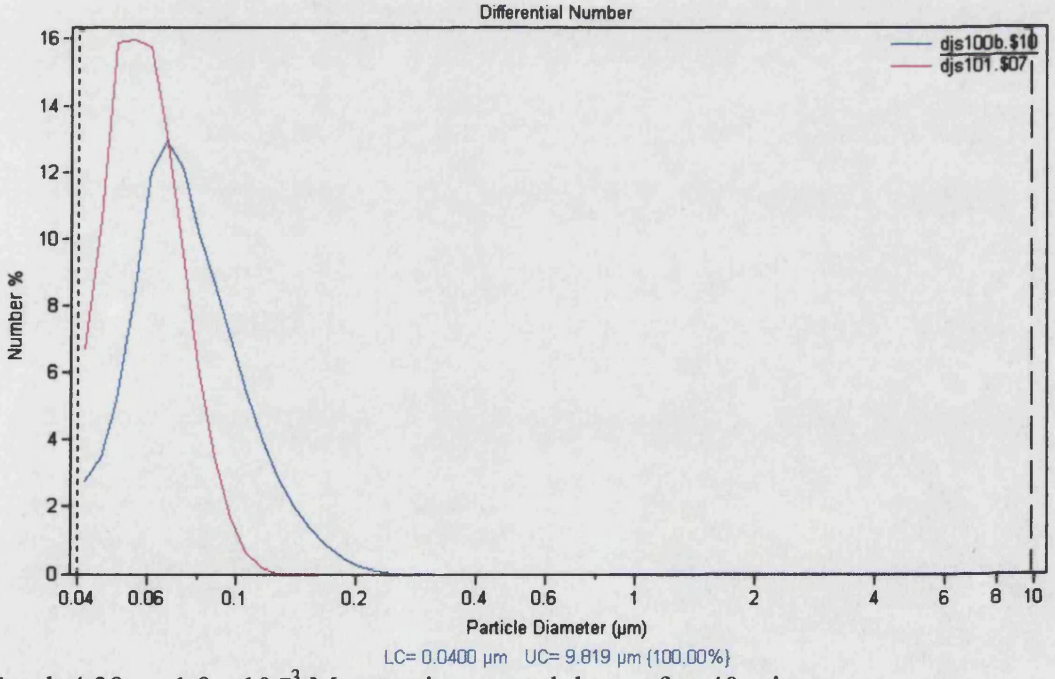

Graph 4.39 1.9×10^{-3} M potassium persulphate, after 40 minutes.

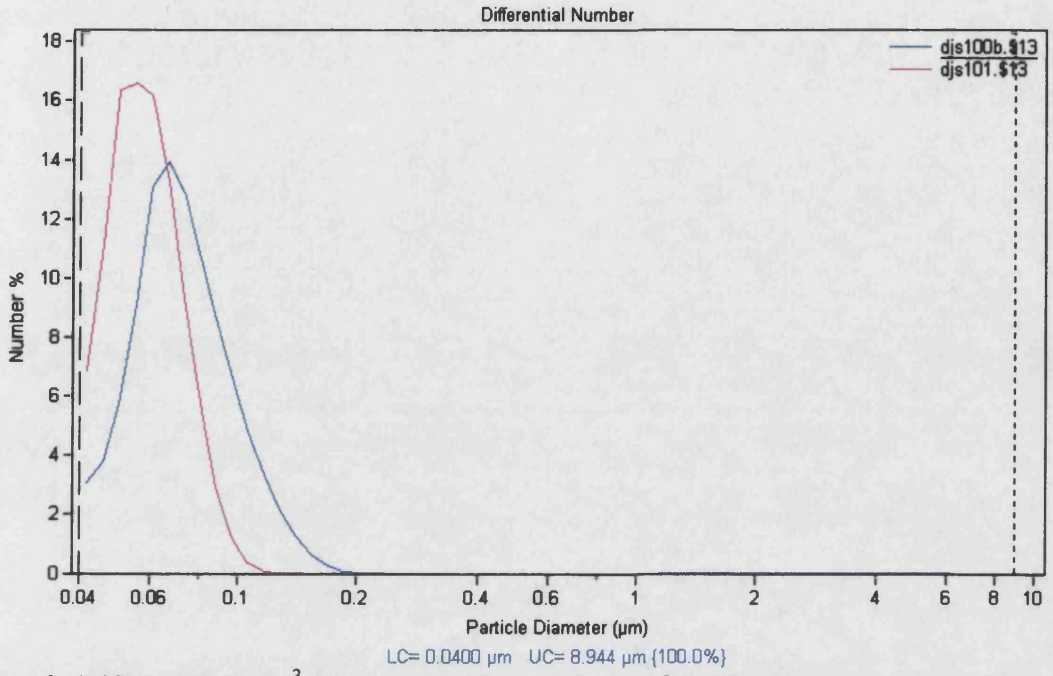

Graph 4.40 1.9×10^{-3} M potassium persulphate, after 60 minutes.

Ultrasonic reaction at 10.66 Wcm^{-2}.				Conventional reaction	
Time	D_n (µm)	$D_{(3,2)}$ (µm)		D_n (µm)	$D_{(3,2)}$(µm)
1	1.799	3.774		1.802	13.420
10	1.550	2.991		0.0807	0.4740
20	0.0809	0.804		0.0589	0.0639
40	0.0793	0.194		0.0604	0.0663
60	0.0754	0.108		0.0599	0.0655

Table 4.3 Average particle sizes for the reaction containing 1.9×10^{-3} M potassium persulphate.

As stated previously these results were surprising given the number of papers that detail how ultrasound can give a smaller particle size in comparison with mechanical agitation. If the Sauter diameter, $D_{(3,2)}$, is studied then there are, however, two issues here, the final particle size and the particle size after 1 minute. After 1 minute then through the use of ultrasound, a considerably smaller particle size is achieved than by mechanical agitation. This is in agreement with

the work conducted by Abismail et.al [173], who sonicated oil-in-water emulsions and studied the particle size every 5 seconds up to 30 seconds.

If the final particle size is studied then the number average and Sauter diameter both show that through the use of a conventional reaction then a smaller particle size is produced. This can be explained if the conditions of ultrasonic radiation are considered. As no gas is bubbling through the solution then transient cavitation is the major type of cavitation occurring within the reaction cell. Hence, higher temperatures, pressures and shear forces are generated when a bubble collapses [1]. This violent shearing action of ultrasound could be either forcing two micelles into each other, or shearing a micelle apart. Therefore causing an apparent increase in the particle size when compared with a conventional reaction.

This hypothesis was tested by comparing latex particles that had been produced, after four hours, in an ultrasonic reaction with those that had been produced in a conventional reaction in a transmission electron microscope (TEM), for an initiator concentration of 9.3×10^{-3} M. Figure 4.2 shows the latex as produced from a conventional reaction, 75°C and stirred. The most important point to note from the photograph is that the particles have a definite edge to them.

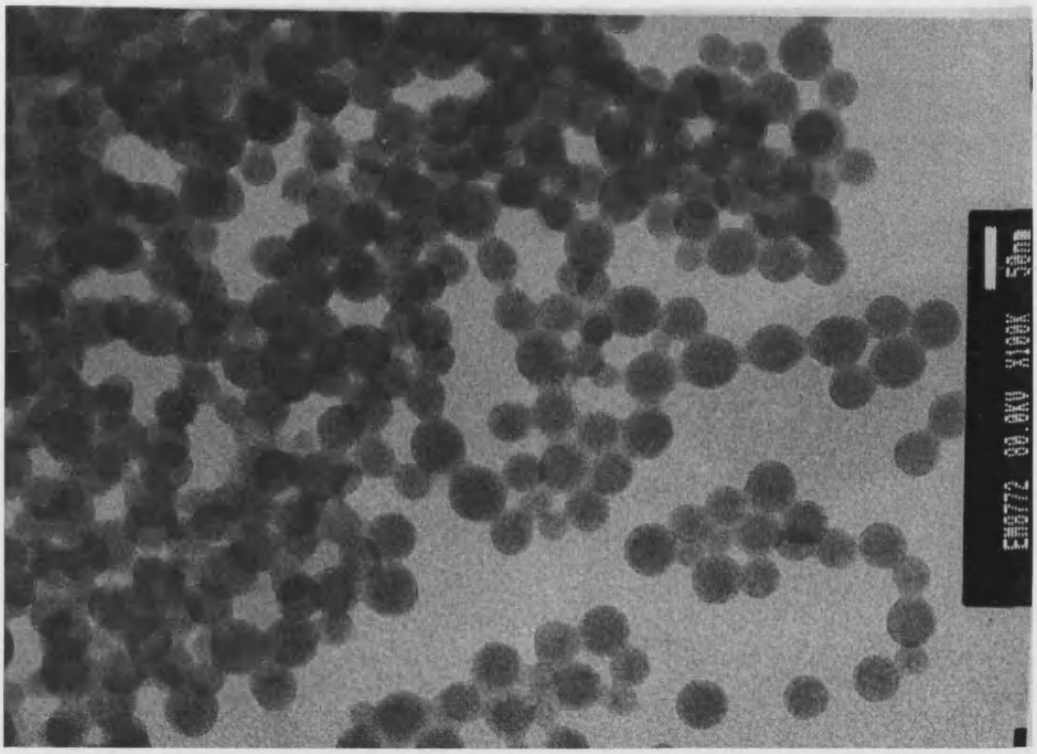

Figure 4.2 TEM image of the latex particles produced by a conventional reaction (100,000-x magnification).

If the magnification is increased to 200,000 then the latex particles can still be seen to have a definite edge to them, although, the carbon support grid becomes a problem for image clarity.

In comparison, those produced from an ultrasonic reaction the particles have a much softer, almost fuzzy outline to them, this is shown in figure 4.3.

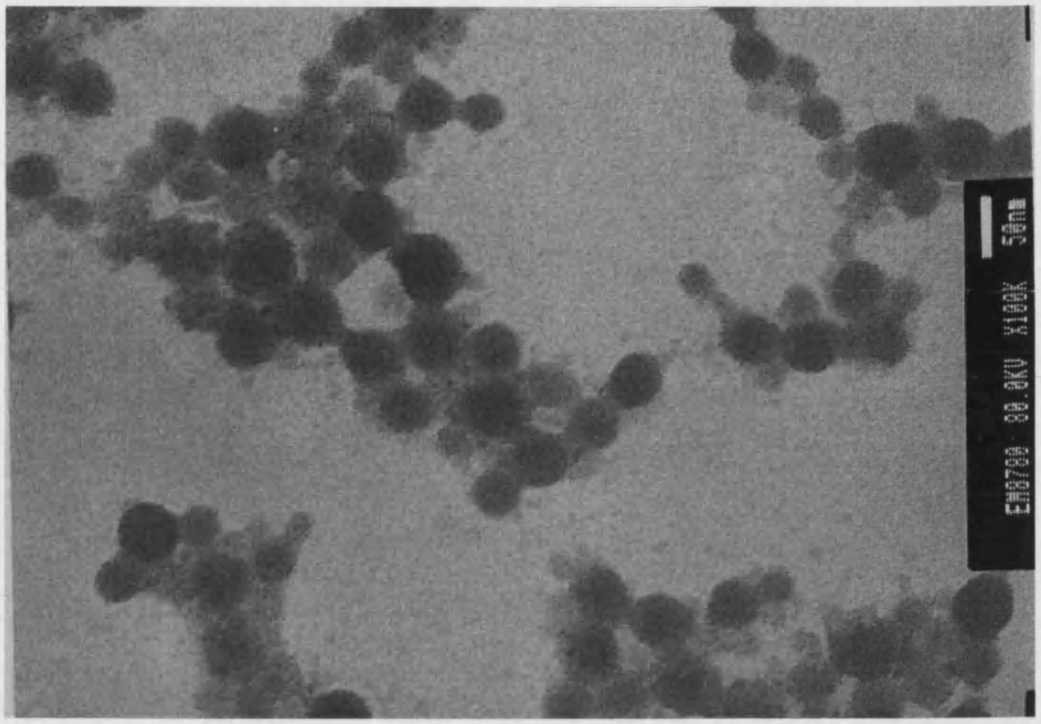

Figure 4.3 TEM image of the latex particles produced by an ultrasonic reaction (100,000-x magnification).

The merging of the latex particles can be seen in close up, as shown in figure 4.4. It is this forcing together of the latex particles which can account for the particle size results as obtained from the Coulter LS230 machine. As the Coulter machine relies upon the scattering angle of an incident beam of laser light, the assumption with the software that controls the optics and detectors is that the particle is spherical. As can be clearly seen from figures 4.4 and 4.5, when two particles are forced together the resultant particle is not always spherical.

This problem of different results from different methods is to be expected, also, even slight differences in sample handling can result in large disparities between results. Even during the early stages of light scattering the results obtained on standard Dow polystyrene latexes found the results to be generally lower, but within 10% of those obtained by electron microscopy [174]. Indeed, there is further evidence for the size disparity between electron microscopy and light scattering measurements [175].

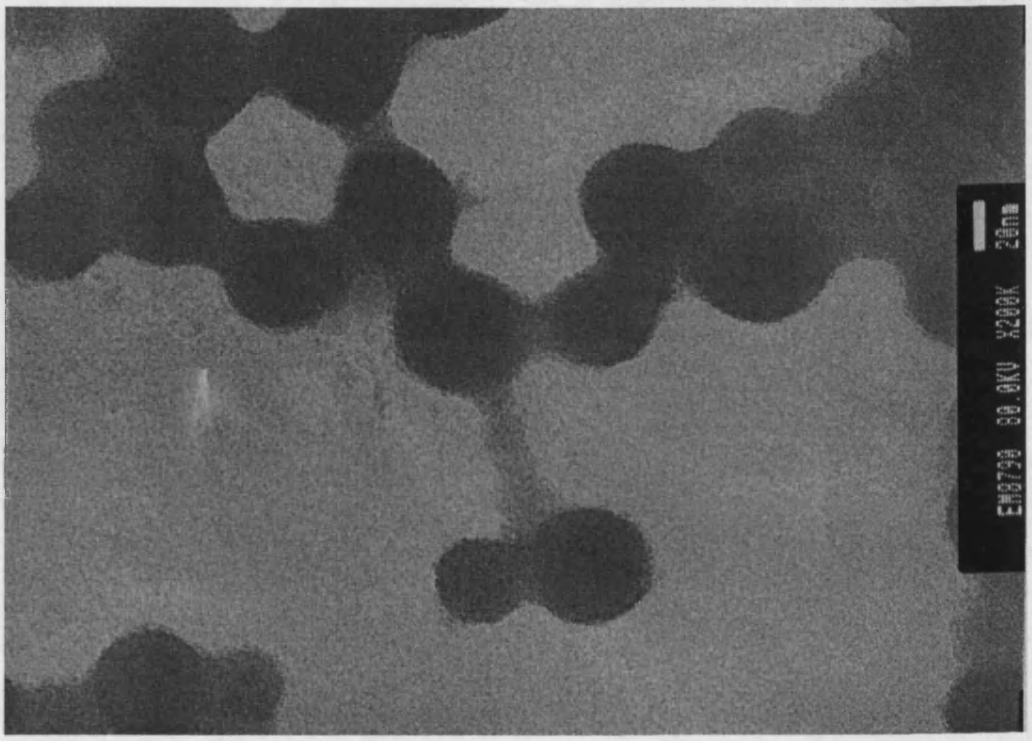

Figure 4.4 TEM image of the latex particles produced by an ultrasonic reaction (200,000-x magnification).

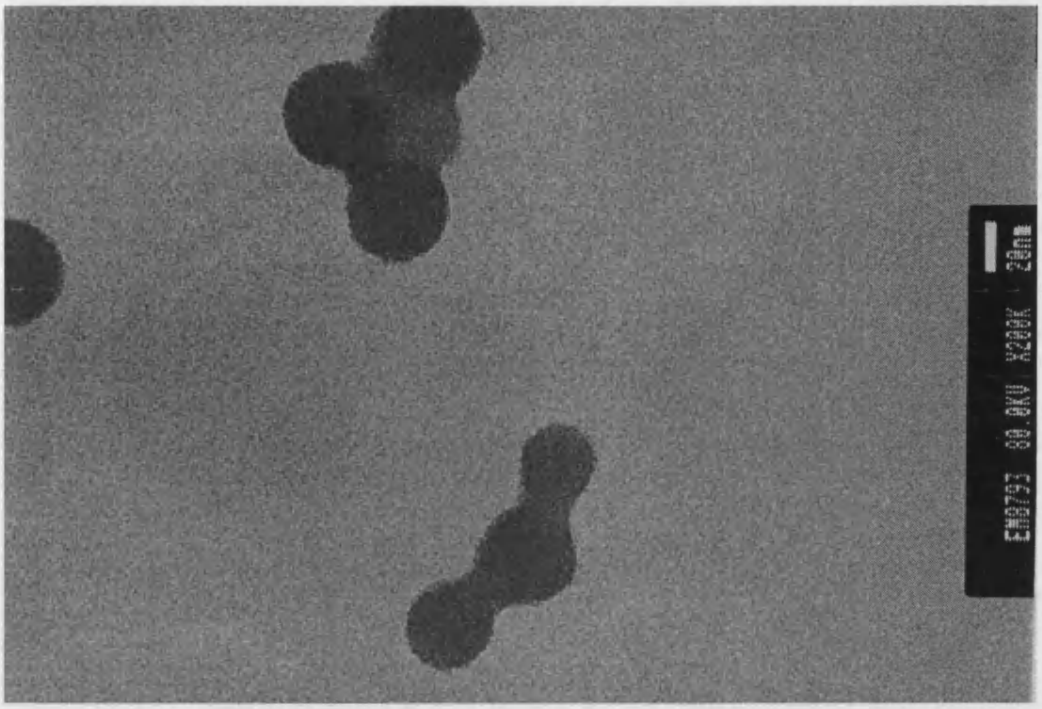

Figure 4.5 TEM image of the latex particles produced by an ultrasonic reaction (200,000-x magnification).

4.4.1.1 Calculation of the total number of latex particles for a change in the initiator concentration.

Using equation 4.7 the number of particles per unit volume can be calculated from the radius of the particle. This is summarised in table 4.4.

Initiator concentration ($moldm^{-3}$)	Ultrasonic reaction at 10.66 Wcm^{-2}	Conventional reaction at 75°C
4.63×10^{-4}	3.80×10^{22}	8.60×10^{22}
9.56×10^{-4}	3.80×10^{22}	7.87×10^{22}
1.85×10^{-3}	4.26×10^{22}	8.51×10^{22}

Table 4.4 Summary of the number of particles per unit volume for a change in the initiator concentration.

The calculation is dependent upon the radius of the particle and it is apparent that the polymer particle number per millilitre of water is typical of the values reported in other investigations of the emulsion polymerisation of styrene [163].

Although, there are only three different concentrations analysed, a graph of the log-log plot of the number of particles produced after sixty minutes of sonication shows it to be increasing to the 0.089 power.

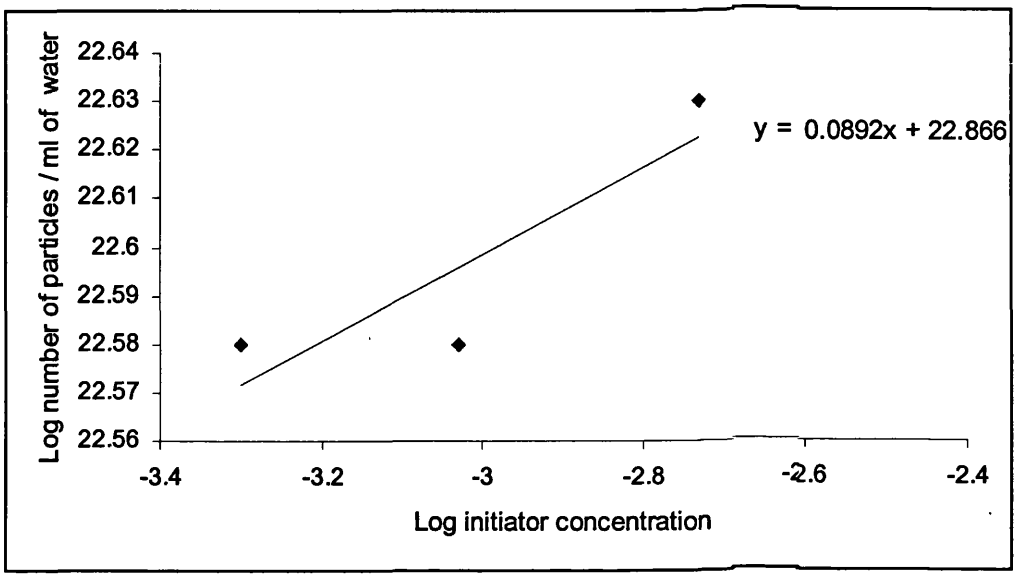

Graph 4.41 The Log –Log plot of the number of particles/ml of water and the initiator concentration for an ultrasonic reaction at 10.66Wcm^{-2}.

Initially this was surprising given that the initiator concentration is expected to change the number of particles to the 0.4 power. However, as stated earlier the Smith-Ewart derivation does contain a number of assumptions, one of these being the fate of radicals upon generation. In the Smith-Ewart theory a radical generated in the aqueous phase enters a monomer-swollen micelle and initiates the polymerisation. If radical absorption/desorption/reabsorption and droplet nucleation [164] occurs then equation 4.6 becomes equation 4.8 [176].

$$N_p = 0.53\left(\frac{\rho_r}{\mu}\right)^{(1-z)}\left(a_s[S]^{(z)}\right) \tag{4.8}$$

where $0.6 < z < 1.0$ and will depend upon the chain transfer constant and the water solubility of the monomer. However, this equation is valid for a conventional reaction, for an ultrasonic reaction where the rate of transfer across the two phases is increased due to the collapsing cavitational bubble the equation

may not be valid. Further concentrations are necessary to firmly establish the relationship.

4.4.2 Change of surfactant concentration.

The Smith-Ewart derived equation, (4.6), although not strictly applicable to an ultrasonic reaction, predicts that by increasing the surfactant concentration then the total number of particles will also increase to the 0.6 power. Therefore, changing the surfactant concentration will have a greater effect upon the particle size than changing the initiator concentration. The change in surfactant concentration is followed as in section 4.4.1.

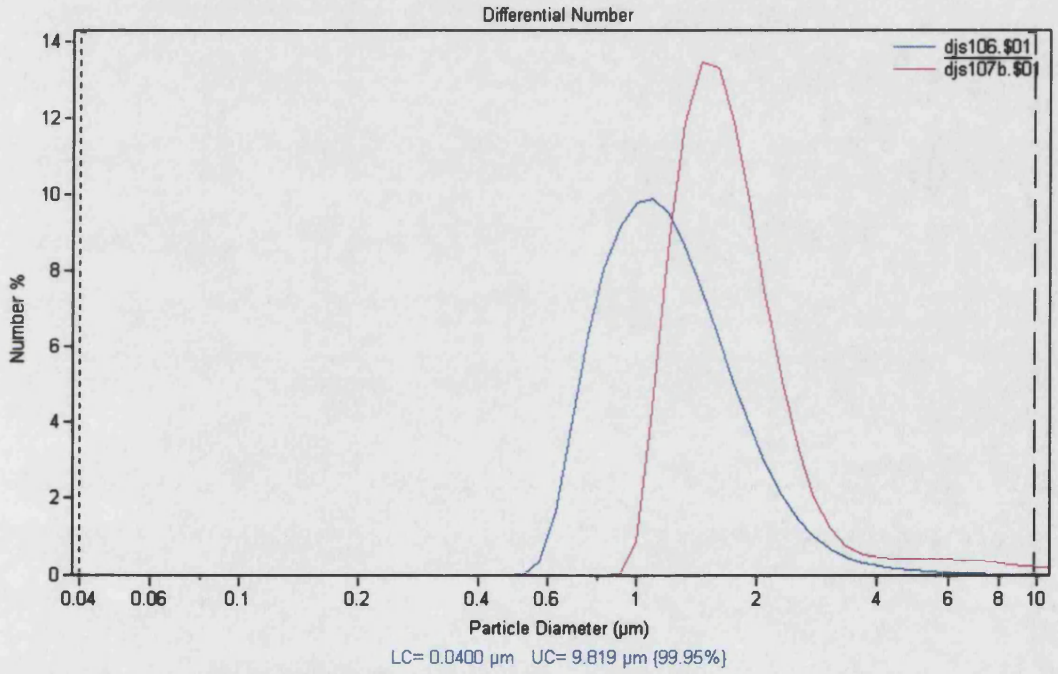

Graph 4.42 0.009 M of surfactant, after 1 minute.

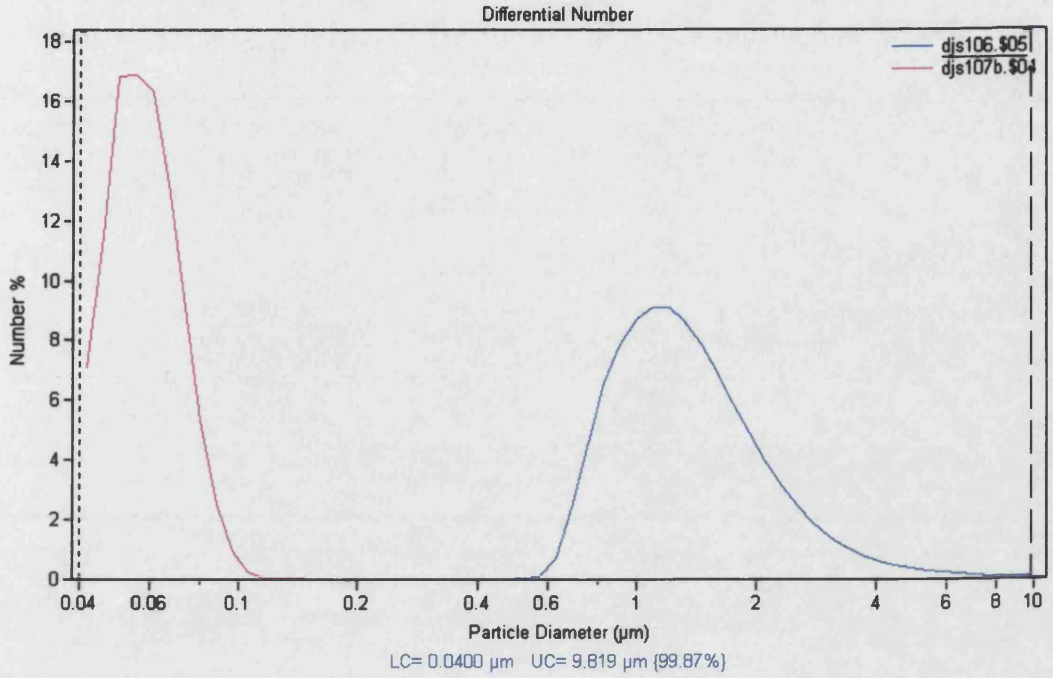

Graph 4.43 0.009 M of surfactant, after 10 minutes.

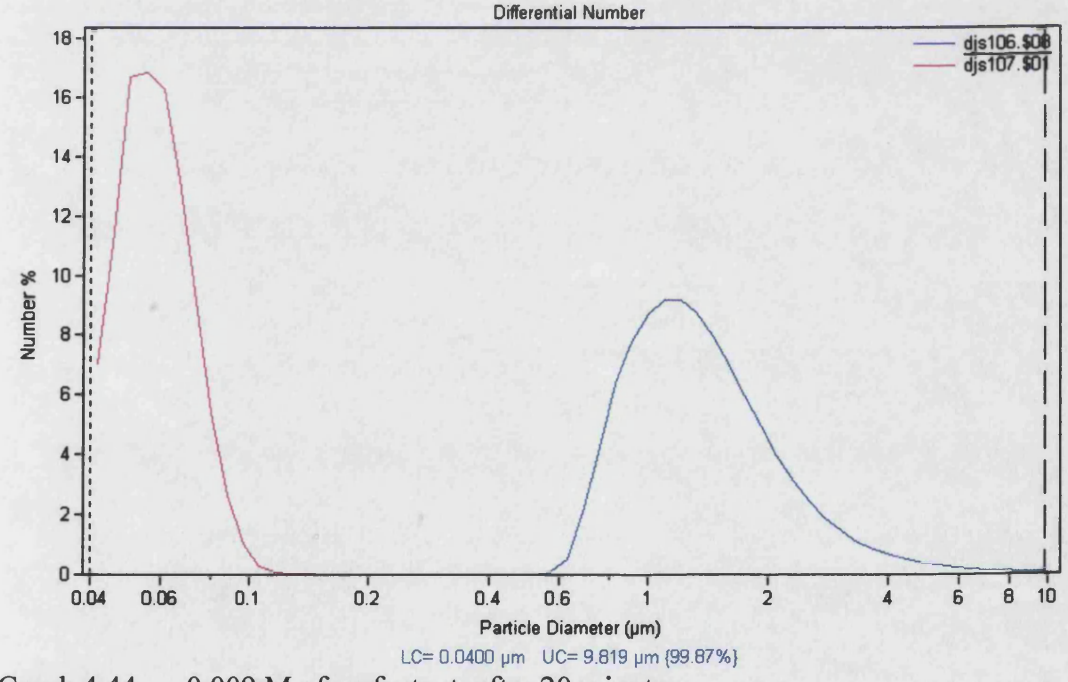

Graph 4.44 0.009 M of surfactant, after 20 minutes.

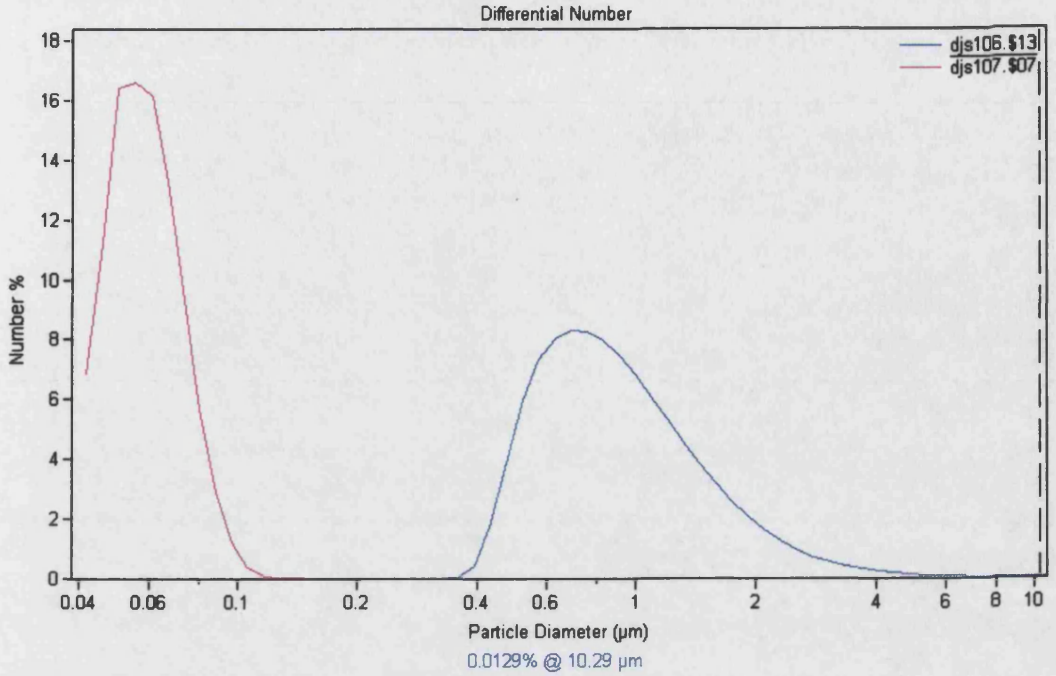

Graph 4.45 0.009 M of surfactant, after 40 minutes.

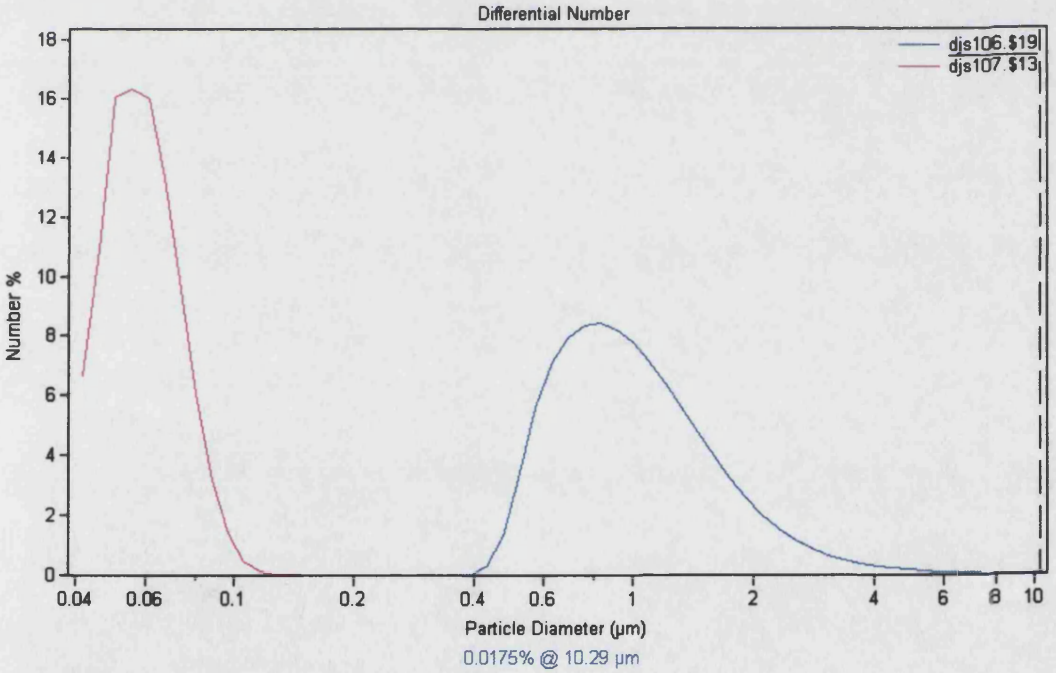

Graph 4.46 0.009 M of surfactant, after 60 minutes.

Ultrasonic reaction at 10.66 Wcm^{-2}			Conventional reaction	
Time (mins)	D_n (μm)	$D_{(3,2)}$ (μm)	D_n (μm)	$D_{(3,2)}$(μm)
1	1.469	2.692	1.564	3.141
10	1.574	2.870	0.0593	0.0645
20	1.533	2.916	0.0594	0.0647
40	1.401	3.424	0.0598	0.0653
60	1.415	3.488	0.0602	0.0660

Table 4.5 Average particle sizes for the reaction containing 0.009 M of surfactant.

The results for 0.0189 M of surfactant are shown in graphs 4.31- 4.35 and are summarised in table 4.5.

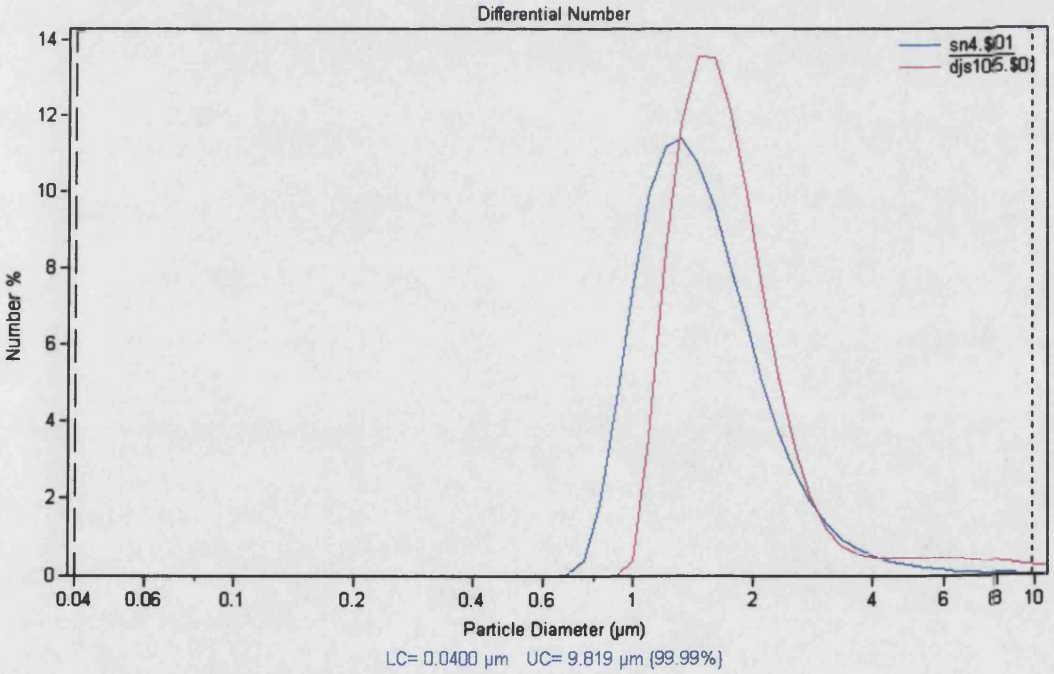

The results for 0.0377 M of surfactant are shown below;

Graph 4.47 0.0377M of surfactant, after 1 minute.

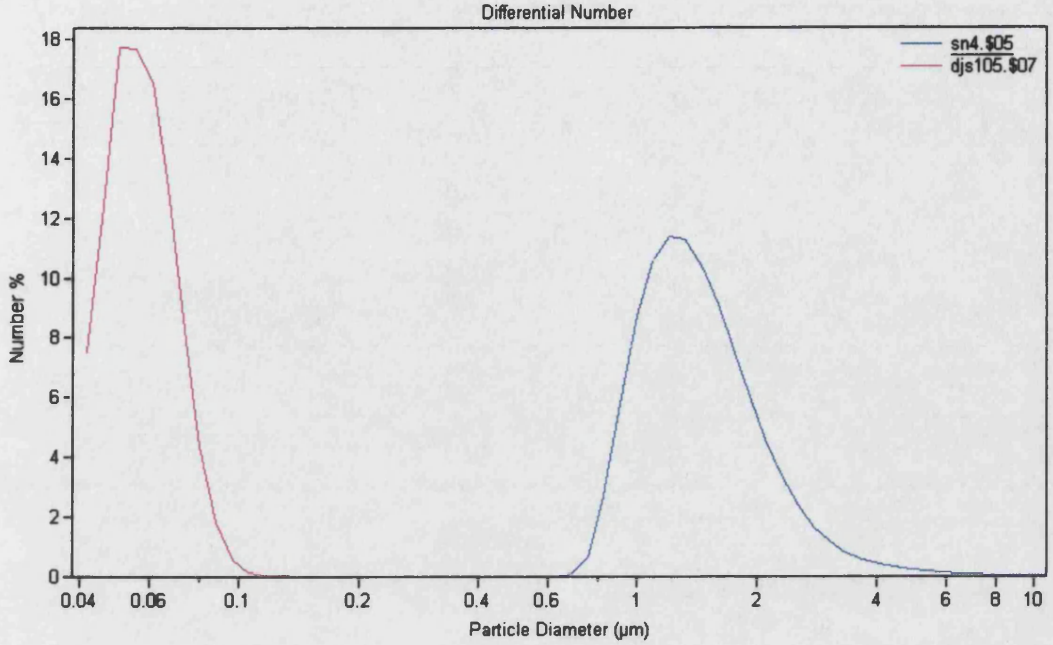

Graph 4.48 0.0377 M of surfactant after 10 minutes.

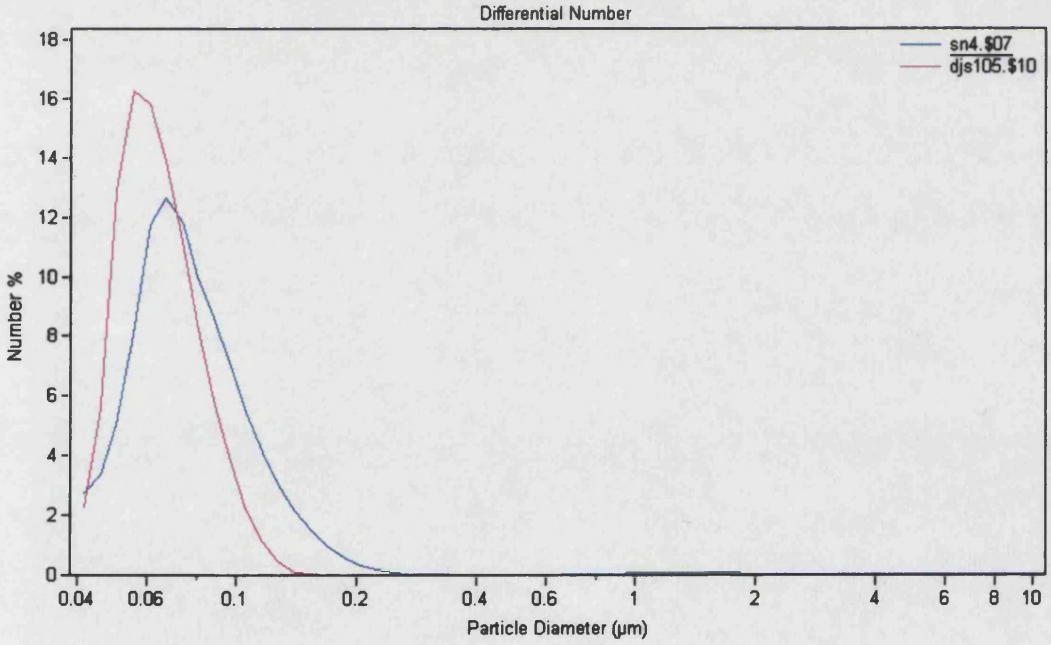

Graph 4.49 0.0377 M of surfactant after 20 minutes.

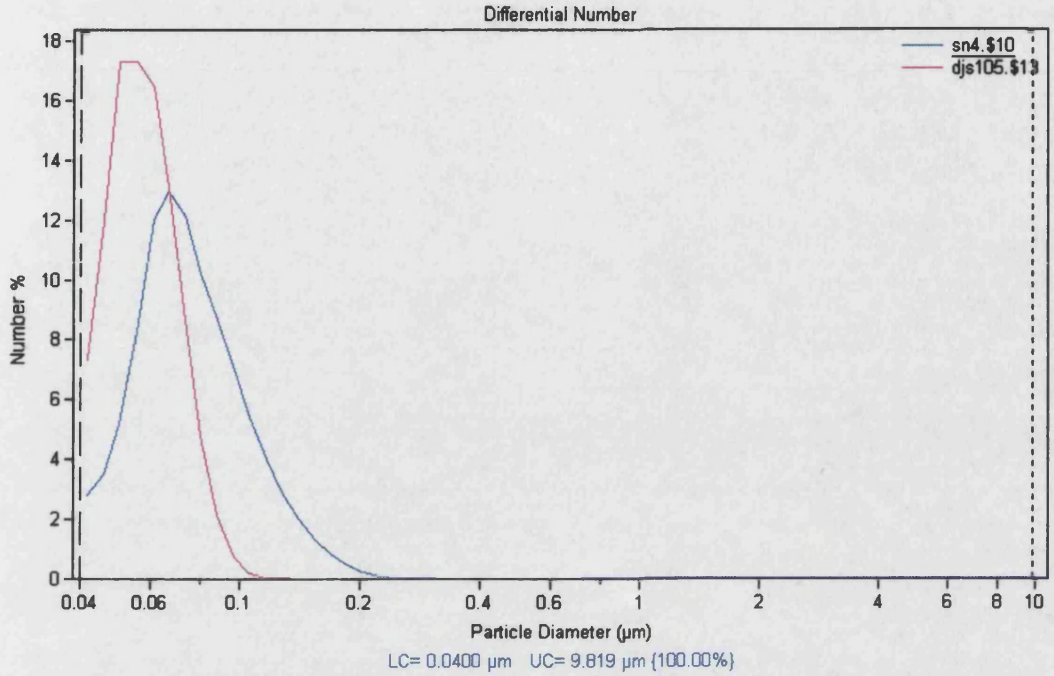

Graph 4.50 0.0377 M of surfactant after 40 minutes.

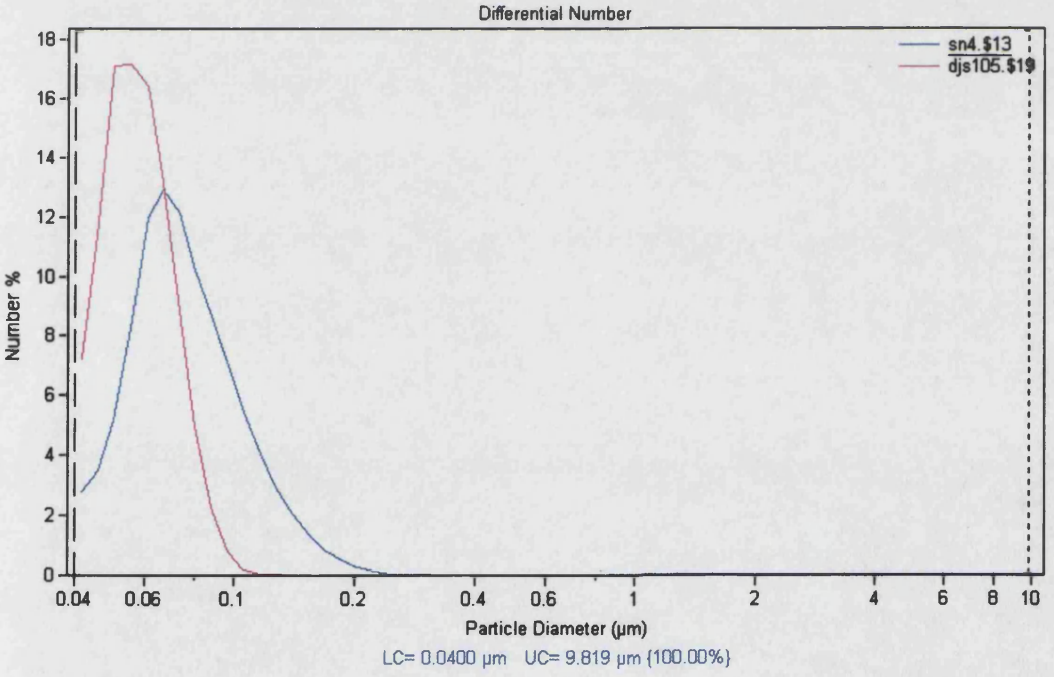

Graph 4.51 0.0377 M of surfactant after 60 minutes.

Ultrasonic reaction at 10.66 Wcm^{-2}			Conventional reaction	
Time (mins)	D_n (μm)	$D_{(3,2)}$ (μm)	D_n (μm)	$D_{(3,2)}$(μm)
1	1.595	2.712	1.769	10.368
10	1.560	2.549	0.0583	0.0630
20	0.0821	1.364	0.0615	0.0737
40	0.081	0.930	0.0588	0.0637
60	0.0802	0.423	0.0589	0.0639

Table 4.6 Average particle sizes for the reaction containing 0.0377 M of surfactant.

Again, this difference can be accounted for by the fact that the violent shearing action of the ultrasound causes the latex particles to be forced together as shown from the TEM pictures, figures 4.2- 4.5.

4.4.2.1 Calculation of the total number of latex particles for a change in surfactant concentration.

Using equation 4.7 the number of particles per unit volume can be calculated from the radius of the particle. This is summarised in table 4.7.

Surfactant concentration ($moldm^{-3}$)	Ultrasonic reaction at 10.66 Wcm^{-2}	Conventional reaction at 75°C
9.43×10^{-3}	6.46×10^{18}	8.39×10^{22}
1.89×10^{-2}	3.80×10^{22}	7.87×10^{22}
3.78×10^{-2}	3.545×10^{22}	8.95×10^{22}

Table 4.7 Summary of the number of particles per unit volume for a change in the surfactant concentration.

The calculation is dependent upon the radius of the particle and it is apparent that the polymer particle number per millilitre of water is typical to the values

reported in other investigations of the emulsion polymerisation of styrene [163]. Although, there are only three points on the graph the log-log plot of the number of particles produced after sixty minutes of sonication shows the number of particles as the CMC of the surfactant, SDS, is surpassed [163].

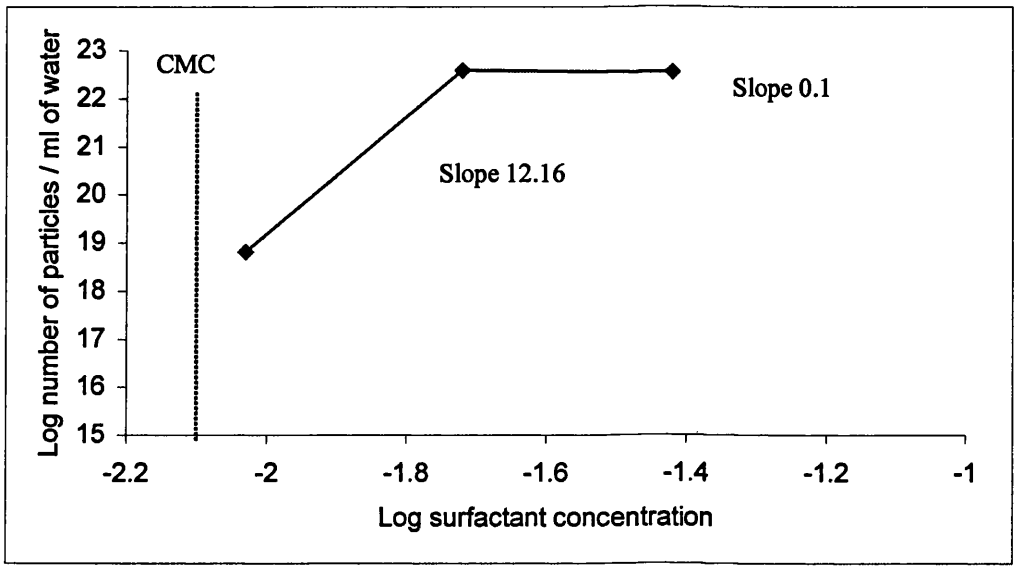

Graph 4.52 The Log –Log plot of the number of particles/ml of water and the surfactant concentration for an ultrasonic reaction at 10.66Wcm^{-2}.

The dependency of the number of particles upon the surfactant concentration is a similar shape to the log- log plot of Chou and Stoffer [169]. They found that the number of particles increased to the 0.3 power in the range of 0.035 M to 0.139 M and to the 1.87 power in the range 0.139 M to 0.243 M. The relationship shown in graph 4.52 implies that the number of particles and the polymerisation rate increases with surfactant concentration due to increasing radical capture by monomer droplets.

The total number of particles for a conventional reaction is similar to that calculated by a number of authors [163,164] and so will not be discussed further.

4.4.3 Effect of intensity upon the particle size.

As stated in section 4.2 the decrease of the ultrasonic intensity is predicted to lower the rate of formation of small monomer droplets capable of directly scavenging free radicals. This is due to the longer time taken to shear large monomer droplets. Therefore, the ultrasonic intensity was reduced from 10.66 to 5.61 Wcm^{-2}, for an initiator concentration of 9.3×10^{-4} M and a surfactant concentration of 1.89×10^{-2} M. Time points of 1, 10, 20, 40 and 60 minutes were recorded. The blue line representing the intensity of 10.66 Wcm^{-2} and the red line representing the intensity of 5.61 Wcm^{-2}.

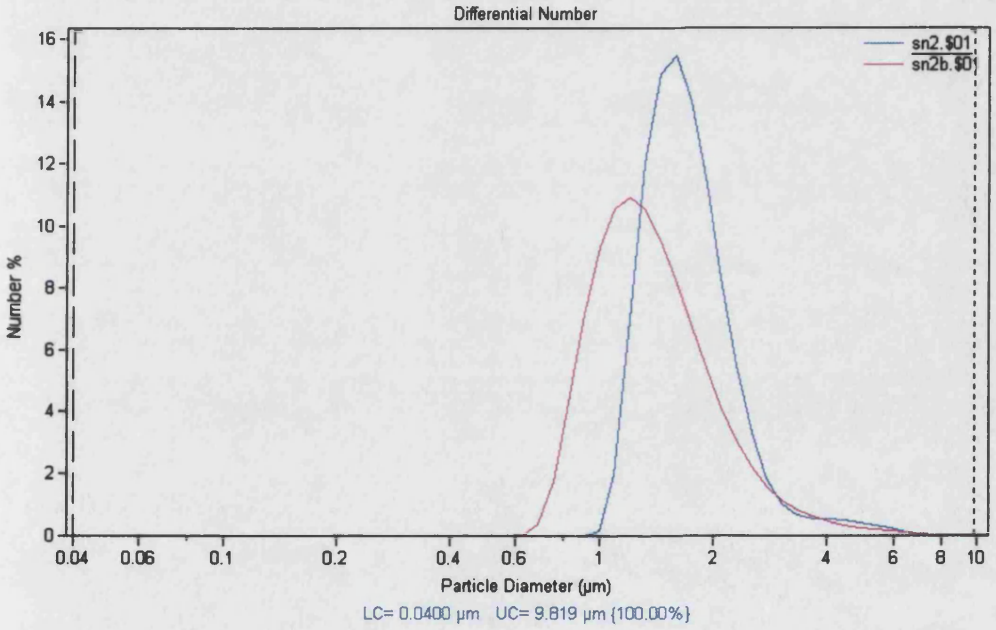

Graph 4.53 Change of intensity after 1 minute.

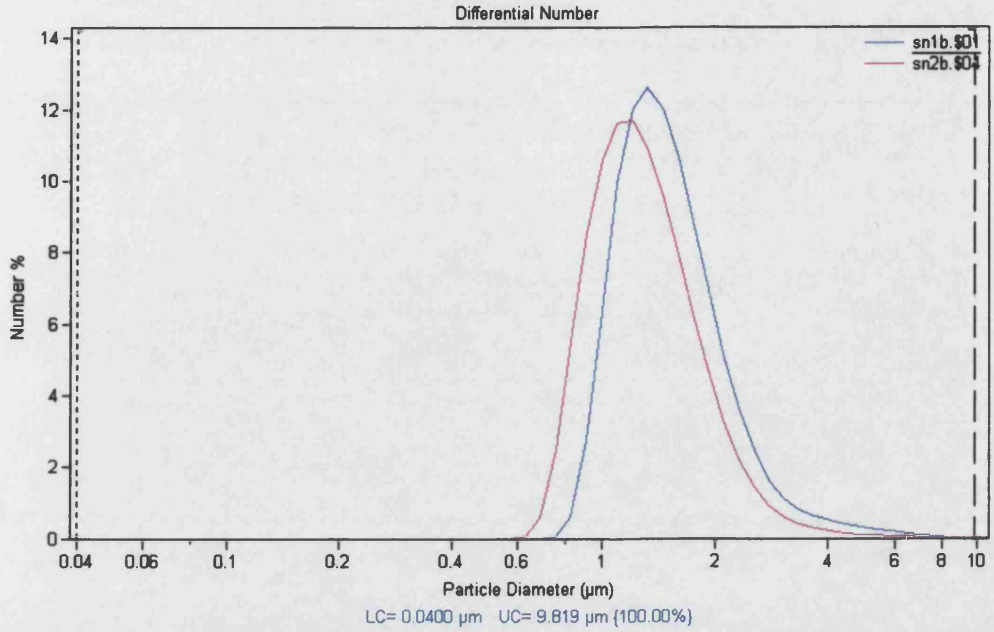

Graph 4.54 Change of intensity after 10 minutes.

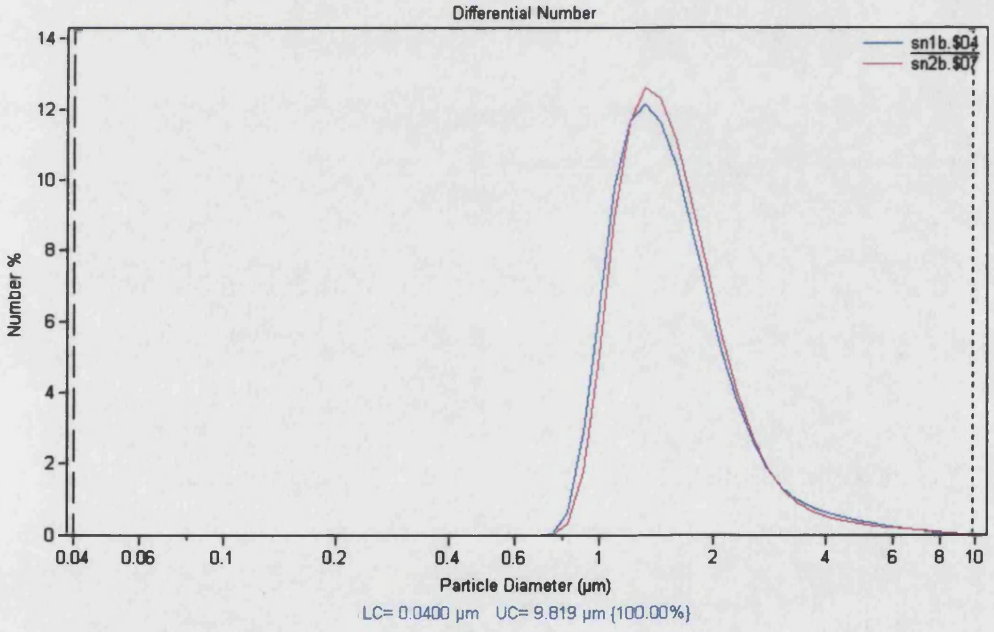

Graph 4.55 Change of intensity after 20 minutes.

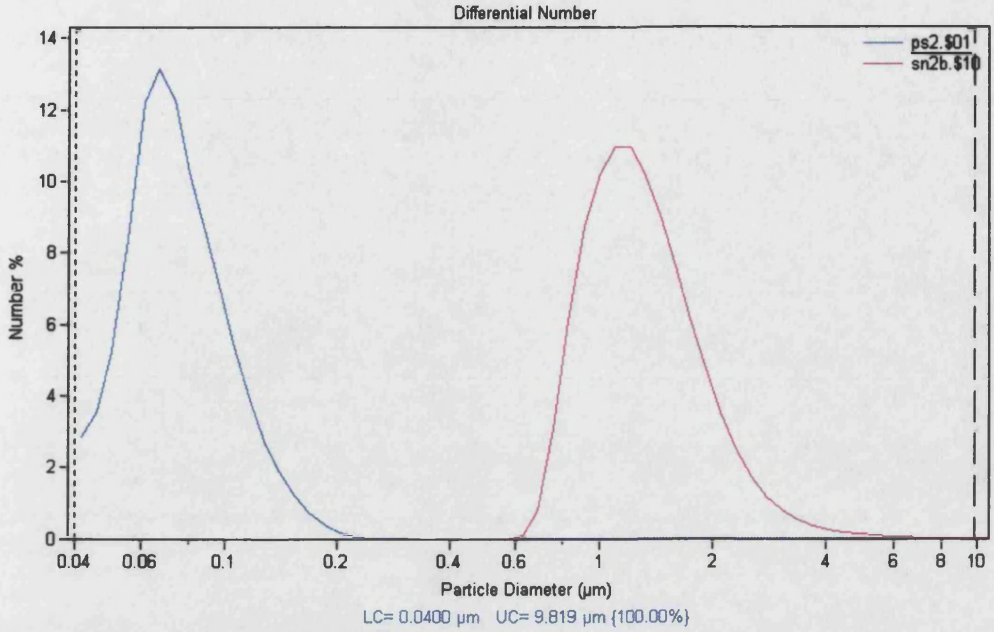

Graph 4.56 Change of intensity after 40 minutes.

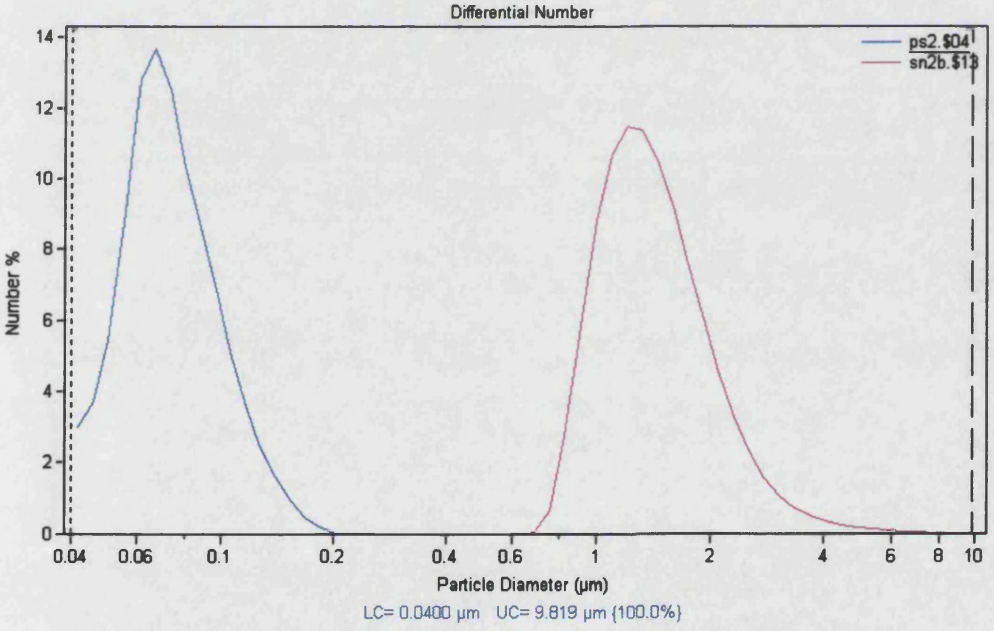

Graph 4.56 Change of intensity after 60 minutes.

These results are summarised in table 4.8.

Ultrasonic reaction at 10.66 Wcm^{-2}			Ultrasonic reaction at 5.61 Wcm^{-2}	
Time	D_n (μm)	$D_{(3,2)}$ (μm)	D_n (μm)	$D_{(3,2)}$(μm)
1	1.832	2.359	1.508	2.447
10	1.665	2.625	1.302	2.011
20	1.679	2.9	1.678	2.689
40	0.0684	0.303	1.403	2.146
60	0.0784	0.403	1.525	2.251

Table 4.8 Average particle sizes for the reaction containing 9.3×10^{-4} M of initiator and 1.89×10^{-2} M of surfactant.

If the total number of particles is calculated, using equation 4.7, then in comparison with the 3.80×10^{22} particles that are present for the reaction at 10.66 Wcm^{-2} there are only 6.15×10^{17} particles for the reaction at 5.61 Wcm^{-2}, after 60 minutes. This reduction in the total number of particles explains the reduced rate of reaction for the ultrasonic reaction at the reduced intensity.

4.4.3 Effect of ultrasound upon a pre-formed latex.

From the particle size work initially conducted and the TEM photographs, it was suggested that the latex particle size could be changed by the action of ultrasound. Therefore, taking a latex that had been prepared by a conventional reaction, i.e. as described in section 2.5, thoroughly de-oxygenating the system and then applying an ultrasonic field of 10.66 Wcm^{-2} intensity any change in the particle size could be monitored. The comparison of the latex prior to sonication, (red line) and after 120 minutes of sonication (blue line) is shown in graph 4.51.

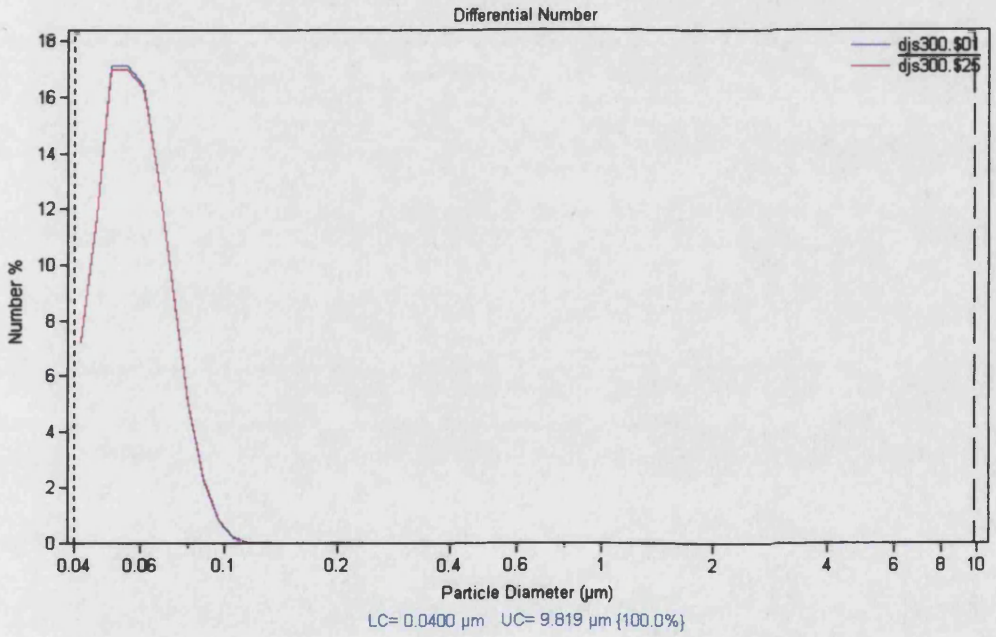

Graph 4.51 Comparison of a pre-formed latex after 120 minutes of sonication (10.66 ±0.6 Wcm^{-2}).

This result was quite surprising, given how during an ultrasonic reaction the latex particles are forced together. However, if the monomer conversion for a conventional reaction is considered then after four hours the conversion has reached 100%. Therefore the latex shell will be composed of polymer, whereas, in a reaction which is still polymerising the shell is surrounded by surfactant which can be easily removed, thus causing two growing chains to coalesce.

Although the particle size is not affected by the action of ultrasound the molecular weight is significantly affected. From the same reaction samples were

withdrawn and 1cm^3 was added to methanol in order to recover the polymer. These samples were analysed courtesy of RAPRA using a PL gel 2*x* mixed bed column 30 cm long @10 microns., with THF set at 1cm^3 per minute as the carrier flow rate. The results are shown in table 4.9.

Time (hours)	M_w	M_n	Polydispersity
0	1,285,000	213,000	6.05
1	1,155,000	196,000	5.85
1.5	698,500	161,000	4.35
2.5	613,500	111,500	5.55
4	814,500	153,500	5.3

Table 4.9 Change in molecular weight with time for a pre-formed latex, after 4 hours of sonication at 10.66 Wcm^{-2}.

This process of changing the molecular weight by ultrasound is well documented [13]. The action involves the longer, higher molecular weight chains breaking due to their poor extensional flow properties when a cavitation bubble collapses near to them. The result of this is that the GPC molecular weight is seen to decrease. This is the process that is occurring here.

Several workers have studied the degradation of polymers in ultrasound. Indeed the effect of intensity and temperature has been studied for a wide number of systems including solutions of polystyrene in toluene [1,13]. For this reason the intensity, although not possible to be increased, was changed to 5.61 Wcm^{-2}. The graph of the particle size distribution is shown in graph 4.52.

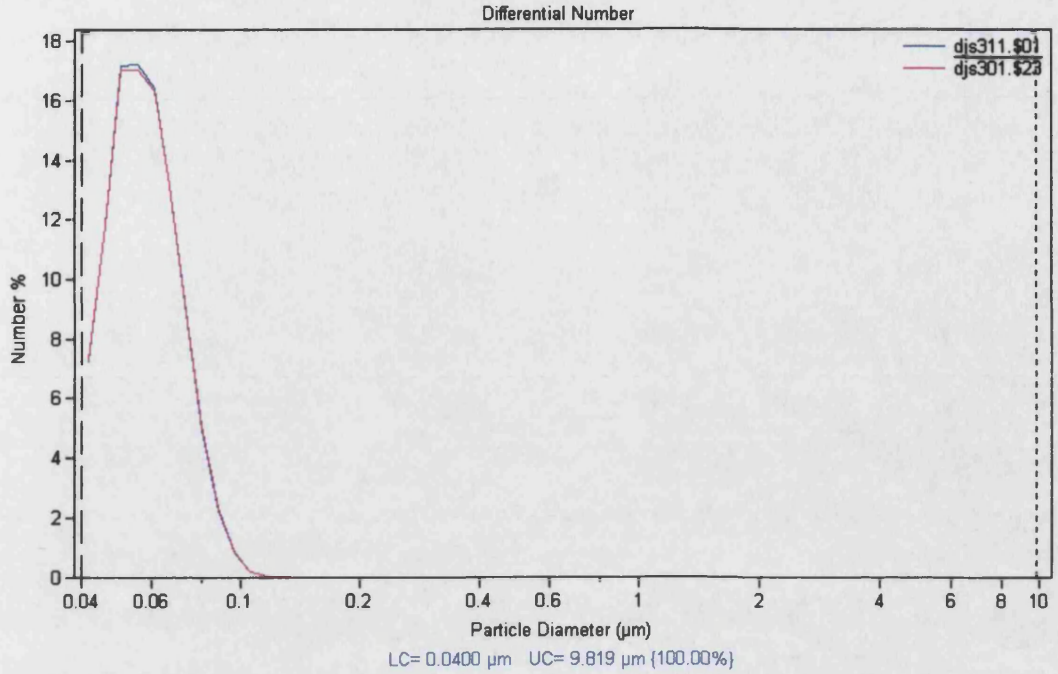

Graph 4.52 Comparison of a pre-formed latex after 120 minutes of sonication ($5.61 Wcm^{-2}$).

This result was expected after sonicating the system at $10.66 Wcm^{-2}$ and not finding any change in the particle size. The molecular weight data were again processed courtesy of RAPRA using the same conditions outlined above. The data is summarised in table 4.10.

Time (hours)	M_w	M_n	Polydispersity
0	1,245,000	300,000	4.15
1	911,000	184,000	4.95
1.5	1,155,000	198,000	5.83
2.5	1,190,000	245,500	4.85
4	1,240,000	182,500	6.8

Table 4.10 Change in molecular weight with time for a pre-formed latex, after 4 hours of sonication ($5.66 \pm 0.35 Wcm^{-2}$).

Although, not as dramatic as the results shown in table 4.8, the change in M_n can be seen.

4.5 Conclusions

Through the collapse of cavitation bubbles, caused by the compression cycle of an ultrasonic wave, high shear rates are set up and radicals are generated within the system. It is these factors which are the cause of the monomer conversion in an emulsion polymerisation. Due to the high shear rates in an ultrasonically assisted polymerisation there is switching of the particle formation mechanism from micellar to a droplet nucleation. Evidence for this comes from the high molecular weights that are produced in an ultrasonic reaction. An ultrasonic reaction yields a molecular weight of ~2.25 $x10^6$, whereas a conventional reaction yields a molecular weight of $1x10^6$. It is this increase in the molecular weight that caused a number of problems when it came to analysing the resultant polymer. Further evidence for a droplet nucleation pathway comes from the ultrasonic reaction where the surfactant concentration is reduced to 9.43 x 10^{-3} $moldm^{-3}$ (0.5g). Here the monomer conversion is significantly reduced even though the CMC of the surfactant was surpassed.

Decreasing the ultrasonic intensity lead to a decrease in the monomer conversion for all reactions. Typically decreasing the intensity from 10.66 Wcm^{-2} to 5.61 Wcm^{-2} decreased the monomer conversion by 40 %, but the molecular weight of the resultant polymer was comparable at both intensities. Due to the experimental design 10.66 Wcm^{-2} was the maximum power that could be delivered to the system, although Chou and Stoffer [**Error! Bookmark not defined.**,169,] suggested that the polymerisation rate increased up to a limiting point of 13.0 Wcm^{-2}. Beyond this point no further benefit was obtained as is usual for sonochemical reactions [13]. The reason for the decrease in monomer conversion is due to the decrease in the ratio of small monomer droplets and hence the total number of polymer particles. This in turn affects the number of primary sites available for radical capture due to the decrease in the relative surface area.

Increasing the temperature of the bulk reaction increases the rate of monomer conversion in an ultrasonic and conventional reaction. For any given time point the ultrasonically assisted polymerisation has a higher monomer conversion than for a conventional reaction. Typically performing a reaction at 25°C at an

intensity of 10.66 Wcm^{-2} is equivalent to carrying out a conventional reaction at 45°C. This gives the possibility of using ultrasound to accelerate the polymerisation and offer energy savings.

Through the use of a Coulter particle size machine the particle size of a number of latex samples was analysed. Although the results generated by the machine show that a slightly smaller particle size is obtained by a conventional reaction at 75°C, rather than through the use of ultrasound, TEM photographs show some of the particles being forced together. It is proposed that the action of the collapsing cavitation bubble causes two or more latex particles to come together and form a larger particle. Thereby causing the optics of the Coulter particle size machine to record a larger particle size. This is the first time that this occurrence has been seen in an emulsion polymerisation.

There is much scope for further work in this aspect of the project. Although styrene has been studied here, an almost water insoluble monomer, hydroxy-ethyl metha acrylate (HEMA), a water soluble monomer, could be investigated. As HEMA is soluble in water the phase properties in an emulsion polymerisation are rather different and therefore the increased mass transport which ultrasound gives offers less of an advantage.

The molecular weights achieved through the use of an emulsion polymerisation are much higher than those achieved for a similar reaction performed in a bulk polymerisation. For this reason it is common to use a charge transfer agent to limit the molecular weight. Haddleton et al.[177,178] have been making novel charge transfer agents and testing how they limit the molecular weight of a styrene emulsion polymerisation. Their conclusion is that the rate of diffusion between the phases is the limiting factor in affecting the molecular weight. The increased mass transport that ultrasound can give is an effective method to determine if that hypothesis is correct.

Other forms of polymerisation could also be investigated in the future such as suspension polymerisations and recently there has been a report that atom

transfer radical polymerisation can be performed in an emulsion [179]. The radical nature of this form of polymerisation is a subject of some debate and therefore through the use of ultrasound the reaction rate could be increased, indicating if the reaction does go via a radical step.

These results show that ultrasound can increase the rate of polymerisation of a styrene emulsion polymerisation and significantly increase the molecular weight of the resultant polymer. The possibility of performing the reaction with reduced amounts of surfactant and initiator can be achieved through the use of ultrasound.

5.0 Copolymerisation of styrene with acrylates.

In the previous chapter the emphasis has been upon the polymerisation of a single monomer to produce a homopolymer. These homopolymers have proven useful for a myriad of applications. However, for some applications it is desirable to have a range of properties which cannot be satisfied by a homopolymer. The development and use of copolymers has therefore become widespread as they can have characteristics of their components.

Copolymerisation is therefore important from a technological viewpoint. It greatly increases the ability to tailor make a polymer product with specifically desired properties. An example of this is the case of polystyrene, which is a brittle plastic with poor impact strength and poor solvent resistance hence it has limited practical utility. Copolymerisation of styrene with acrylonitrile leads to improved impact and solvent resistance, while copolymerisation with butadiene leads to elastomeric properties. Styrene copolymers are useful not only as plastics but also as elastomers.

Very early in the development of copolymers [100] it was realised when two monomers copolymerise the tendency of each monomer to enter the chain can differ markedly. This is due to the greater reactivity of one of the monomers in the reaction, thereby changing the feed ratios of the monomers. This phenomenon known as composition drift is a feature of many copolymerisations. The value of these monomer reactivity ratios is of great interest, in order to understand how the feed composition affects the final polymer structure.

In order to highlight any difference using ultrasound would have in an emulsion copolymerisation reaction, butyl acrylate and methyl methacrylate, were chosen to be copolymerised separately with styrene. Styrene and butyl acrylate are both sparingly soluble in the aqueous phase (3.6×10^{-3} and 6.4×10^{-3} moldm^{-3} in water at 50°C respectively) whereas methyl methacrylate does have a significant solubility in the aqueous phase (1.5×10^{-1} moldm^{-3}). Thus any differences, between the calculated reactivity ratios would be due to changes in the

polymerisation loci, from an emulsion to a microemulsion system, caused by the reduction of the particle size by ultrasound. Any differences should be highlighted through the use of these two acrylates. A further study upon the intensity effects of ultrasound upon the styrene/butyl acrylate system was also carried out.

5.1 Calculation of reactivity ratios.

As explained in section 1.13, the Kelen-Tudos equation is used throughout this work in order to determine the reactivity ratios. This is the preferred method as it is a non linear least squares method, thus giving equal weighting to all experimental points. The Kelen-Tudos equation is shown in equation 5.1.

$$\eta = \left(r_A + \frac{r_B}{\alpha}\right)\xi - \frac{r_B}{\alpha} \tag{5.1}$$

Where

$$\eta = \frac{G}{\alpha + F} \qquad \xi = \frac{F}{\alpha + F} \tag{5.2}$$

and G = h(H-1)/H and F = h^2/H, with h being the monomer feed ratio and H being the copolymer feed ratio. A plot of η against ξ should give a straight line with intercepts of $-r_B/\alpha$ and r_A at ξ=0 and ξ=1 respectively. A value of α of $(F_{max} * F_{min})^{1/2}$ results in equal weighting of the experimental data.

The monomer feed ratio can be calculated easily from the known mass of monomer charged into the reaction vessel. The copolymer composition can be readily determined from the proton nuclear magnetic resonance spectrum, ^{1}H NMR. For the purposes of this study the chemical shift of the phenyl protons and that of the methyl protons were measured, a typical spectrum is shown in figure 5.1. The styrene molar fraction (F_{st}) in the copolymer was calculated from the peak area of the protons due to the phenyl group (A_p) and the peak area of methyl protons in both methyl methacrylate and butyl acrylate (A_m), through use of equation 5.3.

$$F_{st} = \frac{3 * A_p}{(3 * A_p) + (5 * A_m)} \qquad (5.3)$$

5.2 Copolymerisation of styrene with butyl acrylate.

The copolymerisation of styrene and butyl acrylate in an emulsion system has been carried out. Using the experimental apparatus as shown in figure 2.1 and a Sonics and Materials VC 600 horn, the system was flushed with nitrogen for thirty minutes prior to switching on the ultrasound. The mixed monomers (25g) were added to 75g of Milli-Q distilled and de-ionised water containing 3 wt% sodium dodecyl sulphate (SDS), 0.05g sodium hydrogen sulphate and 0.05g of potassium persulphate. In order to restrict the monomer conversion to below 10%, so that the assumptions in the copolymerisation equation are valid, the ultrasound was switched off after 15 minutes. This corresponded to a monomer conversion of approximately 5 – 7 %. A total of nine experiments were carried out for the monomer pair, in order to obtain sufficient samples to calculate the reactivity ratios.

Figure 5.1 shows a typical ^{1}H NMR spectrum of a styrene/butyl acrylate copolymer. Using the method described in equation 5.1, the styrene molar fraction in the copolymer was calculated from the peak area of the protons due to the phenyl group (A_p) at ~7ppm and the peak area of the methyl group (A_m) at ~ 0.9ppm, in the butyl acrylate. These can be related by equation 5.3.

Figure 5.1 A typical ^1H NMR styrene/butyl acrylate copolymer.

A summary of the styrene molar fraction in the copolymers is shown in table 5.2.

Styrene/Acrylate feed ratio (v/v)	Peak height of A_p	Peak height of A_m	$F_{(st)}$
10/90	45	62	0.303
20/80	42.5	36	0.415
30/70	52	29	0.518
40/60	62.5	26	0.591
50/50	83	21.5	0.613
70/30	119	19.5	0.745
80/20	110	14	0.825
90/10	123	11.5	0.865

Table 5.1 The mole fraction of styrene in the poly(styrene-butylacrylate) copolymer prepared using an intensity of 23.8 ± 1.72 Wcm^{-2}.

The reactivity ratios for a styrene (r_A)/butyl acrylate (r_B) emulsion can now be calculated from the graph of η against ξ, as described in equation 5.1. This is shown in graph 5.1. From the graph the values of r_A and r_B are 0.775 ±0.07 and 0.200 ±0.006 respectively.

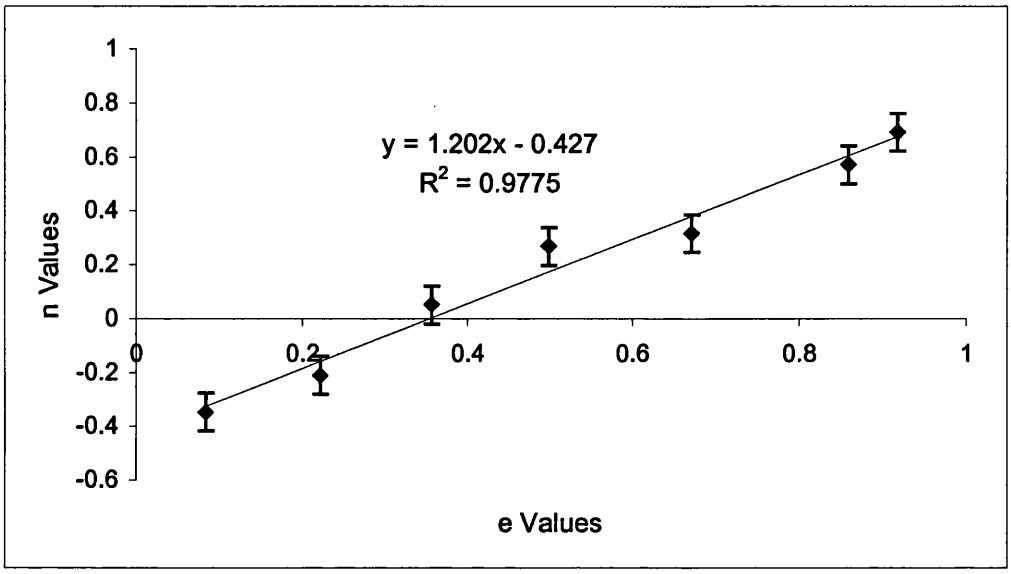

Graph 5.1 A graph to calculate to the reactivity ratios for a styrene/butyl acrylate copolymerisation

Before a comparison can be made with published data, care must be taken to ensure that experimental conditions are similar. The polymer handbook [105] quotes reactivity ratios from 0.66 to 1.23, r_A and -0.106 to 0.38, r_B, for a styrene/butyl acrylate system, respectively. These values represent a range of experimental conditions, temperature, concentration, initiation systems and polymerisation method. This can be summarised in table 5.2, where a sample of published data and the associated method to calculate the reactivity ratios is presented. Therefore, data for the reactivity ratios that are within the experimental range can be found.

Method	r_A	r_B	Temp. (°C)	Ref.
Kelen-Tudos[a]	0.698±0.033	0.164±0.017	50	180
EVM[a]	1.21±0.21	0.17±0.07	70	181
EVM	0.955	0.183	50	182
Kelen-Tudos[a]	0.883	0.207	80	183
Mayo-Huglin[b]	1.006	0.232	80	184
SS space[c]	$0.68 \leq r_A \leq 0.82$	$0.22 \leq r_B \leq 0.26$	110	185

[a] Below 15% conversion. [b] Above 15% conversion. [c] 25-85% conversion.

Table 5.2 Monomer reactivity ratios for a styrene (r_A) and butyl acrylate (r_B) for a sample of conventional reaction conditions and methods of determining the reactivity ratios.

Although there are no comparable results performed using the same conditions as this study, the nearest published results were by Xu et al. [186] who reported the reactivity ratios for styrene and butyl acrylate copolymerisation. In a bulk, emulsion and microemulsion type polymerisation, these were 0.77/0.14, 0.64/0.1 and 0.57/0.21 respectively. However, the method of initiation utilised by Xu was via gamma radiation, 20 $Gy.min^{-1}$ at 25°C, onto a pre-formed latex. Although gamma radiation is very useful in controlling the reaction, radical production can be switched on and off at will. The free radicals generated are OH* and H* [187] rather than SO_4^{*-}.

Although at first this may not appear significant Bartus et al. [188], showed that the copolymerisation of styrene and butyl acrylate is influenced by the initiator type, its position in the polymerisation system i.e. the aqueous or organic phase and the related mechanism of initiation. This was demonstrated through the use of a water soluble initiator (potassium persulphate) and a non-traditional initiator, oxidised isotactic polypropylene (OPP) powder. The hydroperoxidic groups on the surface of PP powder can be used for the initiation of the emulsion polymerisation of styrene in the presence of an amine [189]. Although the mode of initiation has a greater effect upon the molecular weight characteristics of the

copolymer than the reactivity ratios it could explain the differences between the published reactivity ratios and those calculated in this study.

Differences in the initiation step of the radical copolymerisation of styrene with butyl acrylate using ultrasound mainly influence the first three steps in the following reaction scheme, which explains the formation of primary and monomer radicals.

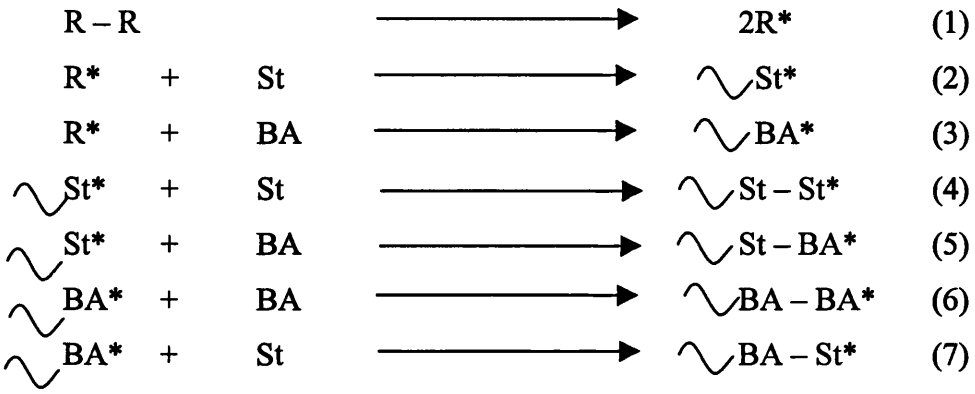

The ability for styrene or butyl acrylate to take part in the propagation reactions, steps 4 to 7, depends mainly upon the reactivity of the monomers, the propagating radicals and the local concentration of monomers in the reaction site. The reactivity ratios calculated in this study of 0.775 ±0.07 and 0.200 ±0.006 respectively, implying that styrene is consumed quicker than butyl acrylate, but why should this be as the vapour pressures and the solubility of the two monomers are very similar [151]. Therefore the chance of a radical entering a monomer droplet should be equal for both styrene and butyl acrylate.

A possible explanation lies in the interaction between the surfactant, SDS and butyl acrylate. The interaction arises from the anionic surfactant, SDS, which forms a double-electron layer [190] around a monomer droplet and the carbonyl carbon that is δ+, due to the electron withdrawing properties of the surrounding oxygens. The pendant chain of four carbons will now act as the hydrophobic part of a surfactant molecule. This will hinder the progress of the organic phase butyl acrylate into the monomer droplet that will become starved of butyl acrylate and

rich in styrene. Therefore, the resultant copolymer will contain more styrene than butyl acrylate.

5.3 Copolymerisation of styrene with methyl methacrylate.

Using the method described above the styrene molar fraction in the copolymer was calculated from the peak area of the protons due to the phenyl group (A_p) at ~7ppm and the peak area of the methyl group (A_m) at ~ 3.5ppm, in the methyl methacrylate. These can be related by equation 5.3. A summary of the styrene molar fraction in the copolymers is shown in table 5.3.

Styrene/Acrylate feed ratio (v/v)	Peak height of A_p	Peak height of A_m	F(st)
10/90	90	14	0.794
20/80	141	43.5	0.660
30/70	69	17	0.709
40/60	61.5	19	0.660
50/50	65.5	13.5	0.744
60/40	83.5	11	0.820
70/30	106.5	12	0.842
80/20	97.5	4	0.936
90/10	155.5	3	0.969

Table 5.3 The mole fraction of styrene in the poly(styrene/methyl methacrylate) copolymer prepared using an intensity of 23.8 ± 1.72 Wcm^{-2}.

Using the equation 5.1, the reactivity ratios for a styrene/methyl methacrylate system can now be found. From the graph, the reactivity ratios are $r_A = 0.651$ ±0.05 and $r_B = 0.415$ ±0.01.

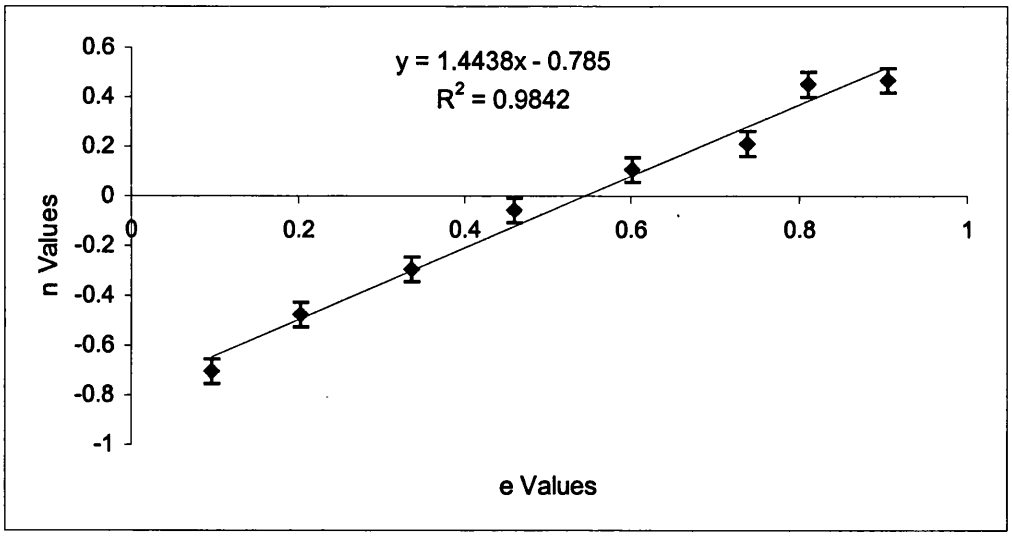

Graph 5.2 A graph to calculate to the reactivity ratios for a styrene/methyl methacrylate copolymerisation

This is in contrast to the situation for the styrene/butyl acrylate system where the reactivity of the styrene monomer is far higher than that of the butyl acrylate. A possible explanation for this may be due to lack of interaction between the anionic surfactant and the monomer methyl methacrylate. Thereby allowing the passage of methyl methacrylate into the monomer droplet and so avoiding styrene rich monomer droplets. Also the collapse of a cavitation bubble creates a large number of nucleation sites, these nucleation sites will be in both the aqueous and organic phase. The difference here is that unlike butyl acrylate which has to compete with styrene in the organic phase, methyl methacrylate can scavenge radicals in the aqueous phase.

The first published results for a styrene/methyl methacrylate microemulsion were by Gan et al. [191], who reported values of $r_A = 0.73$, $r_B = 0.38$, however, these results were commented upon by Klumperman [192] who took issue with the use of the Kelen-Tudos method of analysis. Klumperman then reanalysed the values of Gan et al., using an error invariables method [193] to obtain those shown in table 5.4. It must be noted that the values quoted by Gan/Klumperman, are from a ternary system, i.e. there is no alcohol to act as a co-surfactant, and the surfactant used was 'tetradecyltrimethylammonium bromide' (TTAB).

	r_A	r_B
No correction for composition drift.	0.51	0.32
Mayo-Lewis eq. Integrated	0.6	0.37
Triads plus F_s vs f_s; Mayo-Lewis eq. Integrated	0.55	0.42
Results by Gan	0.73	0.38
Results by Reddy	0.65	0.45

Table 5.4 A comparison of the published results for Gan and Reddy.

The method that Gan et.al used was different to the method described by equation 5.3. Using equation 5.4, he calculated the reactivity ratios.

$$Fs = 8A_p/5A_t \qquad (5.4)$$

Where A_p is the peak area of the protons from the phenyl group and A_t is the total area of all protons. If that method is utilised then the CH_2 group on the styrene is taken into account and so errors in the peak areas of the protons will occur, for this reason this method was not utilised in this study.

The nearest comparable data to the values calculated in this study are those by Reddy [194] who calculated values of $r_A = 0.65$ and $r_B = 0.45$ for a microemulsion copolymerisation, using the Kelen-Tudos method of analysis. Although the monomers were polymerised in a true microemulsion, using n-hexanol as a co-surfactant, the reactivity ratios are in close agreement with the values calculated in this study. This is further evidence (see chapter four) that using ultrasound can cause a switch in the polymerisation pathway from a micellar nucleation mechanism to a droplet nucleation mechanism, which is considered to be the dominant particle formation mechanism in a mini and micro-emulsion.

5.4 Effect of intensity upon the copolymerisation of styrene and butyl acrylate.

In sections 5.3 and 5.4, the intensity used was 23.8 ±1.72 Wcm^{-2}. It was postulated that by changing the ultrasonic intensity the amount of each monomer incorporated into the polymer chain might also be affected, due to the change in the number of nucleation sites, the number of radicals produced and the rate of polymerisation. The experiments were carried out as outlined in section 2.4, except that by changing the intensity then the monomer conversion would also be changed. Thus for an intensity of 36.5 ±2.31 Wcm^{-2}, the reaction was stopped after 12 minutes and for an intensity of 13.6 ±0.97 Wcm^{-2}, the reaction was stopped after 20 minutes. This represents a monomer conversion of less than 10%, necessary for the 'terminal' copolymerisation model to work.

5.4.1 Intensity of 36.5 Wcm^{-2}.

The apparatus was set up as for a copolymerisation reaction at an intensity of 23.8 Wcm^{-2}. However, this time the power on the ultrasonic generator was turned to a higher setting, 36.5 ±2.31 Wcm^{-2}. A summary of the styrene molar fraction in the copolymers is shown in table 5.5

Styrene/Acrylate feed ratio (v/v)	Peak height of A_p	Peak height of A_m	$F_{(st)}$
10/90	36.5	42	0.343
20/80	36	25	0.464
30/70	46	22.5	0.551
40/60	63	25.5	0.597
50/50	84	26.5	0.655
60/40	93.5	25	0.692
70/30	83.5	16	0.758
80/20	139	18	0.822
90/10	128	8	0.906

Table 5.5 The mole fraction of styrene in the poly(styrene/butyl acrylate) copolymer prepared using an intensity of 36.5 ±2.31 Wcm^{-2}.

Using the Kelen-Tudos method the reactivity ratios can now be calculated from the graph of η against ξ as described in equation 5.1. This is shown in graph 5.4. From the graph values of r_A and r_B are 0.79 ±0.07 and 0.12 ±0.009 as shown in graph 5.4.

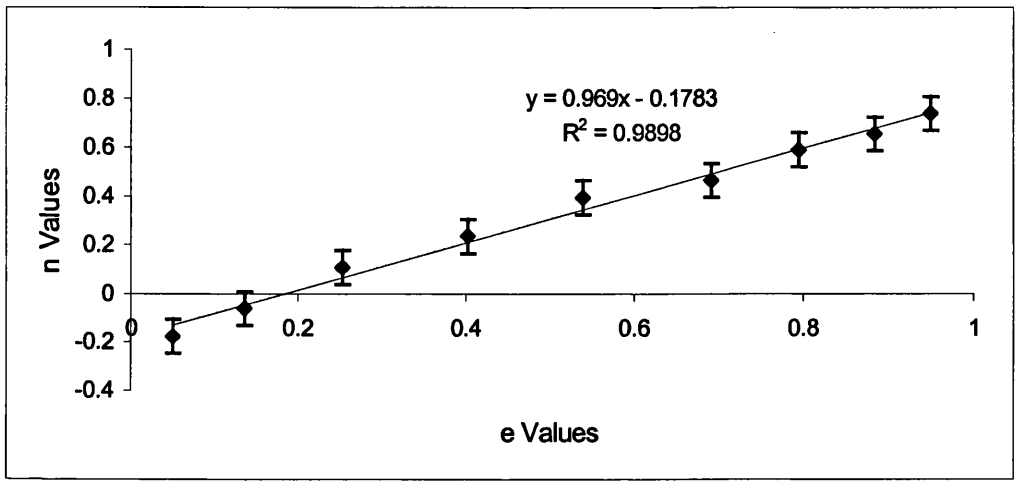

Graph 5.4 Reactivity ratios for styrene/butyl acrylate copolymerisation at an intensity of 36.5 ±2.31 Wcm^{-2}.

5.4.2 Intensity of 13.6 ±0.97 Wcm^{-2}.

The apparatus was set up as for a copolymerisation reaction at an intensity of 23.8 Wcm^{-2}, however, this time the power on the ultrasonic generator was turned to a lower setting, 13.6 ±0.97 Wcm^{-2}. A summary of the styrene molar fraction in the copolymers is shown in table 5.6.

Styrene/Acrylate ratio (v/v)	Peak height of A_p	Peak height of A_m	$F_{(st)}$
10/90	13.5	32	0.202
20/80	26	21.5	0.42
30/70	50.5	31.5	0.49
50/50	76	27	0.628
60/40	7.5	22.5	0.671
70/30	90	20	0.73
80/20	62.5	8	0.824
90/10	101.5	6.5	0.904

Table 5.7 The mole fraction of styrene in the poly(styrene/butyl acrylate) copolymer prepared using an intensity of 13.6 ±0.97 Wcm^{-2}.

Using the Kelen-Tudos method the reactivity ratios can now be calculated from the graph of η against ξ as described in equation 5.1. This is shown in graph 5.5. From the graph values of r_A and r_B are 0.76 ±0.09 and 0.23 ±0.003 as shown in graph 5.4.

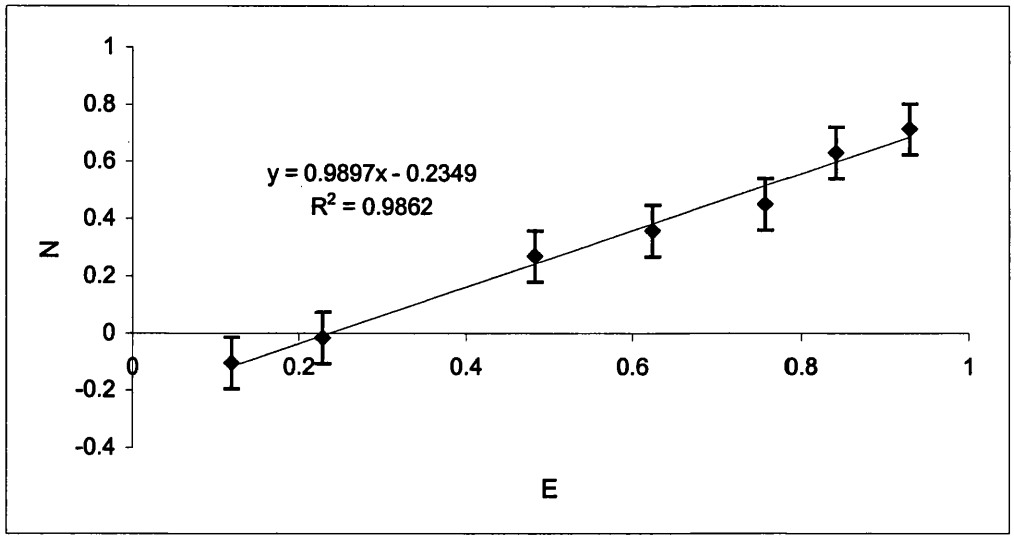

Graph 5.5 Reactivity ratios for styrene/butyl acrylate at an intensity of 13.6 ±0.97 Wcm^{-2}.

Although the calculated reactivity ratios are different for the three intensities studied, summarised in table 5.8, at an initial glance they do not differ as widely as expected.

Ultrasonic Intensity	r_A	r_B
13.6 ±0.97 Wcm^{-2}	0.76 ±0.09	0.23 ±0.003
23.8 ±1.72 Wcm^{-2}	0.78 ±0.07	0.20 ±0.006
36.5 ±2.31 Wcm^{-2}	0.79 ±0.07	0.12 ±0.009

Table 5.8 A summary of the reactivity ratios calculated for the three ultrasonic intensities.

However, if a closer look is cast on the values for r_B then it can be seen that at a decreasing the intensity then r_B tends towards constancy. The tendency of r_B towards unity could be due to the suppression of the termination reaction at lower intensities i.e the chance of another radical entering a monomer droplet is reduced. This is a strange phenomenon and one that requires further investigation at a wider range of intensities to determine the upper and lower limits ultrasound has upon the copolymerisation.

5.5 Conclusion

Previous work has suggested that through the use of ultrasound the ability of a monomer to react with the growing copolymer chain can be changed [195,196]. However, this is the first time that the reactivity ratios have been calculated for an ultrasonic reaction and the first time that a range of ultrasonic intensities has been studied.

The emulsion copolymerisation of styrene/butyl acrylate and styrene/methyl methacrylate has been carried out at 25°C using ultrasound. At an intensity of 23.8 ±1.72 Wcm^{-2} these were 0.78 ±0.07 / 0.20 ±0.006 and 0.651 ±0.05 / 0.415 ±0.01 respectively. The reactivity ratios have been calculated for both monomer pairs, using the Kelen-Tudos least squares method of analysis. The differences in the reactivity ratios can be explained by the interaction between the chosen acrylate and the anionic surfactant, SDS. By considering surfactant type behaviour, i.e. hydrophobic and hydrophilic parts to the molecule, then the interaction of butyl acrylate with SDS causes styrene rich droplets to occur.

The change in ultrasonic intensity has shown that at a high surfactant concentration the reactivity ratio $r_{styrene}$ is not significantly affected. However, the reactivity ratio $r_{B\text{-}acrylate}$ tends towards unity with decreasing ultrasonic intensity. Why this should occur is a matter for further study, by studying a wider range of intensities this phenomenon could be elucidated.

Through the use of ultrasound there is the ability to slightly change the reactivity ratios by merely changing the ultrasonic intensity. This previously has only been achieved by changing the aqueous to organic phase or by changing the monomer ratio in the reaction scheme. Further work to determine the extent of the ultrasonic intensity to effect the reactivity ratios is necessary to encompass soluble monomers.

The reactivity ratios have been compared with published data for such monomer pairs. They indicate that a microemulsion is formed during the polymerisation,

with the polymerisation locus being the monomer droplets. To provide further evidence of this the copolymerisation of styrene, a rather insoluble monomer, with hydroxy ethyl methacrylate, a soluble monomer, could be carried out. In an emulsion the HEMA would be expected to begin polymerising before the styrene due to the fact that the initiator is in the same phase.

6.0 Adhesive preparation

The term 'pressure sensitive adhesive' (PSA) refers to that type of adhesive which, when in a dry state, will adhere to a variety of surfaces merely by application of light hand pressure. Such combinations are inherently soft, permanently tacky materials which exhibit a balance of adhesive and cohesive strength depending upon the viscoelastic nature of the adhesive and the performance requirements of the particular end use.

A number of years ago Smith and Nephew decided to avoid the use of solvents, which are considered to be environmentally undesirable, in their polymerisation processes. One of the reactions which they changed to an emulsion process was the preparation of a pressure sensitive adhesive as described by European patent application number 0194881 [140]. Here the copolymerisation of a number of acrylates, Butyl, hydroxy-ethyl, 2-ethyl hexyl and methyl methacrylate together with a polymerisable surfactant, sodium mono-lauryl itaconoxy propane, produces a pressure sensitive adhesive. The basis of the adhesive is acrylic esters that yield polymers of low glass transition temperatures. The use of a polymerisable surfactant avoids the extra process of removing any residual surfactant.

Polyacrylates of a particular monomer composition are inherently pressure sensitive with the addition of any additives. This single component feature means that low molecular weight ingredients that can migrate to the surface of the coating are absent. As an adhesive bond is a surface phenomenon, minimising the compositional variations at the surface is highly desirable. Polyacrylates also possess other properties superior to many other polymers used for PSA applications. The polymer is saturated and resistant to oxidation, it is water white and does not yellow on exposure to sunlight. Monomers with various functional groups can be introduced during polymerisation and an adhesive with various degrees of thermosetting properties can be prepared.

6.1 Preparation of a pressure sensitive adhesive

Smith and Nephew have attempted to carry out a number of analytical tests on the industrially produced adhesive prior to this study. However, as the adhesive forms a gel when in solution molecular weight analysis is not possible as a proportion of the adhesive gets filtered out when samples are being prepared and another proportion gets held back on the guard column. Therefore, results that have been achieved are not representative of the whole sample. Particle size data could not be obtained due to the adhesive sticking to the side of the viewing cell. Reactivity ratios could not be calculated due to there being five reactants that have to be taken into consideration.

Consequently the only test that is undertaken as part of the quality control procedures is the total solids content of the final adhesive. The formation of a gel presented a great deal of problems in order to analyse the resultant polymer. ^{1}H NMR analysis was a particular problem area with adhesive being prone to sticking on the sides of the NMR tube rather than dropping to the bottom and only a small proportion going into solution. For this reason ^{13}C spectra could not obtained, as there was so little adhesive in solution.

The experiments were carried out as described in section 2.6. The first experiment to be carried out was the sonication of the monomer, water mix and the subsequent addition to a heated and stirred reaction flask. This was carried out in order to provide a benchmark against which all other reactions could be compared. The graph of monomer conversion against time is shown in graph 6.1. As can be seen from this graph the monomer conversion rises steadily with time to a final conversion of 83%. This is comparable with the industrially produced product where the final solids content is between 80 to 94% by weight of the polymer for a reaction time of four hours and a temperature of 85°C.

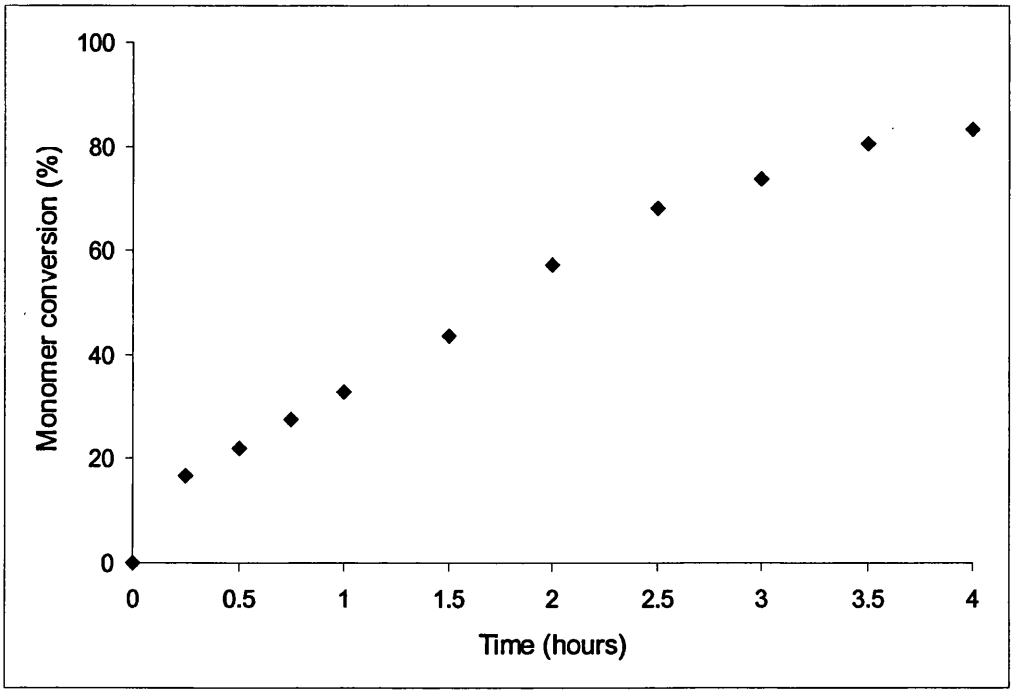

Graph 6.1 Monomer conversion against time for a sonicated emulsion preparation and conventional reaction at 85°C.

Using a similar treatment to that used in chapter four to determine the rate of polymerisation a graph of the rate against time can be drawn for the above reaction, shown in graph 6.2.

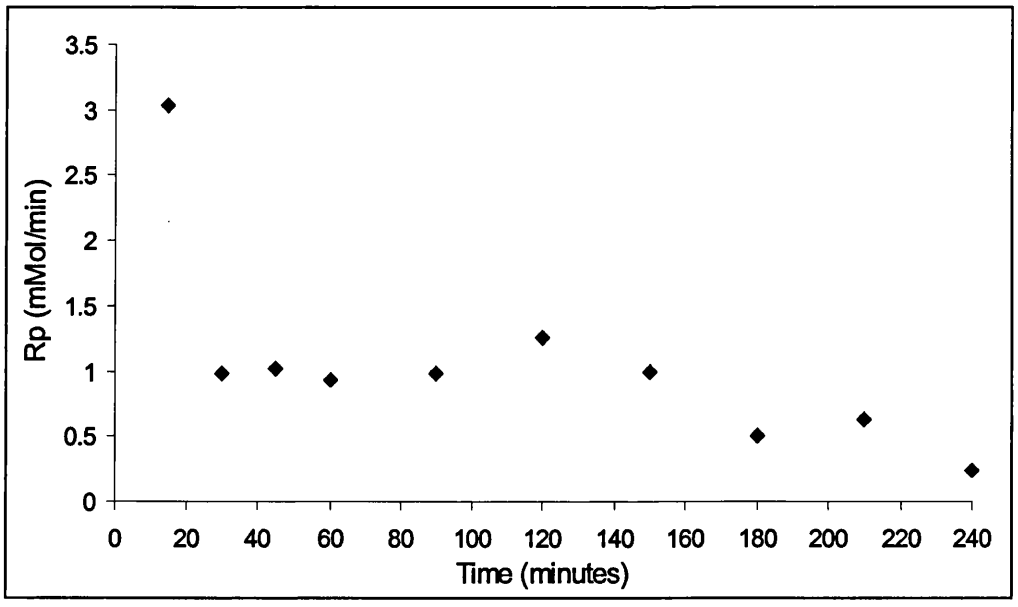

Graph 6.2 The rate of polymerisation against time for the conventional preparation of the PSA at 85°C.

Although no comparable data for this polymerisation system has been published, the process being industrially sensitive, a comparison with the copolymerisation of acrylic acid and acrylic monomers [197] demonstrates that the rate of reaction and the final conversion is of a comparable rate.

As mentioned above the number of analytical tests that can be performed upon the final product are limited, although ^{1}H NMR and detection of the glass transition temperature (T_g) were carried out. The ^{1}H NMR spectrum is shown in figure 6.1. Likewise the DSC trace showing the T_g for the reaction is represented by figure 6.2.

The detection of the T_g was chosen rather than other thermal properties as the dependence of the PSA to wet out and adhere to a surface and the capability for sufficient cold flow to fill surface irregularities are found in PSAs with a low T_g [198]. Although the Tg is neither an accurate measure of polymer stiffness at room temperature nor is it an accurate measure of pressure sensitive properties it is an easy and convenient method to predict the suitability of a polymer for PSA applications. The control of T_g is achieved through copolymerisation of various combinations of high, low and intermediate T_g monomers.

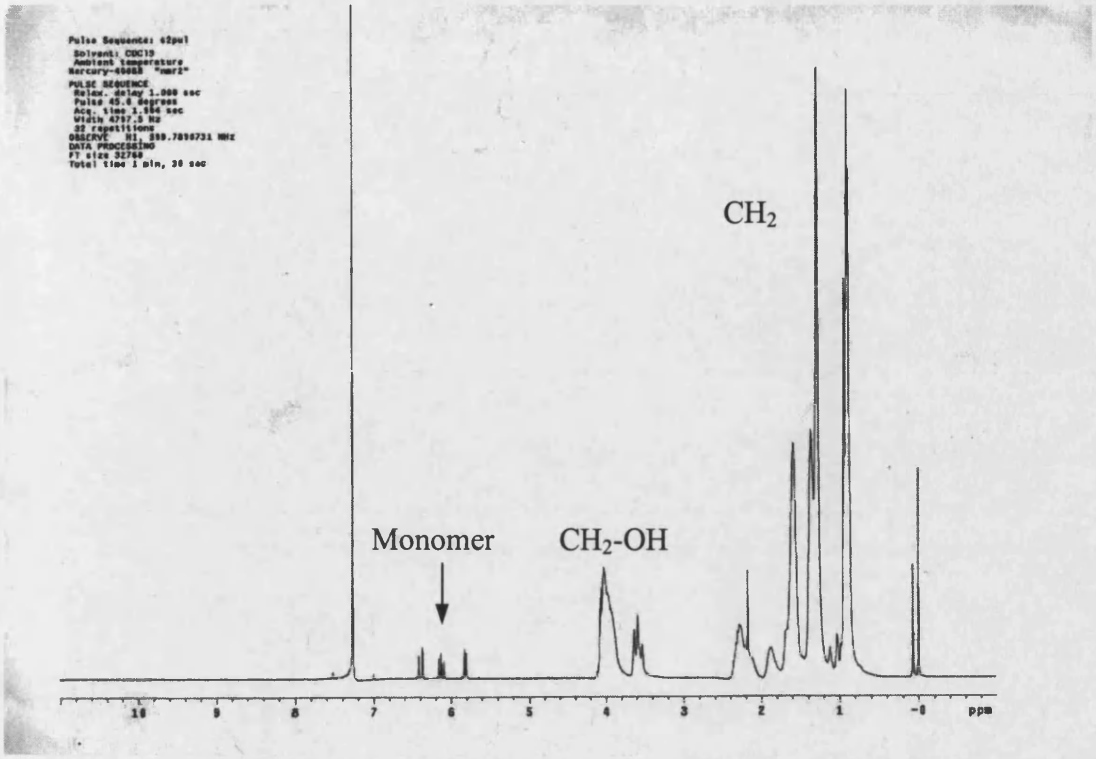

Figure 6.1 ^{1}H NMR spectrum of the pressure sensitive adhesive produced via a conventional reaction.

As can be seen from figure 6.1 there are traces of the monomers in the spectrum. This can be easily seen from the peaks at 6ppm, coming from the protons on the carbon-carbon double bond. The remainder of the spectrum is typical of a acrylate copolymer. Although the peak are labelled further analysis is hampered by the number of monomers in the system, see figure 6.2 and the inclusion of the polymerisable surfactant.

Butyl acrylate 38g

$H_2C{=}CHCO_2(CH_2)_3CH_3$

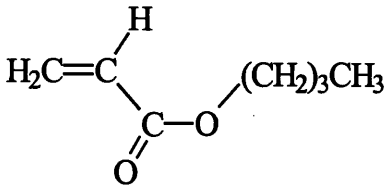

2-ethyl hexyl acrylate 42g

$CH_2{=}CHCOOCH_2CH(CH_2CH_3)(CH_2)_3CH_3$

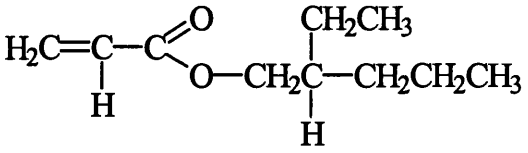

2hydroethyl methacrylate 0.85g

$H_2C{=}C(CH_3)CO_2CH_2CH_2OH$

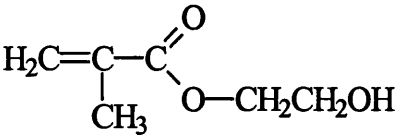

Methyl Methacrylate 4.25g

$H_2C{=}C(CH_3)CO_2CH_3$

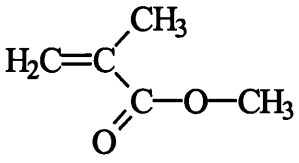

Figure 6.2 The acrylate monomers copolymerised to produce the PSA.

When the sample is analysed using the DSC machine the glass transition temperature (T_g) can clearly be seen to occur between –67 and -55°C with the T_g being recorded as -62°C, shown in figure 6.2.

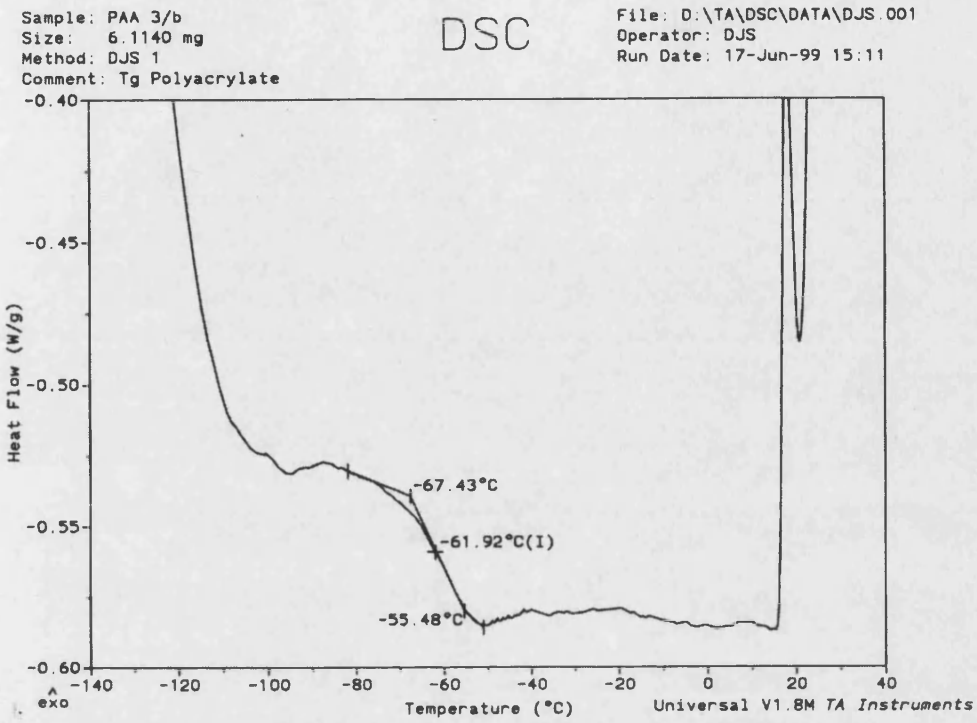

Figure 6.2 DSC trace from the pressure sensitive adhesive as produced via a conventional reaction at 85°C.

The Tg of -62°C is typical of a copolymer of a number of substituted polyacrylates [199]. By incorporating the main building block monomers, butyl, ethyl hexyl acrylate into the polymer backbone the glass transition is representative of these two acrylates. This is readily apparent from the Tg's of the acrylates used for the preparation of the PSA, shown in table 6.1 [200]. The copolymerisation reaction also involves a number of auxiliary acrylates including methyl methacrylate, hydroxy ethyl methacrylate and the polymerisable surfactant. These auxiliary monomers are used to provide crosslinking sites within the copolymer

Monomer	Homopolymer T_g/ °C
n-Butyl acrylate	-54
i-Butyl acrylate	-43
2-Ethylhexyl acrylate	-85
Methyl methacrylate	+105
Hydroxy ethyl methacrylate	+55

Table 6.1 The T_g's for the acrylic homopolymers used in this study.

The same reaction was then repeated at differing temperatures, from 25° to 75°C in 10°C intervals. This was carried out so that not only is the effect of temperature determined but a comparison can be made with the ultrasonic reaction. The graph of monomer conversion is shown in graph 6.3.

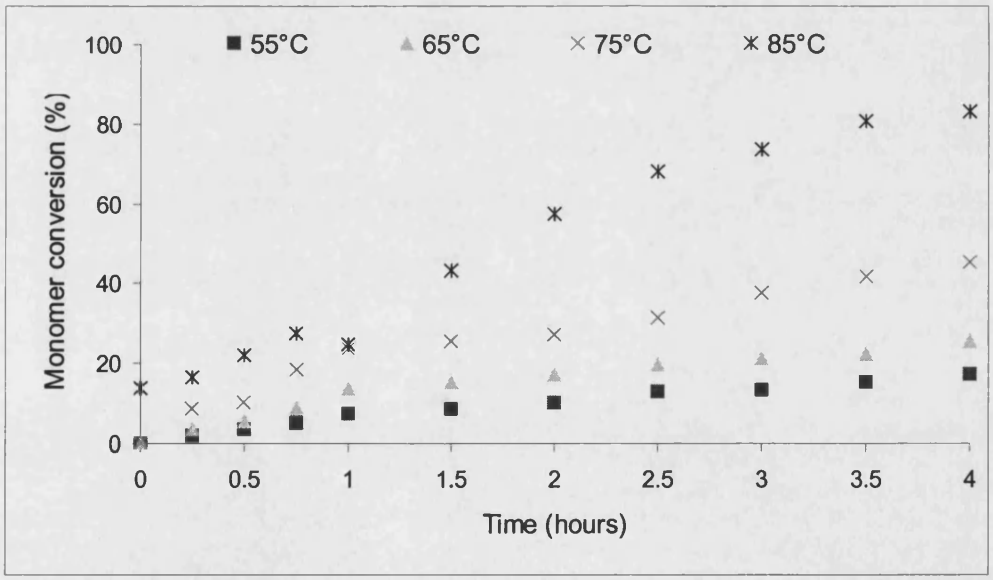

Graph 6.3 Monomer conversion against time for a series of reactions at increasing temperatures.

The monomer conversion for temperatures below 55°C is not shown for clarity. What is surprising from these reactions is that it is not until 75°C that any

significant polymerisation takes place. The rate of persulphate decomposition at 55°C is 2.5×10^{-6} at 85°C the rate is 1.4×10^{-4} [73]. It is apparent that at 55°C the rate of decomposition of persulphate should be sufficient to cause the initiation of the reaction. So why is the conversion so low? Although micellisation is generally an exothermic process and the CMC increases with increasing temperature surfactants exhibit another phenomenon where their solubilities show a rapid increase above a certain temperature. This temperature is known as the Krafft point [168]. Below the Krafft temperature the solubility of the surfactant is insufficient for micelles to form. Increasing the temperature the solubility also increases until, at the Krafft temperature, the CMC is reached.

Increasing the number of carbon atoms in the surfactant will lead to an increase in the Krafft temperature. In the surfactant used in this study there are twenty-one carbon atoms, hence, the high temperature required for solubility.

6.2 Ultrasonic preparation of a pressure sensitive adhesive

All the reactions were carried out as described in section 2.6, using the P100 Sonic Systems ultrasonic horn at an intensity of 10.66 ±0.6Wcm^{-2} and a starting temperature of 25°C.

The graph of monomer conversion against time for the ultrasonically initiated polymerisation is shown in graph 6.4. As can be seen from the graph the monomer conversion is very erratic, with no clear increase in monomer conversion with time as seen for the conventional reaction. Indeed, it could be misinterpreted as degradation occurring in the reaction. This is due to the way the reaction is agitated. In the conventional reaction the whole mixture is continuously stirred and moved around, whilst the outside of the reaction vessel is in contact with oil at an elevated temperature. The result of this is that the mixture does not have a chance to coagulate or agglomerate.

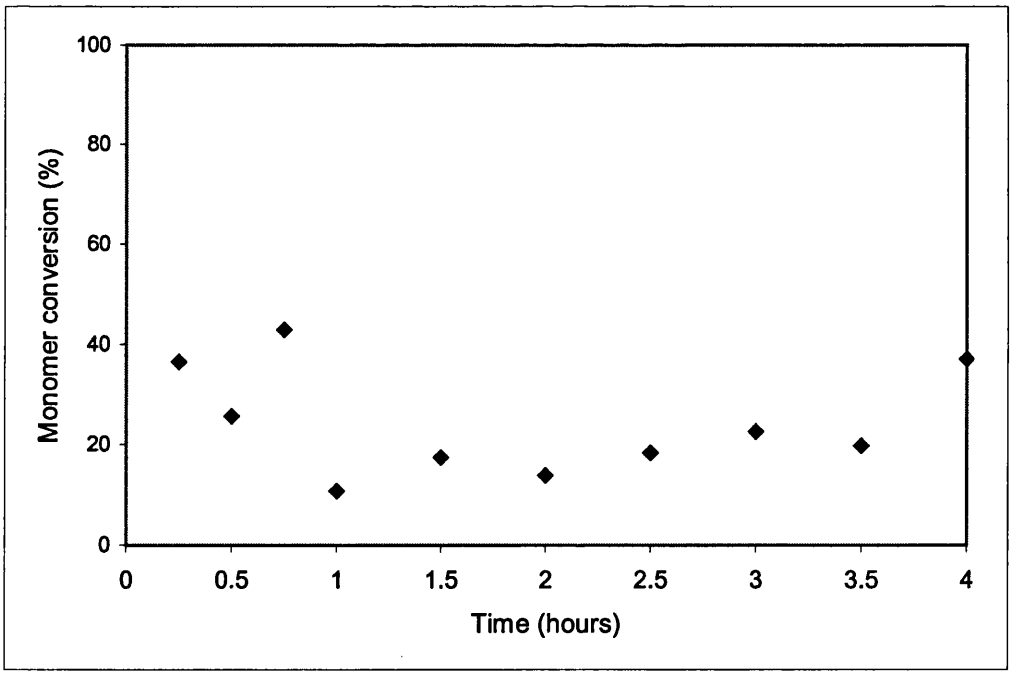

Graph 6.4 Monomer conversion against time for an ultrasonically assisted reaction, (10.66 ±0.6 Wcm^{-2}).

In the ultrasonic reaction the mixture is not moved about by a stirrer, but by the collapse of the cavitation bubbles. Although collapsing bubbles set up very high shear rates they are confined to a local area, therefore, the whole mixture is not subject to a uniform shear rate. The result of this is that as a whole the reaction mixture does not move about as much as a conventional reaction. This causes coagulation on the outside of the reaction vessel where cooling water is circulated around the reaction vessel and this coagulation transfers into the bulk reaction. When a sample is withdrawn via a syringe only the very viscose material can be withdrawn not the coalesced lumps. For this reason the monomer conversion does not increase uniformly with time.

The ^{1}H NMR spectrum of the resultant polymer is shown in figure 6.3.

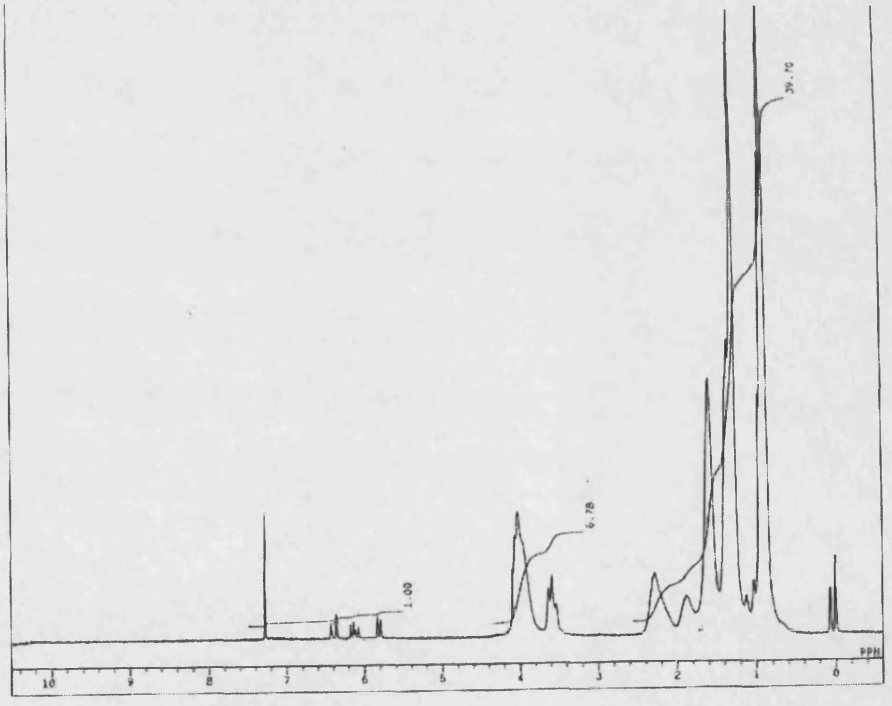

Figure 6.3 ^{1}H NMR spectrum of the pressure sensitive adhesive produced via an ultrasonic reaction (10.66 ±0.6 Wcm^{-2}).

Again, the peaks at 6ppm are indicative of monomer residue in the sample. The spectrum very closely matches the spectrum for a conventional reaction, shown

in figure 6.2. With no change in the spectra it can be concluded that the polymer backbone is similar to that produced via a conventional reaction at 85°C.

However, what cannot be shown is any change in the degree of crosslinking caused by the action of ultrasound upon the polymerisation. An indication of the degree of crosslinking can be determined from the DSC spectrum showing the T_g, as demonstrated in figure 6.4.

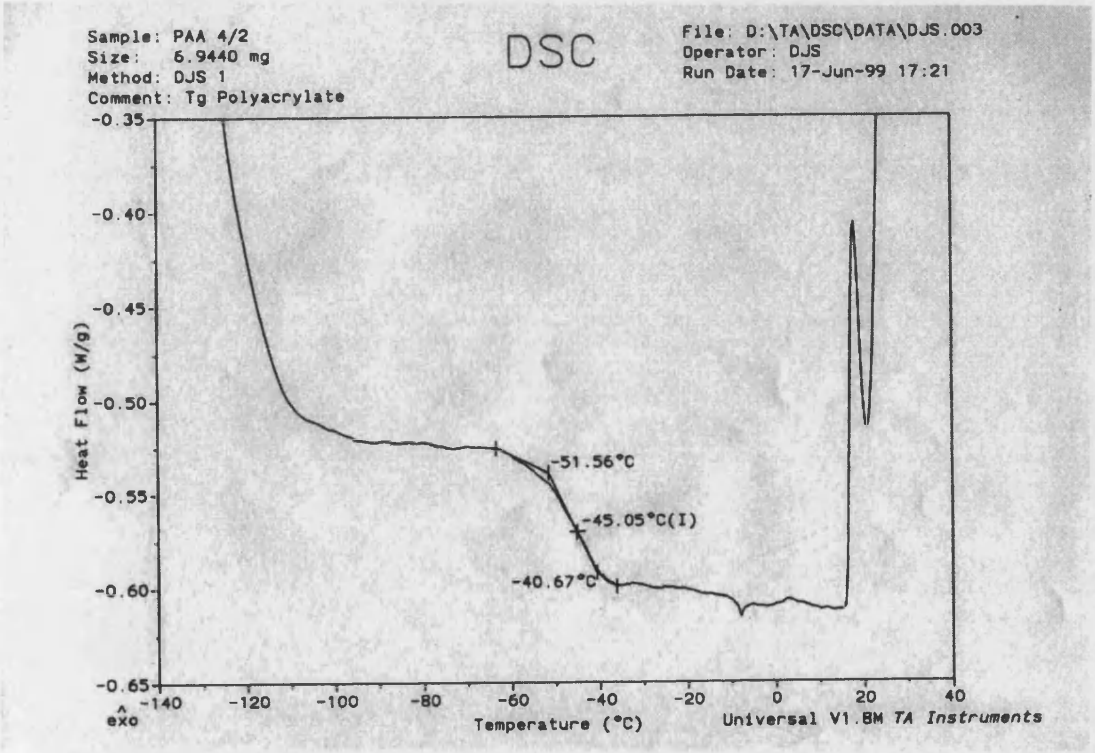

Figure 6.4 DSC trace from the pressure sensitive adhesive as produced via an ultrasonic reaction at 10.36 Wcm^{-2}.

Here, the T_g region occurs between -52° and -41°C with the T_g being recorded as -45°C, which is almost 20°C higher than the conventional reaction. This could be due to a number of factors; steric effects, configurational effects, chain flexibility, the degree of crosslinking and the change in reactivity ratios. It is the last of these factors that is the most significant as it has a knock on effect on to all the other factors in changing the T_g.

The PSA is made up of a number of monomers and a reactive surfactant, sodium mono-lauryl itaconoxy propane sulphonate [201]. If the reactivity ratios are changed, through the application of ultrasound, then the way in which the surfactant becomes part of the PSA will in turn affect the degree of cross-linking in the PSA. The surfactant has to be reactive enough so that it will be incorporated into the growing chain and still function as a surfactant. On the other hand, if the surfactant is too reactive it can become buried inside the latex particle and be unable to provide stability. Through the use of ultrasound it has already been shown, chapters 4 and 5, that the particle size and the reactivity ratios can be affected. These two factors are among several strategies that have been proposed to control reactive surfactant behaviour [202]. The reaction with the monomers and hence the burying of the surfactant in the particles can be minimised if the particles are not allowed to grow significantly, as in the case when ultrasound is used. Although, it is not possible to determine the reactivity ratios for this reaction chapter 5 has shown that ultrasound affects the co-monomer reactivity. These factors are combining to produce a polymer that has a significantly higher number of crosslinks than the conventionally prepared PSA, this is shown by the increase in the T_g.

It was felt that ^{13}C NMR could provide more information than just ^{1}H NMR alone. However, as noted earlier the adhesive does not go into solution, only a gel like solution. Therefore, it did not prove possible to obtain ^{13}C NMR spectra.

As ultrasound can induce bond breakage and hence can create radicals the initiator ammonium persulphate can be induced to break down into sulphate radicals. For this reason the concentration of the initiator was reduced to half the original concentration and finally the initiator was omitted completely for an ultrasonic reaction at 10.66 ±0.6Wcm^{-2} at 25°C. The graph comparing the monomer conversion as obtained from a conventional reaction at 85°C is also included in graph 6.4.

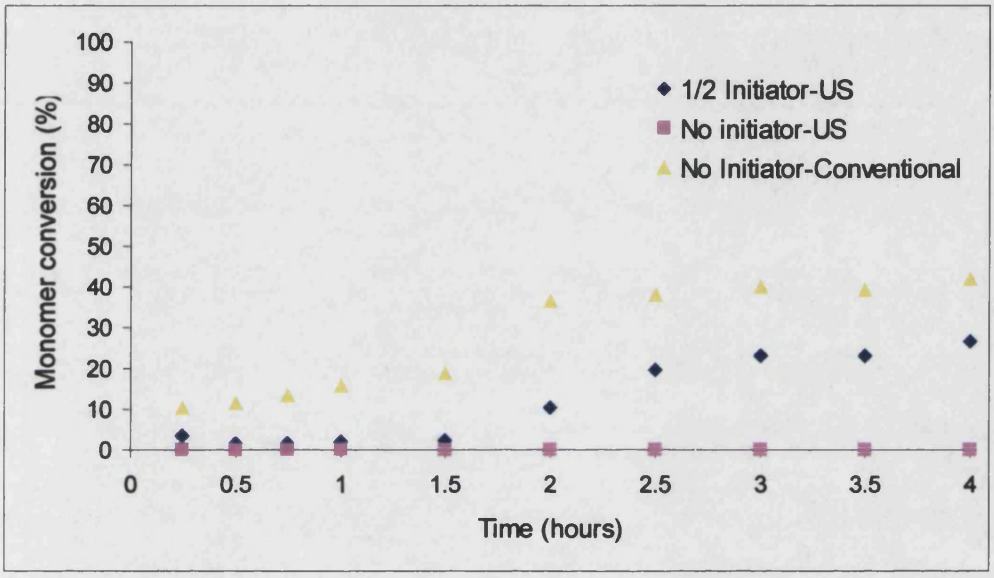

Graph 6.4 Monomer conversion against time for an ultrasonically assisted reaction, (10.66 ±0.6 Wcm^{-2}) and a conventional reaction, with a change in initiator concentration.

As can be seen from the graph the monomer conversion is greatly reduced by the omission of the initiator, ammonium persulphate. Although the conventional reaction gave a poor yield, for the ultrasonic reactions the reaction mixture again coalesced and agglomerated upon the walls of the reaction vessel, so the monomer conversion cannot be a true representation of the reaction. Although the graph of monomer conversion for the reaction with no initiator resulted in poor monomer conversion enough sample could be collected to obtain a DSC spectrum. The summary of the T_gs for this series of reactions is shown in table 6.1.

In the formulation of a PSA the role of the surfactant can be both a passive or and active role, i.e. it can provide stability to the growing polymer chain or it can act a cross-linker to the growing polymer chain. Although the presence of the hydroxyl group from 2-hydroxy-ethyl methacrylate will enable cross-linking to occur, it is the presence of the surfactant that allows sufficient cross-linking of the polymer. The result of this is that the PSA will remain stable when it is spread at high application speeds and as it experiences high shear when it passes under a doctor blade.

In changing the surfactant concentration it was expected that the final tack and adhesion of the PSA would be changed due to the absence of a cross-linking agent, but how the monomer conversion and the chain tacticity would be effected was uncertain. Shown in graph 6.5 is the graph of monomer conversion for the ultrasonic reaction performed at 10.66 ±0.6Wcm^{-2} with half the concentration of the surfactant.

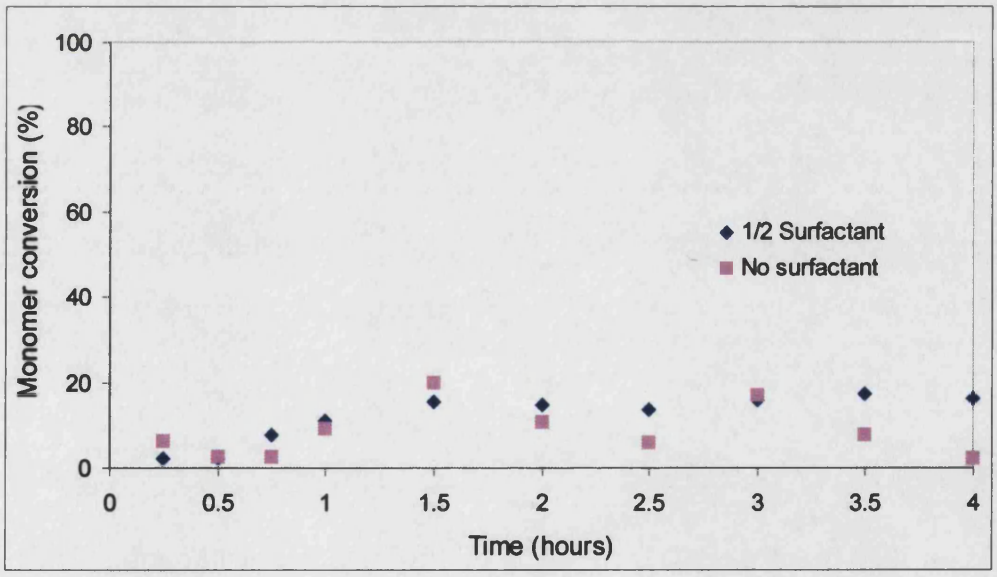

Graph 6.5 Monomer conversion against time for an ultrasonically assisted reaction, (10.66 ±0.6 Wcm^{-2}), with a change in surfactant concentration.

Likewise, the surfactant can be omitted for a conventional reaction, this is shown in graph 6.6.

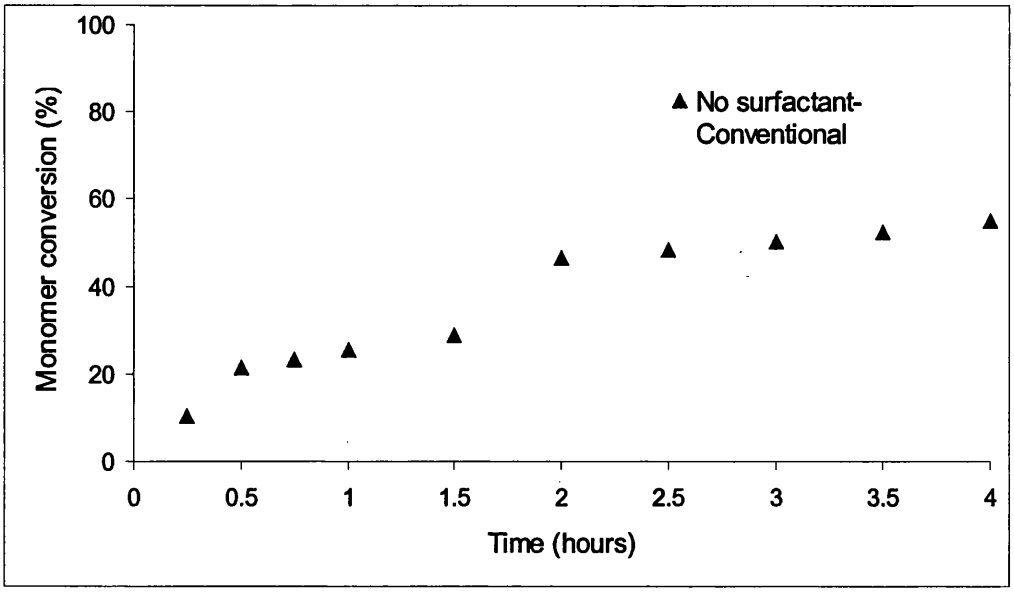

Graph 6.6 Monomer conversion against time for a conventional reaction omitting the surfactant.

All PSA's produced were analysed using ^{1}H NMR, although no differences were found between the spectra. The major differences were to be found in the T_g's of the resultant PSA, summarised in table 6.2. Here the effect of the surfactant acting as a crosslinker can readily be seen. Reducing the concentration from 0.17g to 0.085g decreases the T_g by 3°C, omitting the surfactant decreases the T_g by 10°C, the decrease in the T_g's occurs due the increased mobility of the polymer chain. Likewise for a conventional reaction omitting the surfactant decreases the T_g by 5°C.

Conditions	T_g
Conventional reaction	-63.57°C
Ultrasonic reaction	-45.32°C
Ultrasonic reaction – ½ initiator	-51.99°C
Ultrasonic reaction- no initiator	-50.14°C
Conventional reaction – no initiator	-53.71°C
Ultrasonic reaction – ½ surfactant	-47.88°C
Ultrasonic reaction- no surfactant	-55.36.
Conventional reaction – no surfactant	-67.65

Table 6.2 Summary of the glass transition temperatures for the preparation of a pressure sensitive adhesive.

6.3 Tack testing of the pressure sensitive adhesive

The European patent that describes the preparation of the pressure sensitive adhesive goes on to explain how to thicken the adhesive through the addition of 0.88 ammonia solution and then 4.5% (based on solids) Acusol 830. The addition of the ammonia is necessary in order to create an alkaline solution, so that the Acusol 830, a polyacrylate with free carboxyl groups, gels and thickens the adhesive. The correct viscosity is confirmed by using a Brookfield viscometer spindle 6 and speed setting 10. The viscosity should fall between 55000 and 70000 cp.

Once the adhesive had been thickened then it could be spread onto Rexam 111/80 release paper using a pilot labcoater and the conditions described in table 6.3.

Blade height	0.1mm
Coating speed	$1mMin^{-1}$

Dried at 40°C for 25 seconds, removed from the oven.
Dried at 80°C for 30 seconds, removed from the oven.
Dried at 120°C for 100 seconds, ready to be tested.

Table 6.3 Coating conditions for the pressure sensitive adhesive.

The industrially produced adhesive passes through a number of ovens at differing temperatures. This ramping of the temperature is not possible with a laboratory coating machine. However, using the conditions described in table 6.3. laboratory produced samples closely mimic the industrially produced product.

When the samples that had been prepared at the University of Bath were to be tested it was found that the drying conditions were unsuitable. The adhesive thickened to a suitable viscosity, would be totally dry, or still be wet with water. In either case the adhesive would not be tacky and could not be used for testing. A number of differing viscosities and drying conditions were tried in order to obtain suitable material for tack testing. However, all attempts to produce a tacky substrate failed. This was in contrast to the situation with the industrially produced adhesive, which would give a tacky substrate for all conditions used. Hence, no information on the tack and adhesive properties of the PSA produced using ultrasound was found.

6.3 Conclusions

The use of ultrasound to the Smith and Nephew patent 0194881 did not give the enhanced yield and performance that the studies with styrene emulsions and styrene/acrylate copolymerisations would have suggested. This is due to the very nature of the reagents used in the polymerisation. Unlike a conventional emulsion polymerisation, where the surfactant merely acts to stabilise the growing polymer chain, in this case the surfactant also reacts with the growing chain. This allows the resultant latex not to desorb under the influence of high shear and not to migrate to the surface when it applied to the backing web. Unlike the previous copolymerisation reactions here there are five reagents that are being incorporated into the growing polymer chain, making calculation of the reactivity ratios impossible.

Through the application of ultrasound the number of crosslinks in the PSA increases, restricting the chain flexibility and mobility. This was apparent through the use of DSC analysis, where the glass transition temperature could be monitored for the PSA. A conventional reaction gave a T_g of –63.57°C, whereas an ultrasonic reaction gave a T_g of –45.32°C. Reducing the concentration of the surfactant in the reaction the T_g could be decreased, thereby establishing the link between the reactive surfactant and the T_g. The increase in the number of crosslinks also has a major effect upon the properties of the PSA produced by ultrasound. When the PSA is spread upon release paper either water is retained, so giving a wet surface, or the PSA is dried and it has no adhesive properties.

If ultrasound were to be successful in the preparation of a pressure sensitive adhesive then the formulation would have to be changed to take into account the increase in the number of crosslinks. The starting point for this work would have to be the incorporation of the reactive surfactant into the growing polymer chain and the subsequent calculation of the reactivity ratios.

7.0 Conclusions

The aim of this work was to prepare polymers using the emulsion polymerisation technique. By comparing the same reaction prepared using conventional and ultrasonic methods, an understanding of how ultrasound effects the polymerisation is made. A number of experiments have been carried out in order to comprehend the process that is occurring.

Through the use of a radical trap the activation energies for the sonication of DPPH in *o*-xylene have been calculated. Using a conventional Arrhenius equation the activation energy has been calculated to be $-7.49 kJmol^{-1}$. Using a modified Arrhenius equation the activation energy has been calculated to be $+25.07 kJmol^{-1}$. The difference in the activation energy can be attributed to the choice of temperature and pressure used for the calculations, the bulk temperature or the temperature and pressure generated upon bubble collapse. The bulk sonication of DPPH in *o*-xylene with the organic initiators, AIBN and BPO were also carried out. Again using the conventional Arrhenius equation values of $+24.1 kJmol^{-1}$ and $+15.36 kJmol^{-1}$ respectively were calculated. Using a modified Arrhenius equation, values of $-85.91 kJmol^{-1}$ and $-39.75 kJmol^{-1}$ were calculated. The breakdown of the Arrhenius equation can be attributed to the assumption that the collapsing bubble does some work, this not valid. Although irreversible bubble collapse can be described an Arrhenius equation that takes into account all types of bubble collapse and the correct choice of temperature has yet to be put forward.

The use of DPPH in a two-phase system has also been attempted. Although from the sonication of DPPH in a bulk system has shown that the Arrhenius equation is not valid the activation energy has been calculated using both equations. This is the first time that using a radical trap in a two-phase system has been attempted.

The emulsion polymerisation of styrene has been carried out. It has been found that through the use of ultrasound the particle nucleation pathway shifts from a MICELLAR pathway to a droplet nucleation pathway, due to the high shear rates

caused by a collapsing cavitational bubble. Evidence for this comes from the increased molecular weight in comparison with a conventional reaction and the fact that the monomer conversion is significantly reduced when the surfactant concentration is reduced to 9.43×10^{-3} moldm^{-3} (0.5g), even though this is above the CMC of the surfactant, sodium dodecyl sulphate. It is the increase in the molecular weight of the resultant polymer that was the cause of a number of problems in analysing the polymer. The blocking of two GPC columns was the cause of the curtailment in the molecular weight analysis.

The reduction in the ultrasonic intensity lead to a reduction in the monomer conversion for all the reactions performed here. This is in line with other researchers in this field [169], who have shown that the polymerisation rate increases linearly up to a limiting ultrasonic intensity. The reason for the decrease in the monomer conversion is due to the decrease in the ratio of small monomer droplets and hence total number of particles. This in turn effects the number of primary sites available for radical capture due to the decrease in the relative surface area.

Increasing the bulk temperature of the reaction performed using ultrasound increases the rate of monomer conversion. For a comparable temperature the monomer conversion for an ultrasonic reaction is faster than for a conventional reaction. Through the use of ultrasound, the opportunity to perform the emulsion polymerisation of styrene at either a reduced temperature or with a reduction in the concentration of the initiator or surfactant is possible.

Through the use of a Coulter particle size machine, equipped with a small volume analyser, the evolution of the particle size was followed for a number of reactions. Using this method of analysing the particle size it appears that the particle size for a conventional reaction is smaller than for an ultrasonic reaction. This is in contradiction to a number of other workers who reported that using ultrasound produces a smaller particle size. However, when a latex produced via ultrasound was analysed using a TEM, it appeared that the particles were forced together as a result of the forces generated upon bubble collapse.

The emulsion copolymerisation of styrene/butyl acrylate and styrene/methyl methacrylate has been carried out at 25°C using ultrasound. At an intensity of 23.8Wcm^{-2} these were 0.78 ±0.07 / 0.2 ±0.006 and 0.651 ±0.05 / 0.415 ±0.01 respectively. The reactivity ratios have been calculated using the Kelen-Tudos least squares method of analysis. The differences in the reactivity ratios can be explained by the interaction between the chosen acrylate and the anionic surfactant, SDS.

The preparation of a pressure sensitive adhesive has been attempted using Smith and Nephews European patent number 0194881. The adhesive was compared using spectroscopic methods and by differential scanning calorimetry as these were the only methods that were suitable for the resultant polymer. Due to the change in preparation the amount of cross linking in the adhesive is increased thereby changing the spreading characteristics of the adhesive and not allowing the tack properties to be found.

7.1 Further work

There is much scope for further work in this aspect of the project. Although styrene, an insoluble monomer, has been studied here, hydroxy-ethyl metha-acrylate (HEMA), a soluble monomer could be investigated. As HEMA is soluble in water the phase properties in an emulsion polymerisation are totally different. How ultrasound would effect the reaction is uncertain as the increased mass transport which ultrasound gives would offer less of an advantage.

Due to the kinetics of the reaction the molecular weights achieved are much higher than those achieved for a similar reaction performed in a bulk polymerisation. For this reason it is common to use a charge transfer agent to limit the molecular weight. Haddleton et al.[177,178] have been making novel charge transfer agents and testing how they limit the molecular weight of a styrene emulsion polymerisation. Their conclusion is that the rate of diffusion between the phases is the limiting factor in effecting the molecular weight. The increased mass transport that ultrasound can give is an effective method to determine if that hypothesis is correct.

Other forms of polymerisation could also be investigated in the future such as suspension polymerisations and recently there has been a report that atom transfer radical polymerisation can be performed in an emulsion [179,203]. The radical nature of this form of polymerisation is a subject of some debate and therefore through the use of ultrasound the reaction rate should be increased, indicating if the reaction does go through a radical step. Through the use of a radical trap the activation energies for the emulsion polymerisation can be calculated. However, the conventional Arrhenius equation cannot be applied to an ultrasonic reaction, as the temperature recorded is the bulk temperature and not the temperature where the reaction is occurring, i.e. the collapsing bubble. Therefore through the use of a modified Arrhenius equation the activation energies can be calculated.

8.0 References

1 Mason, T.J., Lorimer, J.P., 'Sonochemistry: Theory, Applications and uses of Ultrasound in Chemistry, Ellis Horwood, Chichester, 1988.

2 Storti G., Hipp A.R., Morbidelli M., Polym. React. Eng. **8**, 77, 2000.

3 Siani A., Storti G., Morbidelli M., J. Appl. Polym. Sci. **72**, 1451, 1999.

4 Canegallo S., Apostolo M., Storti G., Morbidelli M., J. Appl. Polym. Sci. **57**, 1333, 1995.

5 Mason T.J., Lorimer J.P., Chem. Soc. Rev. **16**, 239, 1987.

6 Suslick K., www. scs.uiuc.edu/suslick/

7 Thornycroft J., Barnaby, S.W., Proc. Inst. Civ. Eng. **122**, 67, 1895.

8 Lord Raleigh, Philos. Mag. Ser. **34**, 94, 1917.

9 Suslick K., 'Ultrasound: Its Chemical, Physical and Biological Effects' Suslick K., Ed. VCH, New York 1988.

10 Crum L., Nature, **278**, 148, 1977.

11 Connolly W., Fox F., J. Acoust. Soc. Am. **26**, 843, 1954.

12 Greenspan M., Tschiegg C., J. Res. Natl. Bur. Stds. **71C**, 299, 1967.

13 Price G.J., Ed. 'Introduction to sonochemistry' current trends in sonochemistry RSC. Cambridge 1992.

14 McNamara W.B., Didenko Y.T., Suslick K.S., Nature, **401**, 772, 1999.

15 Suslick K.S., Flint E.B., Grinstaff M.W., Kemper K.A., J. Phys. Chem. **97**, 3098, 1993.

16 Noltingk B.E., Neppiras E.A., Proc. Phys. Soc. **B63**, 674, 1950.

17 Noltingk B.E., Neppiras E.A., Proc. Phys. Soc. **B64**, 1032, 1951.

18 Flynn H.G., 'Physical Acoustics' Vol.1B, Eds. Mason W.P., Academic Press, New York, 1964.

19 SUSLICK IN SCIENCE YR 2000!!!!1!!!!!!!

20 Flint E.B., Suslick K.E., Science, **253**, 1397, 1991.

21 Serpone N., Colarusso P., Res. Chem. Intermed. **20**, 635, 1994.

22 Margulis M.A., Russ. J. Phys. Chem. **59**, 1497, 1985.

23 Margulis M.A.,. Ultrasonic sonochemistry, **S87**, 4, 1994.

24 Margulis M.A., Ultrasonic sonochemistry, **S87**, 1, 1994.

25 Price G.J., West P.J., Smith P.F., Ultra. Sonochem., **1**, S51, 1994.

26 Raso J., Manas P., Pagan R., Sala J., Ultra. Sonochem. **5**, 157, 1999.

27 Chou J.H.C., Stoffer J.O., J. Applied Sci. **72,** 797, 1999.

28 Curie J., Curie P., Bull. Soc. Min. Paris, **3,** 90, 1880.

29 Wood R.W., Loomis A.L., Phil. Mag. **4,** 414, 1927.

30 Richards W.T., Loomis A.L., J. Am. Chem. Soc. **49,** 3086, 1927.

31 Flosdorf E.W., Chambers L.A., J. Am. Chem. Soc. **55,** 3051, 1933.

32 Luche J.L., Einhorn C., Einhorn J., Tetrahedron Lett. **31,** 4125, 1990.

33 Luche J.L., Ultrasonics, **30,** 156, 1992.

34 Kornblum N., Micheal R.E., Kerber R.C., J. Am. Chem. Soc. **88,** 5662, 1966.

35 Russell G.A., Danen W.C., J. Am. Chem. Soc. **88,** 5663, 1966.

36 Luche J.L., Dickens M.J., Tetrahedron Lett. **32,** 4709, 1991.

37 Diaz-Barra E., de la Hoz A., Diaz-Ortiz A., Prieto P., Synth. Commun. **23,** 1935, 1993.

38 De Souza Barboza J.C., Petrier C., Luche J.L., J. Org. Chem. **53,** 1212, 1988.

39 Szalay A., Z. Phys. Chem. **A164,** 234, 1933.

40 Schmid G., Rommel O., Z. Electrochem. **45,** 659, 1936.

41 Schmid G., Phys. Z., **41,** 326, 1940.

42 Basedow A.M., Ebert K.H., Adv. Polym. Sci., **22,** 83, 1977.

43 Price G.J., Chemistry and Industry **3,** Feb. 1993.

44 Price G.J., TRIP, **2,** 174, 1994.

45 Jellinek H.H.G., J. Polym. Sci. **37,** 485, 1959.

46 Henglein A., Makromol. Chem. **15,** 188, 1955.

47 Melville H.W., Murray A.J.R., Trans. Faraday Soc. **46,** 996, 1950.

48 Price G.J., Adv. Sonochem. **1,** 231, 1990.

49 Allen P.E.M., Downer J.M., Hastings G.W., Melville H.W., Molyneux P., Unwin J.R., Nature, **177,** 910, 1956.

50 Henglein A., Makromol. Chem. **18,** 37, 1956.

51 Price G.J., West P.J., Polymer, **37,** 3975, 1996.

52 Lindstrom O., Lamm O., J. Phys. Colloid chem. **55,** 1139, 1951.

53 Kruss P., Adv. Sonochem. **2,** 1, 1991.

54 Kruss P., Patraboy T.J., J. Phys. Chem. **89,** 3379, 1985.

55 Price G.J., Ultra. Sonochem. **3,** S229, 1996.

56 Price G.J., Norris D.J., West P.J., Macromolecules, **25,** 6447, 1992.

57 Ostroski A.S., Stambaugh R.B., J. Appl. Phys. **21,** 478, 1950.

58 Ooi S.K., Biggs S., Ultrason. Sonochem. **7**, 125, 2000.

59 Hatate Y., Ikari A., Kondo K., Nakashio F., Chem. Eng. Commun. **34**, 325, 1985.

60 Lorimer J.P., Mason T.J., Fiddy K., Kershaw D., Groves R., Dodgson D., Ultrasonics International conference proceedings, 1283, (1989) Butterworth-Heinemann.

61 Biggs S., Grieser F., Macromolecules, **28**, 4877, 1995.

62 Liu Y., Chou H.C.J., Stoffer J.D., J. Appl. Polym. Sci. **53**, 247, 1994.

63 Liu J., Chen K., Li Z., Polymer Journal, **32**, 103, 2000.

64 Cheung M., Gaddam K., J. Appl. Polym. Sci., **76**, 101, 2000.

65 Dinsmore R.P., (Goodyear Tire & Rubber Co) BP 297050 (1927) = USP 1732795 (1927), Chem. Abstr. **24**, 266, 1930.

66 Luther M., Heuck C., (I.G. Farbenindustrie) Ger 558890 = USP 1864078 (1928), Chem. Abstr. **26**, 4505, (1932), US Patent 1860681 (1927) Chem. Abstr. **26**, 3804, 1932.

67 Warson H., 'The applications of synthetic resin emulsions' Benn, London 1972.

68 Hohenstein W.P., Mark M., J. Polym. Sci. **1**, 127, 1946.

69 Talalay A., Magat M., 'Synthetic rubber from alcohol' Interscience New York 1945.

70 Dunbrook R.F., 'Historical review' in 'Synthetic rubber' by Whitby G.S., Davis C.C., Dunbrook R.F., (eds) Wiley New York 1954.

71 Fryling C.F., 'Emulsion polymerisation systems' in 'Synthetic rubber' by Whitby G.S., Davis C.C., Dunbrook R.F., (eds) Wiley New York 1954.

72 Bovey E.A., Kolthoff I.M., Medalia A.I., Meehan E.J., 'Emulsion polymerisation' Interscience New York 1955.

73 Behram, E. J., Edwards, J.O., Rev. Inorg. Chem. **2**, 179, 1980.

74 Morris, C.E., Parts, A.G., Makromol. Chem. **119**, 212 1968.

75 Sudol, E., D., El-Aasser, M., S., Vanderhoff, J. W., J.Polym. Sci., Polym. Chem. Edn. **24**, 3515, 1986.

76 Sudol, E., D., El-Aasser, M., S., Vanderhoff, J. W., J.Polym. Sci., Polym. Chem. Edn. **24**, 3499, 1986.

77 Jacobi B., Angew. Chem., **64**, 539, 1952.

78 Priest W.J., J. Phys. Chem., **56**, 1077, 1952.

79 Fitch R.M., Tsai C.H., Polymer colloids, Fitch R.M. (Eds.) plenum, New York, 1971.

80 Hansen F.K., Ugelstad J., Emulsion polymerisation Piirma I., (Eds). Academic: New York, 1982, p51.

81 Ugelstad J., Hansen F.K., Rubb. Chem. Techl., **49**, 536, 1976.

82 Hansen F.K., Ugelstad J., J. Polym. Sci., polym. Chem. Ed., **16**, 1953, 1978.

83 Maxwell I.A., Morrison R.B., Napper D.H., Gilbert D.H., Macromolecules, **24**, 1629, 1991.

84 Harkins W.D., J. Chem. Phys., **13**381, 1945; **14**, 47, 1946.

85 Harkins W.D., J. Polym. Sci., **5, 217**, 1950.

86 Smith W.V., Ewart R.H., J.Chem. Phys., **16**, 592 1948.

87 Smith W.V., J.Amer. Chem. Soc. **70**, 3695, 1948.

88 Parts A.G., Moore D.E., Watterson J.G., Makromol. Chem., **89**, 156, 1965.

89 Gardon J.L., J. Polym. Sci., Polym. Chem., **6**, 623,643, 665, 687, 2853, 2859, 1968, and **9**, 2763, 1971.

90 Harada M., Nomura M., Kojima H., Eguchi W., Nagata S., J. Appl. Polym. Sci., **16**, 811, 1972.

91 Ugelstad J., Mork P.C., Aasen J.O., J. Polym. Chem. **5**, 2281, 1967.

92 Guo J.S., Sudol E.D., Vanderhoff J.W., El-Aasser M.S., Polymer Latexes: Preparation Characterization and Applications, Daniels E.S., Sudol E.D., El-Aasser M.S., (Eds.) American Chemical Society Symposium Series, Vol. 492, Washington DC, 1992, p99.

93 Kuo P.L., Turro N.J., Tseng C.M., El-Aasser M.S., Vanderhoff J.W., Macromolecules, **20**, 1216, 1987

94 Chamberlain B.J., Napper D.H., Gilbert R.G., J. Chem. Soc., Faraday Trans. 1., **78**, 591, 1982.

95 Ugelstad J., El-Aasser M.S., Vanderhoff J.W., J. Polym. Sci., Polym. Letters, **111**, 503, 1973.

96 Tang P.L., Sudol E.D., Silebi C.A., El-Aasser M.S., J. Appl. Polym. Sci., **42**, 2019, 1991.

97 Roe C.P., Ind. Eng. Chem., **60**, 20, 1968.

98 Hansen F.K., Chem. Eng. Sci., **48**, 437, 1993.

99 Casey B.S., Morrison B.R., Gilbert R.G., Prog. Polym. Sci., **18**, 1041, 1993.

100 Staudinger H., Schneiders J., Ann. Chim. (Paris), **541**, 151, 1939.

101 Coote M.L., Johnston L.P.M., Davis T.P., Macromolecules, **30**, 8191, 1997.

102 Maxwell I.A., Aerdts A.M., German A.L., Macromolecules **26**, 1956, 1993.

103 Fukuda T., Ma Y.D., Inagaki H., Macromolecules **18,** 17, 1985.

104 Arehart S.V., Matjaszewski K., Macromolecules, **32**, 2221, 1999.

105 Greenley R.Z., in 'Polymer Handbook' 3rd Edition, Eds Brandup J. and Immergut E.H., p.ii/153, Wiley, New York, 1989.

106 Kelen T., Tudos F., J. Macromol. Sci. Chem. **9,** 1, 1975.

107 Tudos F., Kelen T., Foldes-Bereznich T., Turcsanyi B., J. Macromol. Sci. Chem. **10**, 1513, 1976.

108 Van der Meer R., Linssen H.N., German A.L., J. Polym. Sci. Polym. Chem. Ed. , **16**, 2915, 1978.

109 Fineman M., Ross S.D., J. Polym. Sci., **5**, 259, 1950.

110 Tidwell P.W., Mortimer G.A., J. Macromol. Sci. Rev. Macromol. Chem., **C4**, 281, 1970.

111 Mayo F.R., Lewis F.M., J. Am. Chem. Soc. **66**, 1594, 1944.

112 Alfrey T., Goldfinger G., J. Chem. Phys. **12**, 205, 1944.

113 Mayo F.R., Walling C., Chem. Rev., **46**, 191, 1950.

114 Tidwell P.W., Mortimer G.A., J. Polym. Sci., **A3**, 369, 1965.

115 Meyer V.E., J. Polym. Sci. **A-1(4)**, 2819, 1966.

116 Watts D.G., Linssen H.N., Schrijner J., J. Polym. Sci. Polym. Chem. Ed. **18,** 1285, 1980.

117 Britt H.J., Luecke R.H., Technometrics **15**, 233, 1973.

118 Hill D.J.T., Lang A.P., O'Donnell J.H., O'Sullivan P.W., Eur. Polym. J., **26,** 11, 1989.

119 Moad G., Solomon D.H., Spurling T.H., Stone R.A., Macromolecules, **26,** 1965, 1993.

120 Wang S., Poehlein G.W., J. Applied Polym. Sci.

121 Rudin A., O'Driscoll K.F., Rumack M.S., Polymer, **22**, 740, 1981.

122 Ubel J.J., Dinan F.J., J. Polym. Sci., Polym. Chem. Ed., **21**, 917, 1983.

123 Randall J.C., Polymer Sequence Determination, Academic Press, New York, 1977.

124 Bovey F.A., Chain Structure and Conformation of Macromolecules, Wiley, New York, 1982.

125 Tonelli A.E., NMR Spectroscopy and Polymer Microstructure, VCH, New York, 1989.

126 Maxwell I.A., Aerdts A.M., German A.L., Macromolecules, **26**, 1956, 1993.

127 Aerdts A.M., de Haan J.W., German A.L., Macromolecules **21**, 3536, 1988.

128 Aerdts A.M., de Haan J.W., German A.L., Macromolecules **26**, 1965, 1993.

129 Moad G., Willing R.I., Polym. J. (Tokyo), **23**, 1401, 1991.

130 Moad G., in 'Annual Reports in NMR Spectroscopy' Eds. Webb G.A., Vol. 29, p287, Academic Press, London, 1994.

131 Moad G., Chem. Aust., **58**, 122, 1991.

132 Odian G., Principles of polymerisation 2nd Ed. Wiley, New York, 1988.

133 Ballard M.J., Napper D.H., Gilbert R.G., J. Polym. Sci., Polym.Chem. Ed. **22**, 3225, 1984.

134 Huo B.P., Cambell J.D., Penlidis A., MacGregor J.F., Hamielec A.E., J. Appl. Polym. Sci. **35**, 2009, 1988.

135 Barnes C.E., Elofsen R.M., Jones G.D., J. Am. Chem. Soc. **72**, 210, 1950.

136 Lorimer J.P., Mason T.J., Ultrasonics Sonochemistry **2**, S79, 1995.

137 Lorimer J.P., Mason T.J., J. Chem. Soc. Farad. Trans. **91**, 1067, 1995.

138 Bawn C.E.H., Mellish T.J., J. Chem. Soc. Farad. Trans. **91**, 1067, 1995.

139 Sehgal C., Yu T.J., Sutherland R.G., Verrall R.E., J.Phys. Chem. **86**, 2982, 1982.

140 Howes J.G.B., European patent 0194881 (1986), assigned to Smith and Nephew.

141 Dow J., Proc. Inst. Rubber Ind., **1**, 105, 1954.

142 Condon W.F., S.P.T., 14th Annual Tech. Conf., Section 14, 1, 1959.

143 Hagan J.W., Mallon C.B., Rifi M.R., Adhesives age, **22**, 29, 1979.

144 Aubrey D.W., Devel. In Adhesives, **1**, 127, 1977.

145 Kruus P., Patraboy T.J., J. Phys. Chem., **89**, 3379, 1985.

146 Antonietti M., Bremser W., Muschenborn D., Rosenauer C., Schupp B., Scmidt M., Macromolecules, **24**, 6636, 1991.

147 Sehgal C., Yu Y.T., Sutherland R.G., Verrall R.E., J. Phys. Chem. **86**, 2982, 1982.

148 Lorimer J.P., Kershaw D., Mason T.J., J.Chem. Soc. Faraday Trans. **91,** 1067, 1995.

149 Suslick K.S., Gawienowski J.J., Schubert P.F., Wang H.H., Ultrasonics **22,** 33, 1984.

150 Price G.J., Clifton A.A., Polymer Comms. **37,** 3971, 1996.

151 Brandrup J., Immergut E.H., Polymer Handbook 4th Ed. Wiley, New York, 1995

152 Kulkarni M.G., Mashelkar R.A., J.Polym. Sci., Polym. Letts. Ed., **19,** 507, 1981.

153 Lewis F.M., Matheson M.S., J. Amer. Chem. Soc., **71,** 747, 1949.

154 Overberger C.G., O'Shaughnessy M.T., Shalit H., J. Amer. Chem. Soc., **71,** 2661, 1949.

155 Arnett L.M., J. Amer. Chem. Soc., **74,** 2027, 1952.

156 Smith P., Carbone S., J. Amer. Chem. Soc., **81,** 6174, 1959.

157 Sasaki H., Nagayama M., J. Appl. Polymer Sci., **11,** 2097, 1967.

158 Talat-Erben M., Bywater S., J. Amer. Chem. Soc., **77,** 3712, 1955.

159 Juang R.S., Liang J.F., J. Chem. Tech. Biotechnol. **55,** 379, 1992.

160 Interpretation of mass spectra 4th Ed. Mclafferty F.W., Turecek F., Eds. University Science Books, California, 1992.

161 Introduction to organic spectroscopy, Lambert J.B., Shurvell H.F., Lighter D.A., Cooks R.G., Macmillan, New York, 1987.

162 Lopez de Arbina L., Barandiaran M.J., Gugliotta L.M., Asua J.M., Polymer, **37,** 5907 1999.

163 Gilbert R.G., 'Emulsion polymerisation : A mechanistic approach' Academic Press, London, 1995.

164 El-Aasser M.S., Sudol E.D., 'Emulsion polymerisation' Wiley, New York 1999.

165 Capek I., Adv. Colloid and Interface Sci., **82,** 253, 1999.

166 Chern C.S., Lin S.Y., Hsu T.J., Polymer J., **31,** 516, 1999

167 Xu X., Zhang Z., Wu H., Ge X., Zhang M., Polymer, **39,** 5245, 1998.

168 Shaw D.J., Colloid and surface chemistry 4th Ed. Butterworth Heinemann 1992.

169 Chou H.C., Stoffer J., J. Appl. Polym. Sci., **72,** 827, 1999.

170 Xu X., Zhang Z., Wu H., Ge X., Zhang M., Polymer, **39**, 5245, 1998.

171 Saleh S.I., Ripple E.G., S.T.P. Pharma. Sci., **3**, 220, 1994.

172 Mujumdar S., Kumar P.S., Pandit A.B., Ind. J. Chem. Tech., **4**, 277, 1997.

173 Abismail B., Canselier J.P., Wilhelm A.M., Delmas H., Gourdon C., Ultrason. Chem., **6**, 75, 1999.

174 Deelic G., Kratovil J.P., J. Coll. Sci., **16**, 561, 1961.

175 Davidson J.A., Collins E.A., J. Coll. Sci., **40**, 437, 1972.

176 Hansen F.K., Ugelsted J., Makromol. Chem., **180**, 2423, 1979.

177 Haddleton D.M., Depaquis E., Kelly E.J., Kukalj D., Morsley S.R., Bon S.A.F., Eason M.D., Steward A.G., J. Polym. Sci. A. Polym. Chem., **39**, 2378, 2001.

178 Haddleton D.M., Topping C., Kukalj D., irvine D., Polymer, **39**, 3119, 1998.

179 Shinoda H., Matyjaszewski k., Macromolecules, **34**, 6243, 2001.

180 Kaszas G., Foldes-Berezsnich T., Tudos F., Eur. Polym. J., **20**, 395, 1984.

181 Bar A.S, Sunita C.V.V., Polym. J., **24**, 879, 1992.

182 Dube A.S., Sanayei R.A., Penlidis A., O'Driscoll K.F., Reilly P.M., J. Polym. Sci. Polym. Chem. Ed., **29**, 703, 1991.

183 Ziaee F., Nekoomanesh M., Polymer, **39**, 203, 1998.

184 Ziaee F., Nekoomanesh M., Polymer, **39**, 203, 1998.

185 Arehart S.V., Matyjaszewski K., Macromolecules, **32**, 2221, 1999.

186 Xu X., Ge X., Zhang Z., Zhang M., Polymer, **39**, 5321, 1998.

187 O'Donnell J.H., Sangster D.F., 'Principles of radiation chemistry' Edward Arnold: London 1970.

188 Chrastova V., Citovicky P., Bartus J., J.M.S. Pure Appl. Chem. **A31**, 835, 1994.

189 Mikulasova D., Chrastova V., Citovicky P., Horie K., Makromol. Chem. **178**, 429, 1977.

190 Polymer colloids – A comprehensive introduction, Fitch R.M., Academic press, London, 1997.

191 Gan L.M., Lee K.C., Chew C.H., Ng S.C., Gan L.H., Macromolecules, **27**, 6335, 1994.

192 Klumperman B., Aerdts A.M., Macromolecules, **29**, 6679, 1996.

193 Britt H.J., Luecke R.H., Technometrics, **15**, 233, 1973.

194 Reddy G.V.R., J. Sci. Indust. Research, **58**, 678, 1999.

195 Cooper G., Grieser F., Biggs S., J. Colloid interface Sci. **184**, 52, 1996.

196 Koda S., Amano T., Nomura H., Ultra. Sonochem. **3**, S91, 1996.

197 Morgan L.W., Jensen D.P., Emulsion copolymerisation, mechanisms and processes Guillot J., Pichot C., Eds, Huthig and Wepf, New York, 1985.

198 Aubrey D.W., Developments in Adhesives – 1, Wake W.A. Ed., London, Applied Science Publishers, 1977.

199 Satas D. in Handbook of pressure sensitive adhesive technology, 2nd edn, Satas D., Ed. Van Nostrand Reinhold, New York, 1989.

200 Penzel E., Ullmann's encyclopedia of industrial chemistry, 5th edn, Vol. A21. VCH, New York, p157, 1992.

201 Asua J.M., Schoonbrood H.A.S., Acta . Polym., **49**, 671, 1998.

202 Asua J.M., Schoonbrood H.A.S., Macromolecules, **30**, 6034, 1997.

203 Qiu J., Charleux B., Matyjaszewski K., Polimery **46**, 453, 2001.